Theoretical Approach to the Optical, Thermodynamic and Magnetic Properties of Solid Nitrogen and Solid Oxygen

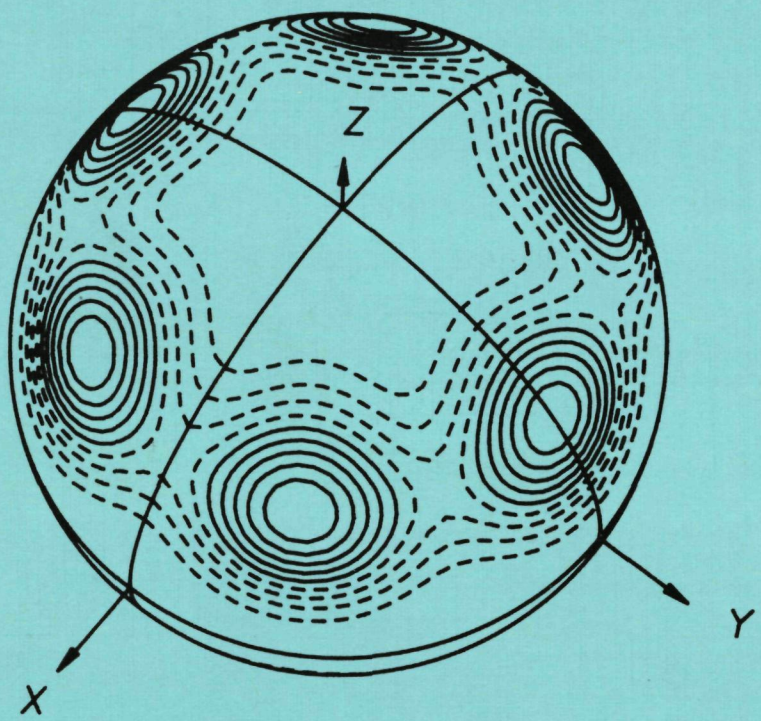

A.P.J. Jansen

Theoretical Approach to the Optical, Thermodynamic and Magnetic Properties of Solid Nitrogen and Solid Oxygen

PROEFSCHRIFT

ter verkrijging van de graad van
doctor in de wiskunde en natuurwetenschappen
aan de Katholieke Universiteit te Nijmegen,
op gezag van de Rector Magnificus
Prof. Dr. B.M.F. van Iersel
volgens besluit van het College van Decanen
in het openbaar te verdedigen
op donderdag 10 september 1987
des namiddags te 3.30 uur

door

Antonius Petrus Johannes Jansen

geboren te Maastricht

druk: Sneldruk Enschede
1987

PROMOTOR: Prof. Dr. Ir. A. van der Avoird

Theoretical Approach to the Optical, Thermodynamic and Magnetic Properties of Solid Nitrogen and Solid Oxygen

Op deze plaats wil ik iedereen bedanken die op een of andere manier heeft bijgedragen aan het tot stand komen van dit proefschrift, en wel met name

- de medewerkers en exmedewerkers van de afdeling Theoretische Chemie van de Universiteit Nijmegen voor alle hulp en suggesties.
- Wim Briels voor de enthousiaste begeleiding.
- de studenten Wilfred Janssen en Rob Schoorl voor het doen van een hoop berekeningen.
- Monique Bongers-de Bie en Ine van Berkel-Meijer voor het vele typewerk.
- Elly voor al het andere.

Aan mijn ouders

CONTENTS

1. The constituents of solids

Solids are made out of atoms or molecules. The word solid implies something that is firm, unmovable. Introductory textbooks on the structure of matter often present a solid as a rigid configuration of atoms or molecules. However, such a view is certainly not correct. Microscopically a solid consists of particles in frantic motions. What is typical for solids is that each atom or molecule moves only in a small region of space; i.e. it vibrates around an equilibrium position.

We need not "look" at individual atoms or molecules in a solid to become aware of the vibrations. There are many macroscopic properties of solids that can be observed (some even without equipment) and which are due to these vibrations. Solids would not expand with increasing temperature, insulators would not conduct heat or sound, and metals would have an infinite thermal conductivity (due to the conduction electrons) if the atoms or molecules would not vibrate. The electrical resistance of a metal would be zero if the atoms would not vibrate. For some metals or compounds the electrical resistance becomes zero below a certain temperature. The vibrations of the atoms in these solids seem to be important for the mechanism that causes this superconductivity. A very important thermodynamic property that is determined by the vibrations of the atoms or molecules is the specific heat. Without these vibrations the specific heat of an insulator would be an exponential function of the reciprocal temperature. Actually at high temperatures the specific heat becomes constant, and at low temperatures (except below $T = 10\,\mathrm{K}$ for metals) a T^3-law holds.

The vibrations of atoms or molecules in solids can be studied most directly by spectroscopic methods. The results of calculations in this thesis will often be compared to experimental results obtained with spectroscopic methods; i.e. absorption of far infrared radiation, Raman spectra, and inelastic scattering of neutrons.

2. Lattice dynamics

Crystals form a special class of solids. They are readily recognized by their geometric shapes. They are bound by planes that are determined by the microscopic structure. In crystals the atoms or molecules are arranged in an array which is periodic in three spatial directions. The equilibrium positions of the atoms or molecules form a set of points called a lattice. Due

to the periodicity of the lattice, there are collective vibrations in which all atoms or molecules participate and which have the form of waves. These collective vibrations constitute the lattice dynamics. In this thesis only crystals are studied, and most calculations that are presented are lattice dynamics calculations.

If the vibrations of the atoms or molecules have only small amplitudes then they can be calculated quite accurately. The potential energy of the crystal can be expanded in a Taylor series in the coordinates describing the displacements of the atoms or molecules from their equilibrium positions. If the amplitudes are small then this series can be truncated after the quadratic terms. With respect to the remaining potential the vibrations can be calculated exactly. This is called the harmonic approximation (see page 33 ff.). With this approximation the properties mentioned in the previous paragraph can be calculated. The harmonic approximation is the standard method for making lattice dynamics calculations.

The terms that are neglected in the harmonic approximation after expanding the potential energy are called anharmonic terms. Inclusion of these terms does not just improve the calculations with the harmonic approximation. There are some properties that are entirely due to these anharmonic terms. The most striking one is the thermal expansion. In the harmonic approximation the average distance between the atoms or molecules does not change with temperature. Another striking property that is due to the anharmonicity is the conductivity of heat. In the harmonic approximation the thermal conductivity is infinite. The finite thermal conductivity is caused by so-called umklapp processes which cannot occur when there are only harmonic terms. Other phenomena due to the anharmonic terms are the failure of the specific heat to approach the Dulong-Petit value at high temperatures, the width of the peaks in spectra, the difference of isothermal and adiabatic properties, the difference between the specific heat at constant pressure and at constant volume, the occurrence of second sound, and the dependence of the positions of the peaks in spectra on the volume.

Anharmonics terms are thus very important. Unfortunately, it is by no means clear how to include them in the calculations. Because the harmonic approximation is simple and yet very powerful, many attempts have been made to extend the harmonic approximation so that the anharmonic terms can be included (see page 36 ff.). However, for many crystals these improvements of the harmonic approximation have met with failure when the amplitudes of the vibrations of the atoms or molecules became too large.

We have developed an altogether different approach, which is inspired by the standard methods of quantum chemistry. We use two methods (see page 48 ff.). First we calculate the vibrations of one atom or molecule in the average field of the others, and then we calculate the collective vibrations. These two methods are called Mean Field theory and the Random Phase Approximation, respectively. Most of this thesis deals with these methods (all sections except 2.3 and 3.3).

3. Molecular crystals

Molecular crystals are built out of molecules (not atoms) that retain in the crystal almost the same properties that they have in the gas phase. As mentioned before, these molecules vibrate in the crystal. Strictly speaking also the atoms in a molecule vibrate with respect to each other. However, as the forces that hold the atoms in a molecule together are much stronger than the forces that hold the molecules together in the crystal, the intramolecular vibrations have a much higher frequency than the intermolecular vibrations. These two types of vibrations are thus well separated, and can often be treated independently. As this thesis deals only with the intermolecular vibrations we treat the molecules as rigid units. This is called the rigid molecule approximation.

Because molecules are not spherically symmetric they can perform two types of motions. We can distinguish a translational motion, in which the orientation does not change, and a rotation in which the position of the centre of gravity does not change. The translational vibrations have been studied for many years and are well understood. In most cases the harmonic approximation gives a good description of these vibrations, or at least a good starting point for including anharmonic corrections by perturbation theory. The second type of motion is called a libration when the molecule has a well-defined equilibrium orientation. Librations are still poorly understood, the main reason being that for them the harmonic approximation and its extensions yield bad results. The librations often have a large amplitude and many terms in the Taylor series of the potential energy should be included in the calculations. It is not unusual that there is no preferred orientation for a molecule, and that the molecules rotate in the crystal. Then we call the crystal "plastic" or "orientationally disordered". In that case the harmonic approximation cannot be used at all.

4. Solid nitrogen and solid oxygen

There are various ways (phases), depending on the temperature and the

pressure, in which molecules assemble to form crystals. In this thesis three phases of solid nitrogen (α-, β-, and γ-N_2), and two phases of solid oxygen (α- and β-N_2) are studied. One of the reasons why we decided to study these crystals is that one needs a good intermolecular potential for the calculations; i.e. one needs to know in detail how molecules attract and repel each other. Such intermolecular potentials are often derived from experiments. However, always a certain model is used in the interpretation of an experiment. Errors due to the approximations made in this model might give an inaccurate intermolecular potential. If the results of calculations deviate from (other) experimental data, it is difficult to know whether this is due to the inaccuracy of the potential or to the approximations in the model. Therefore, it is an advantage if an intermolecular potential is available that has been obtained in a different way. The potentials which are used in this thesis are obtained by state-of-the-art quantum chemical calculations. As the results of the calculations in this thesis will show, these potentials are quite accurate.

The low temperature phases α- and γ-N_2 are both ordered crystals. Especially the α-phase has been studied exhaustively. It has been used as a test for many theories on anharmonicity. The β-phase of solid nitrogen is an orientationally disordered phase. As will be shown the dynamics of such a phase can be quite complex and β-N_2 is by no means just an array of molecules rotating independently of each other. Although it can be studied experimentally as easily as α-N_2, it is much less well understood.

In the lattice dynamics of solid oxygen there are many puzzles. The α- and β-phases are ordered phases, but they are more complex than normal ordered crystals because of magnetic interactions between the molecules. Besides a spatial structure they have also a magnetic structure. With this magnetic structure corresponds a new type of dynamics, i.e. the so-called spin wave dynamics. What makes these crystals complicated is that the spin waves couple to the librations and the translational vibrations. Little is known about this coupling. For β-O_2, the magnetic structure is not even resolved unequivocally. These problems are taken up in this theses and solutions are given which lead to some very remarkable results.

5. This thesis

Chapter 1 provides a survey of the theory of lattice dynamics. Various forms of intermolecular potentials are discussed, and the Hamiltonian of the crystal is introduced. The harmonic approximation is described and two extensions, a perturbation theory and the self-consistent phonon method,

are presented. Molecular Dynamics and Monte Carlo methods are presented in a paragraph on large amplitude motions. In that paragraph also the methods we have developed for lattice dynamics calculations, the Mean Field theory and the Random Phase Approximation, are described. This chapter can be used by someone requiring a general introduction in the lattice dynamics of molecular crystals. Some of the results of the calculations on nitrogen and oxygen are presented in this chapter as well.

In chapter 2 and 3 the results of the calculations on solid nitrogen and solid oxygen are presented and discussed. Comparisons are made with experimental results and other calculations. The Mean Field theory and the Random Phase Approximation are treated in detail. Also some methods are presented that have not been mentioned in chapter 1 (see sections 2.3, 2.5, 3.2, and 3.3). These methods have been developed and used to handle some specific problems.

Chapter 1
General Theory

Dynamics of Molecular Crystals

W. J. BRIELS,* A. P J. JANSEN, and A VAN DER AVOIRD

Institute of Theoretical Chemistry
University of Nijmegen
6525 ED Nijmegen, The Netherlands

I. Introduction

Molecular crystals are solids in which the atoms group together in well-defined stable entities arranged in some periodic way In general, these entities can be molecules or molecular ions, but in this paper we mainly restrict ourselves to crystals built from neutral molecules. The binding forces keeping the atoms together in the molecules are much

* Present address Van't Hoff Laboratorium voor Fysische–en Colloïdchemie, 3584 CH Utrecht, The Netherlands

ADVANCES IN QUANTUM CHEMISTRY, VOLUME 18

stronger than the van der Waals forces that cause the condensation of the molecules in the crystal. As a consequence, the atoms in the solid take part in two types of motions that, to a good approximation, can be assumed to be uncoupled. First, they perform rapid oscillations around instantaneous positions in such a way as to keep the positions, orientations, and geometries of the molecules nearly unchanged. These motions are called intramolecular vibrations. In the solid, when their frequencies are slightly shifted by the crystal field and they are very weakly coupled, they are called vibrons. Second, the equilibrium positions of the atoms undergo displacements that are such that they amount to translations and rotations of the molecules as a whole. These motions, the intermolecular vibrations, usually called lattice vibrations, are much slower than the intramolecular vibrations, and they are the subject of this paper.

Because we are dealing with molecules, two types of lattice vibrations can be distinguished: translational and rotational. In order to describe these motions we have to know the potential energy of the crystal, expressed as a function of the center of mass positions and the orientations of all molecules. In Section II, we give a fairly detailed description of the different ways in which the potential can be expressed, each way having its own merits, depending on the subsequent calculations in which it has to be used.

Depending on the character of the molecular motions, one can distinguish several physical situations. In most cases, the molecules are trapped in relatively deep potential wells. Then, they perform small translational and orientational oscillations around well-defined equilibrium positions and orientations. Such motions are reasonably well described by the harmonic approximation. The collective vibrational excitations of the crystal, which are considered as a set of harmonic oscillators, are called phonons. Those phonons that represent pure angular oscillations, or librations, are called librons. For some properties it turns out to be necessary to look at the effects of anharmonicities. Anharmonic corrections to the harmonic model can be made by perturbation theory or by the self-consistent phonon method. These methods, which are summarized in Section III under the name quasi-harmonic theories, can be considered to be the standard tools in lattice dynamics calculations, in addition to the harmonic model. They are only applicable in the case of fairly small amplitude motions. Only the simple harmonic approximation is widely used; the calculation of anharmonic corrections is often hard in practice. For detailed descriptions of these methods, we refer the reader to the books and reviews by Maradudin *et al.* (1968, 1971, 1974), Cochran and Cowley (1967), Barron and Klein (1974), Birman (1974), Wallace (1972), and Califano *et al.* (1981).

A second situation occurs when the molecules perform angular oscillations, usually with large amplitudes, around one of a set of equilibrium orientations and randomly jump from one orientation to the other. Sometimes the librations are so violent that the molecules perform more or less hindered rotations. An extreme case is solid hydrogen, at normal pressure, in which the free-molecule rotations are only weakly perturbed and one speaks of rotons instead of librons. In all these cases the molecular crystal is called orientationally disordered or plastic, in contrast with the ordered or localized crystals discussed in the preceding paragraph. The only standard method to deal with this type of molecular motion is the mean field or (time-independent) Hartree approximation. By using the mean-field single-particle states as a basis, the collective motions of all molecules in the crystal can be described via the random phase approximation or time-dependent Hartree method. These methods are outlined in Section IV. Mostly the centers of mass of the molecules are thought of as being fixed. This approximation will rarely be justified in practice, however. Most molecular crystals are rather closely packed, which forces the molecules to separate before they can substantially change their orientations. As a result, there will be considerable coupling between the translational vibrations of the molecules and their rotational motions and mixing of the translational phonons and librons. The effects of such coupling on the properties of molecular crystals have been discussed by Michel and co-workers (Michel and Naudts, 1978; de Raedt *et al.*, 1981; Michel, 1984), and by Raich *et al.* (1983) and illustrated by semiempirical model calculations. A way to deal with this coupling via the time-dependent Hartree method has been proposed by ourselves (Briels *et al.*, 1984). This extension of the theory is included in Section IV.

All the lattice dynamics methods that we have just mentioned neglect the exchange of identical molecules. The mean-field method, for instance, is based on the Hartree approximation rather than on the Hartree–Fock model. This concerns, of course, the exchange of identical nuclei, since we are dealing with the nuclear motions and the effects of electron exchange are already contained in the intermolecular potential used. In practically all cases, even for the lightest nuclei, the nuclear wave functions have negligible overlap and the exchange effects may be safely omitted.

Let us now discuss to what extent the lattice vibrations are important for the macroscopic properties of molecular crystals. First of all, we have to consider the zero-point vibrations, i.e., the energy difference between the quantum-mechanical ground state of the system and the minimum of its potential energy. Since the van der Waals interactions among the molecules are rather weak, their zero-point motions affect the cohesion

energy of the crystal to a nonnegligible extent. Second, the characteristic excitation energies of the lattice vibrations are of the same order of magnitude as $k_B T$ (k_B being the Boltzmann constant) in most experimental circumstances. The excited states are populated and thus contribute to the properties of the system. Their effective contributions are strongly dependent on the size of the excitation energies and may vary considerably from one system to the other. As an illustration, let us briefly discuss the phase transition between the ordered and disordered modifications that often exist for the same material. Usually the ordered phase is thermodynamically stable at low temperatures, the plastic phase at high temperatures. The stability of the ordered phase is mainly due to the packing of the molecules in such a manner that the ground-state energy of the system is as low as possible. The stability of the disordered phase at high temperature is caused by its excitation energies, which are typically those of hindered rotors, being much lower than the excitation energies of the ordered phase, which are more like those of harmonic oscillators. Consequently, the excited states in the plastic phase will be more populated, its entropy will be larger, and its free energy ($A = E - TS$) will be lower at high temperature. It will be clear from this example that in order to give a reasonable account of any phase transition, one must accurately calculate the ground state and the excitation energies of the phases involved. The comparison between the calculated and observed phase transition temperatures and pressures yields a sensitive test, both for the potential and for the method used to describe the lattice dynamics.

In most cases, the crystal potential is not known *a priori*. The usual procedure is to introduce some model potential containing several parameters, which are subsequently found by fitting the calculated crystal properties to the observed data available. This procedure has the drawback that the empirical potential thus obtained includes the effects of the approximations made in the lattice dynamics model, which is mostly the harmonic model. It is very useful to have independent and detailed information about the potential from quantum-chemical *ab initio* calculations. Such information is available for nitrogen (Berns and van der Avoird, 1980) and oxygen (Wormer and van der Avoird, 1984), and we have chosen the results calculated for solid nitrogen and solid oxygen to illustrate in Sections V and VI, respectively, the lattice dynamics methods described in Sections III and IV. Nitrogen is the simplest typical molecular crystal;* as such it has received much attention from theorists and

* Hydrogen is even simpler, but solid hydrogen is very atypical. Because of the large splitting between the rotational states of the free H_2 molecule and the weak anisotropy of the H_2–H_2 interaction potential, the free molecule rotations are nearly unperturbed in the solid. This system has been extensively discussed by van Kranendonk (1983).

experimentalists and many data have been collected. It has several phases, ordered as well as disordered. Oxygen is especially interesting because it combines the properties of a molecular crystal with those of a magnetic material. It exhibits both structural and magnetic order–disorder phase transitions.

II. Intermolecular Interactions and the Crystal Hamiltonian

In the Born–Oppenheimer approximation the potential energy of a molecular crystal depends on the internal and external degrees of freedom of all molecules. As mentioned before, it is a very good approximation in most cases to separate the intramolecular vibrations from the center of mass vibrations and rotations of the molecules, i.e., the lattice vibrations. Then one can average the potential energy over the vibrational wave functions of the molecules and obtain the effective potential for the lattice vibrations. If one wishes to obtain this effective intermolecular potential by calculation, it is a good approximation to use the vibrationally averaged molecular geometries from theory or experiment. The (average) geometry of the molecules in the crystal is usually not very different from the free-molecule geometry.

A further approximation, which is applied in almost all practical treatments, is to write the intermolecular potential for the crystal as a sum over molecular pair potentials. For van der Waals solids—in which the electrostatic interactions, the exchange repulsion, and the London dispersion attraction are the main contributors to the potential—this is fairly well justified. However, when the molecules have large dipole moments (in ice, for example) or even more so in ionic crystals, the induction (multipole-induced multipole) interactions become substantial, and the three-body interaction energy will be comparable in size to the pair energy. This is because one has to add pairwise the polarizing electric fields from all neighbors in order to calculate the polarization energy of a given molecule that is quadratic in the field strength. Moreover, one has to take into account self-consistently the mutual interactions among the induced dipole moments. In the present paper, we focus on molecules with relatively small dipole moments, for which we estimate the exchange, induction, and dispersion three-and-more-body contributions to be not larger than about 10% of the pair potential (van der Avoird *et al.*, 1980), and we further neglect these deviations from pairwise additivity.

In order to be useful in crystal dynamics calculations, the intermolecular potential must be represented in a manageable, preferably analytic, form. The form chosen to express the potential will depend on the type of application. If, for example, the intermolecular potential is to be deduced

from the agreement between calculated and observed crystal properties, it is important to have a representation that is as simple as possible, depending only on a few parameters. The same requirement has to be fulfilled when during the calculation the numerical value of the intermolecular potential is needed many times, for instance, in classical molecular dynamics or Monte Carlo simulations. For such purposes a representation in terms of atom–atom interaction potentials is convenient. On the other hand, if one intends to make statistical mechanics calculations with an "*ab initio*" potential without loosing too much accuracy, an expansion of the potential in terms of orthogonal symmetry-adapted functions is suitable. In the sequel, we briefly describe in Section II,A the atom–atom potential model, in Section II,B the representation of the potential in terms of symmetry-adapted functions, and in Section II,C the relation between the two formalisms. Finally, in Section II,D we discuss the full crystal Hamiltonian.

A. Atom–Atom Potentials

The concept of an atom–atom potential (Kitaigorodsky, 1973) is based on the idea that the interaction potential between two molecules P and P' can be approximated by pairwise additive interactions between the constituent atoms, $\alpha \in P$ and $\beta \in P'$, which, in practice, are nearly always taken to be isotropic, i.e., dependent only on the interatomic distances $r_{\alpha\beta}$:

$$V_{PP'} = \sum_{\alpha \in P} \sum_{\beta \in P'} v^{X_\alpha X_\beta}(r_{\alpha\beta}) \tag{1}$$

The labels X_α and X_β denote the types of the atoms α and β. Popular forms for the atom–atom potentials are the Lennard–Jones 12–6 form

$$v^{X_\alpha X_\beta}(r_{\alpha\beta}) = A^{X_\alpha X_\beta} r_{\alpha\beta}^{-12} - B^{X_\alpha X_\beta} r_{\alpha\beta}^{-6} \tag{2}$$

and the Buckingham exp −6 or exp −6−1 form

$$v^{X_\alpha X_\beta}(r_{\alpha\beta}) = A^{X_\alpha X_\beta} \exp(-B^{X_\alpha X_\beta} r_{\alpha\beta}) - C^{X_\alpha X_\beta} r_{\alpha\beta}^{-6} (+ q^{X_\alpha} q^{X_\beta} r_{\alpha\beta}^{-1}) \tag{3}$$

The first term always represents the exchange repulsion and the second term the London dispersion attraction. The Coulomb term is sometimes added in order to represent the electrostatic interactions among molecules, with fractional atomic point charges q^{X_α} and q^{X_β} used. Alternatively, one has included these electrostatic contributions by adding the leading molecular multipole–multipole interaction term to an atom–atom potential of 12–6 or exp −6 type.

The interaction parameters $A^{X_\alpha X_\beta}$, $B^{X_\alpha X_\beta}$, $C^{X_\alpha X_\beta}$, and q^{X_α} are mostly obtained by fitting calculated crystal properties to experimental data. The quality of the resulting empirical potentials is rather uncertain, however,

since the fit will try to compensate for the inaccuracies in the dynamical model used and in the atom–atom model itself. Moreover, the different parameters are often strongly correlated. This implies that such empirical potentials are usually not very effective in predicting properties other than those to which they have been fitted.

In some cases (see van der Avoird *et al.*, 1980, and references therein) atom–atom potentials, which are subsequently used to calculate crystal properties, have been obtained from an independent source, viz., from *ab initio* quantum-chemical calculations. The individual terms in an atom–atom potential of the form in Eq. (3), for example, are then fitted to the corresponding interaction energy contributions calculated for a more or less extensive set of geometries of a molecular pair. It appears that the Buckingham form (in Eq. 3) especially can yield a reasonably accurate representation of an *ab initio* calculated potential, provided that the individual terms are given different force centers (sites) whose positions are shifted away from the atomic nuclei and optimized in fitting the *ab initio* data.

It is convenient for further use to summarize the various atom–atom potentials as given in Eqs. (2) and (3) in the single formula

$$v^{X_\alpha X_\beta}(r_{\alpha\beta}) = \sum_{n,\exp} A^{X_\alpha X_\beta}_{n/\exp} f^{(n/\exp)}(r_{\alpha\beta}) \tag{4}$$

with parameters $A_n^{X_\alpha X_\beta}$, $A_{\exp}^{X_\alpha X_\beta}$ and distance functions $f^{(n)}(r_{\alpha\beta}) = r_{\alpha\beta}^{-n}$ (e.g., $n = 12, 6, 1$) and $f^{(\exp)}(r_{\alpha\beta}) = \exp(-B^{X_\alpha X_\beta} r_{\alpha\beta})$.

B. Intermolecular Potential in Terms of Symmetry-Adapted Functions

In order to describe the orientation of a given molecule we attach a rectangular coordinate frame M to it and specify the Euler angles $\omega = \{\alpha, \beta, \gamma\}$ of this frame relative to a fixed global frame G. The position vector of the center of mass of the molecule is denoted by $\mathbf{r}$. The potential between two molecules at $\mathbf{r}_P$ and $\mathbf{r}_{P'}$, respectively, can then be expanded (Steele, 1963; Yasuda and Yamamoto, 1971; Egelstaff, Gray and Gubbins, 1975; van der Avoird *et al.*, 1980; Briels, 1980) in a complete set of functions of the variables ω_P, $\omega_{P'}$, and $\hat{r}_{PP'}$, where $\hat{r}_{PP'}$ is the unit vector in the direction of $\mathbf{r}_{PP'} = \mathbf{r}_{P'} - \mathbf{r}_P$. The coefficients of the expansion depend on $r_{PP'}$, the length of $\mathbf{r}_{PP'}$. As a basis for the expansion we use the products

$$D^{(l_1)}_{n_1 m_1}(\omega_P) D^{(l_2)}_{n_2 m_2}(\omega_{P'}) C^{(l_3)}_{m_3}(\hat{r}_{PP'})$$

where the $D^{(l)}_{nm}(\omega)$ are Wigner functions and $C^{(l)}_m(\hat{r})$ is a Racah spherical harmonic. For these functions as well as for the Euler angles, we use the definitions of Edmonds (1957). This expansion can be greatly simplified if we exploit the full symmetry of the molecular pair.

In order to incorporate the symmetry requirements into our expansion, we need the transformation properties of the Wigner functions, both with respect to rotations $R^{G}(\omega)$ of the global frame and with respect to rotations $R^{M}(\omega)$ of the molecular frames. If we rotate the global frame through the Euler angles $\tilde{\omega}$, then a scalar quantity that was described in the original frame by a function F will be described in the new frame by $R^{G}(\tilde{\omega})F$; the two functions are related by $R^{G}(\tilde{\omega})F(\omega) = F(\omega')$, where ω and ω' are the Euler angles of the molecular frame relative to the new and old global frames, respectively. Similarly, if we rotate a molecular frame through the Euler angles $\tilde{\omega}$, F will transform into $R^{M}(\tilde{\omega})F$. With the conventions that we have adopted, the transformed Wigner functions are given by

$$R^{G}(\tilde{\omega})D^{(l)}_{nm}(\omega) = \sum_{m'} D^{(l)}_{nm'}(\omega)D^{(l)}_{m'm}(\tilde{\omega}) \tag{5}$$

$$R^{M}(\tilde{\omega})D^{(l)}_{nm}(\omega) = \sum_{n'} D^{(l)}_{n'm}(\omega)D^{(l)}_{n'n}(\tilde{\omega}) \tag{6}$$

The well-known transformation properties of the Racah spherical harmonics can be obtained from the relation

$$C^{(l)}_{m}(\hat{r}) = C^{(l)}_{m}(\theta, \phi) = D^{(l)}_{0m}(\phi, \theta, 0) \tag{7}$$

and Eq. (5):

$$R^{G}(\tilde{\omega})C^{(l)}_{m}(\hat{r}) = \sum_{m'} C^{(l)}_{m'}(\hat{r})D^{(l)}_{m'm}(\tilde{\omega}) \tag{8}$$

The expression for the intermolecular potential must satisfy two symmetry requirements. First, it must be invariant if we rotate the molecular frame of either of the two molecules through specific Euler angles $\tilde{\omega}_g$ that correspond with a symmetry element of the molecule in question. This means that our basis must be invariant under rotations of the outer direct product group $G_P \otimes G_{P'}$, where G_P is the symmetry group of molecule P and $G_{P'}$ that of molecule P'. Acting with the projection operator of the totally symmetric irreducible representation of the group G_P (of order $\#G_P$),

$$P = \frac{1}{\#G_P} \sum_{g \in G_P} R^{M}(\tilde{\omega}_g) \tag{9}$$

on the Wigner functions, and using Eq. (6), we construct linear combinations

$$G^{(l)}_{m}(\omega_P) = \sum_{n} A^{(l)}_{n} D^{(l)}_{nm}(\omega_P) \tag{10}$$

which are invariant under the group G_P. We choose as the expansion basis the set of all products:

$$G^{(l_1)}_{m_1}(\omega_P)G^{(l_2)}_{m_2}(\omega_{P'})C^{(l_3)}_{m_3}(\hat{r}_{PP'}). \tag{11}$$

It may happen that for certain values of l more than one totally symmetric combination (10) may exist. In that case, the l index should be understood as a composite label. As an example, we list in Table I, for values of l up to 10, the tetrahedral rotation functions that transform according to the totally symmetric representation of the tetrahedral group T. These functions are normalized such that

$$(8\pi^2)^{-1}\int d\omega\; T^{(l_1)}_{m_1}(\omega)^* T^{(l_2)}_{m_2}(\omega) = \delta_{l_1 l_2}\,\delta_{m_1 m_2}(2l_1 + 1)^{-1}$$

The coefficients $A^{(l)}_n$ in these functions depend on the way in which the molecular coordinate frame is fixed on the molecule, for which we use the standard convention in this example (see Table I).

TABLE I

TETRAHEDRAL ROTATION FUNCTIONS[a]

l	Function
0	$T^{(0)}_0 = D^{(0)}_{00}$
3	$T^{(3)}_m = -\frac{1}{2}i(2)^{1/2}\{D^{(3)}_{2m} - D^{(3)}_{-2m}\}$
4	$T^{(4)}_m = \frac{1}{2}(\frac{7}{3})^{1/2}\{D^{(4)}_{0m} + (\frac{5}{14})^{1/2}(D^{(4)}_{4m} + D^{(4)}_{-4m})\}$
6	$T^{(6)}_m = \frac{1}{4}(2)^{1/2}\{D^{(6)}_{0m} - (\frac{7}{2})^{1/2}(D^{(6)}_{4m} + D^{(6)}_{-4m})\}$
	$T^{(6)}_m = \frac{1}{4}(\frac{11}{2})^{1/2}\{(D^{(6)}_{2m} + D^{(6)}_{-2m}) - (\frac{5}{11})^{1/2}(D^{(6)}_{6m} + D^{(6)}_{-6m})\}$
7	$T^{(7)}_m = -\frac{1}{4}i(\frac{13}{3})^{1/2}\{(D^{(7)}_{2m} - D^{(7)}_{-2m}) + (\frac{11}{13})^{1/2}(D^{(7)}_{6m} - D^{(7)}_{-6m})\}$
8	$T^{(8)}_m = \frac{1}{8}(33)^{1/2}\{D^{(8)}_{0m} + (\frac{14}{99})^{1/2}(D^{(8)}_{4m} + D^{(8)}_{-4m}) + (\frac{65}{198})^{1/2}(D^{(8)}_{8m} + D^{(8)}_{-8m})\}$
9	$T^{(9)}_m = -\frac{1}{4}i(\frac{3}{2})^{1/2}\{(D^{(9)}_{2m} - D^{(9)}_{-2m}) - (\frac{13}{3})^{1/2}(D^{(9)}_{6m} - D^{(9)}_{-6m})\}$
	$T^{(9)}_m = -\frac{1}{4}i(\frac{17}{3})^{1/2}\{(D^{(9)}_{4m} - D^{(9)}_{-4m}) - (\frac{7}{17})^{1/2}(D^{(9)}_{8m} - D^{(9)}_{-8m})\}$
10	$T^{(10)}_m = \frac{1}{8}(\frac{65}{6})^{1/2}\{D^{(10)}_{0m} - (\frac{66}{65})^{1/2}(D^{(10)}_{4m} + D^{(10)}_{-4m}) - (\frac{187}{130})^{1/2}(D^{(10)}_{8m} + D^{(10)}_{-8m})\}$
	$T^{(10)}_m = \frac{1}{16}(\frac{247}{3})^{1/2}\{(D^{(10)}_{2m} + D^{(10)}_{-2m}) + (\frac{1}{26})^{1/2}(D^{(10)}_{6m} + D^{(10)}_{-6m}) - (\frac{255}{494})^{1/2}(D^{(10)}_{10m} + D^{(10)}_{-10m})\}$

[a] The z axis of the molecule fixed system is a two-fold axis; the [1, 1, 1] axis is a threefold axis.

The second symmetry requirement that the expression for the intermolecular potential has to meet is that it must be invariant under any rotation of the global coordinate frame. The transformation properties of the symmetry-adapted functions $G_m^{(l)}(\omega)$ under such a rotation are easily obtained from Eqs. (10) and (5):

$$R^G(\tilde{\omega})G_m^{(l)}(\omega) = \sum_{m'} G_{m'}^{(l)}(\omega)D_{m'm}^{(l)}(\tilde{\omega}) \tag{12}$$

We now construct the invariant basis in which we shall expand the intermolecular potential by acting on the products (11) with the projection operator

$$(8\pi^2)^{-1}\int d\tilde{\omega}\, R^G(\tilde{\omega}) \tag{13}$$

using the transformation formulas (8) and (12) and the relation

$$(8\pi^2)^{-1}\int d\tilde{\omega}\, D_{m_1'm_1}^{(l_1)}(\tilde{\omega})D_{m_2'm_2}^{(l_2)}(\tilde{\omega})D_{m_3'm_3}^{(l_3)}(\tilde{\omega}) = \begin{pmatrix} l_1 & l_2 & l_3 \\ m_1' & m_2' & m_3' \end{pmatrix}\begin{pmatrix} l_2 & l_2 & l_3 \\ m_1 & m_2 & m_3 \end{pmatrix} \tag{14}$$

The symbols on the right-hand side are 3–j coefficients.

The expansion of the intermolecular potential then reads

$$V(\omega_P, \omega_{P'}, \mathbf{r}_{PP'}) = \sum_{\mathbf{l}} v_{\mathbf{l}}(r_{PP'}) \sum_{\mathbf{m}} \begin{pmatrix} l_1 & l_2 & l_3 \\ m_1 & m_2 & m_3 \end{pmatrix} \times G_{m_1}^{(l_1)}(\omega_P)G_{m_2}^{(l_2)}(\omega_{P'})C_{m_3}^{(l_3)}(\hat{r}_{PP'}) \tag{15}$$

The summation labels are defined as $\mathbf{l} = \{l_1, l_2, l_3\}$ and $\mathbf{m} = \{m_1, m_2, m_3\}$. We note again that for certain values of l_1 and l_2 more than one symmetry-adapted function $G_m^{(l)}$ exists and that in this case $\Sigma_{\mathbf{l}}$ includes all these functions.

From Eq. (15) we observe that the intermolecular potential is completely specified by the coefficients $v_{\mathbf{l}}(r_{PP'})$. These expansion coefficients can be obtained in various ways. If the intermolecular potential is given in terms of atom–atom potentials, it is possible to obtain explicit expressions for these coefficients (see Section II,C). If the long-range part of the potential is known from perturbation theory calculations in the multipole expansion, the expansion coefficients, after some angular momentum recoupling, can also be obtained from explicit formulas (see van der Avoird *et al.*, 1980). If the (short- and intermediate-range) potential is known

numerically from *ab initio* calculations for a grid of distances $r_{pp'}$ and molecular orientations ω_P and $\omega_{P'}$, the expansion coefficients can be found by numerical integration for each value of $r_{PP'}$:

$$v_{\mathbf{l}}(r_{PP'}) = (2l_1 + 1)(2l_2 + 1)(2l_3 + 1)(8\pi^2)^{-2} \times \int d\omega_P \int d\omega_{P'} \sum_{m} \begin{pmatrix} l_1 & l_2 & l_3 \\ m & -m & 0 \end{pmatrix} \times G_m^{(l_1)}(\omega_P)^* G_{-m}^{(l_2)}(\omega_{P'})^* V(\omega_P, \omega_{P'}, r_{PP'})$$

Here we have used the fact that one can always choose to perform the *ab initio* calculations on the pair PP' in a coordinate frame with the z axis along $\mathbf{r}_{PP'}$. Then we have $\hat{r}_{PP'} = (\theta, \phi) = (0, 0)$ and $C_m^{(l)}(\hat{r}_{PP'}) = \delta_{m0}$. The integral can be further simplified by noting that the internal geometry of any molecular pair can be specified by at most five Euler angles, so that one of the six angles ω_P, $\omega_{P'}$ can also be set to zero and left out of the integration. In special cases, even more simplifications can be made. For example, if the molecules P and P' are linear, two more Euler angles can be omitted. Once the coefficients $v_{\mathbf{l}}(r_{PP'})$ are calculated for several values of $r_{PP'}$, it is convenient to fit their $r_{PP'}$ dependence by means of simple analytic forms (r^{-n} in the long range, $\exp(-Br)$ in the short range). For further details of this procedure we refer to the review by van der Avoird *et al.* (1980) and the references therein.

Finally, we observe that, in principle, one may truncate the expansion (15) after a few terms and thus model the anisotropy of the potential (the term $\mathbf{l} = \{0, 0, 0\}$ is the isotropic part). Simple parameterized $r_{PP'}$ functions for the expansion coefficients $v_{\mathbf{l}}(r_{PP'})$ can then be introduced and the parameters can be fitted empirically. The latter procedure is similar to the empirical way of obtaining atom–atom model potentials and the same questions can be raised regarding the validity of the resulting potentials.

C. Expansion of Atom–Atom Potentials in Symmetry-Adapted Functions

In atom–atom potentials the anisotropy of the intermolecular potential, i.e., its dependence on the molecular orientations ω_P and $\omega_{P'}$, is implicitly determined by the model. One can make this dependence explicit by expanding a given atom–atom potential in the form (15). It has been demonstrated by Sack (1964), Yasuda and Yamamoto (1971), and Downs *et al.* (1979) that analytic expressions can be derived for the expansion coefficients $v_{\mathbf{l}}(r_{PP'})$ in (15) for atom–atom potentials (see Section II,A) with $f^{(n)}(r_{\alpha\beta}) = r_{\alpha\beta}^{-n}$ dependence and by Briels (1980) that they can be derived for atom–atom interactions with exponential dependence

$f^{(\exp)}(r_{\alpha\beta}) = \exp(-r_{\alpha\beta})$. In order to derive such expressions these authors use the two-center expansion of the functions:

$$f^{(n/\exp)}(r_{\alpha\beta}) = f^{(n/\exp)}(|\mathbf{r}_{PP'} - \mathbf{d}_\alpha + \mathbf{d}_\beta|)$$

where $\mathbf{d}_\alpha$ is the position vector of atom α relative to the center of mass of the molecule P to which it belongs and $\mathbf{d}_\beta$ is the same vector for atom β in molecule P'. The result is the formula (Briels, 1980):

$$f^{(n/\exp)}(r_{\alpha\beta}) = \sum_{\mathbf{l}} \begin{pmatrix} l_1 & l_2 & l_3 \\ 0 & 0 & 0 \end{pmatrix} g_{\mathbf{l}}^{(n/\exp)}(d_\alpha, d_\beta, r_{PP'}) \times \sum_{\mathbf{m}} \begin{pmatrix} l_1 & l_2 & l_3 \\ m_1 & m_2 & m_3 \end{pmatrix} C_{m_1}^{(l_1)}(\hat{d}_\alpha) C_{m_2}^{(l_2)}(\hat{d}_\beta) C_{m_3}^{(l_3)}(\hat{r}_{PP'}) \quad (16)$$

with

$$g_{\mathbf{l}}^{(1)}(d_\alpha, d_\beta, r_{PP'}) = \delta_{l_1+l_2,l_3}(-1)^{l_2}[\mathbf{l}] \frac{(2l_3)!}{(2l_1+1)!(2l_2+1)!} \frac{l_1! l_2!}{l_3!} \times \frac{1}{r_{PP'}} \left(\frac{d_\alpha}{r_{PP'}}\right)^{l_1} \left(\frac{d_\beta}{r_{PP'}}\right)^{l_2} \quad (17)$$

$$g_{\mathbf{l}}^{(n)}(d_\alpha, d_\beta, r_{PP'}) = (-1)^{l_2} \frac{[\mathbf{l}]}{(n-2)!} \left(\frac{1}{r_{PP'}}\right)^n \left(\frac{d_\alpha}{r_{PP'}}\right)^{l_1} \left(\frac{d_\beta}{r_{PP'}}\right)^{l_2} \times \sum_{m_1=0}^{\infty} \sum_{m_2=0}^{\infty} \left(\frac{d_\alpha}{r_{PP'}}\right)^{2m_1} \left(\frac{d_\beta}{r_{PP'}}\right)^{2m_2} \times \frac{(n-2+l_1+l_2-l_3+2m_1+2m_2)!}{(2l_1+2m_1+1)!!(2m_1)!!(2l_2+2m_2+1)!!(2m_2)!!} \times \frac{(n-2+l_1+l_2+l_3+2m_1+2m_2)!!}{(n-2+l_1+l_2-l_3+2m_1+2m_2)!!} \quad (18)$$

for $n \geq 2$, and

$$g_{\mathbf{l}}^{(\exp)}(d_\alpha, d_\beta, r_{PP'}) = (-1)^{l_2+1}[\mathbf{l}]\{(1+l_1+l_2+l_3) J_{l_1}(d_\alpha) J_{l_2}(d_\beta) K_{l_3}(r_{PP'}) + d_\alpha J_{l_1+1}(d_\alpha) J_{l_2}(d_\beta) K_{l_3}(r_{PP'}) + d_\beta J_{l_1}(d_\alpha) J_{l_2+1}(d_\beta) K_{l_3}(r_{PP'}) - r_{PP'} J_{l_1}(d_\alpha) J_{l_2}(d_\beta) K_{l_3+1}(r_{PP'})\} \quad (19)$$

We use the abbreviated notation $[\mathbf{l}] = (2l_1+1)(2l_2+1)(2l_3+1)$. The functions $J_l(z)$ and $K_l(z)$ are related to the modified spherical Bessel

functions (Antosiewicz, 1970) of the first and third kind, respectively, by $J_l(z) = (\pi/2z)^{1/2}J_{l+(1/2)}(z)$ and $(\pi/2)K_l(z) = (\pi/2z)^{1/2}K_{l+(1/2)}(z)$. It is interesting to notice that Eq. (19) is in closed form, whereas Eq. (18) contains an infinite sum.

Using the general expressions (1) with (4) for an atom–atom model and substituting the two-center expansion (16), we write the intermolecular atom–atom potential as

$$V_{PP'} = V(\omega_P, \omega_{P'}, \mathbf{r}_{PP'}) = \sum_{\mathbf{l}} \begin{pmatrix} l_1 & l_2 & l_3 \\ 0 & 0 & 0 \end{pmatrix} \sum_{a\in P} \sum_{b\in P'} \times \sum_{n,\exp} A_{n/\exp}^{X_a X_b} g_{\mathbf{l}}^{(n/\exp)}(d_a, d_b, r_{PP'}) \times \sum_{\mathbf{m}} \begin{pmatrix} l_1 & l_2 & l_3 \\ m_1 & m_2 & m_3 \end{pmatrix} \left\{ \sum_{\alpha\in a} C_{m_1}^{(l_1)}(\hat{d}_\alpha) \right\} \times \left\{ \sum_{\beta\in b} C_{m_2}^{(l_2)}(\hat{d}_\beta) \right\} C_{m_3}^{(l_3)}(\hat{r}_{PP'}) \tag{20}$$

Here we have partitioned the sums over all atoms α and β in the molecules P and P' in the following manner. First, we sum over equivalent atoms within the same class $\alpha \in a$ and $\beta \in b$, which have the same chemical nature $X_\alpha = X_a$ and $X_\beta = X_b$ and the same distance $d_\alpha = d_a$ and $d_\beta = d_b$ to the respective molecular center of mass. Next, we sum over classes $a \in P$ and $b \in P'$. The orientations $\hat{d}_\alpha$ and $\hat{d}_\beta$ of the position vectors of the atoms $\mathbf{d}_\alpha$ and $\mathbf{d}_\beta$, relative to the molecular centers of mass, are still given with respect to the global coordinate frame. If we denote the polar angles of $\mathbf{d}_\alpha$ and $\mathbf{d}_\beta$ in the molecule fixed frames by $\hat{d}_\alpha^0$ and $\hat{d}_\beta^0$ and remember that the molecular frames are related to the global frame by rotations through the Euler angles ω_P and $\omega_{P'}$, respectively, we find that

$$\sum_{\alpha\in a} C_{m_1}^{(l_1)}(\hat{d}_\alpha) = \sum_{n_1} \left\{ \sum_{\alpha\in a} C_{n_1}^{(l_1)}(\hat{d}_\alpha^0) \right\} D_{n_1 m_1}^{(l_1)}(\omega_P) = k_a^{(l_1)} G_{m_1}^{(l_1)}(\omega_P) \tag{21}$$

and a similar expression for atoms $\beta \in b \in P'$. The latter equality, which is related to Eq. (10), follows from the fact that the left-hand side must be invariant under all rotations of the molecular point group G_P; these rotations just interchange the equivalent atoms $\alpha \in a$. Introducing Eq. (21) and the corresponding result for atoms $\beta \in b$ into Eq. (20), the general atom–atom potential is expressed in the form of Eq. (15), with

$$v_l(r_{PP'}) = \begin{pmatrix} l_1 & l_2 & l_3 \\ 0 & 0 & 0 \end{pmatrix} \sum_{a \in P} \sum_{b \in P'} k_a^{(l_1)} k_b^{(l_2)} \sum_{n,\exp} A_{n/\exp}^{x_a x_b} \times g_l^{(n/\exp)}(d_a, d_b, r_{PP'}) \tag{22}$$

D. The Crystal Hamiltonian

Now that we have expressed the intermolecular potential, it is easy to write down the crystal Hamiltonian. We associate with each point $P = \{\mathbf{n}, i\}$ of the lattice a molecule with position vector $\mathbf{r}_P = \mathbf{R}_P + \mathbf{u}_P$. The vector $\mathbf{R}_P$ denotes the position of the lattice point P, i.e., $\mathbf{R}_P = \mathbf{R}_\mathbf{n} + \mathbf{R}_i$ with $\mathbf{R}_\mathbf{n}$ being the position vector of the origin of the unit cell to which P belongs and $\mathbf{R}_i$ the position vector of P relative to this origin. The displacement vector $\mathbf{u}_P$ describes the position of the center of mass of the molecule at P relative to the lattice point P. The Hamiltonian then reads

$$H = \sum_P \{T(\mathbf{u}_P) + L(\omega_P)\} + \frac{1}{2} \sum_{P \neq P'} \sum V_{PP'}(\mathbf{u}_P, \omega_P; \mathbf{u}_{P'}, \omega_{P'}) \tag{23}$$

where

$$V_{PP'}(\mathbf{u}_P, \omega_P; \mathbf{u}_{P'}, \omega_{P'}) = V(\omega_P, \omega_{P'}, \mathbf{r}_{PP'}) \tag{24}$$

In the latter equation $\mathbf{r}_{PP'} = \mathbf{r}_{P'} - \mathbf{r}_P = \mathbf{R}_{P'} - \mathbf{R}_P + \mathbf{u}_{P'} - \mathbf{u}_P = \mathbf{R}_{PP'} + \mathbf{u}_{P'} - \mathbf{u}_P$, from which the dependence of $V_{PP'}$ on $\mathbf{u}_{P'}$ and $\mathbf{u}_P$ follows. In Eq. (23) the kinetic energy operators for the translational and rotational motions are defined, respectively, as

$$T(\mathbf{u}_P) = -\frac{\hbar^2}{2M} \Delta(\mathbf{u}_P) \tag{25}$$

$$L(\omega_P) = \frac{J_a^2(\omega_P)}{2I_a} + \frac{J_b^2(\omega_P)}{2I_b} + \frac{J_c^2(\omega_P)}{2I_c} \tag{26}$$

Here $\Delta(\mathbf{u}_P)$ is the Laplacian and J_a, J_b, and J_c are the components of the angular momentum operator with respect to the principal a, b, and c axes of the molecule; I_a, I_b, and I_c are the principal values of the molecular moment of inertia. For simplicity we have assumed that the crystal is composed of just one type of molecules. Otherwise, the molecular mass M and the moments of inertia have to carry the sublattice label i, appearing in $P = \{\mathbf{n}, i\}$.

The dependence of the potential $V_{PP'}$ on the translational degrees of freedom $\mathbf{u}_P$ is rather intricate, and in order to use this potential in lattice dynamics calculations, we have to rewrite it in more tractable form. Beforehand, we make some remarks concerning the case when only rotational motions are considered. This is useful when the rotation–transla-

tion coupling is weak, for instance, as in hydrogen or methane crystals, or, in general, at certain points of high symmetry in the Brillouin zone, where the rotation and translation modes are decoupled because of this symmetry. In these cases, the potential for the rotational problem is an effective potential in the sense that it can be obtained from the complete intermolecular potential by averaging over the translational motions. This effective potential can be written in the form of Eq. (15) with coefficients $\langle v_l(r_{PP'})\rangle = v_l(R_{PP'})$. The crystal Hamiltonian then reads

$$H = U^C + \sum_P \{L(\omega_P) + V_P(\omega_P)\} + \frac{1}{2}\sum_{P\neq P'}\sum \Phi_{PP'}(\omega_P, \omega_{P'}) \tag{27}$$

The two-body potential $\Phi_{PP'}$ consists of those terms that depend on the orientations of both molecules; i.e., $\Phi_{PP'}$ is equal to $V_{PP'}$ minus the terms, with one or both of l_1 and l_2 equal to zero. The terms with either l_1 or l_2 equal to zero are contained in V_P, which depends only on the orientation of molecule P, and the isotropic term $l_1 = l_2 = 0$ is just the constant U^C:

$$U^C = \frac{1}{2}\sum_{P\neq P'}\sum v_{0,0,0}(R_{PP'}) = \sum_P U_P \tag{28}$$

$$V_P(\omega_P) = \sum_{l,m}{}' V_m^{(l)}(P) G_m^{(l)}(\omega_P) \tag{29}$$

$$\Phi_{PP'}(\omega_P, \omega_{P'}) = \sum_{l_1,m_1}{}' \sum_{l_2,m_2}{}' G_{m_1}^{(l_1)}(\omega_P) X_{m_1,m_2}^{(l_1,l_2)}(P, P') G_{m_2}^{(l_2)}(\omega_{P'}) \tag{30}$$

with

$$\begin{aligned} V_m^{(l)}(P) &= (2l+1)^{-1/2}(-1)^l \frac{1}{2}\sum_{P'} \{v_{l,0,l}(R_{PP'}) C_m^{(l)}(\hat{R}_{PP'})^* \\ &\quad + v_{0,l,l}(R_{PP'}) C_m^{(l)}(-\hat{R}_{PP'})^*\} \\ &= (2l+1)^{-1/2}(-1)^l \sum_{P'} v_{l,0,l}(R_{PP'}) C_m^{(l)}(\hat{R}_{PP'})^* \end{aligned} \tag{31}$$

$$X_{m_1,m_2}^{(l_1,l_2)}(P, P') = \sum_{l_3,m_3} v_l(R_{PP'}) \begin{pmatrix} l_1 & l_2 & l_3 \\ m_1 & m_2 & m_3 \end{pmatrix} C_{m_3}^{(l_3)}(\hat{R}_{PP'}) \tag{32}$$

In Eq. (31) we have used the relation $v_{0,l,l}(R_{PP'}) = (-1)^l v_{l,0,l}(R_{PP'})$ (Briels, 1980). The primes on the summation signs indicate that the terms with $l = 0$ have to be omitted.

The term $V_P(\omega_P)$ in Eq. (27) is called the crystal field term. From Eqs. (29) and (31) it is clear that this term is invariant under all rotations of the global frame that correspond to symmetry operations on the lattice. As a

result $V_P(\omega_P)$ contains only linear combinations of the functions $G_m^{(l)}(\omega_P)$, which transform according to the totally symmetric representation of the site group S_P. Note that S_P contains all rotations around P that leave the point lattice invariant; this group is larger than the point group of the crystal, which is not yet defined as long as the equation of motion is not solved. The functions adapted to the site symmetry can be obtained by acting with the projection operator:

$$P_S = \frac{1}{\#S_P} \sum_{g \in S_P} R^G(\tilde{\omega}_g) \tag{33}$$

on the functions $G_m^{(l)}(\omega_P)$. In Table II we have given the results for the octahedral group $S_P = O$, which is the site group of all sites in the fcc lattice.

In order to obtain the explicit translational dependence of the complete intermolecular potential (15), we expand the translationally dependent part of Eq. (15) as a Taylor series in the displacement vectors $\mathbf{u}_P$ and $\mathbf{u}_{P'}$:

$$v_l(r_{PP'})C_{m_3}^{(l_3)}(\hat{r}_{PP'}) = \sum_{\alpha_1 \alpha_2} \frac{(-\mathbf{u}_P \cdot \nabla)^{\alpha_1}}{\alpha_1!} \frac{(\mathbf{u}_{P'} \cdot \nabla)^{\alpha_2}}{\alpha_2!} v_l(R_{PP'})C_{m_3}^{(l_3)}(\hat{R}_{PP'}) \tag{34}$$

In principle, the sums over α_1 and α_2 must be extended to infinity. In practice, we apply the truncation condition $\alpha_1 + \alpha_2 \leq \alpha_{\max}$. The terms with $\alpha_1 = \alpha_2 = 0$ give rise to the purely rotational part of the Hamiltonian, which we have just treated. The other terms can be most easily evaluated by applying the gradient formula in spherical tensor form (Edmonds, 1957):

$$\mathbf{u}_P \cdot \nabla F(R_{PP'})C_{m_3}^{(l_3)}(\hat{R}_{PP'}) = u_P \sum_{\lambda} A_{l_3\lambda}(R_{PP'})F(R_{PP'}) \times [C^{(1)}(\hat{u}_P) \otimes C^{(\lambda)}(\hat{R}_{PP'})]_{m_3}^{(l_3)} \tag{35}$$

where A_{lk} is an operator defined by

$$A_{lk}(R) = -\delta_{k,l-1}\left[\frac{l(2l-1)}{2l+1}\right]^{1/2}\left(\frac{d}{dR} + \frac{l+1}{R}\right) + \delta_{k,l+1}\left[\frac{(l+1)(2l+3)}{2l+1}\right]^{1/2}\left(\frac{d}{dR} - \frac{l}{R}\right) \tag{36}$$

The irreducible tensor product between the brackets represents the usual angular momentum coupling

$$[C^{(l_1)}(\hat{r}_1) \otimes C^{(l_2)}(\hat{r}_2)]^{(l_3)}_{m_3} = (-1)^{l_1+l_2-m_3} \sum_{m_1 m_2} \begin{pmatrix} l_1 & l_2 & l_3 \\ m_1 & m_2 & -m_3 \end{pmatrix} C^{(l_1)}_{m_1}(\hat{r}_1) C^{(l_2)}_{m_2}(\hat{r}_2) \quad (37)$$

between two tensors $\{C^{(l_1)}_{m_1}(\hat{r}_1); m_1 = -l_1, \ldots, l_1\}$ and $\{C^{(l_2)}_{m_2}(\hat{r}_2); m_2 = -l_2, \ldots, l_2\}$ to an irreducible tensor that transforms as $C^{(l_3)}_{m_3}$ under rotations of the global frame. Applying Eq. (35) repeatedly to Eq. (34), we find after some tedious algebra (Briels *et al.*, 1984)

$$v_{\mathbf{k}}(r_{PP'}) C^{(l_3)}_{m_3}(\hat{r}_{PP'}) = \sum_{\alpha_1,\alpha_2} \frac{(-u_P)^{\alpha_1}}{\alpha_1!} \frac{(u_{P'})^{\alpha_2}}{\alpha_2!} \times \sum_{\mathbf{k}} \sum_{j} {}^{j}W^{(\mathbf{l})}_{\mathbf{k}}(R_{PP'} \mid \alpha_1, \alpha_2) \times [[C^{(k_1)}(\hat{u}_P) \otimes C^{(k_2)}(\hat{u}_{P'})]^{(j)} \otimes C^{(k_3)}(\hat{R}_{PP'})]^{(l_3)}_{m_3} \quad (38)$$

TABLE II

TETRAHEDRAL ROTATION FUNCTIONS ADAPTED TO THE SITE GROUP O [SEE EQ. (33)][a]

l	Function
0	$O^{(0)}_T = T^{(0)}_0$
3	$O^{(3)}_T = -\frac{1}{2}i(2)^{1/2}\{T^{(3)}_2 - T^{(3)}_{-2}\}$
4	$O^{(4)}_T = \frac{1}{2}(\frac{7}{3})^{1/2}\{T^{(4)}_0 + (\frac{5}{14})^{1/2}(T^{(4)}_4 + T^{(4)}_{-4})\}$
6	$O^{(6)}_T = \frac{1}{4}(2)^{1/2}\{T^{(6)}_0 - (\frac{7}{2})^{1/2}(T^{(6)}_4 + T^{(6)}_{-4})\}$
	$O^{(6)}_T = \frac{1}{4}(\frac{11}{2})^{1/2}\{(T^{(6)}_2 + T^{(6)}_{-2}) - (\frac{5}{11})^{1/2}(T^{(6)}_6 + T^{(6)}_{-6})\}$
7	$O^{(7)}_T = -\frac{1}{4}i(\frac{13}{3})^{1/2}\{(T^{(7)}_2 - T^{(7)}_{-2}) + (\frac{11}{13})^{1/2}(T^{(7)}_6 - T^{(7)}_{-6})\}$
8	$O^{(8)}_T = \frac{1}{8}(33)^{1/2}\{T^{(8)}_0 + (\frac{14}{99})^{1/2}(T^{(8)}_4 + T^{(8)}_{-4}) + (\frac{65}{198})^{1/2}(T^{(8)}_8 + T^{(8)}_{-8})\}$
9	$O^{(9)}_T = -\frac{1}{4}i(\frac{3}{2})^{1/2}\{(T^{(9)}_2 - T^{(9)}_{-2}) - (\frac{13}{3})^{1/2}(T^{(9)}_6 - T^{(9)}_{-6})\}$
	$O^{(9)}_T = -\frac{1}{4}i(\frac{17}{3})^{1/2}\{(T^{(9)}_4 - T^{(9)}_{-4}) - (\frac{7}{17})^{1/2}(T^{(9)}_8 - T^{(9)}_{-8})\}$
10	$O^{(10)}_T = \frac{1}{8}(\frac{65}{6})^{1/2}\{T^{(10)}_0 - (\frac{66}{65})^{1/2}(T^{(10)}_4 + T^{(10)}_{-4}) - (\frac{187}{130})^{1/2}(T^{(10)}_8 + T^{(10)}_{-8})\}$
	$O^{(10)}_T = \frac{1}{16}(\frac{247}{3})^{1/2}\{(T^{(10)}_2 + T^{(10)}_{-2}) + (\frac{1}{26})^{1/2}(T^{(10)}_6 + T^{(10)}_{-6}) - (\frac{255}{494})^{1/2}(T^{(10)}_{10} + T^{(10)}_{-10})\}$

[a] Tetrahedral rotational functions as in Table I.
Site group: z-axis is 4-fold axis, [1, 1, 1] direction is 3-fold axis.

with the following recursion relation for the coefficients:

$$
\begin{aligned}
{}^{j}W^{\mathbf{l}}_{k_1,k_2,k_3}(R_{PP'} \mid \alpha_1 + 1, \alpha_2) &= (-1)^{k_2+k_3+l_3}(2j+1)(2k_1+1) \\
&\times \sum_{k_1'k_3'} \sum_{j'} \begin{pmatrix} 1 & k_1' & k_1 \\ 0 & 0 & 0 \end{pmatrix} \begin{Bmatrix} k_1 & k_2 & j \\ j' & 1 & k_1' \end{Bmatrix} \begin{Bmatrix} j & k_3 & l_3 \\ k_3' & j' & 1 \end{Bmatrix} \\
&\times A_{k_3'k_3}(R_{PP'})\, {}^{j'}W^{(\mathbf{l})}_{k_1,k_2,k_3'}(R_{PP'} \mid \alpha_1, \alpha_2) \qquad (39)
\end{aligned}
$$

and an analogous relation to raise the index α_2. The symbols between braces are 6–j coefficients, which arise from recoupling the spherical harmonics (Edmonds, 1957; Brink and Satchler, 1975). The introduction of Eq. (38) into (15) then yields the final expression for the intermolecular potential:

$$
\begin{aligned}
V_{PP'}(\mathbf{u}_P, \omega_P; \mathbf{u}_{P'}, \omega_{P'}) &= \sum_{\alpha_1,\alpha_2} \frac{(-u_P)^{\alpha_1}}{\alpha_1!} \frac{(u_{P'})^{\alpha_2}}{\alpha_2!} \sum_{\mathbf{l}} \sum_{\mathbf{k}} \sum_{j} {}^{j}W^{(\mathbf{l})}_{\mathbf{k}}(R_{PP'} \mid \alpha_1, \alpha_2) \\
&\times \sum_{\mathbf{m}} \begin{pmatrix} l_1 & l_2 & l_3 \\ m_1 & m_2 & m_3 \end{pmatrix} G^{(l_1)}_{m_1}(\omega_P) G^{(l_2)}_{m_2}(\omega_{P'}) \\
&\times [[C^{(k_1)}(\hat{u}_P) \otimes C^{(k_2)}(\hat{u}_{P'})]^{(j)} \otimes C^{(k_3)}(\hat{R}_{PP'})]^{(l_3)}_{m_3} \qquad (40)
\end{aligned}
$$

Another, equivalent, form in which the potential can be written is

$$
\begin{aligned}
V_{PP'}(\mathbf{u}_P, \omega_P; \mathbf{u}_{P'}, \omega_{P'}) &= \sum_{\alpha_1,\alpha_2} \frac{(-u_P)^{\alpha_1}}{\alpha_1!} \frac{(u_{P'})^{\alpha_2}}{\alpha_2!} \sum_{\mathbf{l}} \sum_{j_1,j_2} \sum_{k_1,k_2} \\
&\times B^{(\mathbf{l})}_{j_1,k_1;j_2,k_2}(R_{PP'} \mid \alpha_1, \alpha_2) \sum_{\mathbf{m}} \begin{pmatrix} l_1 & l_2 & l_3 \\ m_1 & m_2 & m_3 \end{pmatrix} [G^{(j_1)}(\omega_P) \otimes C^{(k_1)}(\hat{u}_P)]^{(l_1)}_{m_1} \\
&\times [G^{(j_2)}(\omega_{P'}) \otimes C^{(k_2)}(\hat{u}_{P'})]^{(l_2)}_{m_2} C^{(l_3)}_{m_3}(\hat{R}_{PP'}) \qquad (41)
\end{aligned}
$$

The expansion coefficients are related to those of Eq. (40) by

$$
\begin{aligned}
B^{(\mathbf{l})}_{j_1,k_1;j_2,k_2}(R_{PP'} \mid \alpha_1, \alpha_2) &= (-1)^{k_1+k_2}(2l_1+1)(2l_2+1) \\
&\times \sum_{a,b} (-1)^a \begin{Bmatrix} l_1 & l_2 & l_3 \\ k_1 & k_2 & a \\ j_1 & j_2 & b \end{Bmatrix} {}^{a}W^{(j_1,j_2,b)}_{k_1,k_2,l_3}(R_{PP'} \mid \alpha_1, \alpha_2) \qquad (42)
\end{aligned}
$$

and they satisfy the recursion relations

$$
\begin{aligned}
B^{(l_1',l_2,l_3)}_{j_1,k_1';j_2,k_2}(R_{PP'} \mid \alpha_1 + 1, \alpha_2) &= (-1)^{1+j_1+l_1+l_2}(2k_1+1)(2l_1+1) \\
&\times \sum_{l_1',l_3',k_1'} \begin{pmatrix} 1 & k_1' & k_1 \\ 0 & 0 & 0 \end{pmatrix} \begin{Bmatrix} k_1 & j_1 & l_2 \\ l_1' & 1 & k_1' \end{Bmatrix} \begin{Bmatrix} l_1 & l_3 & l_2 \\ l_3' & l_1' & 1 \end{Bmatrix} A_{l_3'l_3}(R_{PP'}) \\
&\times B^{(l_1',l_2,l_3')}_{j_1,k_1';j_2,k_2}(R_{PP'} \mid \alpha_1, \alpha_2) \qquad (43)
\end{aligned}
$$

These results [(41) and (42)] are obtained from Eq. (40) by angular momentum recoupling (Brink and Satchler, 1975); the symbol between braces in Eq. (42) is a 9–j coefficient. The recursion relation (43) is derived analogously to Eq. (39) (see Briels *et al.*, 1984).

By introducing the expanded potential [Eq. (40) or Eq. (41)] into the crystal Hamiltonian [Eq. (23)], we can write the latter as

$$H = U^C + \sum_P \{T(\mathbf{u}_P) + V_P^T(\mathbf{u}_P)\} + \sum_P \{L(\omega_P) + V_P^R(\omega_P)\} + \sum_P V_P^{TR}(\mathbf{u}_P, \omega_P) + \frac{1}{2}\sum\sum_{P \neq P'} \{\Phi_{PP'}^T(\mathbf{u}_P; \mathbf{u}_{P'}) + \Phi_{PP'}^R(\omega_P; \omega_{P'}) + \Phi_{PP'}^{TR}(\mathbf{u}_P, \omega_P; \mathbf{u}_{P'}, \omega_{P'})\} \tag{44}$$

in terms of one-body operators and two-body operators affecting the molecular translations T, rotations R, and their coupling TR. This partitioning can give some physical insight; in specific cases, one can study the importance of the different contributions. Just as we did for pure rotational motions, we can use the site symmetry to simplify the expressions. For the crystal field terms V_P^T and V_P^R this can be done exactly as before. For the mixed field terms V_P^{TR} it is somewhat more difficult; one finds that

$$V_P^{TR}(\mathbf{u}_P, \omega_P) = \sum_\alpha (u_P)^\alpha \sum_{l_1 l_2} \sum_\mu V_{l_1 l_2}^{(\mu)}(P \mid \alpha) \times \sum_i C_i^{(l_1 \cdot \mu)}(\hat{u}_P)^* G_i^{(l_2 \cdot \mu)}(\omega_P) \tag{45}$$

where $C_i^{(l_1 \cdot \mu)}$, $i = 1, \ldots, n_\mu$, are linear combinations of $C_m^{(l)}$ that transform according to the unitary representation $\Gamma^{(\mu)}$ of the site group S_P; n_μ is the dimension of this representation. Similarly, $G_i^{(l \cdot \mu)}$, $i = 1, \ldots, n_\mu$, are linear combinations of $G_m^{(l)}$ transforming in the same way. These functions are coupled to an invariant of S_P. An explicit inspection of the separate contributions in Eq. (45) is only useful for small values of $\alpha_{\max}$, since l_1 is at most equal to $\alpha_{\max}$ [see Eqs. (34)–(36)]. Otherwise, the separation becomes too complicated to provide any insight. For the two-body terms this applies *a fortiori*. However, even without the partitioning given by Eq. (44), the crystal Hamiltonian (23) with the potential expanded by Eq. (40) or (41) forms a good basis for discussing any lattice dynamics treatment.

III. Harmonic and Quasi-Harmonic Theories of Lattice Dynamics

In this section we briefly discuss the harmonic and quasi-harmonic models that are commonly used to describe the molecular motions, i.e.,

the lattice vibrations, in molecular crystals. We use the term *quasi-harmonic* for any theory in which the harmonic approximation plays a central role, although strictly speaking the quasi-harmonic model (Barron and Klein, 1974) is a special theory in this category. We include in this section a description of perturbation theory around the harmonic model and of the self-consistent phonon method. In general, as will be clear from the following, quasi-harmonic theories are suitable for describing anharmonic motions with fairly small amplitudes, for example, the translational motions in most crystals. If, however, the vibrational amplitudes are larger, for instance, for the librational motions, especially of small molecules or in the neighborhood of phase transitions, the quasi-harmonic models are of very limited value. They break down completely if the molecules perform hindered rotations as in plastic crystals. In these cases one must resort to completely different treatments, which we discuss in Section IV.

A. Harmonic Approximation

The harmonic approximation consists of expanding the potential up to second order in the atomic or molecular displacements around some local minimum and then diagonalizing the quadratic Hamiltonian. In the case of molecular crystals the rotational part of the kinetic energy, expressed in Euler angles, must be approximated, too. The angular momentum operators that occur in Eq. (26) are given by

$$\begin{aligned} J_a(\omega) &= \frac{\hbar}{i}\left(-\frac{\cos\gamma}{\sin\beta}\frac{\partial}{\partial\alpha} + \sin\gamma\frac{\partial}{\partial\beta} + \cot\beta\frac{\partial}{\partial\gamma}\right) \\ J_b(\omega) &= \frac{\hbar}{i}\left(\frac{\sin\gamma}{\sin\beta}\frac{\partial}{\partial\alpha} + \cos\gamma\frac{\partial}{\partial\beta} - \cot\beta\frac{\partial}{\partial\gamma}\right) \\ J_c(\omega) &= \frac{\hbar}{i}\frac{\partial}{\partial\gamma} \end{aligned} \tag{46}$$

where $\omega = \{\alpha, \beta, \gamma\}$ are the Euler angles of the molecule fixed coordinate frame relative to the global frame. The harmonic approximation implies that one replaces the angles ω in Eq. (46) by their equilibrium values $\omega_0 = \{\alpha_0, \beta_0, \gamma_0\}$ and then substitutes the result into the quadratic kinetic energy expression (26). Thus, one neglects the terms linear in the operators $\partial/\partial\beta$ and $\partial/\partial\gamma$, which occur in the exact expression (26); these terms arise by commuting $\partial/\partial\beta$ and $\partial/\partial\gamma$ with the sine and cosine functions of β and γ in the exact Eq. (46). At the same time, the volume element $\sin\beta\, d\alpha\, d\beta\, d\gamma$ becomes $\sin\beta_0\, d\alpha\, d\beta\, d\gamma$ and the angular displacement coordinates $\Delta\omega = \omega - \omega_0$ become rectilinear and formally run from $-\infty$ to ∞. For

linear molecules this approximation has been applied by Goodings and Henkelman (1971), Schnepp and Jacobi (1972), and Walmsley (1975).

The crystal Hamiltonian now reads

$$H = \frac{1}{2}\sum_{P}\sum_{\lambda,\lambda'} G_P^{\lambda,\lambda'} P_P^{\lambda} P_P^{\lambda'} + \frac{1}{2}\sum_{P,P'}\sum_{\lambda,\lambda'} F_{P,P'}^{\lambda,\lambda'} Q_P^{\lambda} Q_{P'}^{\lambda'} \tag{47}$$

where

$$Q_P^{\lambda} = u_P^{\lambda} \qquad \text{for} \quad \lambda = 1, 2, 3$$
$$Q_P^{\lambda} = \Delta\omega_P^{\lambda-3} \qquad \text{for} \quad \lambda = 4, 5, 6$$

and

$$P_P^{\lambda} = \frac{\hbar}{i}\frac{\partial}{\partial Q_P^{\lambda}}$$

are the momenta conjugate to these coordinates. These operators satisfy the usual commutation rules:

$$[Q_P^{\lambda}, P_{P'}^{\lambda'}] = i\hbar\,\delta_{P,P'}\,\delta_{\lambda,\lambda'}$$

The first term in Eq. (47) represents the kinetic energy operator. The 6×6 matrices $\mathbf{G}_P$ follow from the foregoing discussion; they contain the inverse molecular mass M^{-1} and the inverse inertia tensor depending on the equilibrium angles $\omega_0 = \{\alpha_0, \beta_0, \gamma_0\}$ with respect to the global frame. The second term represents the potential; linear terms are absent because this potential is expanded around a local minimum. The 6×6 matrices $\mathbf{F}_{P,P'}$ are defined as the second derivatives

$$F_{P,P'}^{\lambda,\lambda'} = \left[\frac{\partial^2 V_{PP'}}{\partial Q_P^{\lambda}\,\partial Q_{P'}^{\lambda'}}\right]_0, \qquad F_{P,P}^{\lambda,\lambda'} = \sum_{P'}\left[\frac{\partial^2 V_{PP'}}{\partial Q_P^{\lambda}\,\partial Q_{P'}^{\lambda'}}\right]_0 \tag{48}$$

taken at the equilibrium positions and orientations. The Hamiltonian (47) can easily be diagonalized exactly. First we introduce the operators

$$Q_i^{\lambda}(\mathbf{q}) = \frac{1}{\sqrt{N}}\sum_{\mathbf{n}} \exp(i\mathbf{q}\cdot\mathbf{R}_{\mathbf{n}})Q_P^{\lambda}$$
$$P_i^{\lambda}(\mathbf{q}) = \frac{1}{\sqrt{N}}\sum_{\mathbf{n}} \exp(-i\mathbf{q}\cdot\mathbf{R}_{\mathbf{n}})P_P^{\lambda} \tag{49}$$

with $P = \{\mathbf{n}, i\}$, where N is the number of unit cells in the crystal and $\mathbf{q}$ is a vector in the Brillouin zone. The Hamiltonian transforms into

$$H = \sum_{\mathbf{q}} H(\mathbf{q}) \tag{50}$$

with

$$H(\mathbf{q}) = \frac{1}{2}\sum_{i}\sum_{\lambda,\lambda'} G_i^{\lambda,\lambda'} P_i^{\lambda}(\mathbf{q}) P_i^{\lambda'}(\mathbf{q})^{\dagger} + \frac{1}{2}\sum_{i,i'}\sum_{\lambda,\lambda'} F_{i,i'}^{\lambda,\lambda'}(\mathbf{q}) Q_i^{\lambda}(\mathbf{q}) Q_{i'}^{\lambda'}(\mathbf{q})^{\dagger} \tag{51}$$

and

$$F_{i,i'}^{\lambda,\lambda'}(\mathbf{q}) = \sum_{\mathbf{n}} F_{\{\mathbf{0},i\}\{\mathbf{n},i'\}}^{\lambda,\lambda'} \exp(i\mathbf{q}\cdot\mathbf{R}_{\mathbf{n}}) = F_{i',i}^{\lambda',\lambda}(-\mathbf{q}) = F_{i',i}^{\lambda',\lambda}(\mathbf{q})^{*} \tag{52}$$

Here we have used the property that $\mathbf{G}_P$ and $\mathbf{F}_{PP'}$, are translationally invariant. The commutation rules for the wave-vector-dependent operators are

$$[Q_i^{\lambda}(\mathbf{q}), P_{i'}^{\lambda'}(\mathbf{q}')] = i\hbar\,\delta_{i,i'}\,\delta_{\lambda,\lambda'}\,\delta_{\mathbf{q},\mathbf{q}'}$$

Every $H(\mathbf{q})$, depends on $6Z$ operators $Q_i^{\lambda}(\mathbf{q})$ and $6Z$ operators $P_i^{\lambda}(\mathbf{q})$ if Z is the number of sublattices, i.e., the number of molecules in the unit cell. Finally, we introduce linear combinations

$$\begin{aligned} \overline{Q}_r(\mathbf{q}) &= \sum_{i=1}^{Z}\sum_{\lambda=1}^{6} (\mathbf{c}(\mathbf{q})^{-1})_{i,\lambda}^{r} Q_i^{\lambda}(\mathbf{q}) \\ \overline{P}_r(\mathbf{q}) &= \sum_{i=1}^{Z}\sum_{\lambda=1}^{6} c_r^{i,\lambda}(\mathbf{q}) P_i^{\lambda}(\mathbf{q}) \end{aligned} \tag{53}$$

such that $H(\mathbf{q})$ can be written as

$$H(\mathbf{q}) = \frac{1}{2}\sum_{r}\{\overline{P}_r^{\dagger}(\mathbf{q})\overline{P}_r(\mathbf{q}) + \omega_r(\mathbf{q})^2\overline{Q}_r^{\dagger}(\mathbf{q})\overline{Q}_r(\mathbf{q})\} \tag{54}$$

The coefficients $\mathbf{c}_r(\mathbf{q}) = \{c_r^{i,\lambda}(\mathbf{q}), i = 1, \ldots, Z, \lambda = 1, \ldots, 6\}$ can be obtained from the generalized eigenvalue problem

$$\mathbf{F}(\mathbf{q})\mathbf{c}_r(\mathbf{q}) = \mathbf{G}^{-1}\mathbf{c}_r(\mathbf{q})\omega_r(\mathbf{q})^2 \tag{55}$$

with the normalization condition

$$\mathbf{c}_r^{\dagger}\mathbf{G}^{-1}\mathbf{c}_{r'} = \delta_{rr'} \tag{56}$$

The choice of the transformation (53) ensures that

$$[\overline{Q}_r(\mathbf{q}), \overline{P}_{r'}(\mathbf{q}')] = i\hbar\,\delta_{r,r'}\,\delta_{\mathbf{q},\mathbf{q}'} \tag{57}$$

Introducing phonon creation and annihilation operators

$$\begin{aligned} a_r^\dagger(\mathbf{q}) &= [2\hbar\omega_r(\mathbf{q})]^{-1/2}\{\omega_r(\mathbf{q})\bar{Q}_r^\dagger(\mathbf{q}) - i\bar{P}_r(\mathbf{q})\} \\ a_r(\mathbf{q}) &= [2\hbar\omega_r(\mathbf{q})]^{-1/2}\{\omega_r(\mathbf{q})\bar{Q}_r(\mathbf{q}) + i\bar{P}_r^\dagger(\mathbf{q})\} \end{aligned} \tag{58}$$

with the commutation relations

$$[a_r(\mathbf{q}), a_{r'}^\dagger(\mathbf{q}')] = \delta_{r,r'}\,\delta_{\mathbf{q},\mathbf{q}'} \tag{59}$$

which follow from Eqs. (57) and (58), we can write the Hamiltonian in its well-known form:

$$H = \sum_{\mathbf{q}} \sum_{r} \hbar\omega_r(\mathbf{q}) \left\{ a_r^\dagger(\mathbf{q}) a_r(\mathbf{q}) + \frac{1}{2} \right\} \tag{60}$$

representing a sum of independent harmonic oscillators whose excitations are called phonons. The properties of the crystal can be obtained (see Appendix) from the thermodynamic partition function and its derivatives. The partition function for a system of harmonic oscillators reads

$$Z = \mathrm{Tr}(e^{-\beta H}) = \prod_{\mathbf{q}} \prod_{r} \left\{ 2 \sinh\left(\frac{1}{2} \beta\hbar\omega_r(\mathbf{q}) \right) \right\}^{-1} \tag{61}$$

with $\beta = (k_B T)^{-1}$, k_B being the Boltzmann constant and T the temperature.

B. Anharmonic Corrections by Perturbation Theory

In contrast with atoms and small molecules, the energy levels of extended systems almost invariably appear as broad bands. Degeneracy and near-degeneracy are the rule rather than the exception, and as a consequence, only weak interactions are needed to obtain intermixings of many states. This intermixing will also be caused by external perturbations applied in measurements, such as the electromagnetic fields in spectroscopic experiments. Another consequence of such close-lying states is that many of these states will be thermally populated. The (measured) properties of the system are not determined by the expectation values of operators over pure states, but by thermodynamic (Boltzmann) averages. These two aspects make it less useful to apply straightforward quantum-mechanical perturbation theory to single eigenstates of the Hamiltonian, as one mostly does for atoms and molecules. Instead, it is desirable to use a perturbation theory that describes the response of the whole system. The most powerful theory of this kind is based on the thermal, or imaginary time, Green's function.

In the perturbation theory of lattice dynamics one starts from the

harmonic approximation. The cubic and higher terms in the Taylor expansion of the potential around some local minimum, which are neglected in this approximation, are taken as perturbations of the harmonic model. Accordingly, the Hamiltonian can be written as (Califano, 1981)

$$\begin{aligned} H &= H_0 + H_1 \\ &= \sum_{\mathbf{q}} \sum_{r} \hbar\omega_r(\mathbf{q}) \left\{ a_r^\dagger(\mathbf{q}) a_r(\mathbf{q}) + \frac{1}{2} \right\} \\ &\quad + \sum_{m=3}^{\infty} \sum_{\mathbf{q}_1, \ldots, \mathbf{q}_m} \sum_{r_1, \ldots, r_m} \Phi_{r_1, \ldots, r_m}(\mathbf{q}_1, \ldots, \mathbf{q}_m) A_{r_1}(\mathbf{q}_1) \ldots A_{r_m}(\mathbf{q}_m) \end{aligned} \tag{62}$$

The operators appearing in the interaction Hamiltonian $H_1 = \sum_{m=3}^{\infty} H_m$ are defined as

$$A_r(\mathbf{q}) = a_r(\mathbf{q}) + a_r^\dagger(-\mathbf{q}) \tag{63}$$

and the coupling constants $\Phi_{r_1, \ldots, r_m}(\mathbf{q}_1, \ldots, \mathbf{q}_m)$ are the derivatives of the potential with respect to the coordinates $Q_r(\mathbf{q})$, multiplied by some constant factors. These coupling constants differ from zero only when $\mathbf{q}_1 + \cdots + \mathbf{q}_m$ equals a reciprocal lattice vector. In molecular crystals, the difference between the exact rotational kinetic energy and its harmonic oscillator approximation (see Section III,A) should also be considered as a perturbation. As far as we know, this has never actually been done, however.

The thermal Green's function, or phonon propagator, that is used in lattice dynamics theory is defined as

$$\begin{aligned} G_{r,r'}(\mathbf{q}; \tau) &= \Theta(\tau) \langle e^{\tau H} A_r(\mathbf{q}) e^{-\tau H} A_{r'}(-\mathbf{q}) \rangle \\ &\quad + \Theta(-\tau) \langle A_{r'}(-\mathbf{q}) e^{\tau H} A_r(\mathbf{q}) e^{-\tau H} \rangle \end{aligned} \tag{64}$$

where $\Theta(\tau)$ is the Heaviside step function and $\langle X \rangle$ denotes the thermodynamic average of an operator X over the eigenstates of H, i.e.,

$$\langle X \rangle = Z^{-1} \operatorname{Tr}(X e^{-\beta H}) \tag{65}$$

with

$$Z = \operatorname{Tr}(e^{-\beta H})$$

being the partition function and $\beta = (k_B T)^{-1}$. Using the invariance of the trace for cyclic permutations of the operators, one easily demonstrates that the phonon propagator (64) is a periodic function of the imaginary time τ with period β; we may therefore confine the values of τ to the interval $0 \leq \tau \leq \beta$. The time-dependent perturbation expansion of the

phonon propagator for the Hamiltonian $H = H_0 + H_I$ is given by the formula (Fetter and Walecka, 1971)

$$G_{r,r'}(\mathbf{q};\tau) = \langle S(\beta)\rangle_0^{-1} \sum_{n=0}^{\infty} \frac{(-1)^n}{n!} \int_0^\beta d\tau_1 \ldots \int_0^\beta d\tau_n \times \langle T[\tilde{H}_I^{\tau_1} \ldots \tilde{H}_I^{\tau_n} \tilde{A}_r^{\tau}(\mathbf{q}) \tilde{A}_{r'}^{0}(-\mathbf{q})]\rangle_0 \tag{66}$$

with

$$S(\beta) = \sum_{n=0}^{\infty} \frac{(-1)^n}{n!} \int_0^\beta d\tau_1 \ldots \int_0^\beta d\tau_n \, T[\tilde{H}_I^{\tau_1} \ldots \tilde{H}_I^{\tau_n}] \tag{67}$$

where $\tilde{X}^\tau$ denotes the operator X in the (imaginary time) interaction representation

$$\tilde{X}^\tau = \exp(\tau H_0) X \exp(-\tau H_0) \tag{68}$$

and $\langle X\rangle_0$ is the thermodynamic average of X over the eigenstates of the unperturbed Hamiltonian H_0. The so-called time-ordering operator T places the operators to its right in the order of decreasing times, from left to right. Introduction of the anharmonic interaction operator $H_I = \sum_{m=3}^{\infty} H_m$ defined in Eq. (62) into the expansions (66) and (67) yields many terms of the type written in Eq. (69) below. These can be evaluated by means of the (generalized) Wick theorem (Fetter and Walecka, 1971; Abrikosov *et al.*, 1965):

$$\langle T[\tilde{A}_{r_1}^{\tau_1}(\mathbf{q}_1) \ldots \tilde{A}_{r_{2n}}^{\tau_{2n}}(\mathbf{q}_{2n})]\rangle_0 = \sum_p \langle T[\tilde{A}_{r_i}^{\tau_i}(\mathbf{q}_i)\tilde{A}_{r_j}^{\tau_j}(\mathbf{q}_j)]\rangle_0 \ldots \langle T[\tilde{A}_{r_k}^{\tau_k}(\mathbf{q}_k)\tilde{A}_{r_l}^{\tau_l}(\mathbf{q}_l)]\rangle_0 \tag{69}$$

The summation runs over all $(2n-1)!!$ pairings of the operators $A_{r_i}^{\tau_i}(\mathbf{q}_i)$. The corresponding expectation value for a product of an odd number of operators is zero. The building blocks are the harmonic propagators

$$\langle T[\tilde{A}_r^{\tau}(\mathbf{q})\tilde{A}_{r'}^{\tau'}(\mathbf{q}')]\rangle_0 = \delta_{-\mathbf{q},\mathbf{q}'} \, G_{r,r'}^{(0)}(\mathbf{q};\tau-\tau') \tag{70}$$

given by Eq. (64) for $H = H_0$; they differ from zero only when $\mathbf{q}' = -\mathbf{q}$ and $r' = r$ and can be easily calculated.

The terms in the expansion (66), after substituting Eq. (62) and applying Wick's theorem (69), are usually represented by diagrams, according to the following recipe. For any interaction H_m given by Eq. (62) draw a vertex with m lines. When two operators $A_{r_i}^{\tau_i}(\mathbf{q}_i)$ and $A_{r_j}^{\tau_j}(\mathbf{q}_j)$ are paired in Eq. (69), the corresponding two lines are connected. The two operators $\tilde{A}_r^{\tau}(\mathbf{q})$ and $\tilde{A}_{r'}^{\tau'}(\mathbf{q}')$ defining the propagator (64) appear as vertices with just

a single line. As an example we show

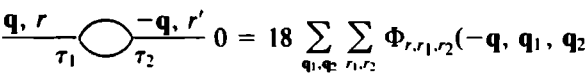

$$= 18 \sum_{\mathbf{q}_1,\mathbf{q}_2} \sum_{r_1,r_2} \Phi_{r,r_1,r_2}(-\mathbf{q}, \mathbf{q}_1, \mathbf{q}_2)$$

$$\times \Phi_{r_1,r_2,r'}(-\mathbf{q}_1, -\mathbf{q}_2, \mathbf{q}) \frac{(-1)^2}{2!} \int_0^\beta d\tau_1 \int_0^\beta d\tau_2$$

$$\times \langle T[\tilde{A}_r^\tau(\mathbf{q})\tilde{A}_{r'}^{\tau_1}(-\mathbf{q})]\rangle_0 \langle T[\tilde{A}_{r_1}^{\tau_1}(\mathbf{q}_1)\tilde{A}_{r_1}^{\tau_2}(-\mathbf{q}_1)]\rangle_0$$

$$\times \langle T[\tilde{A}_{r_2}^{\tau_1}(\mathbf{q}_2)\tilde{A}_{r_2}^{\tau_2}(-\mathbf{q}_2)]\rangle_0 \langle T[\tilde{A}_{r'}^{\tau_2}(\mathbf{q})\tilde{A}_{r'}^{0}(-\mathbf{q})]\rangle_0 \tag{71}$$

The factor 18 appears because there are 18 pairings consistent with this diagram, which all yield the same result; one obtains another 18 diagrams with this result by interchanging the vertices τ_1 and τ_2. There are two kinds of diagrams, those with all lines connected to $(\mathbf{q}, r)$ and/or $(-\mathbf{q}, r')$, which are called connected, and those diagrams consisting of a connected part and one or more parts connected neither to $(\mathbf{q}, \mathbf{r})$ nor to $(-\mathbf{q}, r')$, which are called disconnected. The summation in Eq. (66) contains the contributions from all diagrams, connected or disconnected, that have just two external lines, the $(\mathbf{q}, r)$ and the $(-\mathbf{q}, r')$ lines. It is a simple combinatorial problem to demonstrate that this sum is equal to $\langle S(\beta)\rangle_0$ times the sum over all contributions from connected diagrams only. Thus the expansion (66) for the propagator can be simplified to

$$G_{r,r'}(\mathbf{q}; \tau) = \sum_{n=0}^{\infty} \frac{(-1)^n}{n!} \int_0^\beta d\tau_1 \ldots \int_0^\beta d\tau_n$$

$$\times \langle T[\tilde{H}_I^{\tau_1} \ldots \tilde{H}_I^{\tau_n} \tilde{A}_r^\tau(\mathbf{q})\tilde{A}_{r'}^0(-\mathbf{q})]\rangle_{0,\text{connected}} \tag{72}$$

where the subscript "connected" indicates that only connected diagrams must be taken into account. A final simplification is possible because a permutation of the interaction vertices of equal order does not affect the numerical value of a diagram. Considering only topologically distinct diagrams removes the factor $1/n!$; this is essential for the derivation of the Dyson equation [Eq. (78) below].

In order to relate the thermal or imaginary time propagator to the measured properties of the system, we shall need its Fourier components:

$$\bar{G}_{r,r'}(\mathbf{q}; i\omega_l) = \beta^{-1} \int_0^\beta d\tau\, G_{r,r'}(\mathbf{q}; \tau) \exp(i\omega_l \tau) \tag{73}$$

where $\omega_l = 2\pi l\beta^{-1}$ with integer l, since the thermal propagator has the period β. For the harmonic propagator one derives

$$\bar{G}^{(0)}_{r,r'}(\mathbf{q}; i\omega_l) = \delta_{r,r'}(\beta\hbar)^{-1}\frac{2\omega_r(\mathbf{q})}{\omega_r(\mathbf{q})^2 + \omega_l^2}$$
$$= \delta_{r,r'}\bar{G}^{(0)}_r(\mathbf{q}; i\omega_l) \tag{74}$$

The Fourier representation of the anharmonic propagator is obtained from Eqs. (73) and (72), by using Wick's theorem (69), together with the Fourier representation of the harmonic phonon propagators. The "time" integrations can then explicitly be performed, yielding the condition $\sum_i \omega_i = 0$ and a factor β at every interaction vertex.

The Fourier components of the imaginary time propagator are defined on the imaginary frequency axis. We are interested in the Fourier transform of its real time analog, whose singularities, on the real frequency axis, yield the excitation energies of the system. Therefore, we need expressions for the Fourier components of the thermal phonon propagator that can be analytically continued in the complex plane in such a manner that they correctly yield the shifts of the singularities on the real axis caused by the perturbation. The perturbation expansion (72), truncated at any finite order n, does not satisfy this requirement. In order to calculate the frequency shifts caused by specific interactions, one must sum the corresponding diagrams to infinity. The result can be simplified if we define a "proper" diagram as a diagram that cannot be broken into two parts, each of which as two external lines, by cutting a single phonon line. Then the infinite sum can be symbolically written as

$\bar{G}_{r,r'}(\mathbf{q}; i\omega_l) =$ 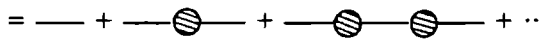 (75)

where the first contribution, the simple line, is the harmonic result $\delta_{r,r'}\bar{G}^{(0)}_r(\mathbf{q}; i\omega_l)$. The second term represents the sum of contributions from all proper diagrams, the third term arises from all diagrams consisting of two proper parts connected by an intermediate line, and so on. The second term is usually written as

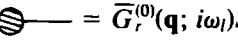 $= \bar{G}^{(0)}_r(\mathbf{q}; i\omega_l)S_{r,r'}(\mathbf{q}; i\omega_l)\bar{G}^{(0)}_{r'}(\mathbf{q}; i\omega_l)$ (76)

thus defining the "self-energy" matrix $\mathbf{S}(\mathbf{q}; i\omega_l)$. Then, one can show that because of the conditions $\sum_i \mathbf{q}_i = 0$ and $\sum_i \omega_i = 0$ at any vertex, which causes all intermediate lines to have momentum $\mathbf{q}$ and frequency ω_l, the third term yields

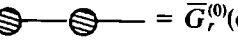 $= \bar{G}^{(0)}_r(\mathbf{q}; i\omega_l)\sum_{r''} S_{r,r''}(\mathbf{q}; i\omega_l)$

$\times\, \bar{G}^{(0)}_{r''}(\mathbf{q}; i\omega_l)S_{r'',r'}(\mathbf{q}; i\omega_l)\bar{G}^{(0)}_{r'}(\mathbf{q}; i\omega_l)$ (77)

This relation can be generalized to diagrams with any number of bubbles, and one can sum Eq. (75) to infinity. The result is the Dyson equation:

$$\bar{\mathbf{G}}(\mathbf{q}; i\omega_l) = \{\mathbf{1} - \bar{\mathbf{G}}^{(0)}(\mathbf{q}; i\omega_l)\mathbf{S}(\mathbf{q}; i\omega_l)\}^{-1}\bar{\mathbf{G}}^{(0)}(\mathbf{q}; i\omega_l) \tag{78}$$

All matrices are of dimension $6Z$ and the harmonic propagator matrix $\bar{\mathbf{G}}^{(0)}(\mathbf{q}; i\omega_l)$ is diagonal. The problem of calculating the phonon propagators thus reduces to the calculation of the self-energy matrices $\mathbf{S}(\mathbf{q}; i\omega_l)$ that contain all anharmonic information. It is not difficult to demonstrate that the self-energy matrix is a Hermitian function of ω_l^2 from which it follows that its analytic continuation in the complex frequency plane, in the neighborhood of the real axis, has the form

$$\lim_{\varepsilon \to 0+} \mathbf{S}(\mathbf{q}; \omega \pm i\varepsilon) = -\beta\hbar\{\mathbf{\Delta}(\mathbf{q}; \omega) \mp i\mathbf{\Gamma}(\mathbf{q}; \omega)\} \tag{79}$$

where $\mathbf{\Delta}$ and $\mathbf{\Gamma}$ are real symmetric and antisymmetric matrices, respectively.

Now we can show the explicit relation with experiment. What is usually measured in spectroscopic or scattering experiments is the spectral density function $I(\omega)$, which is the Fourier transform of some correlation function. For example, the absorption intensity in infrared spectroscopy is given by the Fourier transform of the time-dependent dipole–dipole correlation function $\langle[\mu(t), \mu(0)]\rangle$. If one expands the observables, i.e., the dipole operator in the case of infrared spectroscopy, as a Taylor series in the molecular displacement coordinates, the absorption or scattering intensity corresponding to the phonon branch r at wave vector $\mathbf{q}$ can be written as (Kobashi, 1978)

$$I_{\mathbf{q},r}(\omega) \sim \lim_{\varepsilon \to 0+} i\{\bar{G}_{r,r}(\mathbf{q}; \omega + i\varepsilon) - \bar{G}_{r,r}(\mathbf{q}; \omega - i\varepsilon)\} \tag{80}$$

Usually it is justifiable to neglect the nondiagonal elements of the self-energy matrix; if not so, these can be taken into account as a small perturbation. Then, we arrive at the result

$$I_{\mathbf{q},r}(\omega) \sim (\beta\hbar)^{-1} \frac{8\omega_r(\mathbf{q})^2\Gamma_{r,r}(\mathbf{q}; \omega)}{\{-\omega^2 + \omega_r(\mathbf{q})^2 + 2\omega_r(\mathbf{q})\,\Delta_{r,r}(\mathbf{q}, \omega)\}^2 + 4\omega_r(\mathbf{q})^2\Gamma_{r,r}(\mathbf{q}; \omega)^2} \tag{81}$$

If $\Delta_{r,r}(\omega)$ and $\Gamma_{r,r}(\omega)$ do not vary much with ω, they may be interpreted as the frequency shift, i.e., the resonance shifts from $\omega_r(\mathbf{q})$ to $\omega_r(\mathbf{q}) + \Delta_{r,r}(\mathbf{q}; \omega)$, and the bandwidth, respectively. Note that the actual calculation of these quantities will not be easy, however, since the diagrams involved contain summations over the entire Brillouin zone [see Eq. (71), for instance]. Some simplification may arise from the lattice

symmetry. A perturbation theory has been developed (Briels, 1983; Hamer and Irving, 1984) in which successive perturbation corrections are associated with an increasing sequence of clusters on the (real) lattice, thus avoiding the multiple sums over the Brillouin zone. Up until now, this method has only been applied to relatively simple Hamiltonians.

C. The Self-Consistent Phonon Method

Just as the perturbation theory described in the previous section, the self-consistent phonon (SCP) method applies only in the case of small oscillations around some equilibrium configuration. The SCP method was originally formulated (Werthamer, 1976) for atomic, rare gas, crystals. It can be directly applied to the translational vibrations in molecular crystals and, with some modification, to the librations. The essential idea is to look for an effective harmonic Hamiltonian H_0, which approximates the exact crystal Hamiltonian as closely as possible, in the sense that it minimizes the free energy A_{var}. This minimization rests on the thermodynamic variation principle:

$$A_{\text{var}} = A_0 + \langle H - H_0 \rangle_0 \geq A \tag{82}$$

The angle brackets denote a thermal average over the eigenstates of H_0 [cf. Eq. (65)]. The free energies A and A_0 correspond to the Hamiltonians H and H_0, respectively:

$$\begin{aligned} A &= -k_B T \ln Z, \qquad Z = \text{Tr}[\exp(-\beta H)] \\ A_0 &= -k_B T \ln Z_0, \qquad Z_0 = \text{Tr}[\exp(-\beta H)] \end{aligned} \tag{83}$$

The exact crystal Hamiltonian H is given by Eq. (23) and H_0 is of the form given by Eq. (47); the force constants $F^{\lambda\lambda'}_{P,P'}$ are not given by Eq. (48), however, but they are chosen such as to minimize A_{var}. Neglecting the difference between the exact kinetic energy operators [(25) and (26)] and their harmonic approximations (see Section III,A), one obtains

$$H - H_0 = \frac{1}{2} \sum_{P,P'} V_{PP'}(\mathbf{u}_P, \omega_P; \mathbf{u}_{P'}, \omega_{P'}) - \frac{1}{2} \sum_{P,P'} \sum_{\lambda,\lambda'} F^{\lambda\lambda'}_{P,P'} Q^{\lambda}_{P} Q^{\lambda'}_{P'} \tag{84}$$

with effective force constants $F^{\lambda\lambda'}_{P,P'}$ that still have to be optimized. The displacement coordinates Q^{λ}_{P} are assumed to be rectilinear, as described in Section III,A. The effective harmonic free energy A_0 is given by Eq. (83) with Z_0 as in Eq. (61). The expectation value of the harmonic potential, i.e., the second term in Eq. (84), can be written as

$$-\frac{1}{2} \sum_{P,P'} \sum_{\lambda,\lambda'} F^{\lambda\lambda'}_{P,P'} D^{\lambda\lambda'}_{P,P'} \tag{85}$$

in terms of the effective force constants and the displacement–displacement correlation functions:

$$D^{\lambda,\lambda'}_{P,P'} = \langle Q^{\lambda}_{P} Q^{\lambda'}_{P'} \rangle_0 \tag{86}$$

The expectation value of the exact potential, the first term in Eq. (84), is somewhat more difficult to calculate. Using the properties of the harmonic oscillator eventually leads to (Choquard, 1967; Werthamer, 1976)

$$\begin{aligned}
&\langle V_{PP'}(\mathbf{u}_P, \omega_P; \mathbf{u}_{P'}, \omega_{P'}) \rangle_0 \\
&\quad = \left\langle \exp\left\{ \sum_{\lambda} (Q^{\lambda}_{P} \nabla^{\lambda}_{P} + Q^{\lambda}_{P'} \nabla^{\lambda}_{P'}) \right\} \right\rangle_0 V_{PP'}(\mathbf{0}, \omega_{0P}; \mathbf{0}, \omega_{0P'}) \\
&\quad = \exp\left\{ \frac{1}{2} \sum_{\lambda\lambda'} (D^{\lambda,\lambda'}_{P,P} \nabla^{\lambda}_{P} \nabla^{\lambda'}_{P} + 2D^{\lambda,\lambda'}_{P,P'} \nabla^{\lambda}_{P} \nabla^{\lambda'}_{P'} \right. \\
&\qquad \left. + D^{\lambda,\lambda'}_{P',P'} \nabla^{\lambda}_{P'} \nabla^{\lambda'}_{P'}) \right\} V_{PP'}(\mathbf{0}, \omega_{0P}; \mathbf{0}, \omega_{0P'})
\end{aligned} \tag{87}$$

with $\nabla^{\lambda}_{P} = \partial/\partial Q^{\lambda}_{P}$ acting only on $V_{PP'}$. Substituting the expression for A_0 and the results (85) and (87) for $\langle H - H_0 \rangle_0$ into A_{var} [Eq. (82)] and applying the minimization conditions

$$\partial A_{\text{var}} / \partial F^{\lambda,\lambda'}_{P,P'} = 0$$

one finds the expression for the optimized force constants:

$$F^{\lambda,\lambda'}_{P,P'} = \left\langle \frac{\partial^2 V_{PP'}}{\partial Q^{\lambda}_{P} \partial Q^{\lambda'}_{P'}} \right\rangle_0, \qquad F^{\lambda,\lambda'}_{P,P'} = \sum_{P'} \left\langle \frac{\partial^2 V_{PP'}}{\partial Q^{\lambda}_{P} \partial Q^{\lambda'}_{P}} \right\rangle_0 \tag{88}$$

So, instead of using the second derivatives of the potential in the equilibrium configuration as force constants, the SCP method employs the thermal averages of these derivatives. Equation (88) and the corresponding dynamical equations, given by the generalized eigenvalue problem (55), have to be solved self-consistently. One can do this via the usual iterative procedure, starting with trial values for the effective force constants (88), which can be taken from the harmonic model. The averaging in Eqs. (82) and (88) can be most easily performed (Werthamer, 1976) by first Fourier transforming the function to be averaged, next applying Eq. (87), and then transforming back to the original coordinates, which yields

$$\begin{aligned}
&\langle V_{PP'}(\mathbf{u}_P, \omega_P; \mathbf{u}_{P'}, \omega_{P'}) \rangle_0 \\
&\quad = \int d^6 Q_P \int d^6 Q_{P'} \rho_{PP'}(Q^1_P, \ldots, Q^6_{P'}) V_{PP'}(Q^1_P, \ldots, Q^6_{P'})
\end{aligned} \tag{89}$$

and a similar expression for the second derivatives (88). The width of the Gaussian probability distribution $\rho_{PP'}$ is determined by the Hessian of the

quadratic exponent. This Hessian is the inverse of the 12-dimensional matrix

$$\begin{pmatrix} \mathbf{D}_{PP} & \mathbf{D}_{PP'} \\ \mathbf{D}_{P'P} & \mathbf{D}_{P'P} \end{pmatrix} \tag{90}$$

with elements given by Eq. (86). These elements, the displacement–displacement correlation functions, can easily be calculated by using Eqs. (49), (53), and (58). The result for the minimized free energy A_{var} is

$$\begin{aligned} A = & \sum_{\mathbf{q},r} k_B T \ln\left\{2 \sinh\left(\frac{1}{2}\beta\hbar\omega_r(\mathbf{q})\right)\right\} \\ & + \frac{1}{2}\sum_{P\neq P'}\sum \langle V_{PP'}(\mathbf{u}_P, \omega_P; \mathbf{u}_{P'}, \omega_{P'})\rangle_0 \\ & - \frac{1}{4}\sum_{\mathbf{q},r} \hbar\omega_r(\mathbf{q}) \coth\left(\frac{1}{2}\beta\hbar\omega_r(\mathbf{q})\right) \end{aligned} \tag{91}$$

The calculation of this quantity, and of the displacement–displacement correlation functions, involves a single summation over all wave vectors $\mathbf{q}$ in the Brillouin zone.

From the free energy all thermodynamic properties of the system can be calculated. For example, the entropy is $S = -\partial A/\partial T$ and the energy is $E = A + TS$. For more details we refer to the review by Werthamer (1976). One important point should be mentioned. Expanding the potential $V_{PP'}(Q_P^1, \ldots, Q_{P'}^6)$ as a Taylor series in the displacement coordinates Q_P^λ, we observe, using the analog of Eq. (87) for the force constants (88), that the odd power terms do not contribute to the effective force constants; the SCP method neglects these terms. Their relative importance can, of course, be estimated by perturbation techniques as described in Section III,B.

Here we have formulated the SCP method for molecular crystals. We could easily include the librations because the orientational dependence of the potential $V_{PP'}$ has been explicitly given, in Sections II,B and II,C, in terms of the Euler angles ω_P and thus in terms of the angular displacements $\Delta\omega_P = \omega_P - \omega_{0P}$. In two earlier applications of the SCP method to molecular crystals, one has used atom–atom potentials, however, whose orientational dependence was implicit and the description of librations was still a problem. Raich *et al.* (1974) in their calculations on α-nitrogen (see Section V) have avoided this problem by including the librations implicitly. They did this by considering a molecular crystal as a collection of atoms interacting via strong chemical bonds with their partners within the same molecule and via weak van der Waals potentials with all other

atoms belonging to neighboring molecules. Then they applied the original SCP method to the atomic motions. This approach is, of course, confined to the use of intermolecular potentials of the atom–atom type (see Section II,A). Wasiutynski (1976) has considered the molecular librations explicitly. He has expressed the atom–atom potential as a function of the translational and librational molecular displacements by writing a linear relation between these displacements and the atomic displacements. This relation holds only for small angular displacements.

IV. Dynamical Models for Large-Amplitude Motions

The methods outlined in the preceding section obviously cannot be applied when the molecules in a crystal perform large-amplitude librations or even (hindered) rotations. In this case, one has the tendency to emphasize the motions of the individual molecules rather than the collective motions. Indeed, the most generally applicable method to describe large-amplitude motions is the mean field theory (Kirkwood, 1940; James and Keenan, 1959), which treats the molecules as moving in a field that represents the mean interaction with the neighboring molecules. In a quantum-mechanical description, it is then possible to use the low-lying single-particle states to construct a basis for the whole solid in which the complete crystal Hamiltonian can be diagonalized. Adaptation of this basis to the translational symmetry of the crystal makes this diagonalization practically possible. At the same time, it leads to a labeling of the crystal states by the wave vectors in the Brillouin zone, thus reintroducing the collective aspect of the lattice vibrations. In order to make the frequencies of the acoustical lattice modes go to zero when the wave vector approaches the center of the Brillouin zone, the crystal Hamiltonian has to be diagonalized at the time-dependent Hartree (TDH) or random phase approximation (RPA) level (Fredkin and Werthamer, 1965).

A scheme as described here is indispensable for a quantum dynamical treatment of strongly delocalized systems, such as solid hydrogen (van Kranendonk, 1983) or the plastic phases of other molecular crystals. We have shown, however (Jansen *et al.*, 1984), that it is also very suitable to treat the anharmonic librations in ordered phases. Moreover, the RPA method yields the exact result in the limit of a harmonic crystal Hamiltonian, which makes it appropriate to describe the weakly anharmonic translational vibrations, too. We have extended the theory (Briels *et al.*, 1984) in order to include these translational motions, as well as the coupled rotational–translational lattice vibrations. In this section, we outline the general theory and present the relevant formulas for the coupled

problem. First, we briefly sketch some classical methods, however, that have been used in the literature to study large-amplitude motions in molecular systems.

A. Classical Molecular Dynamics and Monte Carlo Methods

In classical mechanics there exist, apart from the mean field theory, two popular methods to describe the dynamics of molecular systems, viz., the molecular dynamics (MD) method and the Monte Carlo (MC) method (Hansen and McDonald, 1976). In both methods the system is represented by a finite number, usually about 100 to 300, of molecules. In order to reduce boundary effects, this finite system is periodically repeated in all directions.

In the MD method (Rahman, 1966; Verlet, 1967) one specifies the initial conditions, i.e., the positions and orientations of all molecules and their (angular) velocities, and one integrates the classical equations of motion numerically by means of some finite difference scheme. The choice of the time step is mainly determined by the error allowed and the time scale in which one is interested. Usually, one takes time steps of order 10^{-14} sec and follows the trajectory for some 10^3 to 10^5 steps. Along the whole or part of the trajectory all kinds of quantities can be averaged. The method is especially suitable for calculating time-dependent correlation functions that yield information on the dynamics of the system. An example is the so-called intermediate scattering function:

$$F(\mathbf{q}, t) = \frac{1}{4N} \sum_{P,P'}^{N} \langle M_P(\mathbf{q}, t) M_{P'}(\mathbf{q}, 0) \rangle \tag{92}$$

where N is the number of molecules in the system, and the operator

$$M_P(\mathbf{q}, t) = \exp[i\mathbf{q} \cdot \mathbf{r}_P(t)] \sum_{\alpha \in P} \exp[i\mathbf{q} \cdot \mathbf{d}_\alpha(t)] \tag{93}$$

is related to the scattering of neutrons with scattering vector $\mathbf{q}$ by a molecule at the instantaneous position $\mathbf{r}_P(t)$. The atoms α belonging to this molecule have (instantaneous) position vectors $\mathbf{d}_\alpha(t)$ relative to its center of mass; these vectors depend on the orientation of the molecule. The Fourier transform of this particular correlation function

$$S(\mathbf{q}, \omega) = (2\pi)^{-1} \int_{-\infty}^{\infty} dt\, F(\mathbf{q}, t) e^{i\omega t} \tag{94}$$

is called the dynamic structure factor, and it describes the response of the system to a transfer of momentum $\mathbf{q}$ and energy $\hbar\omega$. By the nature of the

MD method, the system studied has constant energy. Its temperature can be defined via the mean kinetic energy. Other thermodynamic properties can be calculated from the numerical derivatives of the energy or by using their relations to certain fluctuations of the system. The specific heat, for instance, can be obtained from the derivative of the energy with respect to the temperature or from the temperature fluctuations. It will be clear that for these derived quantities the uncertainties are larger than for the trajectory itself.

The Monte Carlo method is most easily explained by means of a discrete model. One assumes that the system can only be in a configuration corresponding to one of a finite but large number of grid points on a very fine mesh. The idea is to sample this configuration space and to calculate various mean values. Even with the largest computers, however, it is not possible to sample a substantial part of configuration space, and the possibility exists that one samples many highly improbable configurations. The way to avoid this problem is to generate a Markov chain of successive configurations with step probabilities p_{ij} to get from state i to state j. The probabilities p_{ij} are chosen such that the stationary state of the chain has occupation probabilities in accordance with the canonical Boltzmann distribution law. It is also possible to simulate other thermodynamic ensembles, in which case the Boltzmann distribution has to be replaced by the appropriate probability distribution. Of course, the requirement just stated is not sufficient to completely specify the transition matrix p_{ij}. Among the possible choices for p_{ij} the most popular one, proposed by Metropolis *et al.* (1953), leads to the following scheme. Given a configuration, randomly generate a new one that differs not too much from the previous one and accept it as a sample point if its energy is lower than that of the previous state. If its energy is higher, accept it with probability $\exp(-\beta\,\Delta V_{ij})$, where $\Delta V_{ij} = V(j) - V(i)$. This method is very suitable for calculating static correlation functions. The calculation of thermodynamic properties is similar to that in the MD method; one can use the derivatives of the mean energy or the average fluctuations. Another way is to connect the system reversibly to a model system whose properties are known.

Both the MD and MC methods have some limitations that are mainly due to the finite size of the system and to the periodic boundary conditions. Generally, when the number of molecules is 100 or more, the fluctuations are sufficiently weak for the average properties to approach the bulk properties. Because of the periodic boundary conditions, however, it is impossible to study fluctuations with a wavelength that is larger than the length of the box. This is most unsatisfactory for two-dimensional

systems or for systems in the neighborhood of (second-order) phase transitions, because in these cases the large-scale fluctuations constitute an interesting part of the theory. The same limitation holds in MD calculations for the time-dependent correlations. These may contain spurious contributions when local perturbations are not sufficiently damped, so that they reappear because of the periodic boundary conditions. Another problem occurring especially in small systems is that they can be locked in a small region of phase space. Consequently, it is often difficult to locate phase transitions, because the system remains in a metastable state for a very long time. A third problem is that short-range and long-range interactions have to be included via different methods.

B. The Mean Field Model

Just as the self-consistent phonon method, the mean field approximation (Kirkwood, 1940; James and Keenan, 1959) is based on the thermodynamic variation principle for the Helmholtz free energy:

$$A_{\text{var}} = A_0 + \langle H - H_0 \rangle_0 \geq A \tag{95}$$

The meaning of the symbols is explained in Section III,C [Eq. (83)]; H is the exact crystal Hamiltonian [Eq. (23)]. This time, however, we choose as the approximate Hamiltonian H_0 a sum of single-particle Hamiltonians:

$$H_0 = \sum_P H_P^{\text{MF}}(\mathbf{u}_P, \omega_P) \tag{96}$$

In order to obtain the conditions on $H_P^{\text{MF}}(\mathbf{u}_P, \omega_P)$ that guarantee that H_0 is the best possible Hamiltonian with the form of Eq. (96) in the sense that A_{var} adopts its minimum value, we vary every single-particle Hamiltonian by an arbitrary amount $h_P(\mathbf{u}_P, \omega_P)$:

$$H_0 \to H_0 + h = \sum_P \{H_P^{\text{MF}}(\mathbf{u}_P, \omega_P) + h_P(\mathbf{u}_P, \omega_P)\} \tag{97}$$

and calculate the corresponding variation of the free energy:

$$\begin{aligned} \Delta A_{\text{var}} &= A_{\text{var}}(H_0 + h) - A_{\text{var}}(H_0) \\ &= A(H_0 + h) - A(H_0) \\ &\quad + \text{Tr}[(H - H_0)\{\rho(H_0 + h) - \rho(H_0)\}] \\ &\quad - \text{Tr}[h\rho(H_0 + h)] \end{aligned} \tag{98}$$

This result can easily be obtained by writing the thermodynamic expectation value of an arbitrary operator X as

$$\langle X \rangle = \mathrm{Tr}\{X\rho(H)\} \tag{99}$$

in terms of the density operator

$$\rho(H) = Z^{-1}e^{-\beta H} \tag{100}$$

with

$$Z = \mathrm{Tr}\, e^{-\beta H}$$

To first order in the perturbation h, ΔA_{var} must be zero, while to second order it must be positive for arbitrary h. In order to calculate ΔA_{var} and the density operator on which it depends, up to the second order, we can use the perturbation expansion

$$\exp\{-\beta(H_P^{\mathrm{MF}} + h_P)\} = \exp(-\beta H_P^{\mathrm{MF}}) \times \sum_{n=0}^{\infty} \frac{(-1)^n}{n!} \int_0^\beta d\tau_1 \ldots \int_0^\beta d\tau_n\, T[\tilde{h}_P^{\tau_1} \ldots \tilde{h}_P^{\tau_n}] \tag{101}$$

with

$$\tilde{h}_P^\tau = \exp(\tau H_P^{\mathrm{MF}}) h_P \exp(-\tau H_P^{\mathrm{MF}}) \tag{102}$$

This expansion lies also at the basis of the perturbation expansion given by Eq. (66). The time-ordering operator T orders the (imaginary) times τ_1, ..., τ_n. For brevity we have momentarily stopped indicating the dependence of all quantities on the coordinates $\mathbf{u}_P$ and ω_P. Using the notation $\rho_P^{\mathrm{MF}} = \rho(H_P^{\mathrm{MF}})$ and $\langle X \rangle_{\mathrm{MF}} = \mathrm{Tr}(X\rho_P^{\mathrm{MF}})$, we readily derive

$$\rho(H_P^{\mathrm{MF}} + h_P) = \rho_P^{\mathrm{MF}} + \Delta\rho_P^{(1)} + \Delta\rho_P^{(2)} + \cdots \tag{103}$$

with

$$\Delta\rho_P^{(1)} = \rho_P^{\mathrm{MF}}\{\beta\langle h_P \rangle_{\mathrm{MF}} - \int_0^\beta d\tau_1\, \tilde{h}_P^{\tau_1}\} \tag{104}$$

The explicit expression for $\Delta\rho_P^{(2)}$ will not be needed. Using the perturbation expansion (101) in Eq. (98) we arrive, after some algebra (van der Avoird *et al.*, 1984), at

$$\Delta A_{\mathrm{var}} = \Delta A_{\mathrm{var}}^{(1)} + \Delta A_{\mathrm{var}}^{(2)} + \cdots \tag{105}$$

with

$$\Delta A_{\mathrm{var}}^{(1)} = \sum_P \mathrm{Tr}\{(T_P + L_P + V_P^{\mathrm{MF}} - H_P^{\mathrm{MF}})\, \Delta\rho_P^{(1)}\} \tag{106}$$

and

$$\Delta A_{\text{var}}^{(2)} = \sum_P \text{Tr}\{(T_P + L_P + V_P^{\text{MF}} - H_P^{\text{MF}})\,\Delta\rho_P^{(2)}\}$$

$$+ \frac{1}{2}\sum_{P\neq P'}\sum \text{Tr}\{\Delta\rho_P^{(1)} V_{PP'}\,\Delta\rho_{P'}^{(1)}\}$$

$$+ \beta^{-1}\sum_P \int_0^\beta d\tau_1\,\tau_1\langle \bar{h}_P^{\tau_1} h_P\rangle_{\text{MF}}$$

$$- \frac{1}{2}\beta\sum_P \langle h_P\rangle_{\text{MF}}^2 \tag{107}$$

The kinetic energy operators $T_P = T(\mathbf{u}_P)$ and $L_P = L(\omega_P)$ are defined in Eqs. (25) and (26); the mean field potential is given by

$$V_P^{\text{MF}} = \sum_{P'\neq P} \text{Tr}^{(P')}(V_{PP'}\rho_{P'}^{\text{MF}}) = \sum_{P'\neq P}\langle V_{PP'}\rangle_{P'} \tag{108}$$

From the extremum condition that $\Delta A_{\text{var}}^{(1)}$ should be zero for arbitrary variations h_P and thus for arbitrary changes $\Delta\rho_P^{(1)}$ in the density operator, we derive the expression for the optimized single-particle Hamiltonian

$$H_P^{\text{MF}}(\mathbf{u}_P, \omega_P) = T(\mathbf{u}_P) + L(\omega_P) + \sum_{P'\neq P}\langle V_{PP'}(\mathbf{u}_P, \omega_P; \mathbf{u}_{P'}, \omega_{P'})\rangle_{P'} \tag{109}$$

This defines a set of equations for the mean field Hamiltonians H_P^{MF}. These equations have to be solved self-consistently since the thermodynamic values within the angle brackets in (109) involve the mean field Hamiltonians $H_{P'}^{\text{MF}}$. In principle, all H_P^{MF} can be different; in practice, we impose symmetry relations. Therefore, we choose a unit cell, compatible with the symmetry of the lattice introduced in Section II,D, and we put $H_{P'}^{\text{MF}}$ equal to H_P^{MF} whenever P' and P belong to the same sublattice. Moreover, we apply unit cell symmetry that relates the mean field Hamiltonians on different sublattices. By using the symmetry-adapted functions introduced in Section II,B, the latter symmetry can be imposed as follows. We select a set of molecules constituting the asymmetric part of the unit cell. Then we assign to all other molecules P' Euler angles $\bar{\omega}_{P'}$ through which the mean field Hamiltonian of some molecule P in the asymmetric part has to be rotated in order to obtain $H_{P'}^{\text{MF}}$. As a result, we find

$$\langle C_m^{(l)}\rangle_{P'} = \sum_n \langle C_n^{(l)}\rangle_P D_{nm}^{(l)}(\bar{\omega}_{P'})$$
$$\langle G_m^{(l)}\rangle_{P'} = \sum_n \langle G_n^{(l)}\rangle_P D_{nm}^{(l)}(\bar{\omega}_{P'}) \tag{110}$$

If we substitute these transformation relations into Eq. (109), we observe that the latter equation involves only the mean field Hamiltonians of the molecules in the asymmetric part of the unit cell.

In order to perform the calculations in practice, we introduce a basis in which we diagonalize the mean field Hamiltonians. The density operators ρ_P^{MF} become diagonal, too, and the calculation of the thermodynamic averages is obvious. The most convenient basis consists of the products

$$D_{m_1m_2}^{(l)}(\omega_P)\Psi_{k,m_3}^{(n)}(\mathbf{u}_P) \tag{111}$$

of Wigner functions $D_{m_1m_2}^{(l)}(\omega)$ and three-dimensional harmonic oscillator functions

$$\Psi_{k\,m}^{(n)}(\mathbf{u}_P) = A\left(\frac{2}{u_P}\right)^{1/2} \Lambda_{1/2(n-k)}^{k+1/2}(A^2u_P^2)S_m^{(k)}(\hat{u}_P) \tag{112}$$

with

$$\Lambda_l^{\alpha}(t) = \left[\Gamma(\alpha+1)\binom{l+\alpha}{l}\right]^{-1/2} e^{-t/2}t^{\alpha/2}L_l^{\alpha}(t) \tag{113}$$

The functions $S_m^{(k)}$ are tesseral (i.e., real combinations of spherical) harmonics, L_l^{α} are Laguerre functions, and $\Gamma(\alpha)$ are gamma functions (Powell and Craseman, 1961); k is restricted to $0 \le k \le n$ and it must have the same parity as n. The constant A, in the case of a finite basis, can be used to optimize this basis. The matrix elements required in this basis can be easily computed from Eq. (14) and the relation

$$\int_0^{\infty} u^2\,du\,\Lambda_{1/2(n_1-k_1)}^{k_1+1/2}(u^2)\frac{u^{\alpha}}{u}\Lambda_{1/2(n_2-k_2)}^{k_2+1/2}(u^2)$$
$$= \frac{1}{2}(-1)^{a_1+a_2}\left[\frac{\Gamma(a_1+1)}{\Gamma(a_1+b_1+1)}\frac{\Gamma(a_2+1)}{\Gamma(a_2+b_2+1)}\right]^{1/2}$$
$$\times \sum_{l=l_{\min}}^{l_{\max}}\binom{c-b_1}{a_1-l}\binom{c-b_2}{a_2-l}\binom{c+1}{l}\Gamma(c+1) \tag{114}$$

with

$$a_i = \tfrac{1}{2}(n_i - k_i), \qquad b_i = k_i + \tfrac{1}{2}$$

$$c = \tfrac{1}{2}(k_1 + k_2 + \alpha + 1), \qquad d = \max(a_1 + b_1, a_2 + b_2) - c$$

$$l_{\min} = \begin{cases} d & \text{if } c \text{ is half-integer and } d > 0, \\ 0 & \text{otherwise,} \end{cases} \qquad l_{\max} = \min(a_1, a_2)$$

The factor u^2 in the integrand originates from the volume element in $\mathbf{u}$ space. Matrix elements of the translational kinetic energy operator $T(\mathbf{u}_P)$ follow from the identity

$$-\Delta(\mathbf{u}_P) = A^2[-\Delta(A\mathbf{u}_P) + A^2u_P^2] - A^4u_P^2 \tag{115}$$

The operator between the brackets is the harmonic oscillator Hamiltonian, which has the basis functions (112) as its eigenfunctions; the remaining term is taken into account via Eq. (114). The rotational kinetic energy operator $L(\omega_P)$ [Eq. (26)] can be written in terms of the shift operators $J_\pm = J_a \mp iJ_b$ and the operator J_c, which act on the basis as

$$\begin{aligned} J_c D^{(l)}_{mn}(\omega) &= mD^{(l)}_{mn}(\omega) \\ J_\pm D^{(l)}_{mn}(\omega) &= \{(l \mp m)(l \pm m + 1)\}^{1/2} D^{(l)}_{m\pm1,n}(\omega) \end{aligned} \tag{116}$$

At this point let us make a remark concerning the size of the basis. In order to obtain convergence, one must sometimes include (Briels *et al.*, 1984) basis functions with high values of l and n. High values of l are needed in particular when the orientations of the molecules are fairly well localized. This leads to a rapidly increasing size of the basis. Two measures can be taken to simplify the problem. First, one can adapt the basis of molecule P to the site symmetry at P, which block-diagonalizes the secular problem. If this does not sufficiently reduce the problem, the mean field model Hamiltonian (96) can be further separated by writing

$$H_P^{\mathrm{MF}}(\mathbf{u}_P, \omega_P) = H_P^T(\mathbf{u}_P) + H_P^L(\omega_P) \tag{117}$$

As a result, we now have two "particles" at every lattice point P, one translating and one librating. Expressions for the separate mean field Hamiltonian can be derived as before. The translating particle experiences the mean field of all its neighbors, translating and librating, and of its accompanying librating particle; for the librating particle this relation holds in reverse. The advantage of this separation is that the basis to be used in any cycle of the iterative mean field calculation is either a pure translational basis or a pure rotational basis, and the secular problems are

much smaller than before. The price that we pay is the neglect of correlation between the single-particle translations and librations. This correlation is recovered in the RPA calculations described in the following section.

Once we have obtained the mean field Hamiltonians, we can calculate the thermodynamic properties of the system. The free energy can be found from Eq. (95) and other quantities follow from it:

$$\begin{aligned} A &= -k_B T \sum_P \ln Z_P^{MF} - \frac{1}{2} \sum_P \langle V_P^{MF} \rangle_P \\ S &= -\frac{\partial A}{\partial T} = k_B \sum_P \ln Z_P^{MF} + T^{-1} \sum_P \langle H_P^{MF} \rangle_P \\ E &= A + TS = \sum_P \langle H_P^{MF} \rangle_P - \frac{1}{2} \sum_P \langle V_P^{MF} \rangle_P \end{aligned} \tag{118}$$

The mean field partition function is $Z_P^{MF} = Z(H_P^{MF})$. In order to obtain the entropy in its final form, we have used the relation

$$\sum_P \left\langle \frac{\partial H_P}{\partial T} \right\rangle_P = \frac{1}{2} \sum_P \frac{\partial}{\partial T} \langle V_P^{MF} \rangle_P \tag{119}$$

which follows from Eq. (109).

Before we discuss the stability condition $\Delta A_{var}^{(2)} \geq 0$ on the mean field solution, we first describe the RPA formalism.

C. The Random Phase or Time-Dependent Hartree Approximation

The mean field model outlined in the preceding section provides us with a set of single-particle states

$$H_P^{MF} |\psi_P^{(\alpha)}\rangle = \varepsilon_P^{(\alpha)} |\psi_P^{(\alpha)}\rangle \tag{120}$$

from which we construct the crystal states

$$|\psi_{\{\alpha\}}^{MF}\rangle = \prod_P |\psi_P^{(\alpha_P)}\rangle \tag{121}$$

For all α_P equal to zero, Eq. (121) represents the ground state of the crystal. In order to keep the equations as simple as possible, we have again stopped explicitly indicating the coordinates on which all functions and operators depend. When the mean field Hamiltonian has the form of Eq. (117), the index P, from now on, must be interpreted as $P = \{\mathbf{n}, i, K\}$,

where $K = T, L$ distinguishes between the translating and librating "particles."

The shortcoming of the mean field method is that it admits no correlation between the motions of the individual particles. This correlation can be introduced by means of the random phase approximation (RPA) or time-dependent Hartree (TDH) method. In order to formulate this method, we introduce excitation operators $(E_P^\alpha)^\dagger$, which replace $\psi_P^{(0)}$ by $\psi_P^{(\alpha)}$ when applied to the mean field ground state of the crystal; when applied to any other state, they yield zero. Then, we write the Hamiltonian as a quadratic form in the excitation operators $(E_P^\alpha)^\dagger$ and their Hermitean conjugates E_P^α

$$H = \sum_{P \le P'} \sum_{\alpha\,\alpha'} \{A_{P,P'}^{\alpha\,\alpha'}(E_P^\alpha)^\dagger E_{P'}^{\alpha'} + B_{P\,P'}^{\alpha\,\alpha'}(E_P^\alpha)^\dagger (E_{P'}^{\alpha})^\dagger + (B_{P\,P'}^{\alpha\,\alpha'})^* E_P^\alpha E_{P'}^{\alpha'}\} \quad (122)$$

Linear terms are absent because of the Brillouin theorem. The coefficients $A_{P,P}^{\alpha\,\alpha}$ and $B_{P,P'}^{\alpha\,\alpha'}$ can be calculated by equating the nonzero matrix elements of the RPA Hamiltonian [Eq. (122)], in the basis of Eq. (121), to the corresponding matrix elements of the exact Hamiltonian [Eq. (23)] in the same basis. From the translational symmetry of the mean field states it follows that the A and B coefficients do not depend on the complete labels $P = \{\mathbf{n}, i, K\}$ and $P' = \{\mathbf{n}', i', K'\}$, but only on the sublattice labels $\{i, K\}$ and $\{i', K'\}$. The second ingredient of the RPA formalism is that we assume boson commutation relations for the excitation and de-excitation operators (Raich and Etters, 1968; Dunmore, 1972).

The RPA Hamiltonian [Eq. (122)] can be easily diagonalized. A partial diagonalization is already obtained by writing it in terms of operators

$$E_{i,K}^\alpha(\mathbf{q}) = \frac{1}{\sqrt{N}} \sum_{\mathbf{n}} \exp(i\mathbf{q}\cdot\mathbf{R}_\mathbf{n}) E_P^\alpha \quad (123)$$

with $P = \{\mathbf{n}, i, K\}$, adapted to the translational symmetry of the crystal. Just as in Section III,A, the commutation relations are preserved under this transformation. The next step is to define operators $a_\lambda^\dagger(\mathbf{q})$ that represent the exact excitation operators of the crystal, which satisfy the equations of motion

$$\begin{aligned} [H, a_\lambda^\dagger(\mathbf{q})] &= \omega_\lambda(\mathbf{q}) a_\lambda^\dagger(\mathbf{q}) \\ [H, a_\lambda(\mathbf{q})] &= -\omega_\lambda(\mathbf{q}) a_\lambda(\mathbf{q}) \end{aligned} \quad (124)$$

Expressing these operators as

$$a_\lambda^\dagger(\mathbf{q}) = \sum_{\alpha\,i\,K} \{x_{\alpha\,i\,K}^\lambda(\mathbf{q}) E_{i,K}^\alpha(\mathbf{q})^\dagger + y_{\alpha\,i\,K}^\lambda E_{i,K}^\alpha(-\mathbf{q})\} \quad (125)$$

leads to the RPA eigenvalue problem for the coefficients $x^{\lambda}_{\alpha,i,K}$ and $y^{\lambda}_{\alpha,i,K}$:

$$\begin{pmatrix} \boldsymbol{\chi} - \boldsymbol{\Phi}(\mathbf{q}) & -\boldsymbol{\Phi}(\mathbf{q}) \\ \boldsymbol{\Phi}(\mathbf{q}) & -\boldsymbol{\chi} + \boldsymbol{\Phi}(\mathbf{q}) \end{pmatrix} \begin{pmatrix} \mathbf{x}^{\lambda}(\mathbf{q}) \\ \mathbf{y}^{\lambda}(\mathbf{q}) \end{pmatrix} = \begin{pmatrix} \mathbf{x}^{\lambda}(\mathbf{q}) \\ \mathbf{y}^{\lambda}(\mathbf{q}) \end{pmatrix} \omega_{\lambda}(\mathbf{q}) \tag{126}$$

The diagonal matrix $\boldsymbol{\chi}$ contains the mean field excitation energies

$$\chi_{\alpha,i,K\,\alpha',i',K'} = \delta_{\alpha,\alpha'}\,\delta_{i,i'}\,\delta_{K,K'}[\varepsilon^{(\alpha)}_{\{i,K\}} - \varepsilon^{(0)}_{\{i,K\}}] \tag{127}$$

and the elements of the matrix $\boldsymbol{\Phi}(\mathbf{q})$ are defined as

$$\Phi_{\alpha\, i,K\,\alpha',i',K'}(\mathbf{q}) = \sum_{\mathbf{n}} \exp(i\mathbf{q}\cdot\mathbf{R}_{\mathbf{n}})\langle\psi^{(\alpha)}_{P}\psi^{(0)}_{P'}|\langle V_{\{\mathbf{0},i\}\{\mathbf{n},i'\}}\rangle_{P_c,P'_c}|\psi^{(0)}_{P}\psi^{(\alpha')}_{P'}\rangle$$

$$+ \delta_{i\,i'}\,\delta_{K,K'_c}\sum_{\mathbf{n}''}\sum_{i''}\langle\psi^{(\alpha)}_{P}\psi^{(0)}_{P_c}|\langle V_{\{\mathbf{0},i\}\{\mathbf{n}'',i''\}}\rangle_{Q,Q_c}|\psi^{(0)}_{P}\psi^{(\alpha')}_{P_c}\rangle \tag{128}$$

with $P = \{\mathbf{0}, i, K\}$, $P' = \{\mathbf{n}, i', K'\}$, $Q = \{\mathbf{n}'', i'', K\}$, $P_c = \{\mathbf{0}, i, K_c\}$, K_c is the complement of K and $|\psi^{(\alpha)}_{P}\psi^{(0)}_{P'}\rangle = |\psi^{(\alpha)}_{P}\rangle|\psi^{(0)}_{P'}\rangle$. When the mean field problem is separated for the translations and librations, as reflected by Eq. (117), the matrix $\boldsymbol{\Phi}(\mathbf{q})$ will have a block structure. The blocks $\boldsymbol{\Phi}^{\mathrm{TT}}(\mathbf{q})$ and $\boldsymbol{\Phi}^{\mathrm{LL}}(\mathbf{q})$ correlate the translational and librational motions of the molecules, respectively, and the off-diagonal blocks $\boldsymbol{\Phi}^{\mathrm{TL}}(\mathbf{q})$ and $\boldsymbol{\Phi}^{\mathrm{LT}}(\mathbf{q})$ account for the translation–rotation coupling. The second term of the elements of the latter matrices, given by Eq. (128), includes the coupling between the single-particle librations and translations. The eigenvalues $\omega_{\lambda}(\mathbf{q})$ in Eq. (126) provide the excitation energies of the crystal. The eigenvectors can be conceived as the polarization vectors that, in general, correspond to mixed translational–rotational modes. In using a quadratic Hamiltonian, the RPA model is similar to the harmonic model. The motions in the RPA model can be strongly anharmonic, however; they may even be hindered rotations.

The RPA formalism that we have just presented only applies at zero temperature. It is possible, however, to derive similar eigenvalue equations for the excitation frequencies $\omega_{\lambda}(\mathbf{q})$ by means of the time-dependent Hartree method (Fredkin and Werthamer, 1965; Hüller, 1974; Jansen *et al.*, 1984). The TDH equations are valid for finite temperature; in the limit of $T \to 0$ K, they become identical to the RPA equations. The TDH matrix that replaces the RPA matrix in the eigenvalue equations (126) can be written as

$$\mathbf{M}(\mathbf{q}) = \begin{pmatrix} -\mathbf{P} & \mathbf{0} \\ \mathbf{0} & \mathbf{P} \end{pmatrix} \begin{pmatrix} \boldsymbol{\Phi}(\mathbf{q}) - \boldsymbol{\chi} & \boldsymbol{\Phi}(\mathbf{q}) \\ \boldsymbol{\Phi}(\mathbf{q}) & \boldsymbol{\Phi}(\mathbf{q}) - \boldsymbol{\chi} \end{pmatrix} = \begin{pmatrix} -\mathbf{P} & \mathbf{0} \\ \mathbf{0} & \mathbf{P} \end{pmatrix} \mathbf{N}(\mathbf{q}) \tag{129}$$

where the diagonal matrix χ is given by

$$\chi_{\alpha,\beta,\iota,K,\alpha',\beta',\iota',K'} = \delta_{\alpha,\alpha'}\,\delta_{\beta,\beta'}\,\delta_{\iota,\iota'}\,\delta_{K,K'}\,\frac{\varepsilon_P^{(\alpha)} - \varepsilon_P^{(\beta)}}{P_P^{(\alpha)} - P_P^{(\beta)}} \qquad (\alpha > \beta) \quad (130)$$

and the matrix $\Phi(\mathbf{q})$ by

$$\Phi_{\alpha,\beta,\iota,K,\alpha',\beta',\iota',K'}(\mathbf{q}) = \sum_{\mathbf{n}} \exp(i\mathbf{q}\cdot\mathbf{R}_{\mathbf{n}})\langle\psi_P^{(\alpha)}\psi_{P'}^{(\beta')}|\langle V_{\{\mathbf{0},\iota\}\{\mathbf{n},\iota'\}}\rangle_{P_C,P_C'}|\psi_P^{(\beta)}\psi_{P'}^{(\alpha')}\rangle$$

$$+ \delta_{\iota,\iota'}\,\delta_{K,K_C'}\sum_{\mathbf{n}''}\sum_{\iota''}$$

$$\langle\psi_P^{(\alpha)}\psi_{P_C}^{(\beta')}|\langle V_{\{\mathbf{0},\iota\}\{\mathbf{n}'',\iota''\}}\rangle_{Q,Q_C}|\psi_P^{(\beta)}\psi_{P_C}^{(\alpha')}\rangle \qquad (131)$$

while $\mathbf{P}$ is a diagonal matrix containing population differences:

$$P_{\alpha,\beta,\iota,K,\alpha',\beta',\iota',K'} = \delta_{\alpha,\alpha'}\,\delta_{\beta,\beta'}\,\delta_{\iota,\iota'}\,\delta_{K,K'}\,[P_P^{(\alpha)} - P_P^{(\beta)}] \qquad (132)$$

with

$$P_P^{(\alpha)} = \langle\psi_P^{(\alpha)}|\rho_P^{\mathrm{MF}}|\psi_P^{(\alpha)}\rangle = \exp(-\beta\varepsilon_P^{(\alpha)})\Big/\sum_{\alpha}\exp(-\beta\varepsilon_P^{(\alpha)}) \qquad (133)$$

In the limit of $T \to 0$ K, $P_P^{(0)} = 1$ and $P_P^{(\beta)} = 0$ for $\beta > 0$; the matrix $\mathbf{P}$ becomes the unit matrix $\mathbf{I}$, and obviously, the TDH matrix $\mathbf{M}(\mathbf{q})$ given by Eqs. (129) to (132) reduces to the RPA matrix [see Eqs. (126)–(128)].

D. Stability Conditions for the Mean Field Solution

Just as there exist the so-called Thouless stability conditions on the Hartree–Fock solutions in nuclear physics (Thouless, 1960, 1961; Rowe, 1970) and in quantum chemistry (Čižek and Paldus, 1971), one has stability conditions on the mean field solutions in lattice dynamics problems (Fredkin and Werthamer, 1965). The mean field solutions are obtained from the condition $\Delta A_{\mathrm{var}}^{(1)} = 0$ (see Section IV,A). They are stable; i.e., they correspond with a local minimum in the free energy if $\Delta A_{\mathrm{var}}^{(2)} > 0$. Substituting the mean field solution (109) into the equation (107) for $\Delta A_{\mathrm{var}}^{(2)}$, the term with $\Delta\rho_P^{(2)}$ vanishes and we can express the stability condition as

$$\Delta A_{\mathrm{var}}^{(2)} = \frac{1}{2}\sum_{P\neq P'}\sum \mathrm{Tr}\{\Delta\rho_P^{(1)}\,V_{PP'}\,\Delta\rho_{P'}^{(1)}\}$$

$$+ \beta^{-1}\sum_P\int_0^\beta d\tau_1\,\tau_1\langle\tilde{h}_P^{\tau_1}h_P\rangle_{\mathrm{MF}} - \frac{1}{2}\beta\sum_P\langle h_P\rangle_{\mathrm{MF}}^2 > 0 \quad (134)$$

This condition must hold for arbitrary variations h_P, with the corresponding changes in the density operators $\Delta\rho_P^{(1)}$ as given by Eq. (104). Writing Eq. (134) in the main field basis $|\psi_P^{(\alpha)}\rangle$ and substituting the matrix elements of Eq. (104) in this basis, we find

$$\Delta A_{\text{var}}^{(2)} = \frac{1}{2}\sum_{P}\sum_{P'}\sum_{\alpha,\alpha'}\sum_{\beta,\beta'}\langle\psi_P^{(\alpha)}|\Delta\rho_P^{(1)}|\psi_P^{(\beta)}\rangle\langle\psi_{P'}^{(\beta')}|\Delta\rho_{P'}^{(1)}|\psi_{P'}^{(\alpha')}\rangle \times\left[\langle\psi_P^{(\beta)}\psi_{P'}^{(\alpha')}|V_{PP'}|\psi_P^{(\alpha)}\psi_{P'}^{(\beta')}\rangle - \delta_{\alpha,\alpha'}\,\delta_{\beta,\beta'}\,\delta_{P,P'}\,\frac{\varepsilon_P^{(\alpha)}-\varepsilon_P^{(\beta)}}{P_P^{(\alpha)}-P_P^{(\beta)}}\right] \tag{135}$$

The matrix elements of the variations in the density operators $\Delta\rho_P^{(1)}$ can be interpreted as arbitrary variation coefficients

$$c_{\alpha,\beta,P} = \langle\psi_P^{(\alpha)}|\Delta\rho_P^{(1)}|\psi_P^{(\beta)}\rangle \tag{136}$$

The second-order change in the free energy $\Delta A_{\text{var}}^{(2)}$ thus appears to be a quadratic form in these coefficients. If $\Delta A_{\text{var}}^{(2)}$ has to be positive for arbitrary variation coefficients $c_{\alpha,\beta,P}$, the Hessian of this form has to be positive definite. By Fourier transforming the coefficients, the Hessian can be block-diagonalized with blocks

$$\begin{pmatrix}\boldsymbol{\Phi}(\mathbf{q})-\boldsymbol{\chi} & \boldsymbol{\phi}(\mathbf{q}) & \boldsymbol{\Phi}(\mathbf{q})\\ \boldsymbol{\phi}(\mathbf{q})^{\dagger} & \mathbf{f}(\mathbf{q})-\mathbf{g} & \boldsymbol{\phi}(\mathbf{q})^{\dagger}\\ \boldsymbol{\Phi}(\mathbf{q}) & \boldsymbol{\phi}(\mathbf{q}) & \boldsymbol{\Phi}(\mathbf{q})-\boldsymbol{\chi}\end{pmatrix} \tag{137}$$

which each have to be positive definite. The matrices $\boldsymbol{\chi}$ and $\boldsymbol{\Phi}(\mathbf{q})$ are defined in Eqs. (130) and (131); the other submatrices have similar definitions (van der Avoird *et al.*, 1984), which are not relevant for the conclusion, however. Not only the matrices (137) have to be positive definite, but also all of their diagonal submatrices, in particular the matrices $\mathbf{N}(\mathbf{q})$, defined in Eq. (129), which we obtain from Eq. (137) by omitting the central rows and columns. From Eq. (129) it is not difficult to demonstrate that the eigenvalues of $\mathbf{N}(\mathbf{q})$ will all be positive if and only if the eigenvalues of $\mathbf{M}(\mathbf{q})$, which are the RPA frequencies, are all real (van der Avoird *et al.*, 1984). In that case the matrix $\mathbf{N}(\mathbf{q})$ is positive definite. Therefore, we find the following stability condition: $\Delta A_{\text{var}}^{(2)}$ will only be positive, i.e., the mean field solution will only be stable, if the matrix $\mathbf{N}(\mathbf{q})$ is positive definite. This implies that all TDH frequencies must be real. If at least one of these frequencies is complex, and one can prove that it will be purely imaginary, one finds negative eigenvalues of $\mathbf{N}(\mathbf{q})$ and one can choose variations $\Delta\rho_P^{(1)}$ around the mean field solution ρ_P^{MF} that make $\Delta A_{\text{var}}^{(2)}$ negative. In that case, the mean field solution does not correspond

to a local minimum in the free energy, but to a saddle point [or even a maximum if all eigenvalues of $\mathbf{N}(\mathbf{q})$ would be negative]. Following the direction(s) indicated by the variations that make $\Delta A^{(2)}_{\text{var}}$ negative, one can find a mean field solution of lower free energy.

V. Molecular Motions in Solid Nitrogen

Solid nitrogen is a very suitable system to illustrate the various lattice dynamics theories and to verify how well they describe the different motions that molecules can perform in a solid. Nitrogen has ordered phases in which the molecules librate around well-defined equilibrium orientations, as well as plastic, i.e., orientationally disordered, phases. In the latter case, the x-ray and neutron diffraction studies (Streib *et al.*, 1962; Jordan *et al.*, 1964; Schuch and Mills, 1970; Powell *et al.*, 1983) cannot determine the molecular orientations, and the nature of the molecular motions [i.e., (hindered) rotations or precessions or jumps between different equilibrium orientations] is still uncertain (Schuch and Mills, 1970; Press and Hüller, 1978; Powell *et al.*, 1983). Even in the ordered phases the amplitudes of the molecular librations are not very small, however, especially near the order–disorder phase transition, where "orientational melting" takes place. The ordered α and γ phases that exist at low temperature for pressures below and above 4 kbar, respectively, and the plastic β phase that occurs above $T = 35.6$ K (at zero pressure) have been subject to many experimental investigations. The structures of these phases are shown in Fig. 1. The results prior to 1976 have been collected by Scott (1976). Additional data are still becoming available, and new phases that are stable at higher pressures have been discovered (LeSar *et al.*, 1979; Cromer *et al.*, 1981), for which the molecular ordering is not as yet well established. All the lattice dynamics methods that we have described in Sections III and IV have been applied to the α and γ phases, the methods of Section IV also to the β phase. In this section we discuss the most characteristic results and compare them, with some emphasis on the formalism developed by ourselves, which holds both for small- and large-amplitude motions.

A. Theory for Linear Molecules

The orientations of linear molecules, relative to the global frame, can be specified by two Euler angles $\omega_P = \{\theta_P, \phi_P\}$; the symmetry-adapted functions $G^{(l)}_m(\omega_P)$ that occur in the intermolecular potential [Eq. (15)] reduce to Racah spherical harmonics $C^{(l)}_m(\theta_P, \phi_P)$. If the molecules possess a center of inversion such as N_2 (when we disregard the occurrence of mixed isotopes $^{14}N^{15}N$, the natural abundance of ^{15}N being only 0.37%),

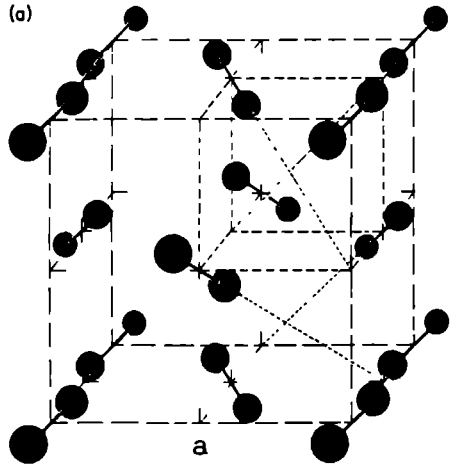

α-N_2, Pa3 (Z=4)
a=5.644 Å

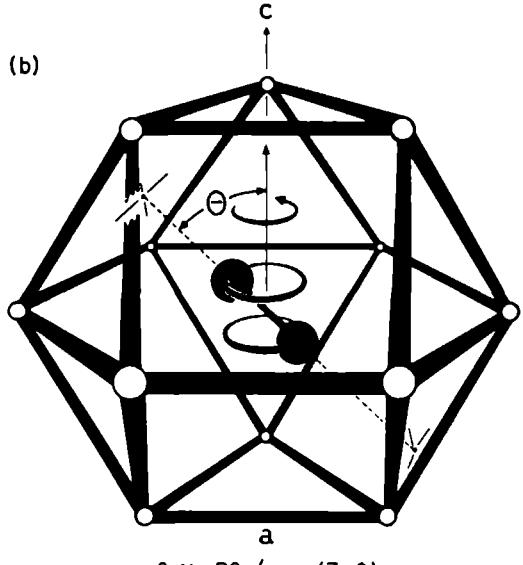

β-N_2, $P6_3/mmc$ (Z=2)
a=4.050 Å, c=6.604 Å

Fig. 1. Crystal structures of (a) α-, (b) β-, and (c) γ-nitrogen, according to Scott (1976).

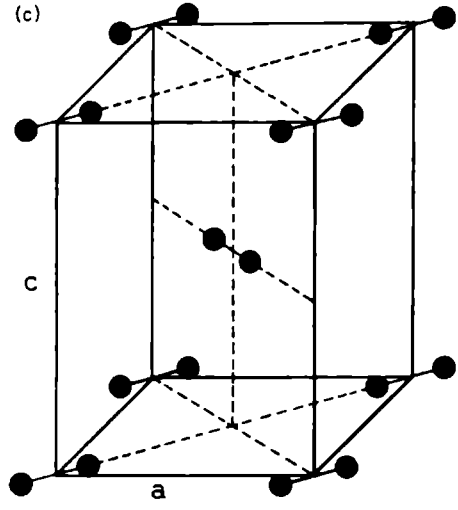

Fig. 1. (*Continued*)

just the even l values occur. The expression (26) for the rotational kinetic energy becomes simply

$$L(\omega_P) = BJ^2(\theta_P, \phi_P) \tag{138}$$

with the rotational constant $B = (2I)^{-1} = (2\mu r_0^2)^{-1}$. For $^{14}N^{14}N$ the average internuclear distance $r_0 = 1.094$ Å, the reduced mass $\mu = 7$ amu, and $B = 2.013$ cm^{-1}. The Wigner $D^{(l)}_{nm}(\omega_P)$ functions in the orientational basis [Eq. (111)] can also be replaced by spherical harmonics $C^{(l)}_m(\theta_P, \phi_P)$, with further restrictions on l depending on the nuclear permutation–inversion symmetry, which is related to the nuclear spin species. Therefore, for ^{14}N the nuclear spin $I = 1$ and the $^{14}N^{14}N$ molecules can be classified as *ortho*-N_2 with $I = 0$ or $I = 2$, and rotational basis functions with even l, and *para*-N_2 with $I = 1$ and a rotational basis with odd l. In lattice dynamics calculations (Dunmore, 1972; Jansen *et al.*, 1984; van der Avoird *et al.*, 1984), one has assumed that the crystal is composed of pure *ortho*-N_2 or pure *para*-N_2. The difference between the libron frequencies for ortho and para crystals is a measure for the quenching of the free N_2 rotations, i.e., the degree of orientational localization, caused by the rotational barriers from the anisotropic potential. In most cases, except for the delocalized solutions in β-nitrogen (van der Avoird *et al.*, 1984), one has found

very small ortho–para differences, which indicate a rather strong localization.

B. Results from Harmonic and Quasi-Harmonic Models

A large majority of the lattice dynamics calculations on nitrogen have employed the harmonic model. Naturally, these calculations concern the

TABLE IIIA

LATTICE FREQUENCIES IN α-N_2 (IN CM^{-1}), $T = 0$ K, $p = 0$

		Experiment[a]	Semiempirical harmonic[b]	*Ab initio* harmonic[c]	SCP[c]	RPA[d]
a (Å)		5.644	5.644	5.611	5.796	5.699
$\Gamma(0, 0, 0)$						
Librations	E_g	32.3	37.5	42.4	41.1	31.0
	T_g	36.3	47.7	52.9	50.7	41.0
	T_g	59.7	75.2	77.7	73.7	68.0
Translational vibrations	A_u	46.8	45.9	52.8	49.2	47.2
	T_u	48.4	47.7	52.6	49.0	48.8
	E_u	54.0	54.0	58.9	54.1	55.6
	T_u	69.4	69.5	78.8	73.3	73.1
$M\left(\frac{\pi}{a}, \frac{\pi}{a}, 0\right)$						
Mixed	M_{12}	27.8	29.6	34.9	32.7	27.6
	M_{12}	37.9	40.6	46.4	43.8	39.1
	M_{12}	46.8	51.8	59.1	55.8	50.2
	M_{12}	54.9	59.0	64.4	60.4	59.1
	M_{12}	62.5	66.4	72.3	67.6	66.5
$R\left(\frac{\pi}{a}, \frac{\pi}{a}, \frac{\pi}{a}\right)$						
Translational vibrations	R_1^-	33.9	34.4	37.1	34.7	34.4
	R_{23}^-	34.7	35.7	39.2	36.5	35.8
	R_{23}^-	68.6	68.3	77.6	72.3	72.3
Librations	R_1^+	43.6	50.7	58.1	55.2	47.9
	R_{23}^+	47.2	57.8	61.0	58.4	50.8
rms deviation of librational frequencies			10.6	14.8	12.2	5.0
rms deviation of translational frequencies			0.6	6.3	2.4	2.1
rms deviation of all lattice frequencies			6.1	10.4	7.6	3.4

[a] From Kjems and Dolling (1975).
[b] From Raich and Gillis (1977).
[c] From Luty *et al.* (1980).
[d] From Briels *et al.* (1984).

ordered α and γ phases, although sometimes the translational vibrations in the β phase have been considered, too, with the molecular rotations neglected. The only nontechnical difference between these harmonic treatments lies in the potentials used, which are practically always empirical model potentials mostly of the atom–atom and/or quadrupole–quadrupole type (see Section II). It is generally believed that, particularly, the phonon frequencies are very sensitive to the shape of the intermolecular potential, the translational frequencies to its distance dependence and the librational modes to its anisotropy. The experimental phonon frequencies from infrared and Raman spectroscopy (for wave vector $\mathbf{q} = \mathbf{0}$) and from inelastic neutron scattering (for any $\mathbf{q}$) have been used to optimize the parameters in the model potentials. As an example of the most sophisticated work of this type, we quote the paper by Raich and Gillis (1977). The results listed in the second columns of Tables IIIA and IIIB are characteristic: fairly good agreement with experiment for the pure translational phonon frequencies and substantially worse agreement for the librational modes even after optimizing the parameters. The discrepancy has been ascribed to the strong anharmonicity and rather large amplitudes of the librations, even at the lowest temperatures. A study by Luty *et al.* (1980) using a nonempirical N_2–N_2 site–site potential obtained from quantum-chemical *ab initio* calculations (Berns and van der Avoird, 1980) yields similar results (see the third columns of Tables IIIA, B). The overall agreement in the *ab initio* treatment, which involves no parameter

TABLE IIIB

LATTICE FREQUENCIES IN γ-N_2 (IN CM^{-1}), $T = 0$ K, $p = 4$ KBAR

		Experiment[a]	Semiempirical harmonic[b]	*Ab initio* harmonic[c]	SCP[c]	RPA[d]
a (Å)		3.957	3.940	4.032	4.100	3.961
c (Å)		5.109	5.086	5.000	5.188	5.104
$\Gamma(0, 0, 0)$						
Librations	E_g	55.0	50.5	60.1	58.7	67.6
	B_{1g}	98.1	74.8	89.2	87.9	103.3
	A_{2g}		105.1	111.2	108.6	124.4
Translational vibrations	E_u	65.0	58.3	71.4	68.7	65.2
	B_{1u}		103.1	113.8	110.9	114.9
rms deviation			14.2	7.0	6.6	7.9

[a] From Thiéry and Fabre (1976) and Fondére *et al.* (1981).
[b] From Raich and Gillis (1977).
[c] From Luty *et al.* (1980).
[d] From Briels *et al.* (1980).

optimization, is slightly worse. We shall illustrate, however, that this is largely due to the harmonic approximation made in the lattice dynamics calculation. We observe, at this point, a weakness of the semiempirical procedure: optimizing a parameterized potential by comparing approximate, mostly harmonic, lattice dynamics results with measured data might lead to incorrect potentials and, at the same time, partly hide the flaws of the approximate lattice dynamics model.

Harris and Coll (1972), Kobashi (1978), and Kuchta and Luty (1983) have used anharmonic perturbation theory (see Section III,B) to study the effect of the cubic and quartic anharmonicities on the libron and phonon frequencies in α-nitrogen. The results are conflicting, however, and the shifts appear to depend very sensitively on the potential. Harris and Coll (1972), using only the quadrupole–quadrupole interactions, find a reduction of the libron frequencies by about 12%, whereas Kobashi (1978), using a 12–6 atom–atom potential, finds an increase in all libron and phonon frequencies by 4 to 14 cm^{-1}, i.e., 7 to 17%. Kuchta and Luty (1983), using a perturbed uncoupled oscillator model starting from the *ab initio* potential of Berns and van der Avoird (1980), obtain a decrease of the harmonic libron frequencies by 18 to 27%. The agreement of the latter results, after the perturbation correction, with experimental data must probably be regarded as fortuitous, however, since the anharmonic corrections for the librations are too large to be treated by perturbation theory up to the second order.

A similar influence of the potential chosen occurs if one tries to calculate the anharmonic effects by the self-consistent phonon (SCP) method. The calculation by Raich *et al.* (1974) is based on the atomic version of the SCP method (see Section III,C). Using an empirical 12–6 atom–atom potential, they found a consistent increase of the harmonic phonon and libron frequencies by 3 to 10%. The calculation by Luty *et al.* (1980), who use the SCP method of Wasiutynski (1976) and the *ab initio* N_2–N_2 potential of Berns and van der Avoird (1980), yields a consistent lowering by about the same amount. It is striking (see Tables IIIA,B, fourth columns) that the *ab initio* results for the pure translational phonon frequencies in α- and γ-nitrogen agree remarkably well with experiment, without any parameter optimization, while the librational frequencies and those of the mixed modes are still substantially too high. Apparently the anharmonicity in the distance dependence of the intermolecular potential, which affects the translational vibrations, is very well accounted for by the SCP method. The orientational dependence of the potential is strongly anharmonic. In combination with the fairly large amplitudes of the rotational oscillations, this causes the SCP method to fail in describing the librational motions. This failure may be related to the additional approximations made in generalizing this method to molecular crystals.

Raich *et al.* (1974) and Goldman and Klein (1975) have applied the SCP method to the translational phonons in β-nitrogen. The molecular rotations were assumed to be completely free and the effective isotropic intermolecular potential used was a rotationally averaged, empirical atom–atom 12–6 potential. The results of such models that completely neglect any translation–rotation coupling are mainly of qualitative interest.

C. Large-Amplitude Motions in the Ordered Phases

Since it became clear from various observations that the librational motions of the molecules, even in the ordered α and γ phases of nitrogen at low temperature, have too large amplitudes to be described correctly by (quasi-) harmonic models, we have resorted to the alternative lattice dynamics theories that were described in Section IV. Most of these theories have been developed for large-amplitude rotational oscillations, hindered or even free rotations, and remain valid when the molecular orientations become more and more localized.

Weis and Klein (1975) made classical molecular dynamics (MD) calculations for 250 N_2 molecules in a cubic box, with periodic boundary conditions. These molecules were initially arranged in the cubic Pa3 structure of α-nitrogen, and they were made to interact via a 12–6 atom–atom potential. The molecular motions were mainly characterized via the calculated dynamic structure factor $S(\mathbf{q}, \omega)$, which describes the response of the system to a transfer of momentum $\mathbf{q}$ and energy $\hbar\omega$ (see Section IV,A). Because for given wave vector $\mathbf{q}$ the peaks in $S(\mathbf{q}, \omega)$ can be identified with phonons, the results of these calculations could be compared with (quasi-) harmonic lattice dynamics studies. The phonon frequencies appeared to be substantially different from the quasi-harmonic results calculated with the same atom–atom potential, and the temperature shifts of some of the peaks were much larger in the MD calculations. These differences and the corresponding peak broadenings have been ascribed by Weis and Klein to the occurrence of strongly anharmonic, large-amplitude motions that cause the breakdown of the quasi-harmonic model. At a temperature, of 35 K, close to the α–β phase transition point, the MD calculations even indicate the existence of "quasi-free" rotations.

Jacobi and Schnepp (1972) and Raich (1972) were the first to develop a quantum-dynamical model for the large-amplitude librations in α-nitrogen. Their formalism is essentially described in Section IV,C. They first calculated single-molecule mean field states that may be localized as well as delocalized, depending on the height of the rotation barriers from the anisotropic potential. These states were used to construct a basis of excitonlike wave functions for the whole crystal. The final step in their calcu-

lation, the diagonalization of the full-crystal Hamiltonian in this basis, amounts to diagonalizing the upper left block of the RPA matrix, Eq. (126). Therefore, this theory is more approximate than the RPA formalism; one of the consequences is that it does not converge to the harmonic solution in the limit of an exactly harmonic crystal Hamiltonian. If the excitonlike model were applied to the translational phonons rather than to the librations, the acoustical modes would not go to zero frequency for $\mathbf{q} = \mathbf{0}$. Employing the full RPA method, as described in Section IV,C, ensures the convergence to the correct limits; this method has been applied to the librations in α-nitrogen by Dunmore (1972, 1976), Raich *et al.* (1974), and Mandell (1974, 1975).

All these authors have used semiempirical N_2–N_2 potentials, often simplified to the utmost by retaining only pure quadrupole–quadrupole interactions or atom–atom 12–6 interactions. Moreover, they have always fixed the molecules with their centers of mass to the lattice points, thus neglecting the translational vibrations and the effects of libron–phonon coupling. We applied the RPA formalism to α- and γ-nitrogen (Jansen *et al.*, 1984) by using the *ab initio* potential of Berns and van der Avoird (1980). This potential was not approximated by a site–site model this time, but expanded in symmetry-adapted functions as in Section II,B. In a subsequent paper (Briels *et al.*, 1984) we extended the theory in order to account explicitly for the translational phonons and for libron–phonon coupling after expanding the crystal Hamiltonian as in Section II,D. The extended formalism is described in Section IV,C. Since this treatment is more complete than any of the previous ones, we shall use its results as an illustration.

We have started by assuming the observed lattice symmetry and by theoretically optimizing the cell parameters for the given *ab initio* potential as follows. For α-nitrogen we have calculated the minimum of the free energy in the mean field approximation as a function of the cubic cell parameter a. This yields the optimum value $a = 5.699$ Å, experimentally (Scott, 1976) $a = 5.644$ Å, and the mean field lattice cohesion energy at $T = 0$ K of $\Delta E = 5.92$ kJ/mol, experimentally $\Delta E = 6.92$ kJ/mol. For the γ phase we have calculated the free energy A for several values of the tetragonal cell parameters a and c and fitted $A(a, c)$ by a second-order polynomial. On each curve of constant molar volume $v = Na^2c/2$, we have determined the optimum a and c by minimizing A. Using the optimum points and the corresponding free energies, we have calculated the pressure as $p = -\partial A/\partial v$. Thus we found at $p = 4$ kbar that $a = 3.961$ Å and $c = 5.104$ Å, in excellent agreement with the experimental values $a = 3.957$ Å and $c = 5.109$ Å (Scott, 1976).

The mean field approximation yields a picture of the single-molecule

motions as determined by the anisotropic *ab initio* potential. The orientational probability distributions in α- and γ-nitrogen are shown in Fig. 2a,b, respectively. We clearly observe that the librations of the molecules in the α phase are localized about the cubic body diagonals, i.e., the [1, 1, 1] direction and three equivalent directions. In γ-nitrogen the N_2 molecules appear to librate about the [1, 1, 0] and [1, −1, 0] directions. Both these findings agree with experiment, cf. Fig. 1. For temperatures up to at least 40 K, these pictures remain qualitatively similar. The amount of delocalization is measured by the decreasing order parameter $S = \langle P_2(\cos\theta)\rangle$ (see Fig. 3), with θ now defined relative to the equilibrium axis. Even at T = 0 K the root-mean-square amplitude of the librations is already substantial, however, about 16° in the α-phase. Similar parameters, including the translational vibrations, are listed in Table IV. We observe that the molecular motions, both librational and translational, in γ-nitrogen at p = 4 kbar are more restricted than in the α phase, at zero pressure.

After calculating the ground and excited mean field states of α- and γ-nitrogen, we have included the correlation between the molecular motions, as well as the translational–rotational coupling, by determining the eigenvalues of the RPA matrix **M(q)** [Eq. (129)]. The expansion of the potential in the translational displacements ($\mathbf{u}_P$) of the molecules [see Eq.

TABLE IV

TRANSLATIONAL AND LIBRATIONAL AMPLITUDES FROM MEAN FIELD CALCULATIONS

α-N_2	T = 0 K	p = 0
$\langle u_\parallel^2\rangle^{1/2}$ = 0 112 Å		$u_\parallel = u_{[1\,1\,1]}$
$\langle u_\perp^2\rangle^{1/2}$ = 0 107 Å		
$\langle u^2\rangle^{1/2}$ = 0 189 Å		
$\arccos(\langle\cos^2\theta\rangle^{1/2})$ = 16.1°		
γ-N_2	T = 0 K	p = 4 kbar
$\langle u_\parallel^2\rangle^{1/2}$ = 0 100 Å		$u_\parallel = u_{[1\,1\,0]}$
$\langle u_{\perp ab}^2\rangle^{1/2}$ = 0 086 Å		$u_{\perp ab} = u_{[1\,-1\,0]}$
$\langle u_{\perp c}^2\rangle^{1/2}$ = 0 087 Å		$u_{\perp c} = u_{[0\,0\,1]}$
$\langle u^2\rangle^{1/2}$ = 0 159 Å		
$\arccos(\langle\cos^2\theta\rangle^{1/2})$ = 12 9°		
asymmetry parameter (rotation out of ab plane − rotation in ab plane): $\dfrac{\langle\sin^2\theta(\sin^2\varphi - \cos^2\varphi)\rangle}{\langle\sin^2\theta\rangle}$ = 0 05		

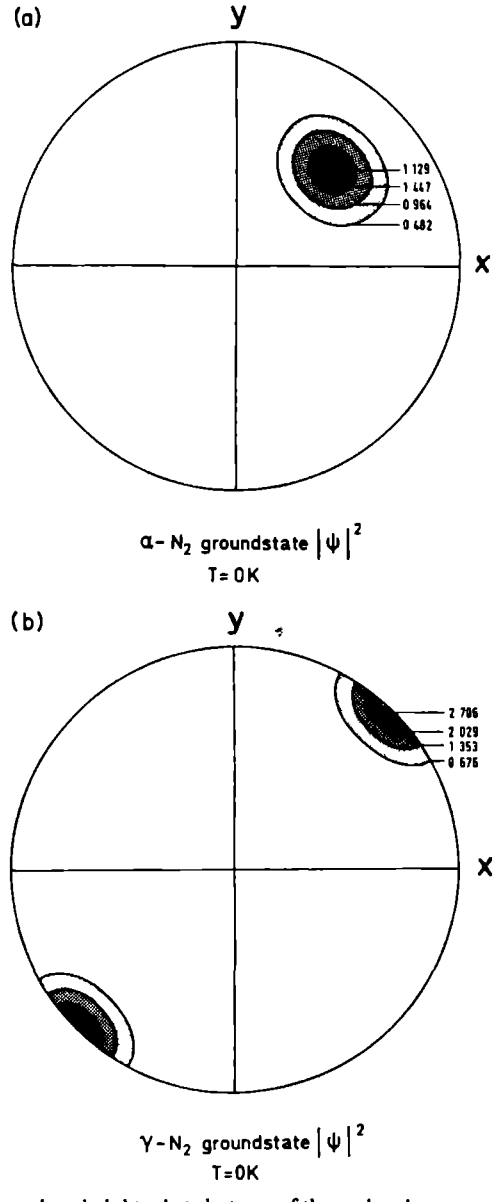

Fig. 2. Orientational probability distributions of the molecular axes in (a) α-nitrogen and (b) γ-nitrogen Contours of constant probability for the molecule in the origin, calculated in the mean field model, are plotted as functions of the polar angles (θ, ϕ) with respect to the crystal axes (Fig 1) The angle θ increases linearly with the radius of the plots from 0 (in the center) to $\pi/2$ (at the boundary), ϕ is the phase angle

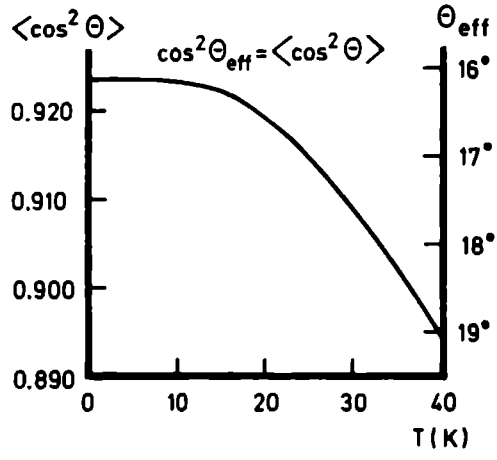

Fig. 3. Temperature dependence of the (mean field) order parameter in α-N_2.

(40)] has been truncated at three different levels. Taking $\alpha_{max} = 2$ corresponds to a harmonic model for the translational phonons; taking $\alpha_{max} = 3$ and $\alpha_{max} = 4$ includes the cubic and quartic anharmonicities, respectively. The orientational (ω_p) dependence of the *ab initio* potential has always been included exactly, which is important because of the large amplitude of the librons. Some typical results are shown in Table V. The size of the anharmonic corrections to the translational phonon frequencies is comparable with that of the self-consistent phonon corrections calculated with the same *ab initio* potential (Luty *et al.*, 1980); the corrected frequencies agree equally well with experiment. There is an important difference, however, between our RPA formalism and the SCP method. The latter neglects those terms in the potential that depend on the odd powers of the molecular displacements. The cubic terms have sometimes been added perturbationally (Goldman *et al.*, 1968; Koehler, 1969), but not so by Luty *et al.* (1980). Our formalism includes the effects of the cubic terms directly in the mean field and RPA results. In α-nitrogen, however, because of the inversion symmetry, they vanish at the mean field level and have no effect on the purely translational phonon frequencies of Table V. In the mixed phonon–libron modes the cubic corrections mostly lower the frequencies, while the quartic corrections are always positive and dominant.

We wish to emphasize that the most essential advantage of the RPA method discussed here over the previous (quasi-) harmonic treatments is the correct description of the large-amplitude libron modes and the mixed libron–phonon modes. This is reflected by the substantial anharmonic corrections in the frequencies of these modes; compare the last column of

TABLE V

α_{max} DEPENDENCE OF SOME RPA LATTICE FREQUENCIES FOR α-N_2 (a = 5.644 Å, T = 0 K)

		Frequency ω (cm^{-1})		
		$\alpha_{max} = 2^a$	$\alpha_{max} = 3$	$\alpha_{max} = 4$
$\Gamma(0, 0, 0)$				
Librations	E_g	32.8	32.8	32.8
	T_g	43.4	43.4	43.4
	T_g	71.6	71.6	71.5
Translations	A_u	42.3	42.3	50.6
	T_u	48.7	48.7	52.7
	E_u	55.7	55.7	60.2
	T_u	73.0	73.0	79.4
$M\left(\frac{\pi}{a}, \frac{\pi}{a}, 0\right)$				
Mixed	M_{12}	28.8	25.7	28.8
	M_{12}	40.4	38.5	41.5
	M_{12}	52.2	51.7	53.3
	M_{12}	60.0	61.2	63.7
	M_{12}	67.0	68.6	72.0

[a] Harmonic model for translations.

Table III with the preceding columns. The new results calculated with the *ab initio* potential agree very well with the frequencies from inelastic neutron scattering (Kjems and Dolling, 1975) and from infrared and Raman spectroscopy (Thiéry and Fabre, 1976; Fondère *et al.*, 1981) for all types of modes. Also the phonon dispersion relations, displayed in Fig. 4, are in good agreement with the neutron-scattering data. Since most of the lattice modes are actually mixed libron–phonon modes, this indicates that the translation–rotation coupling is correctly included in the RPA formalism.

D. The Plastic Phase and the Orientational Order–Disorder Phase Transition

Lattice dynamics calculations on the plastic β-nitrogen phase are relatively scarce because, obviously, the standard (quasi-) harmonic theory cannot be applied to this phase. Classical Monte Carlo calculations have been made by Gibbons and Klein (1974) and Mandell (1974) on a face-centered cubic (α-nitrogen) lattice of 108 N_2 molecules, while Mandell has also studied a 32-molecule system and a system of 96 N_2 molecules on a hexagonal close-packed (β-nitrogen) lattice. Gibbons and Klein used 12–6

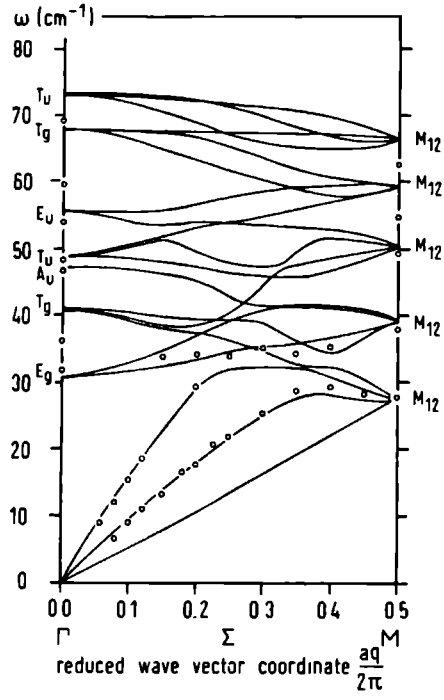

Fig. 4. Calculated (TDH) dispersion curves for α-N_2, for phonon–libron modes propagating along the [110] direction. The circles correspond to inelastic neutron scattering data measured at T = 15 K by Kjems and Dolling (1975).

and 9–6 atom–atom potentials and fairly high temperatures, T = 96 and 192 K; they found only complete orientational disorder. Mandell made his N_2 molecules interact as pure point quadrupoles, and he showed that even the smaller 32-molecule system already yields a fairly realistic order–disorder phase transition.

Another simple, quantum-mechanical, model for the phase transition has been proposed by Raich and Etters (1972). They studied N_2 molecules on an fcc lattice, again interacting as pure point quadrupoles. Using a mean field model for the librations in the α phase, a free rotor model for β-nitrogen, and calculating the corresponding free-energy curves, they found an α–β phase transition at somewhat too high a temperature. This model has been refined by Raich *et al.* (1974) and Goldman and Klein (1975), who applied the self-consistent phonon method to the translational and librational motions in the α phase and to the pure translational phonons in the β phase (cf. Section V,B). The rotational motions in β-nitrogen were still assumed to be completely free, however, and any

translation–rotation coupling was neglected. Classical molecular dynamics calculations by Klein *et al.* (1977, 1981) on a 288-molecule model for β-nitrogen at $T = 47$ K indicate that this coupling is probably important, since the translational phonon frequencies derived from these MD calculations, while using the same 12–6 atom–atom potential, are substantially different from the SCP results of Raich *et al.* (1974). The rotational motions in the β phase were found to be "quasi-free" in the classical MD model.

Finally, we discuss the mean field and RPA calculations made on β-nitrogen (van der Avoird *et al.*, 1984) by using the *ab initio* potential of Berns and van der Avoird (1980) again. We started our calculations on this phase, just as those for α- and γ-nitrogen, by assuming the experimentally observed lattice symmetry. Thus, the two molecules in the hexagonal unit cell (see Fig. 1) were given translationally equivalent mean field solutions. The orientational probability distribution that results for the pure *ortho*-N_2 crystal is shown in Fig. 5a. The ground state of the *para*-N_2 species is twofold degenerate; the average probability distribution $\frac{1}{2}|\psi_1|^2 + \frac{1}{2}|\psi_2|^2$ is similar to Fig. 5a. This picture suggests that the orientational motions in β-nitrogen are quasi-free precessions around the crystal c axis, modulated by small sixfold barriers. In accordance with the ideas of Press and Hüller (1978) and the earlier mean field calculations by Dunmore (1976), the precession angle θ between the molecular axis and the c axis is not sharply defined, but it shows a rather broad distribution with the maximum at the "experimental" value of $\theta = 56°$ (Scott, 1976).

The mean field ground state yielding this delocalized picture appeared to be unstable, however. This could be concluded from the ensuing RPA calculations yielding imaginary libron frequencies and the stability conditions in Section IV,D. We have searched for a stable mean field solution by independently varying the orientational wave functions of the two molecules in the unit cell, and we have indeed found such a solution, which is lower in (free) energy by 0.87 kJ/mol than the previous delocalized solution at $T = 0$ K. In this new solution the orientations of the N_2 molecules are clearly localized (see Fig. 5b). They librate about an equilibrium axis that makes an angle of 52° with the crystal c axis. The equilibrium axes for the two neighboring molecules in the hexagonal unit cell are not the same, but they are rotated through 180° about the c axis. This 180° rotation avoids the steric hindrance between neighbors that would occur when the molecules were freely precessing (Schuch and Mills, 1970) and, thus, leads to the lower free energy.

The problem with this localized, stable, mean field solution is that it has a much lower symmetry than the experimentally observed hexagonal symmetry of β-nitrogen. We have conjectured that the higher symmetry is

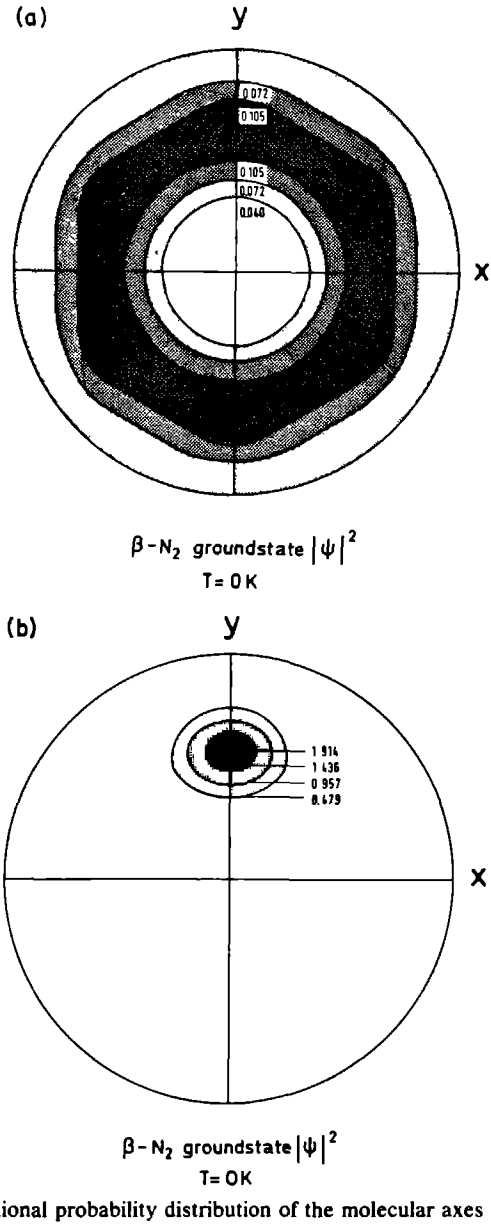

Fig. 5. Orientational probability distribution of the molecular axes for the delocalized (a) and localized (b) mean field states in β-nitrogen. (a) applies to both molecules in the unit cell. (b) is drawn for one molecule in the unit cell; the other molecule in the cell is rotated over $\phi = 180°$. The distribution does not change qualitatively up to (at least) $T = 70$ K; it just becomes slightly wider with increasing temperature. Reading of the contour plot as in Fig. 2.

observed because of rapid jumps of the molecular axes between six localized librational states of the type found in the final mean field calculation. The six equilibrium axes will be located at $\theta \simeq 52°$ and $\phi = 0°$, 60°, 120°, 180°, 240°, and 300°. The characteristic time for these jumps should be less than the inverse frequency of the nuclear quadrupole resonance measurements (de Reggi *et al.*, 1969), i.e., about 10^{-7} sec. In order to preserve the lower energy of the stable mean field solution, the jumps of neighboring molecules must be correlated; two neighbors have the tendency to remain 180° out of phase in their ϕ angles.

With the different models emerging for the molecular motions in the β phase and the mean field model for localized, large-amplitude librations in the α phase (see Section V,C), we have studied the α–β phase transition. The calculated free-energy curves corresponding with these models are shown in Fig. 6. The free energy for the delocalized precession model of β-nitrogen decreases much more steeply, with increasing temperature, than that for α-nitrogen. This is caused by the spectrum of the delocalized β-N_2 model being like a free rotor, with considerably smaller excitation

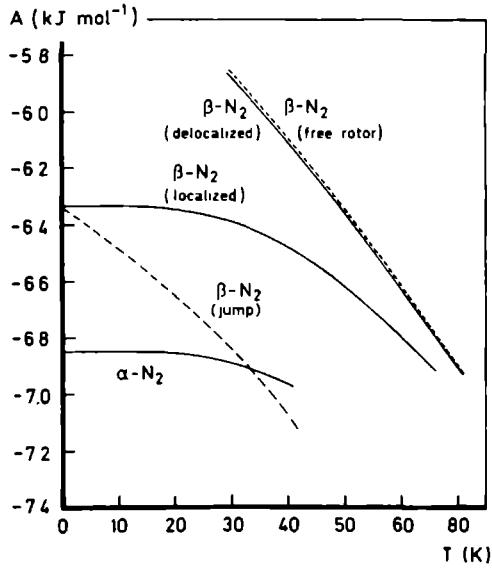

Fig. 6. Free energy (at zero pressure) for α-nitrogen and β-nitrogen, in different mean field models (closed lines). The dashed free rotor curve has been calculated from the isotropic $(l_1, l_2, l_3) = (0, 0, 0)$ term of the *ab initio* potential by adding the free rotor expression for the free energy. The dashed jump model curve has been obtained from the localized mean field solution (with the full anisotropic potential) by adding an entropy term $-k_B T \ln 6$ (see the text).

energies than the harmonic oscillatorlike spectrum of α-N_2. As shown in Fig. 6, a free rotor model for β-N_2 yields almost the same free-energy curve as the delocalized precession model. However, both these models cannot give a free energy lower than that for α-N_2, and thus a phase transition, at any reasonable temperature. On the other hand, the localized librational solution for β-N_2 is much lower in energy, but its free-energy curve does not sufficiently fall off with temperature to cross the α-N_2 curve. Now we invoke the jumps of the molecules between the localized solutions. Ignoring, for the moment, the correlations between these jumps and assuming that each molecule has access to six localized states yields an entropy term $-k_B T \ln 6$. Adding this term to the free-energy curve of a particular localized solution leads to the curve in Fig. 6 marked "β-N_2 jump." This model predicts an α–β phase transition temperature of 34 K, very close to the experimental value $T = 35.6$ K.

Starting from the localized mean field wave functions, we have also calculated the libron frequencies in β-nitrogen via the RPA formalism. All frequencies appeared to be real, as they should be for a stable mean field solution. The infrared spectrum (Medina and Daniels, 1976) shows two very broad peaks around 25 to 36 cm^{-1} and 50 to 68 cm^{-1}, depending on the pressures. The first one has been interpreted as a translational phonon band, the second one as a libron band. Neutron scattering (Kjems and Dolling, 1975) yields broad peaks at 25 and 64 cm^{-1} attributed to translational phonons. We have calculated optical libron frequencies of 34, 41, 56, and 59 cm^{-1}. The observed broad peaks may well contain these libron excitations in addition to the translational phonon bands. We assign the broadening of these peaks to the occurrence of more or less random transitions, classically called jumps, between the different localized libron states.

In summary, we think that our calculations suggest a model with localized librations and 60° jumps for the orientational motions in β-nitrogen. This model gives a reasonable account of the α–β phase transition and the libron spectrum of β-N_2. A dynamical model for the 60° jumps, which must include strong short-range pair correlations, is still lacking, however. Possibly this correlation can be introduced by using Jastrov functions (van Kranendonk, 1983).

VI. Dynamics and Magnetism of Solid Oxygen

Oxygen, with its $^3\Sigma_g^-$ ground state, is one of the few stable molecules with a nonvanishing electronic spin momentum. The potential between O_2 molecules is not only determined by the usual van der Waals interactions occurring between closed shell molecules, but it contains, moreover, the

coupling between the electronic spins. In addition to their positional and orientational coordinates, the O_2 molecules have an extra degree of freedom: the orientations of their triplet spin momenta. Consequently, in the solid we must consider the molecular motions, translational and rotational, as well as the spin dynamics.

This extra degree of freedom makes solid O_2 one of the most interesting molecular crystals. Even at low pressure one finds three different phases: the α phase between 0 and 23.8 K, the β phase between 23.8 and 43.8 K, and the γ phase between 43.8 K and the melting point at 54.4 K. These phases have structural as well as magnetic order. The α and β phases are orientationally ordered; the γ phase is plastic. The α phase is antiferromagnetic, with the usual (spin up, spin down) two-sublattice structure; α-oxygen is the only homogeneous antiferromagnet known. The β phase probably has short-range antiferromagnetic order with a three-sublattice 120° spin arrangement. The γ phase is paramagnetic, just like liquid oxygen. Both in the α and β phases the molecules are packed in layers, the a–b planes, with their axes perpendicular to these planes (see Fig. 7). In the β phase this packing is hexagonal; in the monoclinic α phase the hexagons are slightly distorted by a contraction in the **a** direction and a dilation in the **b** direction. This distortion is driven by the magnetic coupling: the α–β phase transition is called magnetoelastic. The spins in the α phase are preferentially directed in the $\pm$**b** directions.

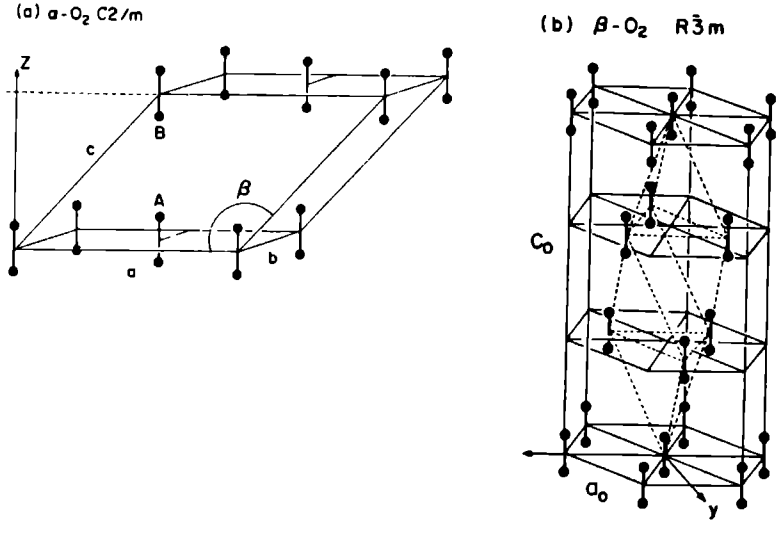

Fig. 7. Crystal structures of (a) α-oxygen and (b) β-oxygen, according to De Fotis (1981).

The excitations in such a magnetic solid are not only due to the lattice vibrations, phonons, and librons, but also to the spin waves; the corresponding quasi-particles are called magnons. The magnetic excitations in α-O_2 have been directly observed by infrared and Raman spectroscopy and by inelastic neutron scattering. In general, they determine, of course, the magnetic properties of the system, susceptibilities, spin flop processes, etc. They also affect other properties, though, such as the specific heat and the thermal expansion coefficients. For the experimental and theoretical work prior to 1981 we refer to De Fotis's (1981) review, which begins by stating that "the magnetic, structural, thermodynamic and spectroscopic properties of the condensed phases of oxygen have been under study for nearly a century. Yet important aspects of their behavior remain poorly understood." Work by Slyusarev *et al.* (1980, 1981), Gaididei and Loktev (1981), Stephens *et al.* (1983), Meier *et al.* (Meier *et al.*, 1982; Meier and Helmholdt, 1984; Meier, 1984), Etters *et al.* (Etters *et al.*, 1983; Helmy *et al.*, 1984), and van der Avoird *et al.* (van Hemert *et al.*, 1983; Wormer and van der Avoird, 1984; Jansen and van der Avoird, 1985) has provided additional information.

A. Lattice Dynamics and Spin Wave Calculations

Until very recently, the lattice vibrations in solid O_2 and its magnetic properties have always been treated separately. As far as the packing in the crystal and the lattice vibrations are concerned, one can consider the O_2 molecules as resembling N_2. An important quantitative difference lies in the O_2 molecule's quadrupole moment, however, which is about four times smaller than that of N_2 (in absolute value). This smaller quadrupole moment, together with the exchange coupling between the open-shell O_2 molecules (see the subsequent discussion), probably explains why the packing in the ordered α and β phases of solid O_2 (see Fig. 7) is very different from the ordered N_2 structures (see Fig. 1) (English and Venables, 1974; English *et al.*, 1974). The lattice dynamics calculations that have been made for α- and β-oxygen (Kobashi *et al.*, 1979; Etters *et al.*, 1983; Kuchta, 1985) are very similar to the standard harmonic calculations made on solid nitrogen (see Section V); they have used empirical atom–atom 12–6 or exp −6 potentials. The calculated optical libron frequencies are generally in reasonable agreement with the experimental data. One important observation could not be explained by these calculations, however, In β-oxygen there is a degenerate optical ($\mathbf{q} = \mathbf{0}$) libron mode of E_g symmetry with a frequency of about 50 cm^{-1}. This mode corresponds with the in-phase librations of all O_2 molecules around the crystal **a** and **b** axes, and the degeneracy occurs because of the equivalence of these axes in the hexagonal β phase. When the hexagonal sym-

metry is distorted by going through the β–α phase transition, this mode will be split, in principle. The librations around the monoclinic **b** axis in α-O_2 have A_g symmetry; those around the **a** axis have B_g symmetry. The splitting actually observed by Raman spectroscopy is so large, however, that it cannot be explained by any of the lattice dynamics calculations. The experimental spectrum of α-O_2 shows two peaks at 43 and 79 cm^{-1}, whereas the lattice dynamics calculations yield a splitting of about 10 cm^{-1} at most. The latter result is not surprising in view of the small structural distortion that accompanies the β–α phase transition. Most authors have assumed, therefore, that the A_g and B_g modes remain very nearly degenerate in α-O_2 and that the higher-frequency peak represents a two-libron, two-phonon, or libron–magnon transition. Experiments by Bier and Jodl (1984) indicate, however, that the mode at 43 cm^{-1} is probably the B_g mode and the mode at 79 cm^{-1} the A_g mode. We shall give an explanation of this phenomenon in the next section.

The magnetic properties of α-O_2, which is the most extensively studied phase, have always been interpreted on the basis of the following phenomenological spin Hamiltonian:

$$H_{\text{spin}} = -\frac{1}{2}\sum_{P\neq P'}\sum 2J_{PP'}\mathbf{S}_P \cdot \mathbf{S}_{P'} + \sum_P (AS_{zP}^2 + BS_{yP}^2) \qquad (139)$$

where z is the preferred magnetization axis, the **b** axis, the x axis is the orientation of the molecular axes (i.e., the crystallographic **c*** direction), and the y axis coincides with the crystal **a** axis. The first term in this Hamiltonian is the Heisenberg exchange coupling between the triplet O_2 molecules. The dominant, intersublattice exchange coupling is antiferromagnetic, i.e., $J_{PP'} < 0$, and it occurs between a given molecule and its four nearest neighbors in the a–b plane. In the more recent work, moreover, the in-plane intrasublattice coupling with the two next-nearest neighbors and the interplanar coupling with four additional neighbors have been included. The interplanar coupling was found (Burakhovich *et al.*, 1977; Stephens *et al.*, 1983) to be very weak, which makes α-oxygen, and β-oxygen, a quasi-two-dimensional magnetic system. The single-particle term AS_z^2 is due to the intramolecular spin–orbit and spin–spin interactions; the free-molecule value of A is equal to 3.96 cm^{-1} = 5.72 K. This term tends to keep the directions of the molecular spin momenta perpendicular to the molecular axes, such that in α- and β-oxygen the spins will lie in the a–b plane. The additional single-particle term BS_y^2 is then added *ad hoc* in order to impose the observed in-plane anisotropy that forces the spins to lie parallel to the **b** axis. Classical dipole models yielding the preferred magnetization axis and the order of magnitude of the empirical

B values suggest that the term BS_y^2 actually represents the magnetic dipole–dipole interactions between the molecular spin moments.

With the use of the phenomenological spin Hamiltonian [Eq. (139)], mean field and spin-wave calculations have been made that yield the observed magnetic, optical, and thermodynamic properties. The antiferromagnetic spin-wave calculations are mostly based on the RPA method outlined in Section IV,C. The formalism is very simple in this case, because the basis for every molecule consists only of the three triplet spin states. By taking the mean field ground state on each molecule and the first excited state, which provides the single magnon states, the RPA equations can be solved exactly for the magnon frequencies. The calculated properties have been compared with experimental data and the coupling constants J, A, and B in the Hamiltonian (139) have thus been determined empirically. The situation is not very satisfactory, however, since the various semiempirical studies on α-O_2 have yielded substantially different sets of coupling constants, depending on the type of experimental data fitted. The discrepancies have been pointed out most clearly by De Fotis (1981), but also the more recent studies still yield rather different J, A, and B values. Moreover, most of the empirical A and B values in solid O_2 deviate considerably from the values corresponding with the free-molecule zero-field splitting and the magnetic dipole moment, respectively. This is surprising since we expect the distortions of the molecular electronic charge distributions, due to the weak van der Waals interactions in the solid, to be minor.

B. The Complete Crystal Hamiltonian and the Coupling between Lattice Vibrations and Spin Dynamics

In a recent paper (Jansen and van der Avoird, 1985), two of us have proposed replacing the phenomenological spin Hamiltonian (139) by a spin Hamiltonian from first principles. By this qualification we mean that our Hamiltonian can be derived directly from the known properties of the O_2 molecules and their interactions. Such a Hamiltonian, which applies not only to α-O_2, but also to any of the condensed phases, looks as follows:

$$\begin{aligned} H_{\text{spin}} = & -\frac{1}{2}\sum_{P}\sum_{P'\neq P} 2J(\omega_P, \omega_{P'}, \mathbf{r}_{PP'})\mathbf{S}_P \cdot \mathbf{S}_{P'} \\ & + \sum_{P}\sum_{m} (-1)^m A_{-m}(\omega_P)[\mathbf{S}_P \otimes \mathbf{S}_P]^{(2)}_m \\ & + \frac{1}{2}\sum_{P}\sum_{P'\neq P}\sum_{m} (-1)^m T_{-m}(\mathbf{r}_{PP'})[\mathbf{S}_P \otimes \mathbf{S}_{P'}]^{(2)}_m \end{aligned} \tag{140}$$

The irreducible tensor product between two (spherical) vectors is defined in Eq. (37). An important feature of this Hamiltonian is that it explicitly describes the dependence of the coupling "constants" J, A_m, and T_m on the distance vectors $\mathbf{r}_{PP'}$ between the molecules and on the orientations $\omega_P = \{\theta_P, \phi_P\}$ of their axes, in contrast with the phenomenological Hamiltonian (139). Another important difference with the latter is that the *ad hoc* single-particle spin anisotropy term BS_z^2, which probably stands implicitly for the magnetic dipole–dipole interactions, has been replaced by a two-body operator that correctly represents these interactions. The distance and orientational dependence of the coupling parameters J, A_m, and T_m has been obtained as follows.

The Heisenberg exchange coupling parameter J is a scalar quantity; its dependence on $\mathbf{r}_{PP'}$, ω_P, and $\omega_{P'}$ is described by expanding it in symmetry-adapted angular functions, just as the intermolecular potential in Eq. (15). The distance-dependent expansion coefficients have been explicitly obtained from *ab initio* quantum-chemical calculations (van Hemert *et al.*, 1983; Wormer and van der Avoird, 1984). These coefficients could be represented by steeply decaying exponential functions of the distance. The *ab initio* calculations refer to $(O_2)_2$ dimers with the triplet O_2 spins coupled to a singlet, a triplet, or a quintet. The exchange splitting between the dimer spin states has been obtained from a second-quantized hole–particle formalism, generalized to nonorthogonal orbitals (Wormer and van der Avoird, 1984), It was found that this exchange splitting could indeed be represented accurately by a Heisenberg effective spin Hamiltonian. The coupling parameter J appeared to depend very sensitively on the distance between the O_2 molecules and, particularly, on their orientations (see Fig. 8). In Fig. 9 we have plotted the dependence of J on the librational coordinates in α-oxygen.

The molecular spin–anisotropy term, the second term in Eq. (140), depends on the angle between the O_2 spin momentum $\mathbf{S}_P$ and the molecular axis. With respect to the global frame, this dependence can be expressed as in Eq. (140) with the second-rank tensor

$$A_m(\omega_P) = \tfrac{1}{3}A\sqrt{30}\, C_m^{(2)}(\theta_P, \phi_P) \tag{141}$$

The constant $A = 3.96\ \mathrm{cm}^{-1}$ has been obtained from the free-molecule zero-field splitting (Mizushima, 1975) and $C_m^{(2)}$ is a Racah spherical harmonic with $l = 2$. The tensor that describes the interaction between the magnetic dipole moments $g_e\mu_B\mathbf{S}_P$, where g_e equals 2.0023 and μ_B is the Bohr magneton, can be written immediately as

$$T_m(\mathbf{r}_{PP'}) = -g_e^2\mu_B^2\sqrt{30}\, r_{PP'}^{-3} C_m^{(2)}(\hat{r}_{PP'}) \tag{142}$$

In summing this term over the lattice, in the calculations described subsequently, the Ewald method (Born and Huang, 1954) had to be invoked.

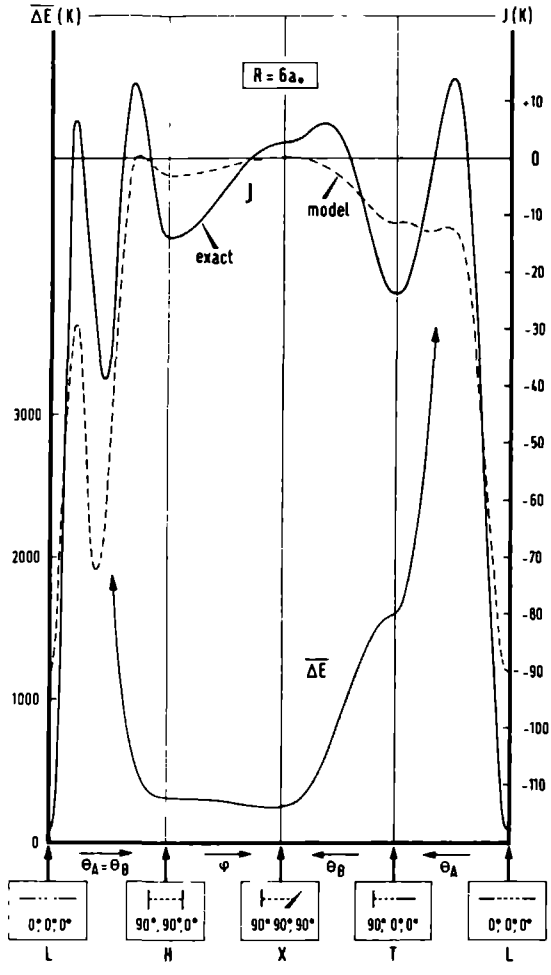

Fig. 8. Orientational dependence of the average (spin-independent) exchange interaction energy $\overline{\Delta E} = V(\omega_P, \omega_{P'}, \mathbf{r}_{PP'})$ and the Heisenberg exchange coupling constant $J(\omega_P, \omega_{P'}, \mathbf{r}_{PP'})$ in the O_2–O_2 dimer at $r_{PP'} = 6$ bohrs. The full lines represent the results of all-electron calculations; the dashed line refers to a four-electron model. The multipole contributions to $\overline{\Delta E}$ are now drawn explicitly because they are negligible at $r_{PP'} = 6a_0$.

Since the O_2 molecule carries a triplet spin momentum, the spin Hamiltonian (140) has to be added to the Hamiltonian (23), which contains the kinetic energies and the spin-independent part of the intermolecular O_2–O_2 potential, in order to obtain the crystal Hamiltonian for solid O_2. The spin-independent O_2–O_2 potential can be partly extracted from the *ab initio* calculations on the $(O_2)_2$ dimer by averaging the calculated interac-

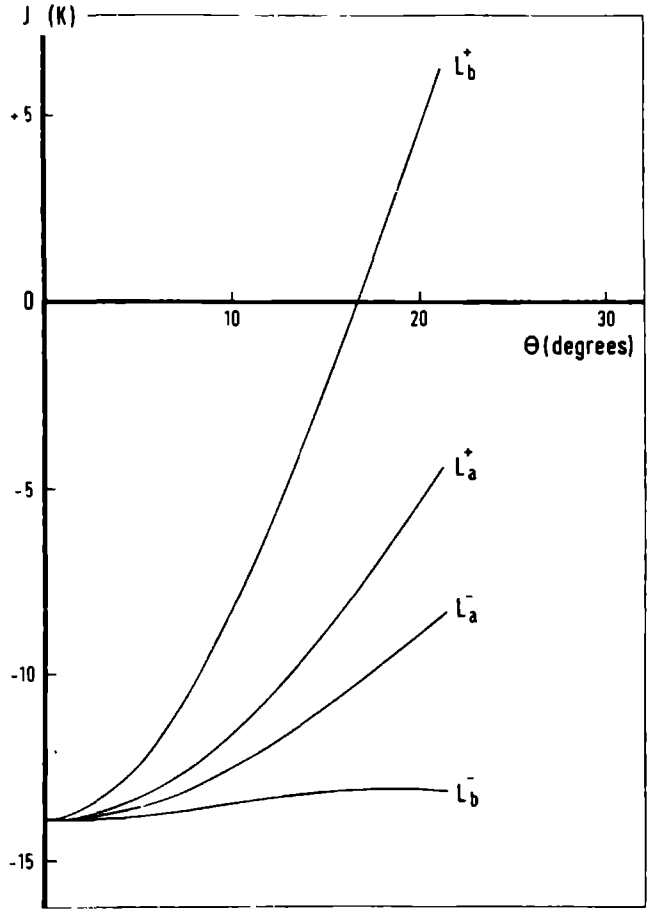

Fig. 9. Variation of the (intersublattice) exchange coupling parameter J between the nearest neighbors in solid α-O_2 along some normal coordinates of libration. The labels L_a and L_b refer to librations around the crystal **a** and **b** axes, respectively; see Fig. 7. The plus and minus signs denote in-phase and out-of-phase librations of the molecules on different sublattices.

tions over the dimer spin multiplets. The *ab initio* calculations do not yet contain the long-range dispersion attractions, however, and so the corresponding terms in the potential must still be included semiempirically. The approximate solutions for the complete crystal Hamiltonian, which describe the coupled lattice vibrations (phonons, librons, mixed modes) and spin waves (magnons), can be obtained very elegantly via the mean field and RPA methods described in Sections IV,B and IV,C. This has

actually been done by Jansen and van der Avoird (1985) for α- and β-oxygen. All they had to add to the formalism applied by Briels *et al.* (1984) to solid nitrogen, was to multiply the basis (111) by the triplet spin functions

$$\Theta^{(S)}_{M_S}(\sigma_P) \qquad \text{with} \quad S = 1 \quad \text{and} \quad M_S = 1, 0, -1$$

to add a spin term $H^S_P(\sigma_P)$ to the mean field Hamiltonian (117) and to extend the particle label $P = \{\mathbf{n}, i, K\}$ in the RPA Hamiltonian (122) to translations, librations, and spin "motions": $K = \{T, L, S\}$. This extension leads to extra blocks in the RPA eigenvalue equations (126) that correlate the spin excitations and couple them to the phonons and librons. In principle, one can obtain mixed phonon–libron–magnon modes. Such modes are not found in solid oxygen, however. The bilinear coupling terms between the lattice modes and the single-magnon spin modes vanish from the RPA Hamiltonian (122) because of symmetry. The excitations are either pure lattice vibrations, of (mixed) phonon–libron type, or pure magnons. The effective Hamiltonian for the lattice modes is obtained from the complete Hamiltonian by spin averaging Eq. (140), i.e., replacing $\mathbf{S}_P$ by $\langle \mathbf{S}_P \rangle$, and adding it to Eq. (23). The amplitude of the librations, 11° in α-oxygen at $T = 0$ K, appears to be substantially smaller than in solid nitrogen. This agrees with the experimental data (Cahill and Leroi, 1969). The effective spin Hamiltonian is given by Eq. (140) with the coupling constants $\langle J(\omega_P, \omega_{P'}, \mathbf{r}_{PP'}) \rangle$, $\langle A_m(\omega_P) \rangle$, and $\langle T_m(\mathbf{r}_{PP'}) \rangle$ averaged over the translations and librations. Proceeding in this way, several of the problems outlined in Section VI,A can be solved.

The problem of the splitting of the E_g libron in β-oxygen into an A_g, B_g doublet in α-oxygen appears to have the following explanation. Given the small structural distortion at the β–α phase transition, this splitting is indeed far too large to be obtained from lattice dynamics calculations employing the usual spin-independent Hamiltonian (23). The spin orderings in β and α-oxygen are very different, however, yielding a strong discontinuity of $\langle \mathbf{S}_P \rangle \cdot \langle \mathbf{S}_{P'} \rangle$ at the β–α transition. More precisely, one finds for the 120° spin arrangement in β-O_2 that $\langle \mathbf{S}_P \rangle \cdot \langle \mathbf{S}_{P'} \rangle \simeq -0.5$ and for the antiferromagnetic ordering in α-O_2 that $\langle \mathbf{S}_P \rangle \cdot \langle \mathbf{S}_{P'} \rangle \simeq -1$ for nearest neighbors. Introducing these values into the effective Hamiltonian for the lattice modes, the Heisenberg coupling parameter $J(\omega_P, \omega_{P'}, \mathbf{r}_{PP'})$ in Eq. (140) gets a very different weight in the β and α phases. We have mentioned already that this parameter is extremely anisotropic, and thus it has a strong influence on the librational motions (see Fig. 9). The A_g mode in α-O_2 indeed obtains a much higher frequency than the E_g mode in β-O_2, while the B_g mode is somewhat lowered. Using the anisotropic $J(\omega_P, \omega_{P'}, \mathbf{r}_{PP'})$ from *ab initio* calculations (Wormer and van der Avoird, 1984) gives

quantitative agreement with the experimental splitting and shifts. Omitting the Heisenberg term yields a small splitting, just as in the earlier lattice dynamics calculations. This confirms the crucial role of this term in the libron-splitting mechanism.

Jansen and van der Avoird (1985) have also made spin-wave calculations as described earlier. The RPA equations with the effective spin Hamiltonian (140), averaged over the translations and librations, could be solved analytically for any wave vector $\mathbf{q}$. The optical ($\mathbf{q} = \mathbf{0}$) magnon frequencies emerging from these calculations are 6.3 and 20.9 cm^{-1}, in reasonable agreement with the experimental values 6.4 and 27.5 cm^{-1}. This agreement is very satisfactory if we realize that the spin Hamiltonian has been obtained from first principles, with none of its parameters fitted to the magnetic data.* We conclude that the RPA model, both for the lattice modes and the spin waves, when based on a complete crystal Hamiltonian from first principles, yields a realistic description of several properties of solid O_2 that were not well understood before.

Appendix

In this article we have used some of the concepts of quantum-statistical mechanics. These concepts can, of course, be found in the textbooks (Ter Haar, 1966; Feynman, 1972; McQuarrie, 1976), but the ideas that are most relevant to this paper are summarized in this appendix. In particular, we prove the thermodynamic variation principle, which has been applied several times.

In quantum-statistical physics, just as in the classical counterpart, one introduces a density operator ρ such that the average value of any mechanical observable X can be calculated as

$$\langle X \rangle = \mathrm{Tr}(\rho X) \tag{A.1}$$

Depending on the boundary conditions imposed on the system and on the specific form of ρ, several ensembles are distinguished. Most often the system is assumed to have constant volume V and the density operator is chosen to be

$$\rho = e^{\beta(A-H)} \tag{A.2}$$

* Actually, the long-range dispersion term in the spin-independent potential of Eq (23), which affects the lattice vibrations and thus the averaged coupling parameters in Eq (140), has been fitted to obtain the best lattice constants in α-O_2. The magnetic data, and the libron splitting discussed, are very insensitive to this term, however

The corresponding ensemble is therefore called canonical. The constant A is chosen such that $\mathrm{Tr}(\rho) = 1$, from which it follows that ρ can be interpreted as defining a probability distribution over the eigenstates of the Hamiltonian H. It is easy to demonstrate that

$$A = -\beta^{-1} \ln Z \tag{A.3}$$

with $Z = \mathrm{Tr}(e^{-\beta H})$ and $\beta^{-1} = k_B T$, k_B being the Boltzmann constant. The quantity A corresponds with the Helmholtz free energy of the system.

The thermodynamic variation principle reads

$$A \leq A_0 + \langle H - H_0 \rangle_0 \tag{A.4}$$

with the free energy A_0 and the average $\langle\rangle_0$ referring to an approximate Hamiltonian H_0. The inequality holds for any H_0. In the classical limit it is a simple consequence of Jensen's inequality known from integration theory (Rudin, 1966). In the quantum-mechanical case, its proof is more elaborate (Girardeau and Mazo, 1973; Feynman, 1972). Here we reproduce the proof of Girardeau and Mazo and define

$$Z(\lambda) = \mathrm{Tr}(e^{X+\lambda Y}) \tag{A.5}$$

We need the derivatives of this quantity with respect to λ. The derivatives of an exponential operator are given by the rule

$$\frac{d}{d\lambda} e^{H(\lambda)} = e^{H(\lambda)} \int_0^1 dx\, e^{-xH(\lambda)} \frac{dH(\lambda)}{d\lambda} e^{xH(\lambda)} \tag{A.6}$$

This rule is proved by writing

$$\frac{d}{d\lambda} e^{yH(\lambda)} = e^{yH(\lambda)} F(y)$$

and demonstrating, via some simple differentiations, that

$$\frac{dF(y)}{dy} = e^{-yH(\lambda)} \frac{dH(\lambda)}{d\lambda} e^{yH(\lambda)}$$

Since

$$\lim_{y \to 0} F(y) = 0$$

it follows that

$$F(y) = \int_0^y dx\, e^{-xH(\lambda)} \frac{dH(\lambda)}{d\lambda} e^{xH(\lambda)}$$

which, for $y = 1$, proves the rule (A.6). Applying this rule, with $H(\lambda) = X + \lambda Y$, and using the invariance of the trace with respect to cyclic permutations of the operators, one finds for the derivatives of the quantity $Z(\lambda)$ defined by Eq. (A.5) that

$$Z'(\lambda) = \mathrm{Tr}(Ye^{X+\lambda Y}) \tag{A.7}$$

$$Z''(\lambda) = \mathrm{Tr}\left(Y \frac{d}{d\lambda} e^{X+\lambda Y}\right) \tag{A.8}$$

Applying the rule (A.6) to Eq. (A.8) and using the cyclic invariance of the trace again, it follows for Hermitian operators X and Y that

$$Z''(\lambda) = \int_0^1 dx\, \mathrm{Tr}\{C(x)C(x)^\dagger\} \tag{A.9}$$

with

$$C(x) = e^{1/2x(X+\lambda Y)} Y e^{1/2(1-x)(X+\lambda Y)}$$

Knowing the derivatives of the quantity $Z(\lambda)$, we can expand it as a Taylor series:

$$Z(\lambda) = Z(0) + \lambda Z'(0) + \tfrac{1}{2}\lambda^2 Z''(\lambda')$$

for some λ' lying in the interval $0 \le \lambda' \le \lambda$. Since the second derivative, expressed as in Eq. (A.9), must satisfy the relation

$$Z''(\lambda) \ge 0 \tag{A.10}$$

we find the inequality

$$Z(1) \ge Z(0) + Z'(0) \tag{A.11}$$

When choosing

$$X = -\beta H_0 - \beta\langle H - H_0\rangle_0, \qquad Y = -\beta(H - H_0) + \beta\langle H - H_0\rangle_0$$

it can be shown, using Eq. (A.7), that $Z'(0) = 0$, and the inequality (A.11) becomes

$$\begin{aligned} \mathrm{Tr}[\exp(-\beta H)] &= \mathrm{Tr}[\exp(X + Y) \ge \mathrm{Tr}[\exp(X)] \\ &= \mathrm{Tr}[\exp(-\beta H_0)]\, \exp(-\beta\langle H - H_0\rangle_0) \end{aligned} \tag{A.12}$$

Taking the logarithm of this inequality and multiplying by $-\beta^{-1}$ yields the thermodynamic variation principle, Eq. (A.4).

When the free energy A is given as a function of its characteristic variables, viz., T and V, it is possible to calculate all thermodynamic properties of the system. We list, for instance, the

$$\text{(entropy)} \qquad S = -\left(\frac{\partial A}{\partial T}\right)_V$$

$$\text{(energy)} \qquad E = A + TS$$

$$\text{(pressure)} \qquad p = -\left(\frac{\partial A}{\partial V}\right)_T$$

$$\text{(specific heat)} \qquad C_v = T\left(\frac{\partial S}{\partial T}\right)_V = -T\left(\frac{\partial^2 A}{\partial T^2}\right)_V$$

$$C_p = T\left(\frac{\partial S}{\partial T}\right)_p = C_v + \alpha_p^2 \frac{TV}{\kappa_T}$$

$$\text{(thermal expansion coefficient)} \qquad \alpha_p = \frac{1}{V}\left(\frac{\partial V}{\partial T}\right)_p$$

$$\text{(compressibility)} \qquad \kappa_T = -\frac{1}{V}\left(\frac{\partial V}{\partial p}\right)_T$$

For details we refer the reader to the textbooks mentioned.

ACKNOWLEDGMENT

This investigation was supported in part by the Netherlands Foundation for Chemical Research (SON) with financial aid from the Netherlands Organization for the Advancement of Pure Research (ZWO)

One of us (W J B) is grateful to the Van't Hoff Laboratory for granting him the time to spend on writing this article

REFERENCES

Abrikosov, A A , Gorkov, L. P , and Dzyaloshinski, I E. (1965) "Methods of Quantum Field Theory in Statistical Physics." Dover, New York.

Antosiewicz, H. A., (1970). *In* "Handbook of Mathematical Functions" (M. Abramowitz and I A Stegun, eds.). Dover, New York

van der Avoird, A., Wormer, P. E. S., Mulder, F., and Berns, R M (1980). *Top. Curr. Chem.* **93,** 1.

van der Avoird, A., Briels, W. J , and Jansen, A P. J (1984) *J. Chem Phys.* **81,** 3658.

Barron, T. H. K., and Klein, M L (1974). *In* "Dynamical Properties of Solids" (G K Horton and A. A. Maradudin, eds), Vol 1 North Holland, Amsterdam, p 391.

Berns, R. M., and van der Avoird, A (1980) *J Chem Phys.* **72,** 6107.

Bier, K. D., and Jodl, H. J. (1984). *J. Chem. Phys.* **81,** 1192.

Birman J L (1974) *In* "Dynamical Properties of Solids" (G K Horton and A A Maradudin, eds) Vol 1 North Holland, Amsterdam, p 83
Born, M, and Huang, K (1954) "Dynamical Theory of Crystal Lattices" Clarendon, Oxford
Briels, W J (1980) *J Chem Phys* **73,** 1850
Briels, W J (1983) *J Chem Phys* **79,** 969
Briels, W J, Jansen, A P J, and van der Avoird, A (1984) *J Chem Phys* **81,** 4118
Brink, D M, and Satchler, G R (1975) "Angular Momentum" Clarendon, Oxford
Burakhovich, I A, Krupskii, I N, Prokhvatilov, A I, Freiman, Yu A, and Erenburg, A I (1977) *JETP Lett* **25,** 32
Cahill, J E, and Leroi, G E (1969) *J Chem Phys* **51,** 97
Califano, S, Schettino, V, and Neto, N (1981) "Lattice Dynamics of Molecular Crystals" Lecture Notes in Chemistry, Vol 26 Springer, Berlin
Choquard, P F (1967) "The Anharmonic Crystal" Benjamin, New York
Čižek, J and Paldus, J (1971) *Phys Rev* **A3,** 525
Cochran W and Cowley, R A (1967) *In* "Encyclopedia of Physics," Vol XXV, 2a Springer Berlin
Cromer, D T, Mills, R L, Schiferl, D, and Schwalbe, L A (1981) *Acta Crystallogr* **B37,** 8
DeFotis, G C (1981) *Phys Rev* **B23,** 4714
Downs, J, Gubbins, K E, Murad, S, and Gray, C G (1979) *Mol Phys* **37,** 129
Dunmore, P V (1972) *J Chem Phys* **57,** 3348
Dunmore, P V (1976) *J Low Temp Phys* **24,** 397
Dunmore, P V (1977) *Can J Phys* **55,** 554
Edmonds, A R (1957) "Angular Momentum in Quantum Mechanics" Princeton Univ Press, Princeton, New Jersey
Egelstaff, P A, Gray, C G, and Gubbins, K E (1975) *In* "Molecular Structure and Properties" (Physical Chemistry, Ser 2, Vol 2) MTP Internatl Rev Sci, Butterworths, London
English, C A, and Venables, J A (1974) *Proc R Soc London Ser A* **340,** 57
English, C A, Venables, J A, and Salahud, D R (1974) *Proc R Soc London Ser A* **340,** 81
Etters, R D, Helmy, A A, and Kobashi, K (1983) *Phys Rev* **B28,** 2166
Fetter, A L, and Walecka, J D (1971) "Quantum Theory of Many Particles Systems" McGraw-Hill, New York
Feynman, R P (1972) "Statistical Mechanics" Benjamin, Reading, Massachusetts
Fondère, F, Obriot, J, Marteau, Ph, Allavena, M, and Chakroun, H (1981) *J Chem Phys* **74,** 2675
Fredkin, D R, and Werthamer, N R (1965) *Phys Rev* **A138,** 1527
Gaididei, Yu B, and Loktev, V M (1981) *Sov J Low Temp Phys* **7,** 1305
Gibbons, T G, and Klein, M L (1974) *Chem Phys Lett* **29,** 463
Girardeau, M D, and Mazo, R M (1973) *Adv Chem Phys* **24,** 187
Goldman, V V, Horton, G K, and Klein, M L (1968) *Phys Rev Lett* **21,** 1527
Goldman, V V, and Klein, M L (1975) *J Chem Phys* **64,** 5121
Goodings, D A, and Henkelman, M (1971) *Can J Phys* **49,** 2898
ter Haar, D (1966) "Elements of Thermostatics" Holt, New York
Hamer, C J, and Irving, A C (1984) *Nucl Phys* **B230(FS10),** 336
Hansen, J P, and McDonald, I R (1976) "Theory of Simple Liquids" Academic Press, New York
Harris, A B, and Coll, C F (1972) *Solid State Commun* **10,** 1029

Helmy, A A , Kobashi, K , and Etters, R D (1984) *J Chem Phys* **80,** 2782
van Hemert, M C , Wormer, P E S , and van der Avoird, A (1983) *Phys Rev Lett* **51,** 1167
Huller, A (1974) *Phys Rev* **B10,** 4403
Jacobi, N , and Schnepp, O (1972) *Chem Phys Lett* **13,** 344
James, H M , and Keenan, T A (1959) *J Chem Phys* **31,** 12
Jansen, A P J , Briels, W J , and van der Avoird, A (1984) *J Chem Phys* **81,** 3648
Jansen A P J , and van der Avoird, A (1985) *Phys Rev* **B31,** 7500
Jordan, T H , Smith, H W , Streib, W E , and Lipscomb, W N (1964) *J Chem Phys* **41,** 756
Kirkwood, J G (1940) *J Chem Phys* **8,** 205
Kitaigorodsky, A I (1973) "Molecular Crystals and Molecules " Academic Press, New York
Kjems, J K , and Dolling, G (1975) *Phys Rev* **B11,** 1639
Klein, M L , and Weis, J J (1977) *J Chem Phys* **67,** 217
Klein, M L , Lévesque, D , and Weis, J J (1981) *J Chem Phys* **74,** 2566
Kobashi, K (1978) *Mol Phys* **36,** 225
Kobashi, K , Klein, M L , and Chandrasekharan, V (1979) *J Chem Phys* **71,** 843
Koehler, T R (1969) *Phys Rev Lett* **22,** 777
van Kranendonk, J (1983) "Solid Hydrogen " Plenum, New York
Kuchta, B , and Luty, T (1983) *J Chem Phys* **78,** 1447
Kuchta, B (1985) *Chem Phys* **95,** 391
LeSar, R , Ekberg, S A , Jones, L H , Mills, R L , Schwalbe, L A , and Schiferl, D (1979) *Solid State Commun* **32,** 131
Luty, T , van der Avoird, A , and Berns, R M (1980) *J Chem Phys* **73,** 5305
McQuarrie, D A (1976) "Statistical Mechanics " Harper, New York
Mandell, M J (1974) *J Chem Phys* **60,** 1432
Mandell, M J (1974) *J Chem Phys* **60,** 4880
Mandell, M J (1974) *J Low Temp Phys* **17,** 169
Mandell, M J (1975) *J Low Temp Phys* **18,** 273
Maradudin, A A , Montroll, E W , Weiss, G H , and Ipatova, P (1971) "Theory of Lattice Dynamics in the Harmonic Approximation " Academic Press, New York
Maradudin, A A , and Vosko, S H (1968) *Rev Mod Phys* **40,** 1
Maradudin, A A (1974) *In* "Dynamical Properties of Solids" (G K Horton and A A Maradudin, eds) Vol 1 North Holland, Amsterdam, p 1
Medina, F D , and Daniels, W B (1976) *J Chem Phys* **64,** 150
Meier, R J , Schinkel, C J , and de Visser, A (1982) *J Phys* **C15,** 1015
Meier, R J , and Helmholdt, R B (1984) *Phys Rev* **B29,** 1387
Meier, R J (1984) Unpublished thesis, University of Amsterdam
Metropolis, M , Rosenblut, A W , Rosenblut, M N , Teller, A N , and Teller, E (1953) *J Chem Phys* **21,** 1087
Michel, K H , and Naudts, J (1978) *J Chem Phys* **68,** 216
Michel, K H (1984) *Z Physik* **B54,** 129
Mizushima, M (1975) "The Theory of Rotating Diatomic Molecules " Wiley, New York
Powell, B M , Dolling, G , and Nieman H F (1983) *J Chem Phys* **79,** 982
Powell, J L , and Craseman, B (1961) "Quantum Mechanics " Addison-Wesley, Reading, Massachusetts
Press, W , and Huller, A (1978) *J Chem Phys* **68,** 4465
de Raedt, B , Binder, K , and Michel, K H (1981) *J Chem Phys* **75,** 2977
Rahman, A (1966) *J Chem Phys* **45,** 258

Raich, J C , and Etters, R D (1968) *Phys Rev* **168,** 425
Raich, J C (1972) *J Chem Phys* **56,** 2395
Raich, J C , and Etters, R D (1972) *J Low Temp Phys* **7,** 449
Raich, J C , Gillis, N S , and Anderson, A B (1974) *J Chem Phys* **61,** 1399
Raich, J C , Gillis, N S , and Koehler, T R (1974) *J Chem Phys* **61,** 1411
Raich, J C , and Gillis, N S (1977) *J Chem Phys* **66,** 846
Raich, J C , Yasuda, H , and Bernstein, E R (1983) *J Chem Phys* **78,** 6209
de Reggi, A S , Canepa, P C , and Scott, T A (1969) *J Magn Reson* **1,** 144
Rowe, D J (1970) "Nuclear Collective Motion " Methuen, London
Rudin, W (1966) "Real and Complex Analysis " McGraw-Hill, New York
Sack, R A (1964) *J Math Phys* **5,** 260
Scott, T A (1976) *Phys Rep* **27,** 89
Schnepp, O , and Jacobi, N (1972) *Adv Chem Phys* **22,** 205
Schuch, A F , and Mills, R L (1970) *J Chem Phys* **52,** 6000
Slyusarev, V A , Freiman, Yu A , and Yankelevich, R P (1980) *Sov J Low Temp Phys* **6,** 105
Slyusarev, V A , and Freiman, Yu A , and Yankelevich, R P (1981) *Sov J Low Temp Phys* **7,** 265
Steele, W A (1963) *J Chem Phys* **39,** 3197
Stephens, P W , Birgenau, R J , Majkrzak, C F , and Shirane, G (1983) *Phys Rev* **B28,** 452
Streib, W E , Jordan, T H , and Lipscomb, W N (1962) *J Chem Phys* **37,** 2962
Thiéry, M M , and Fabre, D (1976) *Mol Phys* **32,** 257
Thouless, D J (1960) *Nucl Phys* **21,** 225
Thouless, D J (1961) "The Quantum Mechanics of Many-Body Systems " Academic Press, New York
Verlet, L (1967) *Phys Rev* **159,** 98
Wallace, D C (1972) "Thermodynamics of Crystals " Wiley, New York
Walmsley, S H. (1975) *In* "Lattice Dynamics and Intermolecular Forces" (S Califano, ed) (Proc Enrico Fermi, Vol 55) North Holland, Amsterdam
Wasiutynski, T (1976) *Phys Status Solidi* **B76,** 175
Weis, J J , and Klein, M L (1975) *J Chem Phys* **63,** 2869
Werthamer, N R (1976) *In* "Rare Gas Solids" (M L Klein and J Venables, eds), Vol I Academic Press, London
Wormer, P E S , and van der Avoird, A (1984) *J Chem Phys* **81,** 1929
Yasuda, H , and Yamamoto, T (1971) *Progr Theor Phys* **45,** 1458

Chapter 2
Solid Nitrogen

Ab initio description of large amplitude motions in solid N_2. I. Librons in the ordered α and γ phases

A P J Jansen, W J Briels, and A van der Avoird
Institute of Theoretical Chemistry, University of Nijmegen Toernooiveld 6525 ED Nijmegen, The Netherlands

(Received 18 April 1984, accepted 12 June 1984)

Starting from an *ab initio* intermolecular potential, we have calculated the mean field states for the librations in the ordered α and γ phases of solid N_2, using a basis of spherical harmonics up to $l_{max} = 12$ The correlation between the mean field solutions was then taken into account via a libron model based on the random-phase approximation or time-dependent Hartree method The calculated librational frequencies are rather accurate, showing that the discrepancies in earlier results with the *ab initio* potential are mainly due to the breakdown of (quasi-)harmonic models for the librations, even in the ordered phases

I. INTRODUCTION

Solid nitrogen under its own vapor pressure can exist in two phases, the low temperature α phase and the high temperature β phase The α–β phase transition occurs at temperature $T_{\alpha\beta} = 35\,6$ K Above 4 kbar a third phase is known, the γ phase, and at still higher pressures, above 49 kbar, a new phase (δ) has recently been found[1,2] and another phase (ϵ) has been predicted [3] In these papers we shall look at the α, β, and γ modifications which have been extensively studied experimentally The α and γ phases are ordered solids in which the molecules perform oscillations around their equilibrium positions and equilibrium orientations, especially the angular oscillations have considerable amplitudes In the disordered β phase the angular motions are even more violent such that the orientational distribution function is expected to be almost constant for all angles A schematic drawing of the structures of these phases is given in Figs 1(a), (b), and (c) For more information on the results of experimental and theoretical work on solid nitrogen prior to 1976 we refer to the review of Scott [4]

In the following we report the results of a new theoretical study of the molecular motions in solid nitrogen There are two main reasons which make a study like this highly interesting

(i) The starting point of any study of the dynamics of molecular crystals is the description of the intermolecular potential Normal practice is to introduce a model description of this potential in which several parameters are free to be chosen Next the dynamics calculations are performed for different values of the model parameters, and finally these parameters are fixed by a minimization of the difference between the calculated and observed properties of the crystals, such as structures and phonon frequencies Much work has been done[5–7] on the choice of the model potentials and there exist now several models which seem to do their job reasonably well A great disadvantage of the procedure described above, however, is that the final parameters depend largely on the approximations made in the dynamics calculations The model potentials thus obtained may be satisfactory for representing the (solid state) data to which they have been fitted, but in the cases where this has been investigated, they did not yield other (gas phase and liquid state) properties very well It is therefore of great value that, for nitrogen, we can use a potential which was obtained from quantum chemical calculations,[8,9] independent of any dynamics study This potential has now been tested in several bulk properties virial coefficients,[10] transport properties, Rayleigh linewidths, and rotational relaxation coefficients[11] of gaseous N_2 and liquid state properties,[12] which are generally found to be quite accurate It has been used in self-consistent phonon (SCP) calculations on solid N_2[13] with good results for the static properties and excellent agreement with experiment for the translational phonon frequencies The librational phonon frequencies came out about 30% too high, but this was believed to be due mainly to the failure of the dynamical (SCP) model to account for the strongly anharmonic librations In the present paper we investigate these librations

(ii) In most molecular crystals the molecules are trapped in deep potential wells The lattice dynamics calculations can be done within the harmonic approximation, and they are by now fairly standard [5] In some cases anharmonic effects appear to be important and these are most often introduced perturbatively [5] At higher temperatures, however, especially in the neighborhood of phase transitions, molecular motions are so violent that perturbation calculations do not seem to be of much value (Moreover, in view of the fact that the perturbation series for a quartic anharmonic oscillator has a vanishing range of convergence,[14] one should be very careful with lattice dynamics perturbation calculations) In solid nitrogen, especially in the β phase, but, to a lesser degree also in α and γ nitrogen, the molecules perform angular motions which are intermediate between harmonic librations and free rotations The study of molecular motions in this region is far from standard, and poses a challenging problem

In this paper we confine ourselves to the pure rotational motions of the molecules In a harmonic approximation this would be possible exactly at certain points in the Brillouin zone In general the decoupling of the translational and the rotational motions can only be justified approximately Examples of systems in which it has been successfully applied are the methane and deuterated methane crystals[15–17] and the hydrogen crystals [18–20] Also in the case of nitrogen decoupling has been applied previously [21–24] In a forthcoming

 0021 9606/84/203648 10$02 10

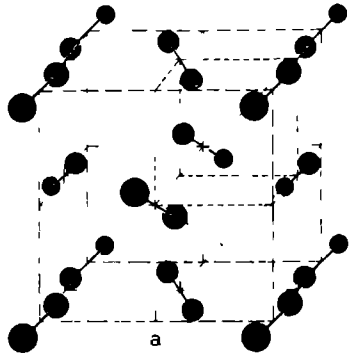

α-N_2, Pa3 (Z=4)
a = 5.644 Å

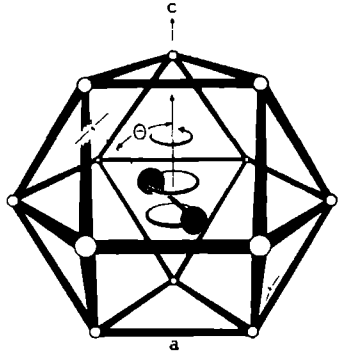

β-N_2, $P6_3/mmc$ (Z=2)
a=4.050 Å c=6.604 Å

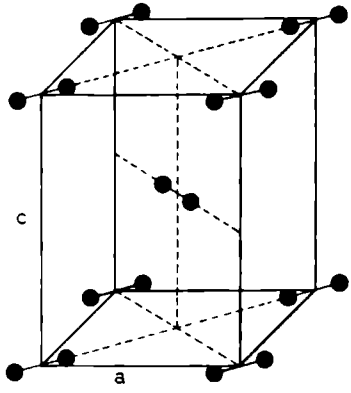

γ-N_2, $P4_2/mmm$ (Z=2)
a=3.957 Å c=5.109 Å

FIG. 1. Crystal structures of α, β, and γ nitrogen according to Ref. 4.

paper we will describe the coupled rotational-translational motions of the molecules.

Let us briefly outline the theoretical model that we have used. In contrast with the SCP scheme[5,25] which is essentially a (quasi-)harmonic model, we approach the solution from the side of freely rotating molecules. Using free rotor states as a basis we construct states for each particle, which describe its rotational motion and which effectively contain the influence of all neighboring molecules. Thus it is possible to retain the full anharmonic potential, without any further approximation. After we have constructed the single particle states, we use these states to build the states of the whole crystal and we calculate the corresponding energies. Again it is possible to include the full potential without further approximation. The approximation in the above procedure is introduced by employing only part of the single particle states. The above procedure is not at all new but it has not been applied very extensively, and never with an *ab initio* potential. Moreover, we shall extend the existing theory, by looking at the stability conditions for the mean field solutions (in paper II) and by including explicitly the translational coupling (in paper III). Therefore we give in Sec. II the formulas that we have programmed, references to the original literature can also be found in this section.

II. MODEL AND THEORETICAL METHODS

A. The Hamiltonian

The system we are concerned with consists of a periodic crystal of librating molecules with their centers of mass fixed at the equilibrium positions, the lattice sites P. After the introduction of a suitably chosen unit cell for the "center of mass crystal," the position vector of $P = \{\mathbf{n},t\}$ can be written as $\mathbf{R}_P = \mathbf{R}_\mathbf{n} + \mathbf{r}_t$, where $\mathbf{n}$ represents the three indices of the unit cell to which P belongs, $\mathbf{R}_\mathbf{n}$ the position vector of the origin of this unit cell, and $\mathbf{r}_t$ the position vector of P relative to this origin. The orientation of a molecule at position P will be described by the polar angles $\Omega_P = \{\theta_P,\varphi_P\}$ of its molecular axis. The intermolecular energy of two molecules at positions P and P', respectively can then be written as

$$\Phi(\mathbf{R}_{PP'},\Omega_P,\Omega_{P'}) = \sum_{\mathbf{l}} \varphi_{\mathbf{l}}(R_{PP'}) \sum_{\mathbf{m}} \begin{pmatrix} l_1 & l_2 & l_3 \\ m_1 & m_2 & m_3 \end{pmatrix} \times C^{(l_1)}_{m_1}(\Omega_P) C^{(l_2)}_{m_2}(\Omega_{P'}) C^{(l_3)}_{m_3}(\hat{\mathbf{R}}_{PP'}) \quad (1)$$

Here, $\mathbf{R}_{PP'} = \mathbf{R}_{P'} - \mathbf{R}_P$ and $\hat{\mathbf{R}}_{PP'}$ is the unit vector along $\mathbf{R}_{PP'}$, $\mathbf{l}$ and $\mathbf{m}$ denote the index sets $\{l_1,l_2,l_3\}$ and $\{m_1,m_2,m_3\}$, respectively, $C^{(l)}_m(\Omega)$ is a Racah spherical harmonic,[26] and the symbol following the second summation sign is a 3-j coefficient. The coefficients $\varphi_{\mathbf{l}}(R_{PP'})$ are related to the *ab initio* calculated coefficients $V_{l_1 l_2 l_3}(R_{PP'})$ of Berns and van der Avoird[9] by $\varphi_{\mathbf{l}}(R_{PP'}) = [(2l_1+1)(2l_2+1)(2l_3+1)]^{1/2} V_{l_1 l_2 l_3}(R_{PP'})$. In general they satisfy several symmetry relations,[27,28] which in the case of homonuclear diatomic molecules imply that only coefficients with l_1, l_2, and l_3 even can be nonzero.

We write the crystal Hamiltonian as a sum of one-particle terms and two-particle terms plus a constant

$$H = U^c + \sum_P L_P(\Omega_P) + \frac{1}{2}\sum_{P}\sum_{P'\neq P}\Phi_{PP'}(\Omega_P,\Omega_{P'}), \tag{2}$$

where

$$L_P(\Omega_P) = B\,|\mathbf{J}(\Omega_P)|^2 + \sum_{lm}{}' V_m^{(l)}(P)C_m^{(l)}(\Omega_P), \tag{3a}$$

$$\Phi_{PP'}(\Omega_P,\Omega_{P'}) = \sum_{l_1 m_1}{}' \sum_{l_2 m_2}{}' C_{m_1}^{(l_1)}(\Omega_P)X_{m_1 m_2}^{(l_1 l_2)}(P,P')C_{m_2}^{(l_2)}(\Omega_{P'}) \tag{3b}$$

The primes at the summation signs in Eqs (3a) and (3b) indicate that the value $l = 0$ should be omitted from the summations (this convention is used throughout this paper) $\mathbf{J}(\Omega_P)$ is the angular momentum vector operator associated with the molecule at position P, and B its rotation constant Because we assume that the centers of mass of the molecules are fixed to their equilibrium positions, the first term in Eq (3a) represents the complete kinetic energy of the molecule at position P The constant U^c and the coefficients $V_m^{(l)}(P)$ and $X_{m_1 m_2}^{(l_1 l_2)}(P,P')$ are given by

$$U^c = \frac{1}{2}\sum_{P}\sum_{P'\neq P}\varphi_{0,0,0}(R_{PP'}) = \sum_P U_P, \tag{4a}$$

$$V_m^{(l)}(P) = (2l+1)^{-1/2}(-1)^l \sum_{P'\neq P}\varphi_{l0l}(R_{PP'})C_m^{(l)}(\hat{R}_{PP'})^*, \tag{4b}$$

$$X_{m_1 m_2}^{(l_1 l_2)}(P,P') = \sum_{l_3 m_3}\varphi_{l_3}(R_{PP'})\begin{pmatrix} l_1 & l_2 & l_3 \\ m_1 & m_2 & m_3 \end{pmatrix} C_{m_3}^{(l_3)}(\hat{R}_{PP'}) \tag{4c}$$

These quantities are invariant under any lattice translation of the center of mass crystal, in fact in the nitrogen crystals U_P and $V_m^{(l)}(P)$ are also independent of the sublattice index i, so that we can omit the label P Finally, because we neglect the translational displacements, many terms will cancel in Eq (4b) at points of high site symmetry For example, in α–N_2 the $l = \{2,0,2\}$ and $l = \{0,2,2\}$ terms drop out completely

B. The mean field approximation

The mean field approximation[15,17,29] is based on the Gibbs–Bogoliubov inequality[30,31]

$$A_{\text{var}} = A_0 + \langle H - H_0\rangle_0 > A, \tag{5}$$

where H_0 can be any Hamiltonian $\langle X\rangle_0$ is the thermodynamic average of the operator X over the eigenstates of H_0, i e, $\langle X\rangle_0 = Z_0^{-1}\,\mathrm{Tr}\,X\exp(-\beta H_0)$ with $Z_0 = \mathrm{Tr}\exp(-\beta H_0)$ and $\beta = (k_B T)^{-1}$ as usual (k_B is Boltzmann's constant), $A_0 = -k_B T \ln Z_0$ and A is the free energy of the system with Hamiltonian H The approximation then consists of letting H_0 be a sum of one-particle operators

$$H_0 = \sum_P H_P^{\text{MF}}(\Omega_P), \tag{6}$$

such that A_{var} is stable against all variations of $H_P^{\text{MF}}(\Omega_P)$ This leads to the coupled set of equations

$$H_P^{\text{MF}}(\Omega_P) = L(\Omega_P) + \sum_{P'\neq P}\langle\Phi_{PP'}(\Omega_P,\Omega_{P'})\rangle_{P'} = L(\Omega_P) + \Phi_P^{\text{MF}}(\Omega_P) \tag{7}$$

Here $\langle X\rangle_P$ denotes the thermodynamic average of X over the eigenstates of $H_P^{\text{MF}}(\Omega_P)$ The Eqs (7) have to be solved self-consistently In principle, H_P^{MF} can be different for every P In practice, of course, one imposes symmetry relations on the solutions of Eq (7) This means that one chooses a unit cell, compatible with the symmetry of the center of mass crystal, and then puts H_P^{MF} equal to $H_{P'}^{\text{MF}}$ for all P and P' for which $\mathbf{R}_{PP'}$ is equal to a lattice vector Next, one introduces unit cell symmetry, also compatible with the symmetry of the center of mass crystal, such that the mean field Hamiltonians on different sublattices are related

In this paper we restrict ourselves to those solutions of Eq (7) that have the experimentally observed symmetry As a result we have, in all cases, only one independent molecule per unit cell, whose mean field is given by

$$\Phi_P^{\text{MF}}(\Omega_P) = \sum_{lm}{}' F_m^{(l)}(P)C_m^{(l)}(\Omega_P), \tag{8a}$$

$$F_m^{(l)}(P) = \sum_{kn}{}' \sum_{P'\neq P} X_{mn}^{(lk)}(P,P')\langle C_n^{(k)}\rangle_{P'} \tag{8b}$$

The molecular field acting on a molecule at position P' is then completely determined by the symmetry of the unit cell, and can be obtained by a rotation of the mean field of the independent molecule over the Euler angles $\omega_{P'} = \{\alpha_{P'}, \beta_{P'}, \gamma_{P'}\}$ As a result, the mean field of the molecule at P', when measured in a coordinate frame which is rotated over the Euler angles $\omega_{P'}$ relative to the laboratory frame, is given by $\Phi_{P'}^{\text{MF}}(\tilde{\Omega}_{P'})$, where $\tilde{\Omega}_{P'}$ denotes the polar angles of the molecule at P' relative to the rotated coordinate frame Because in all cases the Euler angles are such that $L(\Omega_{P'})$ is invariant under the corresponding transformation, the mean field Hamiltonian at P' is given by $H_{P'}^{\text{MF}}(\tilde{\Omega}_{P'})$ From this we conclude that the thermodynamic average of $C_m^{(k)}(\tilde{\Omega}_{P'})$ is equal to $\langle C_m^{(k)}\rangle_{P'}$, and therefore that

$$\langle C_n^{(k)}\rangle_{P'} = \sum_m \langle C_m^{(k)}\rangle_{P'} D_{mn}^{(k)}(\omega_{P'}) \tag{9}$$

For the Euler angles and the Wigner matrices $D^{(k)}(\omega)$ we use the conventions of Edmonds [26] Introducing Eq (9) into Eq (8b), we find

$$F_m^{(l)}(P) = \sum_{kn}{}' Y_{mn}^{(lk)}(P)\langle C_n^{(k)}\rangle_{P'}, \tag{10a}$$

$$Y_{mn}^{(lk)}(P) = \sum_{P'\neq P}\sum_{m} X_{mm}^{(lk)}(P,P')D_{nm}^{(k)}(\omega_{P'}) \tag{10b}$$

Equations (7), (8a), and (10) constitute the set of equations that we shall solve self-consistently In order to calculate $\langle C_n^{(k)}\rangle_{P'}$, we first diagonalize $H_P^{\text{MF}}(\Omega_P)$, and then perform the averaging in the obvious way The diagonalization gives us eigenfunctions of the mean field Hamiltonian, which will be used in the next section In order to perform the diagonalization in practice we must introduce a basis the most convenient basis for the current problem is the basis of tesseral harmonics because the mean field Hamiltonian is real and symmetric in this basis

Once we have obtained the mean field Hamiltonians we can calculate the thermodynamic properties[17] of the system The free energy is found from Eqs (5) and (6), and other quantities follow from it

$$A = -k_B T \sum_P \ln Z_P^{MF} + \sum_P U_P - \frac{1}{2} \sum_P \langle \Phi_P^{MF} \rangle_P , \quad (11a)$$

$$S = -\frac{\partial A}{\partial T} = k_B \sum_P \ln Z_P^{MF} + \frac{1}{T} \sum_P \langle H_P^{MF} \rangle_P , \quad (11b)$$

$$E = A + TS = \sum_P U_P + \sum_P \langle H_P^{MF} \rangle_P - \frac{1}{2} \sum_P \langle \Phi_P^{MF} \rangle_P \quad (11c)$$

In order to get the entropy in its final form [Eq (11b)] we have made use of $\Sigma_P \langle \partial H_P^{MF}/\partial T \rangle_P = \frac{1}{2} \Sigma_P \partial/\partial T \langle \Phi_P^{MF} \rangle_P$, which follows from Eq (7)

C. Simple libron theory

The mean field treatment described above provides us with a set of single particle states $|\psi_P^{(\alpha)}(\Omega_P)\rangle$ and corresponding single particle energies $\epsilon^{(\alpha)}$ given by

$$H_P^{MF}(\Omega_P)|\psi_P^{(\alpha)}(\Omega_P)\rangle = \epsilon^{(\alpha)}|\psi_P^{(\alpha)}(\Omega_P)\rangle , \quad (12)$$

where all mean field Hamiltonians have the same symmetry, and therefore all energies are independent of P Because $H_P^{MF}(\Omega_P)$ depends on the temperature T, the states and energies also depend on T From the single particle states we now obtain mean field states for the crystal

$$|\Psi_{|\alpha|}^{MF}\rangle = |\psi_1^{(\alpha}{}^{)}(\Omega_1)\rangle |\psi_2^{(\alpha_2)}(\Omega_2)\rangle \ldots |\psi_{ZN}^{(\alpha_{ZN})}(\Omega_{ZN})\rangle , \quad (13)$$

where Z is the number of molecules in the unit cell and N the number of unit cells In the construction of these states we have taken into account the complete anisotropy and anharmonicity of the Hamiltonian The mean field states do not show, however, any correlation between the motion of different molecules The simplest way to obtain "correlated states" is by diagonalization of the full Hamiltonian in the subspace spanned by the mean field states (13) (at $T = 0$ K) with at most one α_i different from zero, where $|\psi_P^{(0)}(\Omega_P)\rangle$ denotes the ground state at position P It is not difficult to show that the Brillouin theorem is valid in this case (i e , when $T = 0$ K)

$$\langle \Psi_0^{MF}|H|\Psi_{\alpha P}^{MF}\rangle = 0 \quad (14)$$

Here $|\Psi_0^{MF}\rangle$ denotes the mean field ground state of the crystal and $|\Psi_{\alpha P}^{MF}\rangle$ a crystal state with an excitation to the single particle state α at position P From this theorem it follows that the ground state remains unchanged and that we can find the excitation energies of the crystal from a diagonalization of $\tilde{H} = H - \langle \Psi_0^{MF}|H|\Psi_0^{MF}\rangle$ in a basis of excited states In order to diagonalize $\tilde{H}$, we adapt this basis to the translation symmetry of the crystal, i e , we take basis functions

$$|\Psi_{\alpha,i}^{q}\rangle = \frac{1}{\sqrt{N}} \sum_n e^{i\mathbf{q}\cdot\mathbf{R}_n} |\Psi_{\alpha|n,i|}^{MF}\rangle \quad (15)$$

In this basis $\tilde{H}$ is diagonal in $\mathbf{q}$, and its elements are

$$\langle \Psi_{\alpha,i}^{q}|\tilde{H}|\Psi_{\alpha,i}^{q}\rangle = \delta_{i,i}\delta_{\alpha\alpha}\{\epsilon^{(\alpha)} - \epsilon^{(0)}\} + \Phi(\mathbf{q})_{\alpha i\alpha i} , \quad (16a)$$

$$\Phi(\mathbf{q})_{\alpha i\alpha i'} = \sum_n e^{i\mathbf{q}\cdot\mathbf{R}_n} \langle \Psi_{\alpha|0,i|}^{MF}|\Phi_{|0,i||n,i'|}|\Psi_{\alpha|n,i'|}^{MF}\rangle \quad (16b)$$

In the derivation of this result we have used the translational symmetry, and the fact that at $T = 0$ the ground state average is equivalent to the thermodynamic average, which allowed us to substitute Eq (7) In the sum in Eq (16b) the self-interaction Φ_{PP} must be put equal to zero Introducing Eq (13b) into Eq (16b) we find

$$\Phi(\mathbf{q})_{\alpha i\alpha i'} = \sum_{l}{}' \sum_{m_1}{}' \sum_{l_2,m_2}{}' \langle \Psi_{|0,l|}^{(\alpha)}|C_{m_1}^{(l_1)}|\Psi_{|0,i|}^{(0)}\rangle Z_{m_1,m_2}^{(l_1,l_2)}(\mathbf{q}|i,i') \times \langle \Psi_{|0,l|}^{(0)}|C_{m_2}^{(l_2)}|\Psi_{|0,l|}^{(\alpha)}\rangle , \quad (17a)$$

$$Z_{m_1,m_2}^{(l_1,l_2)}(\mathbf{q}|i,i') = \sum_n e^{i\mathbf{q}\cdot\mathbf{R}_n} X_{m_1,m_2}^{(l_1,l_2)}(|\mathbf{0},i|,|\mathbf{n},i'|) \quad (17b)$$

From the discussion preceding Eq (9) it is clear that we need to calculate only the matrix elements of the standard molecule P; the others follow from

$$\langle \Psi_P^{(\alpha)}|C_n^{(k)}|\Psi_P^{(\alpha)}\rangle = \sum_m \langle \Psi_P^{(\alpha)}|C_m^{(k)}|\Psi_P^{(\alpha)}\rangle D_{mn}^{(k)}(\omega_P) \quad (18)$$

The diagonalization of $\tilde{H}$ leads to a set of approximate crystal states, which are linear combinations of the functions defined by Eq (15), and which have the wave vector $\mathbf{q}$ as one of their quantum labels These states are called librons, the theory was first formulated in this context by Raich [18]

D. The random phase or time-dependent Hartree approximation

A shortcoming of the theory described in the preceding subsection is the absence of correlation between the molecular motions in the ground state The simplest theory which incorporates correlation effects into the ground state is based on the random phase approximation In this approximation,[21 23 24] the Hamiltonian is written as a quadratic form in the excitation operators $(E_P^{\alpha})^{\dagger}$ and their Hermitean conjugates E_P^{α}, the operator $(E_P^{\alpha})^{\dagger}$ excites a molecule at position P from its mean field ground state to the excited state α Linear terms are absent because of the Brillouin theorem, Eq (14) Because the Hamiltonian contains all quadratic terms, certain matrix elements between states that differ in two excitations are taken into account, and this will affect the ground state The next step is to restrict α to a few excited mean field states on each molecule and to approximate the commutators of E_P^{α} and $(E_P^{\alpha})^{\dagger}$ as boson commutators In Dunmore's application of the random-phase approximation to α–N_2 only the lowest (twofold degenerate) excited mean field state was included[23 24], we investigate the effect of the higher states Finally, the quadratic boson Hamiltonian is diagonalized which leads to the elementary excitations of the crystal

It is well known[32 33] in the case of many-fermion systems, that the equations which result from the random phase approximation can be derived in many alternative ways In our case too, the final equations can be found[34] in several ways In an Appendix we shall give a derivation by means of the time dependent Hartree (TDH) method [16 35 36] We do this because the TDH formulas are related to the stability conditions for the mean field solutions which we investigate in paper II and, moreover, because we wish to generalize the theory, in paper III, in order to attack the problem of rotation translation coupling

With any lattice Hamiltonian it is possible to label the states and corresponding energies with a vector q from the first Brillouin zone The result of the Appendix is that the excitation energies of the crystal $E_\alpha(\mathbf{q}) - E_\beta(\mathbf{q})$ can be found as the eigenvalues $\Lambda^{(k)}(\mathbf{q})$ of a matrix $\mathbf{M}(\mathbf{q})$ which has the structure

$$M(\mathbf{q}) = \begin{pmatrix} \mathbf{A} - \mathbf{B}(\mathbf{q}) & -\mathbf{B}(\mathbf{q}) \\ \mathbf{B}(\mathbf{q}) & -\mathbf{A} + \mathbf{B}(\mathbf{q}) \end{pmatrix} = \begin{pmatrix} \mathbf{P} & \mathbf{O} \\ \mathbf{O} & -\mathbf{P} \end{pmatrix} \begin{pmatrix} \chi - \Phi(\mathbf{q}) & -\Phi(\mathbf{q}) \\ -\Phi(\mathbf{q}) & \chi - \Phi(\mathbf{q}) \end{pmatrix} \tag{19}$$

It is not difficult to demonstrate that to every positive eigenvalue there corresponds a negative eigenvalue of the same absolute value, this is related to the fact that with any excitation $E_\alpha(\mathbf{q}) - E_\beta(\mathbf{q})$ there is a deexcitation $E_\beta(\mathbf{q}) - E_\alpha(\mathbf{q})$ Moreover, it is not difficult to prove[33] that the squares of the $\Lambda^{(k)}(\mathbf{q})$ are determined by the symmetric generalized eigenvalue problem

$$[\chi - 2\Phi(\mathbf{q})]\mathbf{c} = [\Lambda^{(k)}(\mathbf{q})]^2 \mathbf{P}^{-1}\chi^{-1}\mathbf{P}^{-1}\mathbf{c} \tag{20}$$

with $\Phi(\mathbf{q})_{\alpha\alpha'}$ given by Eq (16b) The diagonal matrices P and χ are defined by

$$P_{\alpha\alpha'} = \delta_{\alpha\alpha}\delta_{\alpha'\alpha'}(P^{(\alpha)} - P^{(0)}),$$

$$\chi_{\alpha\alpha'} = \delta_{\alpha\alpha}\delta_{\alpha'\alpha'}\frac{\epsilon^{(\alpha)} - \epsilon^{(0)}}{P^{(\alpha)} - P^{(0)}}, \tag{21a}$$

and the matrices A and B by

$$\mathbf{A} = \mathbf{P}\chi,$$

$$\mathbf{B}(\mathbf{q}) = \mathbf{P}\Phi(\mathbf{q}) \tag{21b}$$

In the limit $T \to 0$, the occupation numbers $P(0)$ and $P(\alpha)$ are 1 and 0, respectively, and Eqs (19) and (21a) and (21b) are identical to the RPA equation For $T > 0$, there is a slight difference between the time-dependent Hartree method and the RPA method

There exists a simple relation between the RPA results and the results of Raichs libron theory (see Sec II C) In the limit $T \to 0$, the left upper matrix $\mathbf{A} - \mathbf{B}(\mathbf{q})$ of $\mathbf{M}(\mathbf{q})$, with A and B(q) given by Eqs (21a) and (21b) is identical to the matrix defined by Eqs (16a) and (16b) If one restricts the basis to the first excited mean field level for each particle, A is a constant times the unit matrix In that case, one finds[34] the following simple relation

$$\Lambda^{(k)}(\mathbf{q}) = [2(\epsilon^{(1)} - \epsilon^{(0)})\hbar\omega_1^{(k)}(\mathbf{q}) - (\epsilon^{(1)} - \epsilon^{(0)})^2]^{1/2} \tag{22}$$

between the RPA excitation energies $\Lambda^{(k)}(\mathbf{q})$ and the excitation energies $\hbar\omega^{(k)}(\mathbf{q})$ obtained by means of the simple libron theory of Sec II C

III. RESULTS AND DISCUSSION

A. General remarks

We have performed our calculations with the *ab initio* calculated potential of Berns and van der Avoird [9] The coefficients in the spherical expansion of this potential are given by

$$\varphi_1(R) = C_1^{\exp}\exp[aR^2 + bR + c] + C_1^{\text{mult}} R^{-(l_1 + l_2 + 1)} + C_1^{[6]} R^{-6} + C_1^{[8]} R^{-8} + C_1^{[10]} R^{-10} \tag{23}$$

For the sake of completeness we have reproduced in Table I the coefficients which together specify the potential

In order to solve the mean field equation we have imposed the experimentally observed symmetry on the solutions A schematic drawing of the crystal structures is given in Fig 1 As to the choice of the cell parameters, let us make a few remarks In a combined mean field treatment of the translational and rotational degrees of freedom, which will be given in paper III, one can vary the cell parameters in order to obtain the free energy A as a function of V and T Using the thermodynamic data of the vapor, which are easy to calculate, one can then calculate the cell parameters of the crystal along the solid–vapor equilibrium line These cell parameters should actually be used in a study of the dynamics of the crystals, i e , in the formulas which eventually yield the libron frequencies Since we treat only the rotational degrees of freedom in the present paper, however, this procedure would lead to too small values of the cell parameters, and it would be unreasonable to compare the calculated libron frequencies with the experimental ones Therefore, we have chosen to effectively average over the translational phonons by using the experimental cell parameters, which are given in Fig 1

We have performed the mean field calculations not in the usual basis of spherical harmonics, but in a basis of tesseral harmonics, because then the mean field Hamiltonian is real and symmetric The tesseral harmonics are defined as

$$S_{lm}(\Omega) = \left\{\frac{2l+1}{8\pi}\right\}^{1/2}\{(-1)^m C_m^{(l)}(\Omega) + C_{-m}^{(l)}(\Omega)\}, \qquad m > 0,$$

$$S_{l0}(\Omega) = \left\{\frac{2l+1}{4\pi}\right\}^{1/2} C_0^{(l)}(\Omega), \qquad m = 0,$$

$$S_{lm}(\Omega) = -i\left\{\frac{2l+1}{8\pi}\right\}^{1/2}\{(-1)^m C^{(l)}{}_m(\Omega) - C_m^{(l)}(\Omega)\}, \quad m < 0 \tag{24}$$

Matrix elements are easily obtained by use of [26]

$$\int \frac{d\Omega}{4\pi} C_m^{(l)}(\Omega)\, C_{m_1}^{(l_1)}(\Omega)\, C_{m_2}^{(l_2)}(\Omega) = \begin{pmatrix} l_1 & l_2 & l_3 \\ 0 & 0 & 0 \end{pmatrix}\begin{pmatrix} l_1 & l_2 & l_3 \\ m_1 & m_2 & m_3 \end{pmatrix} \tag{25}$$

TABLE I Expansion coefficients of the *ab initio* N–N potential
$a = -20.5$ nm^{-2} $b = -23.3$ nm^{-1} $c = 8\,833.47$

l_1	l_2	l	C_l^{exp}	C_l^{multi}	C_l^{6r}	C_l^{8r}	C_l^{10r}
0	0	0	44 258		-4.231×10^{1}	-2.946×10^{4}	-2.239×10^{5}
2	0	2	119 355		-9.075×10^{1}	-2.639×10^{4}	-2.987×10^{5}
2	2	0	14 735		-1.882×10^{1}	-3.049×10^{4}	-1.128×10^{6}
2	2	2	−52 928		-5.037×10^{1}	1.147×10^{5}	4.128×10^{6}
2	2	4	197 31	2.774×10^{1}	-5.457×10^{4}	-7.398×10^{5}	-1.829×10^{7}
4	0	4	38 781				
4	2	2	4 710				
4	2	4	−14 731				
4	2	6	76 213	1.851×10^{1}			
4	4	0	0 045				
4	4	2	−0 121				
4	4	4	0 702				
4	4	6	−4 251				
4	4	8	38 407	2.255×10^{4}			
6	0	6	5 057				
6	2	4	0 266				
6	2	6	−1 657				
6	2	8	13 263	2.814×10^{5}			

[a] In kJ mol^{-1}
[b] In kJ mol^{-1} nm$^{l_1+l_2+l}$
[c] In kJ mol^{-1} nm^{6}
[d] In kJ mol^{-1} nm^{8}
[e] In kJ mol^{-1} nm^{10}

We have always assumed that the crystal was composed of either *ortho* molecules only, or *para* molecules only In those cases the basis was restricted to tesseral harmonics with even or odd l, respectively All functions were included up to $l_{max} = 10/9$ inclusive for *ortho/para* α-nitrogen, and to $l_{max} = 12/11$ for *ortho/para* γ-nitrogen This was always sufficient[37] to have the ground state energy converged to within 0 5 cm^{-1} and the first excited state to within 1 cm^{-1}

In α-nitrogen we have extended the lattice summations over six shells This means that we have neglected the potential for all values of the intermolecular distance beyond 9 87 Å The same interaction radius has been used in β and γ nitrogen In Dunmore's calculations[23,24] on α–N_2 he has assumed that the effective lattice potential has cylindrical symmetry around the molecular equilibrium axes (the body diagonals of the cubic unit cell, see Fig 1) We have not made this assumption, but we have found that the only noncylindrical $C_m^{(l)}(\Omega_p)$ contributions to the potential [see Eq (8a)] which are not vanishing because of the symmetry, i e , the $m = \pm 3$ (in a local frame with the Z axis along the body diagonal), have actually very small effects on the final results

Finally, we have used the value $B = 24\,080\,977$ J mol^{-1} = 2 012 986 4 cm^{-1} for the rotation constant of N_2

B. Mean field results

In Fig 2 we have presented the single particle excitation energies obtained from the mean field calculations Although the mean field excitation energies do not readily compare with the excitation energies of the whole crystal, the mean field spectra nevertheless give some interesting information on the average motions of the individual molecules Additional information can be obtained from the probability densities which we have calculated from the mean field wave functions and presented in Fig 3 In the following we shall discuss these results for each modification separately The thermodynamic properties and the α–β phase transition will be discussed in paper II

In α-nitrogen the single particle energy levels group together in such a way that the spectrum becomes very similar to that of a two-dimensional harmonic oscillator This is true for the *ortho* as well as for the *para* species Moreover, the

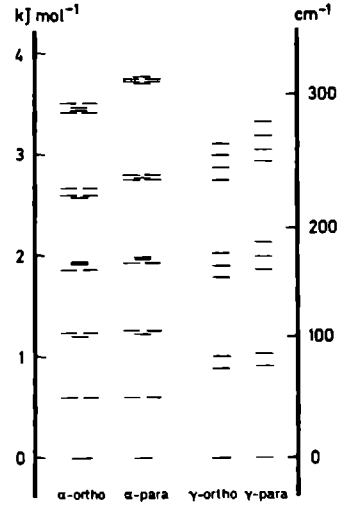

FIG 2 Calculated mean field levels for the librations in α and γ nitrogen

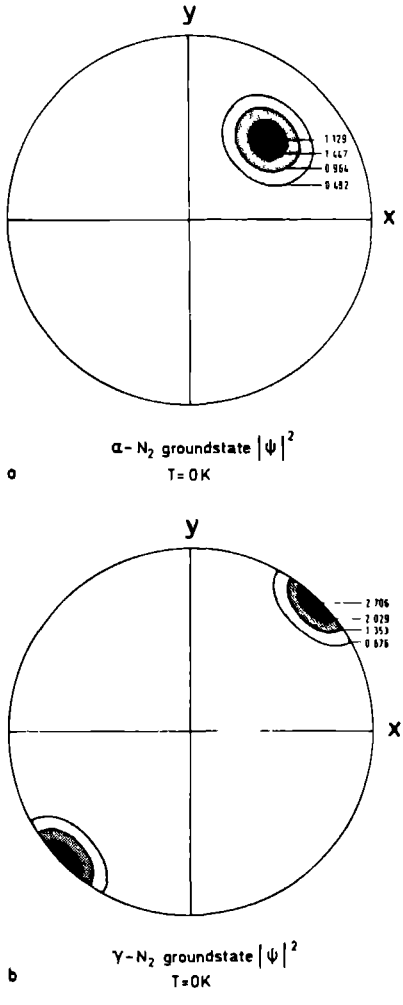

FIG 3 Orientational probability distributions of the molecular axes in α [Fig 3(a)] and γ [Fig 3(b)] nitrogen Contours of constant probability for the molecule in the origin calculated in the mean field model are plotted as functions of the polar angles (θ ϕ) with respect to the crystal axes (Fig 1) The angle θ increases linearly with the radius of the plots from 0 (in the center) to $\pi/2$ (at the boundary), ϕ is the phase angle

oscillation frequencies associated with the spectra are the same in both cases ($\omega = 50\,4$ cm $^{-1}$) This result is remarkable because we have started with free rotor states but it has been obtained previously[23,24] using empirical potentials It suggests that the molecules in the α modification are localized in rather deep potential wells and perform nearly isotropic oscillations around their equilibrium orientations

This suggestion is confirmed by the probability densities in Fig 3(a) This figure pertains to the *ortho* species at temperature $T = 0$ K, analogous figures for nonzero temperatures below 40 K, and also those for *para*-nitrogen are qualitatively similar We clearly observe that the orientations of the molecules are localized around the [1,1,1] axes, which is in agreement with the experimental findings [see Fig 1(a)] Because of the special way of plotting, i e , θ being proportional to the radius of the representation point, we also see clearly the symmetry of the density as a function of θ and ϕ An interesting quantity, measuring the amount of delocalization, is the order parameter $S = \langle P_2(\cos\theta)\rangle$ where θ is now taken relative to the equilibrium [1,1,1] axes and the brackets denote a thermodynamic average At $T = 0$ K we find $S = 0\,885$, which should be compared with the experimental[4] result $S^{\text{exp}} = 0\,863$ The fact that our value is somewhat larger than the experimental one means that our ground state wave function is not sufficiently delocalized Previous mean field calculations,[14] using only quadrupole–quadrupole interactions, also led to too large a value of S ($S = 0\,890$)

In Fig 4 we have plotted the variation of the order parameter S with the temperature The calculated variation is mainly caused by the changes in the occupation numbers of the mean field levels, these levels themselves change only very little We observe that the calculated order parameter does not fall off sufficiently with increasing temperature as compared with the experimental one This result is typical for mean field calculations[4,18,19]

Also in γ-nitrogen the mean field single particle excitation energies for the *ortho* and *para* species are almost identical, the small differences in the higher part of the spectrum are due to the fact that the energy levels here are not yet converged to their correct position ($l_{max} = \infty$) The spectrum, in both cases, resembles that of a system of two independent harmonic oscillators with slightly different frequencies ($\omega_1 = 72\,1$, $\omega_2 = 81\,3$ cm^{-1}) Again this suggests that the molecules perform small oscillations around their equilibrium orientations which, as can be seen from Fig 3(b), are directed along the local [1,1,0] axes, in agreement with ex-

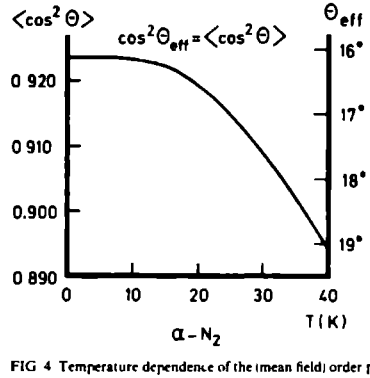

FIG 4 Temperature dependence of the (mean field) order parameter in α N

TABLE II Librational frequencies in α nitrogen (in cm^{-1}) $T = 0$ K

		Γ q = (0 0 0)			R q = $\left(\frac{\pi}{a}\ \frac{\pi}{a}\ \frac{\pi}{a}\right)$		rms deviation
		E_g	T_g	T_g	R_1^+	R_{25}^+	
	Experiment (Ref 44)	32 3	36 3	59 7	43 6	47 2	
	Harmonic (Ref 13)	40 8	50 7	74 3	55 6	58 3	12 3
	SCP (Ref 13)	39 5	48 5	70 3	52 7	55 7	9 7
ab initio	Raich s libron (this work)*	34 5	41 8	71 7	48 0	51 0	6 5
potential	RPA (this work)	30 7	41 0	68 5	47 9	51 0	5 2
	One-dimensional model (Ref 40)	30 1	43 3	67 2			6 1
	One-dimensional model (Ref 41)	32 0	37 2	61 0			0 9
	Harmonic (Ref 6)	37 5	47 7	75 2	50 7	57 8	10 6
Semiempirical	RPA (Ref 23)	31 5	40 3	66 4			4 5
potential	RPA Raich–Mills potential (Ref 24)	34 4	45 4	67 4	47 0	52 8	6 2

*Results for $l_{max} = 10$ and 2 excited mean field states per molecule for five excited states the frequencies are 34 4 41 1 and 69 3 cm^{-1} (in the Γ point)

periment [4] Looking at Fig 1(c), we might guess that the smaller oscillation frequency pertains to an oscillation in the (a,b) plane, while the larger one pertains to an oscillation perpendicular to this plane By inspection of the vectors corresponding to the mean field energy levels we have found that this guess is consistent with the wave functions of the first two excited states but not with those of the higher levels The order parameter for the ground state equals 0 921, which indicates that the molecules in γ nitrogen are slightly more localized than those in α-nitrogen The mean field results and the corresponding orientational probability distributions for the β phase will be discussed in paper II

C. Libron frequencies

In Tables II and III we have collected the librational phonon frequencies in α and γ nitrogen, respectively We have included in these tables the results of previous harmonic and self-consistent phonon (SCP) calculations[13] which were based on the same *ab initio* potential [9] These calculations have used a site–site representation of this potential, whereas we now have employed the potential in the form of a spherical expansion [see Eqs (1) and (23) and Table I], the differences between these two representations are small, however [9] Also included are the results of simple one-dimensional model calculations[40,41] which correct the SCP results for the strong anharmonicity of the librational potential Furthermore, we compare some values from harmonic[6] and libron model[23,24] calculations based on the best available semiempirical potentials Going downwards in these tables, we observe a systematic improvement in the results of different dynamical models based on the same *ab initio* potential harmonic, SCP, Raich's libron model, and RPA (or time-dependent Hartree) libron model The results of the RPA model, and already those of Raich's libron model, are substantially better than those of the SCP model The one-dimensional model results[40,41] have indicated already that this is due to the failure of the SCP model (or any other quasiharmonic model) in describing large amplitude orientational oscillations The libron results practically do not change when higher excited mean field states are included, apparently it is sufficient to take only the lowest two excited states for each particle into account (corresponding with the two angular degrees of freedom) This might be different, however, when the mean field excitation energies are lower and the states are more delocalized, as one expects in the β phase Our best results, the RPA libron results, are considerably better also than the results of the harmonic calculations,[6] and comparable with the best libron results,[23,24] using optimized empirical potentials In the *ab initio* potential which we have used no fitting of the parameters to any solid state data has been involved, however

TABLE III Librational frequencies in γ nitrogen (in cm^{-1}) $T = 0$ K

		Γ q = (0 0 0)			rms deviation
		E_g	B_{1g}	A_{2g}	
	Experiment (Ref 43)	55 0	98 1		
	Harmonic (Ref 13)	57 9	86 5	109 7	8 5
ab initio	SCP (Ref 13)	56 5	85 2	107 1	9 2
potential	Raich s libron (this work)	64 3	101 6	129 0	7 0
	RPA (this work)*	63 8	99 6	119 9	6 3
	One-dimensional model (Ref 40)	56 5	87 6	104 6	7 5
Semiempirical potential	Harmonic (Ref 6)	50 5	74 8	105 1	16 8

*Results for $l_{max} = 12$ and 2 excited mean field states included per molecule For $l_{max} = 10$ and 2 excited states the frequencies are 64 9 101 9 and 122 7 cm^{-1} and for $l_{max} = 10$ and 5 excited states 64 7 101 9 and 122 7 cm^{-1}

IV. CONCLUSION

From the results discussed in the previous section we can observe that the libron models presented in this paper, when applied with the *ab initio* N_2–N_2 potential of Berns and van der Avoird,[9] yield very good agreement with the experimental data for α and γ nitrogen Assuming the center of mass lattice without predetermined orientations of the N_2 molecules, the experimentally observed structures come out of mean field calculations The collective orientational oscillations of the molecules (librational phonons or librons) around these equilibrium structures are described by means of the libron models The frequencies emerging from these libron models are very accurate indeed, for all the measured points[42,43] where the translational phonons may be considered to be decoupled from the librations, because of the symmetry This leads to the following conclusions

(i) The *ab initio* N_2–N_2 potential of Berns and van der Avoird is quite realistic, also in its orientational dependence (anisotropy) Its distance dependence has already been tested in SCP calculations[13] which gave accurate results for the translational phonon frequencies

(ii) The libron model works very well, at least for the pure librational motions in the ordered molecular solids, α and γ nitrogen In the next paper (II) we look at orientationally disordered solids, β nitrogen, and in a subsequent paper (III), at the effect of translational-rotational coupling which should be included at least for those lattice vibrations where no decoupling occurs due to symmetry Actually, this decoupling holds only for some specific points in the Brillouin zone In calculating observable properties as thermodynamic averages one should (numerically) integrate over the complete zone, including all the mixed mode points

ACKNOWLEDGMENTS

This investigation was supported in part by the Netherlands Foundation for Chemical Research (S O N) with financial aid from the Netherlands Organization for the Advancement of Pure Research (Z W O)

APPENDIX

In this Appendix we briefly present the time-dependent Hartree theory for the dynamics of molecular crystals which can be used to derive Eqs (19) and (20) It starts by applying a small perturbation $\lambda h(t)$ to the crystal The Hamiltonian of the system is then

$$H(t) = H + \lambda h(t), \tag{A1}$$

where H is given by Eq (2) We write the statistical density operator $D(t)$ as

$$D(t) = D + \lambda \Delta(t), \tag{A2}$$

where $D = \exp(-\beta H)/Z$ is the time-independent canonical density operator The time evolution of $D(t)$ is given by the Liouville equation, which to first order in λ reads

$$i\hbar \dot{\Delta}(t) = [h(t), D] + [H, \Delta(t)] \tag{A3}$$

We solve this equation by taking its Fourier transform, for $\tilde{\Delta}(\omega) = \int e^{i\omega t} \Delta(t) dt$ we obtain

$$\tilde{\Delta}(\omega) = \sum_{\alpha\beta} \frac{|\psi_\alpha\rangle\langle\psi_\alpha|[\tilde{h}(\omega), D]|\psi_\beta\rangle\langle\psi_\beta|}{\hbar\omega - (E_\alpha - E_\beta)} \tag{A4}$$

Here $\tilde{h}(\omega) = \int e^{i\omega t} h(t) dt$ and $|\psi_\alpha\rangle$ is an exact eigenstate of H with corresponding eigenvalue E_α The important point now is that $\tilde{\Delta}(\omega)$ has singularities for those values of ω which are equal to some energy difference $(E_\alpha - E_\beta)/\hbar$; we shall approximately calculate these singularities for the case that either E_α or E_β is the ground state energy

We use a perturbation of the form $h(t) = \Sigma_P h_P(\Omega_P, t)$, and we write the statistical density operator in the time-dependent Hartree approximation

$$D(t) = \prod_P d_P(\Omega_P, t), \tag{A5a}$$

$$d_P(\Omega_P, t) = d_P^{\mathrm{MF}}(\Omega_P) + \lambda \delta_P(\Omega_P, t) \tag{A5b}$$

Here $d_P^{\mathrm{MF}}(\Omega_P)$ is the time-independent mean field single particle density operator $\exp\{-\beta H_P^{\mathrm{MF}}(\Omega_P)\}/Z^{\mathrm{MF}}$, with $H_P^{\mathrm{MF}}(\Omega_P)$ given by Eq (7) As a result, in the limit $\lambda \to 0$, the system is described by the mean field approximation To first order in λ we get

$$\tilde{\Delta}(\omega) = \sum_P d_1^{\mathrm{MF}}(\Omega_1) \ \delta_P(\Omega_P, \omega) \ d_{ZN}^{\mathrm{MF}}(\Omega_{ZN}), \tag{A6}$$

where $\tilde{\delta}_P(\Omega_P, \omega) = \int e^{i\omega t} \delta_P(\Omega_P, t) dt$ It follows that $\tilde{\Delta}(\omega)$ has singularities at the values of ω where $\tilde{\delta}_P(\Omega_P, \omega)$ has singularities

In order to calculate the singular points of $\tilde{\delta}_P(\Omega_P, \omega)$ we write down the Liouville equation to the first order in λ, and perform the trace over all one-particle Hilbert spaces except for that of molecule P.

$$\begin{aligned} i\hbar\, \mathrm{Tr}^{(\neq P)} \sum_P d_1^{\mathrm{MF}}(\Omega_1) \ \dot{\delta}_P(\Omega_P, t) \ d_{ZN}^{\mathrm{MF}}(\Omega_{ZN}) &= i\hbar \dot{\delta}_P(\Omega_P, t) \\ &= \mathrm{Tr}^{(\neq P)}\left[H, \prod_P d_P^{\mathrm{MF}}(\Omega_P)\right] + \mathrm{Tr}^{(\neq P)}\left[H, \sum_P d_1^{\mathrm{MF}}(\Omega_1) \ \delta_P(\Omega_P, t) \ d_{ZN}^{\mathrm{MF}}(\Omega_{ZN})\right] \\ &\quad + \mathrm{Tr}^{(\neq P)}\left[\sum_P h_P(\Omega_P, t), \prod_P d_P^{\mathrm{MF}}(\Omega_P)\right] \\ &= [H_P^{\mathrm{MF}}(\Omega_P), d_P^{\mathrm{MF}}(\Omega_P)] + [H_P^{\mathrm{MF}}(\Omega_P), \delta_P(\Omega_P, t)] + [\Phi_P(\Omega_P, t), d_P^{\mathrm{MF}}(\Omega_P)] + [h_P(\Omega_P, t), d_P^{\mathrm{MF}}(\Omega_P)], \end{aligned} \tag{A7a}$$

$$\Phi_P(\Omega_P, t) = \sum_P{}' \mathrm{Tr}^{(P)} \delta_P(\Omega_P, t) \Phi_{PP}(\Omega_P, \Omega_P) \tag{A7b}$$

The superscripts of the trace operators are self-explanatory In the first step we have made use of $\mathrm{Tr}\, \delta_P(\Omega_P, t) = 0$, which follows from Eq (A5b) Verification of the last step in Eq (A7a) is somewhat tedious but straightforward The first commuta-

tor following the last equal sign in Eq (A7a) is of course equal to zero The next step is to Fourier transform Eqs (A7a) and (A7b) and to calculate the matrix elements $\langle \psi_P^{(\alpha)} | \tilde{\delta}_P(\omega) | \psi_P^{(\beta)} \rangle$, the operator then follows from

$$\tilde{\delta}_P(\Omega_P, \omega) = \sum_{\alpha \beta} |\psi_P^{(\alpha)}(\Omega_P)\rangle \langle \psi_P^{(\alpha)} | \tilde{\delta}_P(\omega) | \psi_P^{(\beta)} \rangle \langle \psi_P^{(\beta)}(\Omega_P)| \tag{A8}$$

Because all manipulations are fairly elementary, and moreover are essentially identical to those of Hüller,[16] we just give the final result

$$\langle \psi_P^{(\alpha)} | \tilde{\delta}_P(\omega) | \psi_P^{(\beta)} \rangle = \sum_{\mathbf{q}} \sum_{K} \frac{B^{(K)}_{\alpha \beta P}(\mathbf{q})}{\hbar\omega - \Lambda^{(K)}(\mathbf{q})} \tag{A9}$$

The precise form of $B^{(K)}_{\alpha \beta P}(\mathbf{q})$ is not important, suffice it to say that it originates from the last commutator in Eq (A7a) $\Lambda^{(K)}(\mathbf{q})$ are the eigenvalues of a matrix $\mathbf{M}(\mathbf{q})$ with elements

$$M_{\alpha\, \beta\, l\alpha\, \beta\, l'}(\mathbf{q}) = \delta_{\alpha\alpha}\delta_{\beta\beta}\delta_{ll'}(\epsilon^{(\alpha)} - \epsilon^{(\beta)}) - (P^{(\alpha)} - P^{(\beta)}) \sum_{\mathbf{n}} e^{i\mathbf{q}\cdot\mathbf{R}_n} \langle \psi^{(\alpha)}_{|0\,l|}\, \psi^{(\beta)}_{|\mathbf{n}\,l'|}\, |\Phi_{|0\,l||\mathbf{n}\,l'|}|\, \psi^{(\beta)}_{|0\,l|}\, \psi^{(\alpha)}_{|\mathbf{n}\,l|} \rangle\,, \tag{A10}$$

where $P^{(\alpha)} = \langle \psi_P^{(\alpha)} | d_P^{MF} | \psi_P^{(\alpha)} \rangle$ From Eqs (A4), (A6), (A8), and (A9) we conclude that the eigenvalues $\Lambda^{(K)}(\mathbf{q})$ provide the approximate energy differences $E^{(\alpha)} - E^{(\beta)}$ It is clear from Eq (A10) that the rows of $\mathbf{M}(\mathbf{q})$ for which $\epsilon^{(\alpha)} = \epsilon^{(\beta)}$ are identically equal to zero We shall omit these rows and the corresponding columns, because we are only interested in the eigenvalues $\Lambda^{(K)}(\mathbf{q})$ that are not trivially equal to zero (the zeros correspond to the diagonal terms in Eq (A4) Finally, if we use the fact that the mean field states are real, we can arrange the indices such that $\mathbf{M}(\mathbf{q})$ has the structure given in Eq (19)

[1] R le Sar, S A Ekberg, L H Jones, R L Mills, L A Schwalbe, and D Schiferl, Solid State Commun 32, 131 (1979)
[2] D T Cronen, R L Mills, D Schiferl, and L A Schwalbe, Acta Crystallogr Sect B 37, 8 (1981)
[3] K Kobashi, A A Helmy, R D Etters, and I L Spain, Phys Rev B 26, 5986 (1982)
[4] T A Scott, Phys. Rep 27, 89 (1976)
[5] S Califano, V Schettino, and N Neto, *Lattice Dynamics of Molecular Crystals, Lecture Notes in Chemistry* (Springer, Berlin, 1981), Vol 26
[6] J C Raich and N S Gillis, J Chem Phys 66, 846 (1977)
[7] C S Murphy, S. F O'Shea, and I R. McDonald, Mol Phys 50, 531 (1983)
[8] F Mulder, G van Dijk, and A van der Avoird, Mol Phys. 39, 407 (1980)
[9] R M Berns and A van der Avourd, J Chem Phys 72, 6107 (1980)
[10] M C van Hemert and R M Berns, J Chem Phys 76, 354 (1982)
[11] C Nyeland, L L Poulsen, and G D Billing, J Phys Chem 88, 1216 (1984)
[12] A R Allnatt (private communication)
[13] T Luty, A van der Avoird, and R M Berns, J Chem Phys. 73, 5305 (1980).
[14] B Simon and A Dicke, Ann Phys 58, 76 (1970)
[15] H M James and T A Keenan, J Chem Phys 31, 12 (1959)
[16] A Huller, Phys Rev B 10, 4403 (1974)
[17] T Yamamoto, Y Katsoka, and K Okade, J Chem Phys 66, 2701 (1977)
[18] J C Raich, J Chem Phys 56, 2395 (1972)
[19] I F Silvera, Rev Mod Phys 52, 393 (1980)
[20] J van Kranendonk, *Solid Hydrogen* (Plenum, New York, 1983)
[21] J C Raich and R D Etters, Phys Rev 168, 425 (1968)
[22] M J Mandell, J Low Temp Phys. 17, 169 (1974), 18, 273 (1975)
[23] P V Dunmore, J Chem Phys 57, 3348 (1972)
[24] P V Dunmore, Can J Phys. 55, 554 (1977)
[25] N R Werthamer, in *Rare Gas Solids*, edited by M L Klein and J Venables (Academic, London, 1976), Vol I
[26] A R Edmonds, *Angular Momentum in Quantum Mechanics* (Princeton University, Princeton, 1957)
[27] W J Briels, J Chem Phys 73, 1850 (1980)
[28] A van der Avoird, P E S Wormer, F Mulder, and R M Berns, Top Curr Chem 93, 1 (1980)
[29] J G Kirkwood, J Chem Phys 8, 205 (1940)
[30] M D Girardeau and R M Mazo, Adv Chem Phys 24, 187 (1973)
[31] R P Feynman, *Statistical Mechanics* (Benjamin, Reading, Mass. 1972)
[32] D J Rowe, *Nuclear Collective Motion* (Methuen, London, 1970)
[33] J Linderberg and Y Ohrn, *Propagators in Quantum Chemistry* (Academic, New York, 1973)
[34] J C Raich, N S Gillis, and A B Anderson, J Chem Phys 61, 1399 (1974)
[35] W Brenig, Z Phys. 171, 60 (1963)
[36] D R Fredkin and N R Werthamer, Phys. Rev A 138, 1527 (1965)
[37] W J Briels, J Tennyson, M Claessens, Th van der Lee, and A van der Avoird, Int J Quantum Chem 23, 1091 (1983)
[38] V A Slyusarev, Yu A Freiman, J N Krupskii, and J A Burakhovich, Phys Status Solidi B. 54, 745 (1972)
[39] H E Stanley, *Introduction to Phase Transitions and Critical Phenomena* (Oxford University, Oxford, 1971)
[40] B Kuchta and T Luty, Chem Phys Lett 92, 462 (1982)
[41] B Kuchta and T Luty, J Chem Phys 78, 1447 (1983)
[42] F D Medina and W B Daniels, J Chem Phys 64, 150 (1976)
[43] M M Théry and D Fabre, Mol Phys 32, 257 (1976)
[44] J K Kjems and G Dolling, Phys Rev B 11, 1639 (1975)

Ab initio description of large amplitude motions in solid N_2. II. Librons in the β-phase and the α–β phase transition

A. van der Avoird, W. J. Briels,[a] and A. P. J. Jansen
Institute of Theoretical Chemistry, University of Nijmegen, Toernooiveld, 6525 ED Nijmegen, The Netherlands

(Received 18 April 1984; accepted 12 June 1984)

Using an *ab initio* pair potential, we have performed mean field and time-dependent Hartree calculations for the reorientational motions in disordered β nitrogen, in a basis of tesseral harmonics The results show that orientationally localized librational solutions with neighboring molecules rotated over 180° around the crystal c axis are energetically more favorable than (nearly) free precession of the molecules. The experimental symmetry can be obtained by allowing rapid jumps between six equivalent localized states; such a jump model predicts the α–β phase transition at the correct temperature.

I. INTRODUCTION

In the preceding paper I[1] we have described a model for the librations in the ordered α and γ phases of solid N_2. In contrast with the more common (quasi-) harmonic models, this "libron" model holds even for the larger amplitude librations. In the present paper we apply it to the β phase of solid nitrogen where the molecules are orientationally disordered.

Two pictures have been accepted for β-nitrogen and it was not possible from the experimental data[2–8] (x-ray diffraction, neutron scattering, nuclear magnetic resonance, and nuclear quadrupole resonance) to discriminate between these pictures. In both pictures the molecular centers are located on a hexagonal lattice with a c/a ratio close to the ideal hexagonal close packed value. There are two molecules in the unit cell and the space group is $P6_3/mmc$ [see Fig. 1(b) of paper I]. In the first picture the N_2 molecules are freely precessing around the crystal c axis with an angle of $56° \pm 2.5°$ between the molecular axes and the c axis. In the second picture the nitrogen atoms are randomly distributed among 24 equivalent positions of the space group $P6_3/mmc$, with the same angle of about 56° between the molecular axes and the c axis. It has been pointed out,[4] on the basis of the overlap between specific molecular density contours, that there will probably be some hindrance between neighboring molecules at specific precession angles. This would prevent completely free precessions.

Theoretical treatments of the lattice dynamics in β-nitrogen are not very numerous. This is obviously due to the fact that it is impossible to apply the standard harmonic model. Some authors[9,10] have assumed that the intermolecular potential may be averaged over freely rotating N_2 molecules. This yields an effective isotropic potential between N_2 pseudoatoms, which was used in a self-consistent phonon calculation of the translational lattice modes The reorientational contributions to the free energy were then superimposed, using a free rotor or 12-fold jump model.[9] Explicit treatments of the reorientational motions on the basis of an anisotropic potential have been given by Mandell[11]—a classical Monte Carlo simulation with a pure quadrupole–quadrupole interaction—by Klein *et al*[12,13]—a classical molecular dynamics calculation with atom–atom plus quadrupole–quadrupole potential—and by Dunmore.[14] The latter, quantum mechanical mean-field calculation is similar to the first part of our study and will be discussed below. Optical (infrared, Raman)[15] and inelastic neutron scattering[5,6] studies of the phonon spectrum of β-N_2 are rather scarce as well.

In the present paper we first present a mean-field solution for the reorientational motions in β-N_2 which has the experimentally observed symmetry When we tried to treat the correlations between the molecular reorientations by means of the time-dependent Hartree (TDH) or the random phase approximation (RPA), the libron frequencies came out purely imaginary, however. It is demonstrated in Sec II, that this implies the instability of the mean-field solution. So, we have looked for a stable mean-field solution of lower symmetry and calculated the libron frequencies (in Sec III). Next we discuss the α–β phase transition and the physical picture that emerges for the reorientational motions in β-nitrogen.

II. STABILITY CONDITIONS FOR THE MEAN-FIELD MODEL

It has been demonstrated by Fredkin and Werthamer[16] that the stability of the solutions of the mean-field (MF) or time-independent Hartree equations for lattice dynamics is related to the eigenvalues of the time-dependent Hartree equations. For zero temperature the latter are identical to the RPA equations (see paper I) Imaginary eigenfrequencies of the TDH equations imply that the original MF solution does not correspond to a local minimum of the free energy The result in the Appendix of Ref (16) is a generalization to nonzero temperature of the stability conditions for Hartree–Fock solutions in many-fermion systems [17–20] We give a slightly different proof which follows closely the presentation of the theory in paper I

We start with the thermodynamic variation principle for the Helmholtz free energy

$$A_{\text{var}} \geqq A_0 + \langle H - H_0 \rangle_0 \geqq A, \tag{1}$$

[a] Laboratoire de Dynamique des Cristaux Moleculaires (ERA 465), Universite des Sciences et Techniques de Lille I, 59655 Villeneuve d'Ascq Cedex, France

 0021-9606/84/203658-08$02 10

where H is the exact lattice Hamiltonian (omitting the constant term from paper I)

$$H = \sum_P L_P(\Omega_P) + \frac{1}{2}\sum_{P\neq P}{}' \Phi_{PP'}(\Omega_P,\Omega_{P'}) \tag{2}$$

and H_0 may be any Hamiltonian The thermodynamic expectation value $\langle X\rangle_0$ is defined as

$$\langle X\rangle_0 = \mathrm{Tr}(D_0 X), \tag{3}$$

where $D_0 = Z_0^{-1} e^{-\beta H}$ is the density operator associated with the approximate Hamiltonian H_0 and A_0 is the corresponding free energy

$$A_0 = -\beta^{-1}\ln Z_0 \tag{4}$$

The partition function reads

$$Z_0 = \mathrm{Tr}(e^{-\beta H_0}) \tag{5}$$

and $\beta = (k_B T)^{-1}$ The exact quantities are given by $A = -\beta^{-1}\ln Z$ with $Z = \mathrm{Tr}(e^{-\beta H})$ The MF or Hartree equation will be found by defining H_0 as a sum of one-particle operators

$$H_0 = \sum_P H_P^{\mathrm{MF}}(\Omega_P), \tag{6}$$

from which it follows that

$$D_0 = \prod_P d_P^{\mathrm{MF}}(\Omega_P) \tag{7}$$

with

$$d_P^{\mathrm{MF}}(\Omega_P) = (Z_P^{\mathrm{MF}})^{-1} e^{-\beta H_P^{\mathrm{MF}}(\Omega_P)},$$
$$Z_P^{\mathrm{MF}} = \mathrm{Tr}^{(P)}(e^{-\beta H_P^{\mathrm{MF}}(\Omega_P)}), \tag{8}$$

and making A_{var} stationary with respect to variations of H_0

$$H_P^{\mathrm{MF}}(\Omega_P) \to H_P^{\mathrm{MF}}(\Omega_P) + h_P(\Omega_P) \tag{9}$$

In order to derive the effect of such variations on the free energy, we use the following well-known expansion[21]

$$\begin{aligned} e^{-\beta(H_P^{\mathrm{MF}}+h_P)} &= e^{-\beta H_P^{\mathrm{MF}}} T\exp\left[-\int_0^\beta d\beta\ \bar{h}_P(\beta')\right] \\ &= e^{-\beta H_P^{\mathrm{MF}}}\left[1 - \int_0^\beta d\beta_1\,\bar{h}_P(\beta_1) \right. \\ &\quad \left. + \int_0^\beta d\beta_1 \int_0^\beta d\beta_2\,\bar{h}_P(\beta_1)\bar{h}_P(\beta_2) - \ \right] \end{aligned} \tag{10}$$

with

$$h_P(\beta) = e^{\beta H_P^{\mathrm{MF}}} h_P e^{-\beta H_P^{\mathrm{MF}}}, \tag{11}$$

where T is the Dyson time-ordering operator, acting here on the inverse temperatures β_1, β_2, etc In order to simplify the notation we have stopped indicating the dependence of all quantities on Ω_P Expanding the logarithm in Eq (4) we obtain for the first order variation in A_0

$$\begin{aligned} A_0^{(1)} &= \beta^{-1}\sum_P \left\langle \int_0^\beta d\beta_1 \bar{h}_P(\beta_1)\right\rangle_P \\ &= \sum_P \langle h_P\rangle_P \end{aligned} \tag{12}$$

The single-particle expectation value is defined as

$$\langle x_P\rangle_P = \mathrm{Tr}^{(P)}(d_P^{\mathrm{MF}} x_P) \tag{13}$$

with d_P^{MF} given by Eq (8)

The same variation (9) of H_P^{MF} by h_P makes the corresponding density operator vary as

$$\begin{aligned} d_P &= e^{-\beta(H_P^{\mathrm{MF}}+h_P)}/\mathrm{Tr}^{(P)}(e^{-\beta(H_P^{\mathrm{MF}}+h_P)}) \\ &= d_P^{\mathrm{MF}} + \delta_P^{(1)} + \end{aligned} \tag{14}$$

with

$$\delta_P^{(1)} = -d_P^{\mathrm{MF}}\left[\int_0^\beta d\beta_1\,\bar{h}_P(\beta_1) - \beta\langle h_P\rangle_P\right] \tag{15}$$

It is easy to verify that $\mathrm{Tr}^{(P)}(\delta_P^{(1)}) = 0$ The same result holds for the higher order terms, so that the density operator remains normalized, $\mathrm{Tr}^{(P)}(d_P) = \mathrm{Tr}^{(P)}(d_P^{\mathrm{MF}}) = 1$, in every order For the first order variation of A_{var} we find the following expression

$$\begin{aligned} A_{\mathrm{var}}^{(1)} &= A_0^{(1)} + \sum_P \mathrm{Tr}^{(P)}(\delta_P^{(1)} L_P) + \sum_{P\neq P}{}' \mathrm{Tr}^{(PP')}(\delta_P^{(1)} d_P^{\mathrm{MF}}\Phi_{PP'}) \\ &\quad - \sum_P \mathrm{Tr}^{(P)}(\delta_P^{(1)} H_P^{\mathrm{MF}}) - \sum_P \mathrm{Tr}^{(P)}(d_P^{\mathrm{MF}} h_P) \end{aligned} \tag{16}$$

Substituting Eqs (12) and (13), we observe immediately that the first term cancels the last term Putting $A_{\mathrm{var}}^{(1)} = 0$ for arbitrary variations $\delta_P^{(1)}$, which are related to the variations h_P via Eq (15), we obtain the MF result

$$\begin{aligned} H_P^{\mathrm{MF}} &= L_P + \sum_{P'\neq P} \mathrm{Tr}^{(P')}(d_{P'}^{\mathrm{MF}}\Phi_{PP'}) \\ &= L_P + \Phi_P^{\mathrm{MF}} \end{aligned} \tag{17}$$

In order to investigate whether the MF solution corresponds to a local minimum of A_{var}, we must look at the second order variation $A_{\mathrm{var}}^{(2)}$ All quantities occurring in A_{var} can be expanded via Eq (10), now taken up to the second order terms inclusive Expanding the logarithm in Eq (4) again, we get

$$\begin{aligned} A_0^{(2)} &= -\beta^{-1}\sum_P \left[\left\langle \int_0^\beta d\beta_1 \int_0^\beta d\beta_2\,\bar{h}_P(\beta_1)\bar{h}_P(\beta_2)\right\rangle_P \right. \\ &\quad \left. -\frac{1}{2}\left\langle \int_0^\beta d\beta_1\,\bar{h}_P(\beta_1)\right\rangle_P^2\right] \\ &= -\beta^{-1}\sum_P \int_0^\beta d\beta_1 \int_0^\beta d\beta_2 \langle \bar{h}_P(\beta_2) h_P\rangle_P \\ &\quad + \frac{1}{2}\beta\sum_P \langle h_P\rangle_P^2 \end{aligned} \tag{18}$$

The total second order variations in A_{var} can then be written as

$$\begin{aligned} A_{\mathrm{var}}^{(2)} &= A_0^{(2)} + \frac{1}{2}\sum_{P\neq P}{}' \mathrm{Tr}^{(PP')}(\delta_P^{(1)}\delta_{P'}^{(1)}\Phi_{PP'}) \\ &\quad + \sum_P \mathrm{Tr}^{(P)}(\delta_P^{(2)} L_P) + \frac{1}{2}\sum_{P\neq P}{}' \mathrm{Tr}^{(PP')}(\delta_P^{(2)} d_P^{\mathrm{MF}}\Phi_{PP'}) \\ &\quad - \sum_P \mathrm{Tr}^{(P)}(\delta_P^{(2)} H_P^{\mathrm{MF}}) - \sum_P \mathrm{Tr}^{(P)}(\delta_P^{(1)} h_P) \end{aligned} \tag{19}$$

The terms with $\delta_P^{(2)}$ cancel after substituting the MF Hamiltonian (17) and the remaining terms

$$A^{(2)}_{\text{var}} = A^{(2)}_0 + \frac{1}{2}\sum_P{}' \mathrm{Tr}^{(P,P)}(\delta^{(1)}_P \delta^{(1)}_P \Phi_{PP}) - \sum_P \mathrm{Tr}^{(P)}(\delta^{(1)}_P h_P) \tag{20}$$

can be worked out by substituting Eqs. (15) and (18). Taking the traces with respect to the eigenstates $|\alpha_P\rangle = |\psi^{(\alpha)}_P\rangle$ of the MF Hamiltonian

$$H^{\text{MF}}_P |\alpha_P\rangle = \epsilon^{(\alpha)} |\alpha_P\rangle, \tag{21}$$

it is not difficult to obtain the result

$$A^{(2)}_{\text{var}} = \frac{1}{2}\sum_P{}' \sum_{\alpha_P \beta_P} \sum_{\alpha'_P \beta'_P} \langle \alpha_P \alpha'_P | \Phi_{PP} | \beta_P \beta'_P \rangle \langle \beta_P | \delta^{(1)}_P | \alpha_P \rangle \langle \beta'_P | \delta^{(1)}_P | \alpha'_P \rangle - \frac{1}{2}\sum_P \sum_{\alpha_P \beta_P} \frac{P^{(\alpha)} - P^{(\beta)}}{\epsilon^{(\alpha)} - \epsilon^{(\beta)}} \langle \alpha_P | h_P | \beta_P \rangle \langle \beta_P | h_P | \alpha_P \rangle + \frac{1}{2}\sum_P \sum_{\alpha_P} \beta P^{(\alpha)} \langle \alpha_P | h_P | \alpha_P \rangle^2 - \frac{1}{2}\sum_P \beta \langle h_P \rangle^2_P \tag{22}$$

The second term has been simplified via interchanging α_P and β_P. The occupation numbers $P^{(\alpha)}$ are given by

$$P^{(\alpha)} = \langle \alpha_P | d^{\text{MF}}_P | \alpha_P \rangle = e^{-\beta\epsilon^{(\alpha)}} \Big/ \sum_\alpha e^{-\beta\epsilon^{(\alpha)}} \tag{23}$$

In Eq. (21), and also later, we use the fact that in all our applications the spectra of all H^{MF}_P are equal (see paper I), i.e., $\epsilon^{(\alpha)}$ does not depend on P. Equation (22) contains both the variations h_P in the MF Hamiltonian and the variations $\delta^{(1)}_P$ in the density operator. Via relation (15) it could be expressed in terms of h_P only, but we find it more convenient to write Eq. (15) in matrix element form

$$\langle \alpha_P | \delta^{(1)}_P | \beta_P \rangle = \frac{P^{(\alpha)} - P^{(\beta)}}{\epsilon^{(\alpha)} - \epsilon^{(\beta)}} \langle \alpha_P | h_P | \beta_P \rangle \quad \text{for } \epsilon^{(\alpha)} \neq \epsilon^{(\beta)}$$
$$= -\beta P^{(\alpha)} [\langle \alpha_P | h_P | \alpha_P \rangle - \langle h_P \rangle_P] \quad \text{for } \epsilon^{(\alpha)} = \epsilon^{(\beta)} \tag{24}$$

and to use this relation backwards, in order to express Eq. (22) completely in terms of the matrix elements of $\delta^{(1)}_P$

$$A^{(2)}_{\text{var}} = \frac{1}{2}\sum_P{}' \sum_{\alpha_P \beta_P} \sum_{\alpha'_P \beta'_P} \langle \alpha_P \alpha'_P | \Phi_{PP} | \beta_P \beta'_P \rangle \langle \beta_P | \delta^{(1)}_P | \alpha_P \rangle \langle \beta'_P | \delta^{(1)}_P | \alpha'_P \rangle - \frac{1}{2}\sum_P \sum_{\alpha_P \beta_P} \frac{\epsilon^{(\alpha)} - \epsilon^{(\beta)}}{P^{(\alpha)} - P^{(\beta)}} \langle \alpha_P | \delta^{(1)}_P | \beta_P \rangle \langle \beta_P | \delta^{(1)}_P | \alpha_P \rangle \tag{25}$$

The last two sums over diagonal terms in Eq. (22) correspond with the diagonal ($\alpha_P = \beta_P$) terms in the last summation of Eq. (25). These terms have been formally included in this summation via the relation

$$\lim_{\epsilon^{(\beta)} \to \epsilon^{(\alpha)}} \frac{\epsilon^{(\alpha)} - \epsilon^{(\beta)}}{P^{(\alpha)} - P^{(\beta)}} = -\frac{1}{\beta P^{(\alpha)}} \tag{26}$$

Equation (25) is identical to the expression obtained by Fredkin and Werthamer,[16] who did not explicitly consider the diagonal terms.

It is easy to adapt this expression to the translational symmetry of the crystal. Defining the first order variations in the symmetry adapted density matrix as variational coefficients

$$C(\mathbf{q})_{\alpha\beta,i} = N^{-1/2} \sum_{\mathbf{n}} e^{i\mathbf{q}\cdot\mathbf{R}_{\mathbf{n}}} \langle \alpha_P | \delta^{(1)}_P | \beta_P \rangle \tag{27}$$

with $P = \{\mathbf{n}, i\}$, and the Fourier transformed pair interaction matrix

$$\Phi(\mathbf{q})_{\alpha\beta,i\alpha'\beta',i'} = \sum_{\mathbf{n}} e^{i\mathbf{q}\cdot\mathbf{R}_{\mathbf{n}}} \langle \alpha_P \alpha'_P | \Phi_{PP'} | \beta_P \beta'_{P'} \rangle \tag{28}$$

with $P = \{\mathbf{0}, i\}$ and $P' = \{\mathbf{n}, i'\}$, and $\Phi_{PP} = 0$, just as in paper I, we find that $A^{(2)}_{\text{var}}$ becomes additive in the wave vector $\mathbf{q}$

$$A^{(2)}_{\text{var}} = \sum_{\mathbf{q}} A^{(2)}_{\text{var}}(\mathbf{q})$$

with

$$A^{(2)}_{\text{var}}(\mathbf{q}) = \frac{1}{2}\sum_{ii'} \sum_{\alpha\beta} \sum_{\alpha'\beta'} \Phi(\mathbf{q})_{\alpha\beta,i\alpha'\beta',i'} C(\mathbf{q})_{\beta\alpha,i} C(-\mathbf{q})_{\beta'\alpha',i'} - \frac{1}{2}\sum_i \sum_{\alpha\beta} \frac{\epsilon^{(\alpha)} - \epsilon^{(\beta)}}{P^{(\alpha)} - P^{(\beta)}} C(\mathbf{q})_{\alpha\beta,i} C(-\mathbf{q})_{\beta\alpha,i} \tag{29}$$

It can be assumed, without imposing any restriction, that the MF states $|\alpha_P\rangle$ are real. Then the matrix $\Phi(\mathbf{q})$ satisfies the following symmetry relations

$$\Phi(\mathbf{q})_{\alpha\beta,i\alpha'\beta',i'} = \Phi(\mathbf{q})_{\beta\alpha,i\alpha'\beta',i'} = \Phi(\mathbf{q})_{\alpha\beta,i\beta'\alpha',i'} = \Phi(\mathbf{q})_{\beta\alpha,i\beta'\alpha',i'} \tag{30}$$

in addition to the usual properties

$$\Phi(\mathbf{q}) = \Phi(\mathbf{q})^\dagger = \Phi(-\mathbf{q})^* \tag{31}$$

For Hermitean variations h_P, Eq. (24) yields the following relation for the variation coefficients (27)

$$C(\mathbf{q})_{\alpha\beta,i} = C(-\mathbf{q})^*_{\beta\alpha,i} \tag{32}$$

If we now order the MF states such that $\alpha > \beta$ implies $\epsilon^{(\alpha)} > \epsilon^{(\beta)}$ and $P^{(\alpha)} < P^{(\beta)}$, relabel the coefficients

$$C(\mathbf{q})_{\alpha\beta,i} = u(\mathbf{q})_{\alpha\beta,i} \quad \text{for } \alpha > \beta,$$
$$C(\mathbf{q})_{\alpha\beta,i} = v(\mathbf{q})_{\alpha,i} \quad \text{for } \alpha = \beta, \tag{33}$$
$$C(\mathbf{q})_{\alpha\beta,i} = w(\mathbf{q})_{\beta\alpha,i} \quad \text{for } \alpha < \beta,$$

and use the relations (30) to (32), we can rewrite Eq (29) in matrix form

$$A^{(2)}_{\mathrm{var}}(\mathbf{q}) = \frac{1}{2} \times \begin{pmatrix} \mathbf{u}(\mathbf{q}) \\ \mathbf{v}(\mathbf{q}) \\ \mathbf{w}(\mathbf{q}) \end{pmatrix}^{\dagger} \begin{pmatrix} \Phi(\mathbf{q}) - \chi & \phi(\mathbf{q}) & \Phi(\mathbf{q}) \\ \phi(\mathbf{q})^{\dagger} & \mathbf{f}(\mathbf{q}) - \mathbf{g} & \phi(\mathbf{q})^{\dagger} \\ \Phi(\mathbf{q}) & \phi(\mathbf{q}) & \Phi(\mathbf{q}) - \chi \end{pmatrix} \begin{pmatrix} \mathbf{u}(\mathbf{q}) \\ \mathbf{v}(\mathbf{q}) \\ \mathbf{w}(\mathbf{q}) \end{pmatrix} \quad (34)$$

with the matrices $\Phi(\mathbf{q})$, $\phi(\mathbf{q})$, and $\mathbf{f}(\mathbf{q})$ all being subblocks of the matrix $\Phi(\mathbf{q})$ in Eq (28) with $\{\alpha > \beta,\ \alpha' > \beta'\}$, $\{\alpha > \beta, \alpha' = \beta'\}$, and $\{\alpha = \beta, \alpha' = \beta'\}$, respectively The diagonal matrices χ and $\mathbf{g}$ are defined as

$$\chi_{\alpha\beta,i\alpha'\beta'} = \delta_{\alpha\alpha'}\delta_{\beta\beta'}\delta_{ii'}\frac{\epsilon^{(\alpha)} - \epsilon^{(\beta)}}{P^{(\alpha)} - P^{(\beta)}} \quad \text{for } \alpha > \beta,$$

$$g_{\alpha i,\alpha' i'} = -\delta_{\alpha\alpha'}\delta_{ii'}(\beta P^{(\alpha)})^{-1} \quad (35)$$

The matrix occurring in Eq (34) is related to the matrix $\mathbf{M}(\mathbf{q})$ occurring in the TDH equations (cf paper I) by

$$\mathbf{M}(\mathbf{q}) = \begin{pmatrix} -\mathbf{P} & \mathbf{0} \\ \mathbf{0} & \mathbf{P} \end{pmatrix} \begin{pmatrix} \Phi(\mathbf{q}) - \chi & \Phi(\mathbf{q}) \\ \Phi(\mathbf{q}) & \Phi(\mathbf{q}) - \chi \end{pmatrix} = \begin{pmatrix} -\mathbf{P} & \mathbf{0} \\ \mathbf{0} & \mathbf{P} \end{pmatrix} \mathbf{N}(\mathbf{q}), \quad (36)$$

where $\mathbf{P}$ is a diagonal population difference matrix

$$P_{\alpha\beta i,\alpha'\beta' i'} = \delta_{\alpha\alpha'}\delta_{\beta\beta'}\delta_{ii'}(P^{(\alpha)} - P^{(\beta)}) \quad \text{for } \{\alpha > \beta, \alpha' > \beta'\} \quad (37)$$

The matrix $\mathbf{N}(\mathbf{q})$ is obtained from the matrix in Eq (34) by erasing the central rows and columns

The second variation $A^{(2)}_{\mathrm{var}}(\mathbf{q})$ is positive for any set of variation coefficients (33) if and only if the matrix in Eq (34) is positive definite Via the separation theorem for the eigenvalues of Hermitean matrices and their principal minors[22] it follows then, that its submatrix $\mathbf{N}(\mathbf{q})$ must be positive definite, too The latter matrix can be blocked by means of a simple similarity transformation $\mathbf{T}$ adding and subtracting its rows and columns, which corresponds with taking the real and imaginary parts of the variation coefficients $\mathbf{u}$ and $\mathbf{w}$ as new variables This yields

$$\mathbf{N}'(\mathbf{q}) = \mathbf{T}^{-1}\mathbf{N}(\mathbf{q})\mathbf{T} = \begin{pmatrix} 2\Phi(\mathbf{q}) - \chi & \mathbf{0} \\ \mathbf{0} & -\chi \end{pmatrix} \quad (38)$$

The diagonal submatrix $-\chi$ is clearly positive definite, see Eq (35) As a result, the matrices $\mathbf{N}'(\mathbf{q})$ and $\mathbf{N}(\mathbf{q})$, and therefore $A^{(2)}_{\mathrm{var}}$ as given by Eq (34), can only be positive definite if the submatrix $2\Phi(\mathbf{q}) - \chi$ is positive definite The latter matrix occurs in the generalized eigenvalue problem, Eq (20) of paper I, which yields the squares of the TDH frequencies Multiplying this eigenvalue equation by -1 and using the fact that the metric matrix $-\mathbf{P}^{-1}\chi^{-1}\mathbf{P}^{-1}$ is diagonal and positive definite, one easily shows that the squares of the TDH frequencies are all positive if and only if $2\Phi(\mathbf{q}) - \chi$ is positive definite

In summary, we have proved that the squares of the TDH eigenfrequencies are positive, provided that the mean-field solution corresponds with a local minimum in A_{var} So, if one or more of these squares are negative, i e , if one or more of the TDH frequencies $A^{(k)}(\mathbf{q})$ are imaginary, then the matrices $\mathbf{N}(\mathbf{q})$ and $\mathbf{N}(\mathbf{q})$ have negative eigenvalues Choosing the variation coefficients $\mathbf{u}(\mathbf{q})$ and $\mathbf{w}(\mathbf{q})$ in Eq (33) as one of the eigenvectors of $\mathbf{N}(\mathbf{q})$ associated with these negative eigenvalues and $\mathbf{v}(\mathbf{q}) = 0$ yields a negative value of $A^{(2)}_{\mathrm{var}}$ and thus a free energy which is lower than the MF value Inspecting these eigenvectors can help us in finding a more stable MF solution

III. MEAN FIELD AND LIBRON CALCULATIONS

The methods applied for the lattice dynamics calculations on β-nitrogen are the same as those used in paper I Also, we have employed the same *ab initio* potential[23] with the anisotropy expressed in the form of a spherical expansion, including spherical harmonics up to $l = 6$ on each molecule We have used the experimental[14] unit cell parameters $\mathbf{a}$ and $\mathbf{c}$ [see Fig 1(b) of paper I], at zero pressure and temperature 46 K The mean-field states of the molecules on each lattice site have been expanded in tesseral harmonics with even or odd l for pure *ortho* or *para* nitrogen, respectively Lattice summations over the potential have been extended over eight shells, $R < 9\ 87$ Å We have not assumed the mean-field potential to have axial symmetry around the c axis, as Dunmore[14] has done For the existence of localized solutions with broken symmetry, see below, the nonaxial components are crucial

Just as in Paper I we have started by assuming the experimentally observed crystal symmetry Thus, the two molecules in the hexagonal unit cell have been given identical

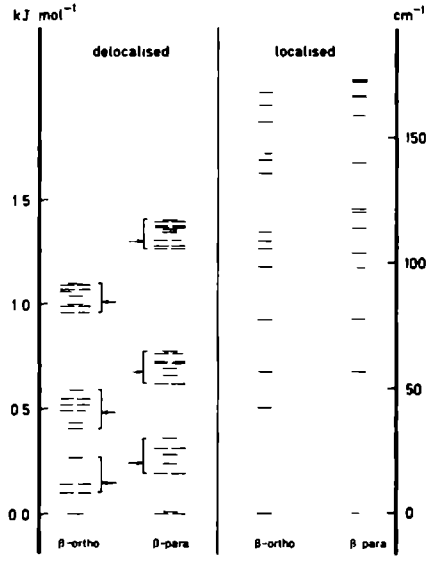

FIG 1 Calculated mean field levels for β-nitrogen corresponding with the delocalized (unstable) mean field states and the (stable) localized states The arrows which are the free rotor levels, indicate that the delocalized mean field spectrum resembles a perturbed rotor spectrum

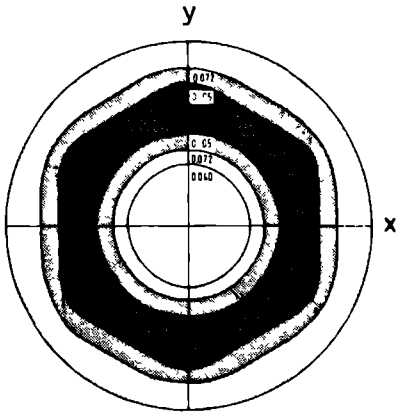

FIG 2 Orientational probability distribution of the molecular axes for the delocalized mean field states in β nitrogen, for both molecules in the unit cell This picture is almost independent of the temperature up to (at least) 70 K Reading of the contour plot as in paper I, Fig 3

mean-field solutions That is, the Euler angles in the matrices $D^{(k)}(\alpha,\beta,\gamma)$ which rotate mean-field expectation values from the original site in the unit cell to the equivalent sites, see Eq (9) of paper I, have all been put to zero The mean-field spectrum and the ground state wave function which result from these calculations are shown in Figs 1 and 2, respectively It is obvious from the contour plot in Fig 2 that the orientations of the molecular axes in the mean-field states are delocalized The motions can be described as precessions around the c axis which are just slightly hindered by small sixfold barriers In accordance with the picture of Press and Huller,[24] the angle θ between the molecular axes and the c axis is not fixed, but it shows a rather broad distribution The maximum of this distribution lies at the "experimental"[3,4,7,8] precession angle, about 56° We can easily calculate the coefficients C_{lm} in the orientational form factors[6,24]

$$F^{\text{rot}}(\mathbf{q}) = \sum_{lm} (i)^l C_{lm} S_{lm}(\theta,\phi)\, j_l(qd/2), \tag{39}$$

where $S_{lm}(\theta,\phi)$ are tesseral harmonics, j_l are spherical Bessel functions, d is the molecular bond length, and q is the wave vector Our results are given in Table I The experimental results are rather uncertain,[6] but the general feature that C_{20} is relatively very small, which is confirmed by the NMR and NQR data,[7,8] agrees with our calculations Also the mean-field spectrum at the left-hand side of Fig 1, is characteristic for delocalized reorientational motions It has the appearance of a perturbed free rotor spectrum, with significant differences between *ortho* and *para* nitrogen Apart from the small sixfold modulation in Fig 2, our results are similar to Dunmore's,[14] although the intermolecular potentials used are different (see also paper I)

From the mean-field states thus obtained we wanted to calculate the libron frequencies by means of the TDH method Using a basis of two or five excited mean-field states per molecule and 2 molecules in the unit cell, while conserving the full translational symmetry of the problem, one has to solve a four or ten dimensional complex generalized eigenvalue problem, respectively, in order to calculate the squares of the libron frequencies [cf paper I, Eq (20)] Some of these frequencies (for $\mathbf{q} = 0$) came out imaginary, however, i e, their squares were negative, in both cases According to the theory of Sec II, this implies that the delocalized mean-field states do not correspond to a local minimum of the free energy It should be possible to find a more stable mean-field solution which still has the correct translational symmetry Inspecting the eigenvectors of the TDH problem belonging to the imaginary frequencies has taught us that the free energy could be lowered by out-of-phase motions of the two neighboring molecules in the unit cell

Thus, we have modified our MF program in such a way that the two molecules in the unit cell are treated independently, within each others mean field This leads to two steps in each cycle of the iterative MF procedure, which were previously reduced to one step by rotating the mean-field solution from the first molecule to the second one in the unit cell (over angles zero, in this case) Indeed, we have found a MF solution which is lower in free energy than the delocalized solution, by 0 87 kJ/mol at zero temperature In this new solution, the orientations of the molecular axes are clearly localized, see Fig 3 The MF states for the two neighboring molecules in the unit cell appear to be equivalent, but rotated over 180° around the c axis, just as expected from the TDH eigenvectors for the previous, unstable, solution This 180° rotation avoids the hindrance which would occur between

TABLE I Orientational form factors in β-nitrogen from mean field calculations, see Eq. (39)

	Calculated					Experiment
	Delocalized		Localized		Ref 14	Ref 6[a]
	$T = 30$ K	45 K	30 K	55 K	35 K	55 K
$C_{2,0}$	− 0 027	− 0 020	0 048	0 032	− 0 003	0 004 ± 0 085
$C_{4,0}$	− 0 082	− 0 060	− 0 233	− 0 167	− 0 043	− 0 311 ± 0 326
$C_{6,0}$	0 029	0 020	0 042	0 023	–	0 99 ± 1 95
$C_{6,6}$	− 0 016	− 0 013	− 0 035	− 0 013	–	− 0 18 ± 2 30

[a] Converted to normalized tesseral harmonics.

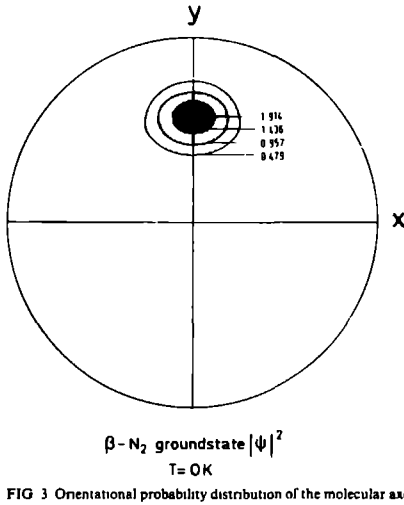

FIG 3 Orientational probability distribution of the molecular axes for the localized mean field states in β nitrogen drawn for one molecule in the unit cell the other molecule in the cell is rotated over $\phi = 180°$ The distribution does not change qualitatively up to (at least) $T \approx 70$ K it just becomes slightly wider with increasing temperature Reading of the contour plot as in paper I Fig 3

neighboring molecules when they precess freely [4]

The motions of the molecules in this new MF solution can be described as localized librations about equilibrium orientations of the molecular axes which point to one of the square faces of the hexagonal cage,[2] see Fig 1(b) of paper I The angle $\theta \cong 52°$ between the molecular axes and the crystal c axis is slightly smaller than for the delocalized case The coefficients in the form factor are similar, see Table I In particular, the coefficient C_{20} is still relatively small, as expected from the experimental data The much higher excitation energies in the MF spectrum, Fig 1 right-hand side, and the similarity between the *ortho* and *para* nitrogen solutions are typical for localized librations (cf the α and γ nitrogen results in I)

The most remarkable feature of the localized MF states is that the experimentally observed hexagonal symmetry of the crystal is completely lost This experimental symmetry will be restored if we assume that, for each molecule, six equivalent MF solutions are available, which are related to each other by rotations of 60° around the c axis, and that the molecules can jump from one localized solution to another within the time that is characteristic for the observation process (the inverse NMR frequency, for example) We shall digress on this hypothesis in Sec IV, when discussing the α–β phase transition Our jump model thus assumes six localized orientations for each molecule in the unit cell, i e , 12 molecular positions or 24 atomic positions in each primitive cell These are not the 24-fold degenerate Wyckoff positions[25] of the space group $P6_3/mmc$, however, but two sets of 12-fold degenerate positions Actually, as observed in Ref 2, with the molecules in alternate layers packed as they are in the (near) hcp lattice, it is not possible that the atoms occupy just one set of 24-fold degenerate positions This can easily be seen by checking that the centers of inversion of the space group are not located on the lattice sites occupied by the molecular midpoints

Next we calculated the libron frequencies by the TDH method with two excited, localized, MF states on each molecule All these frequencies are real now, as they should be for a stable MF solution As can be expected from the localized nature of the MF states, we find that the libron frequencies (see Table II) are of similar size as those for the ordered α and γ phases, and comparable also with the translational phonon frequencies [9 15] The experimental spectra[5 15] show two very broad peaks of which the higher one around 50 cm^{-1} (depending on the temperature and pressure) has been interpreted as a libron band and the lower one around 25 cm^{-1} as a translational phonon band (Table II) The higher libron frequency agrees reasonably well with our results, but according to our calculated frequencies, the libron modes might cause some absorption in the lower band as well (apart from symmetry and intensity considerations, which we have not looked at) Our results indicate that the broadening of the observed libron band is caused by coupling localized librational modes with more or less random jumps in the orientations of the molecules by multiples of 60°

IV. THE α–β PHASE TRANSITION

In Fig 4 we have plotted the free energy A_{var} calculated from the different MF solutions of α and β nitrogen, accord-

TABLE II Optical (q = 0) frequencies in β-nitrogen (in cm^{-1})

	Calculated (libron)		Experiment					
	TDH	TDH	Ref 15				Kjems and Dolling[a]	
Temperature (K)	0	55	55	55	55	55	36	
Molar volume (cm^3 mol^{-1})	28 26	28 26	26 87	25 90	25 05	23 59		
Frequencies			25 ± 3	28 ± 3	31 ± 3	36 ± 3	25 64	translational phonon
	34 9 56 7 65 7 73 3	33 9 40 8 55 8 58 8	50 ± 3	54 ± 3	58 ± 3	68 ± 3		libron

[a] As quoted in Ref 15

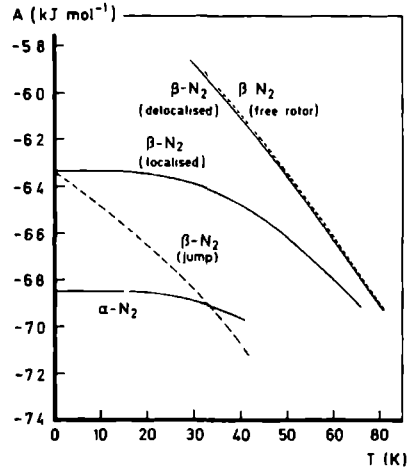

FIG 4 Free energy (at zero pressure) for α nitrogen (see paper I) and β nitrogen in different mean field models (closed lines) The dashed free rotor curve has been calculated from the isotropic $(l_1\ l_2\ l_3) = (0\ 0\ 0)$ term of the *ab initio* potential (Ref 23) by adding the free rotor expression for the free energy as in Ref 9 The dashed jump model curve has been obtained from the localized mean field solution (with the full anisotropic potential) by adding an entropy term $-k_B T \ln 6$ (see the text)

ing to Eq (1) or, in more detail, Eq (11a) of paper I The contribution from the translational phonons is not included in this picture, it will be considered in paper III, but we do not expect a great difference in this contribution between the α and β phases The curve for the delocalized MF solution of β nitrogen falls off much steeper, with increasing temperature, than the localized β-N_2 curve and the α-N_2 curve This is caused by the considerably lower excitation energies for the delocalized states which can be conceived as perturbed free rotor states (see the MF spectra in Fig 1) It is characteristic that the free rotor model, which has been used also by Raich *et al*,[9,26] produces almost the same free energy curve (see Fig 4) as the delocalized MF model in β-N_2 The (free) energy at zero temperature for the delocalized model is too high, however, to make the β-N_2 curve cross the α-N_2 curve at any reasonable temperature So this model fails to explain the α–β phase transition

For the localized β-N_2 model, the energy is substantially lowered, due to a more favorable packing of nearest neighbors But, for this model, the free energy curve runs almost parallel to the α-N_2 curve, which is related to the similar size of the MF excitation frequencies, and we still find no crossing between the α and β curves It should be remembered that the localized MF solution for β nitrogen has much lower symmetry than observed experimentally We conjecture that the experimental symmetry will be restored by assuming more or less random jumps of each molecule between six localized librational states, symmetrically positioned about the c axis Because of important energy effects, the orientations of the molecules will not be completely randomly distributed over the six possibilities but, on the contrary, they will show a strong short range correlation The effect of this correlation is to substantially lower the energy of the whole crystal and make it approximately equal to the energy calculated in our "correlated" localized mean-field model

The entropy of the crystal can be assumed to be the sum of two contributions The first part originates from the librations of the molecules around their equilibrium orientations and it is approximately the entropy calculated in the localized mean-field model The second part is due to the distribution of the molecules over their six positions Although the latter distribution is strongly correlated, it is in the spirit of the present MF approach to put the corresponding entropy equal to $-k_B T \ln 6$ The free energy per particle will thus be equal to the result of the localized model, minus $k_B T \ln 6$ This yields the dashed curve in Fig 4 marked "β-N_2 jump" This curve crosses the free energy curve for α-N_2 at $T = 34$ K, in close agreement with the experimental α–β phase transition temperature, $T = 35.6$ K

In principle, one could suggest that the same type of jumps occur between four equivalent localized solutions in α-N_2, with the molecules oriented along one of the body diagonals of the cubic lattice (see paper I) One can argue, however, that such jumps of the individual molecules are energetically much more unfavorable in α-N_2 than they are in β-N_2 The strongest indication for this is the experimentally observed crystal symmetry which agrees with the symmetry of a specific localized MF solution for α-N_2 Further arguments can be found from the MF calculations themselves In the first place, the overlap between the sixfold localized MF states in β-N_2 is substantially larger than the overlap between the four states in α-N_2 and, therefore, tunneling will be faster in β-N_2 Secondly, we have tried to generate delocalized solutions for α-N_2 by forcing all four molecules in the unit cell to have identical MF states as in the delocalized β-N_2 model The molecules in α N_2 remain still localized, however, with their axes oriented along one of the cube edges So, even at the expense of a substantial amount of lattice energy, the molecules in α-N_2 will not reorient themselves as in β-N_2 Apparently, the rotation barriers are substantially higher in α-N_2 than they are in β-N_2 A definite theoretical confirmation of the jump model in β-N_2 must wait for a sound theoretical formulation of the dynamics of this model, though

Our jump model seems related to the 12-fold jump model invoked by Raich *et al*,[9] who have also used their model to study the α–β phase transition However, our results show that it is essential that the jumps occur between localized librational states of the molecules which lie in deep wells that can only be obtained from the full anisotropic potential Raich *et al*[9] have used an effective, orientationally averaged, isotropic potential, which in our case would produce a free energy curve close to the free rotor curve in Fig 4 and, thus, too high to cross the α-N_2 curve A certain amount of localization seems to be required, even in the β phase, in order to stabilize this phase and obtain the α–β phase transition at the observed temperature

So the physical picture for β-nitrogen that emerges from our calculations is that of a sixfold jump model between orientationally localized librational states of the molecules

There is a tendency for neighboring molecules to stay 180° out of phase, in order to achieve a favorable lattice energy Thus, it is clear that an appropriate quantum dynamical model for the jump process, which is still to be developed, must include the intermolecular (pair) correlations from the outset

ACKNOWLEDGMENTS

This investigation was supported in part by the Netherlands Foundation for Chemical Research (SON) with financial aid from the Netherlands Organization for the Advancement of Pure Research (ZWO).

[1]A P J Jansen, W J Briels, and A van der Avoird, J Chem Phys. 81, 3648 (1984)
[2]W E Streib, T H Jordan, and W N Lipscomb, J Chem Phys. 37, 2962 (1962)
[3]T H Jordan, H W Smith, W E Streib, and W N Lipscomb, J Chem Phys. 41, 756 (1964)
[4]A F Schuch and R L Mills, J Chem Phys 52, 6000 (1970).
[5]J K Kjems and G Dolling, Phys Rev B 11, 1639 (1975)
[6]B M Powell, G Dolling, and H F Nieman, J Chem Phys 79, 982 (1983)
[7]A S de Reggi, P C Canepa, and T A Scott, J Magn Reson 1, 144 (1969)
[8]T A Scott, Phys Rept 27, 89 (1976)
[9]J C Raich, N S Gillis, and T R Koehler, J Chem Phys 61, 1411 (1974)
[10]V V Goldman and M L Klein, J Chem Phys. 64, 1521 (1975)
[11]M J Mandell, J Chem Phys 60, 4880 (1974)
[12]M L Klein and J J Weis, J Chem Phys 67, 217 (1977)
[13]M L Klein, D Levesque, and J J Weis, J Chem Phys. 74, 2566 (1981)
[14]P V Dunmore, J Low Temp Phys. 24, 397 (1976)
[15]F D Medina and W B Daniels, J Chem Phys 64, 150 (1976)
[16]D R Fredkin and N R Werthamer, Phys Rev A 138, 1527 (1965)
[17]D J Thouless, Nucl Phys 21, 225 (1960)
[18]N D Mermin, Ann Phys. (N Y) 21, 99 (1963)
[19]D J Rowe, *Nuclear Collective Motion* (Methuen, London, 1970).
[20]J Čížek and J Paldus, Phys Rev A 3, 525 (1971)
[21]D J Thouless, *The Quantum Mechanics of Many-Body Systems* (Academic, New York, 1961)
[22]G G Hall, *Matrices and Tensors* (Pergamon, Oxford, 1963)
[23]R M Berns and A van der Avoird, J Chem Phys 72, 6107 (1980)
[24]W Press and A Huller, J Chem. Phys 68, 4465 (1978)
[25]*International Tables for X-ray Crystallography* (Kynoch, Birmingham, England, 1967), Vol I
[26]J C Raich and R D Etters, J Low Temp Phys. 7, 449 (1972).

Section 2.3

NEW APPROACH TO ORIENTATIONALLY DISORDERED MOLECULAR CRYSTALS

A.P.J. Jansen
Institute of Theoretical Chemistry
University of Nijmegen
Toernooiveld
6525 ED Nijmegen
The Netherlands

Abstract

A new theory is presented for the description of orientationally disordered molecular crystals. The theory is based on the thermodynamic variation principle with a generalized Ising Hamiltonian. The optimized single-molecule states are calculated, and the occupation of these states and the correlation in the occupation for pairs of molecules is determined via the cluster variation method. The theory is applied to the β-phase of solid nitrogen. A delocalized orientational probability distribution is found that is formed by six localized states which are equally occupied. Correlation functions for the orientations of nearest-neighbours are given.

1. Introduction

Interest in orientationally disordered or "plastic" molecular crystals has been growing over the last years. This may be partially due to the fact that it is quite common for a molecular substance to have an orientationally disordered solid phase. Molecular crystals often show an order-disorder phase transition. The disordered phase at the higher temperatures is stabilized by a high entropy. In solid hydrogen the zero-point motions are so large that even at $T = 0$ K the crystal is orientationally disordered.[1]

The standard (quasi-)harmonic methods obviously do not work for the dynamics of these kinds of crystals. No other method has emerged yet that has been regarded widely as an appropriate method to describe the reorientations of the molecules. The most versatile (classical) method is Molecular Dynamics. A large number of orientationally disordered molecular crystals has been studied using this method, notably by Klein *et al.*[2-8], Lynden-Bell *et al.*[7-9] and Dove *et al.*[9,10] The major drawback of Molecular Dynamics is that it is a classical method. It fails where quantum effect are concerned. Furthermore, it is a simulation method, whereas one often prefers an analytical method in which the relations between various properties are more transparent.

The only quantum mechanical methods that have been used to our knowledge are the Time Independent and Time Dependent Hartree approximations, and the pseudo-spin method. The first two approximations are most frequently encountered in the form of a susceptibility approach (see the work of Michel).[11-14] In our work we have usually called them Mean Field (MF) and Random Phase Approximation (RPA). These approximations seem to work quite satisfactorily. However, as we have shown in the case of β-N_2, there are crystals where a more sophisticated formalism is needed to treat the correlation in the occupation of different states. The pseudo-spin method attempts to do just that.[15,16] This method however is only capable of handling two states per molecule. We will comment on all these methods later on.

The standard model for an order-disorder phase transition is the Ising model.[17] In this paper we will show how to extend the Ising Model so that it can be applied to molecular crystals. The main problem is what states to choose for the individual molecule. We will show how to calculate those states that yield the minimal free energy. In subsection 2A the method is outlined. In subsection 2B the cluster variation method for obtaining occupation numbers is presented. In section 3 the results of the calculations

on β-N_2 and the α-β phase transition in solid nitrogen are presented. In section 4 the results are discussed, the method is compared to the methods mentioned above, and some improvements are suggest. The appendices serve to clarify some of the problems encountered in section 2.

2. Theory

A. Derivation of the method

The method that we present in this paper is based on the thermodynamic variation principle or Gibbs-Bogoliubov inequality[18]

$$A_{var} \equiv A_0 + \langle H - H_0 \rangle_0 \geq A, \tag{1}$$

with

$$A = -\beta^{-1} \ln \mathrm{Tr}[e^{-\beta H}], \tag{2a}$$

$$A_0 = -\beta^{-1} \ln \mathrm{Tr}[e^{-\beta H_0}], \tag{2b}$$

$$\langle X \rangle_0 = \frac{1}{Z_0} \mathrm{Tr}[e^{-\beta H_0} X], \tag{3a}$$

and

$$Z_0 = \mathrm{Tr}[e^{-\beta H_0}]. \tag{3b}$$

Here H is the exact Hamiltonian of the system, A is the exact free energy, and X is any operator. The general form of the exact Hamiltonian can be written as

$$H = \sum_P L_P + \frac{1}{2} \sum_{PP'} \Phi_{PP'}, \tag{4}$$

when we assume that there are no three- or more-particle interactions. The summation indices P and P' denote the molecules in the crystal. The one-particle terms L_P contain the kinetic energy and possibly the crystal field. The two-particle terms $\Phi_{PP'}$ contain the intermolecular interactions. As it is almost always impossible to calculate properties with the exact Hamiltonian H, we use an approximate Hamiltonian H_0 for the calculations. The variational method consists of choosing a (parametrized) functional form for the Hamiltonian H_0. The "best" Hamiltonian H_0 is then obtained by varying it and thereby minimizing A_{var}. If a sum of one-particle operators is chosen for H_0 then this yields the Mean Field (MF) approximation.[19,20] If a harmonic Hamiltonian is chosen for H_0 then this yields the Self-Consistent Phonon (SCP) approximation.[21]

We can write the exact Hamiltonian H in terms of an orthonormal basis of single-molecule states as

$$H = \sum_{P} \sum_{\alpha\beta} \langle \alpha(P) \mid L_P \mid \beta(P) \rangle \, E^{(P)}_{\alpha\beta} + \sum_{PP'} \sum_{\alpha\beta\gamma\eta} \langle \alpha(P)\gamma(P') \mid \Phi_{PP'} \mid \beta(P)\eta(P') \rangle \, E^{(P)}_{\alpha\beta} E^{(P')}_{\gamma\eta}, \tag{5}$$

with

$$E^{(P)}_{\alpha\beta} \equiv |\alpha(P)\rangle\langle\beta(P)|. \tag{6}$$

The states $|\alpha(P)\rangle$ and $|\beta(P)\rangle$ are the states of the orthonormal basis.

In our method we approximate the Hamiltonian H by an operator H_0 which does not contain any non-diagonal terms; that is we write

$$H_0 = \sum_{P} \sum_{\alpha} c^{(1)}_{P\alpha} E^{(P)}_{\alpha\alpha} + \frac{1}{2} \sum_{PP'} \sum_{\alpha\beta} c^{(2)}_{P\alpha,P'\beta} E^{(P)}_{\alpha\alpha} E^{(P')}_{\beta\beta}. \tag{7}$$

In the minimisation of A_{var} we vary both the coefficients $c^{(1)}_{P\alpha}$ and $c^{(2)}_{P\alpha,P'\beta}$ and the basis of single-molecule states. If there are only two states per molecule then, apart from a constant, the Hamiltonian H_0 can be written as an classical Ising Hamiltonian

$$H_{\text{Ising}} = -\sum_{PP'} J_{PP'} \sigma_{Pz} \sigma_{P'z} + g\mu_B \sum_{P} H_P \sigma_{Pz}. \tag{8}$$

The Hamiltonian H_0 is thus a generalisation of the Hamiltonian that is used in the pseudo-spin method. Our method can therefore be regarded as an extension of the pseudo-spin method. The Ising Hamiltonian and H_0 have the same properties. The eigenstates of H_0 are product functions

$$|\{\alpha\}\rangle = \prod_{P} \otimes |\alpha(P)\rangle, \tag{9}$$

just as for the Ising Hamiltonian. Its eigenvalues are

$$E_{\{\alpha\}} = \sum_{P} \sum_{\alpha} c^{(1)}_{P\alpha_P} + \frac{1}{2} \sum_{PP'} \sum_{\alpha\beta} c^{(2)}_{P\alpha_P,P'\beta_{P'}}. \tag{10}$$

Consequently, the methods that have been devised for the Ising model to calculate thermodynamic averages $\langle X \rangle_0$ may be used for H_0 as well.

To facilitate the variation of the basis states $\{|\alpha(P)\rangle\}$, we introduce a fixed orthonormal basis $\{|i(P)\rangle\}$ that is known. We define unitary matrices $U_{\alpha i}^{(P)}$ by

$$|\alpha(P)\rangle = \sum_i U_{\alpha i}^{(P)} |i(P)\rangle. \tag{11}$$

Using this equation we can effect the variation of the basis $\{|\alpha(P)\rangle\}$ by varying the unitary matrices $U_{\alpha i}^{(P)}$. The basis $\{|i(P)\rangle\}$ will be called a reference basis. By substituting Eq. (11) into Eq. (7), and then substituting the resulting expression into Eq. (1), we obtain A_{var} as a function of the $c_{P\alpha}^{(1)}$'s, the $c_{P\alpha,P'\beta}^{(2)}$'s and the $U_{\alpha i}^{(P)}$'s. The functional form is intractable however, because we obtain thermodynamic averages of the form $\langle\, |\, i(P)\rangle\langle j(P)\,|\,\rangle_0$ which depend on the $c_{P\alpha}^{(1)}$'s, the $c_{P\alpha,P'\beta}^{(2)}$'s, and the $U_{\alpha i}^{(P)}$'s in a very complicated way. Instead, we express H_0 and H in terms of the operators $E_{\alpha\beta}^{(P)}$. Equation (5) can be rewritten using the reference basis $\{|i(P)\rangle\}$ as follows

$$\begin{aligned} H = & \sum_P \sum_{\alpha\beta} E_{\alpha\beta}^{(P)} \sum_{ij} U_{\alpha i}^{(P)*} \langle i(P) \mid L_P \mid j(P)\rangle U_{\beta j}^{(P)} \\ & + \sum_{PP'} \sum_{\alpha\beta\gamma\eta} E_{\alpha\beta}^{(P)} E_{\gamma\eta}^{(P')} \\ & \times \sum_{ijkl} U_{\alpha i}^{(P)*} U_{\gamma k}^{(P')*} \langle i(P)k(P') \mid \Phi_{PP'} \mid j(P)l(P')\rangle U_{\beta j}^{(P)} U_{\eta l}^{(P')}. \end{aligned} \tag{12}$$

Substituting this equation, and Eq. (7), into Eq. (1) we obtain

$$\begin{aligned} A_{var} = & A_0 \\ & - \sum_P \sum_\alpha \left\langle E_{\alpha\alpha}^{(P)} \right\rangle_0 \left[c_{P\alpha}^{(1)} - \sum_{ij} U_{\alpha i}^{(P)*} \langle i(P) \mid L_P \mid j(P)\rangle U_{\alpha j}^{(P)} \right] \\ & - \frac{1}{2} \sum_{PP'} \sum_{\alpha\beta} \left\langle E_{\alpha\alpha}^{(P)} E_{\beta\beta}^{(P')} \right\rangle_0 \left[c_{P\alpha,P'\beta}^{(2)} - \sum_{ijkl} U_{\alpha i}^{(P)*} U_{\beta k}^{(P')*} \right. \\ & \left. \times \langle i(P)k(P') \mid \Phi_{PP'} \mid j(P)l(P')\rangle U_{\alpha j}^{(P)} U_{\beta l}^{(P')} \right]. \end{aligned} \tag{13}$$

The traces hidden in this expression can be worked out using the states of Eq. (9). We then see that A_{var} is again a function of the $c_{P\alpha}^{(1)}$'s, the $c_{P\alpha,P'\beta}^{(2)}$'s, and the $U_{\alpha i}^{(P)}$'s, but that A_0, $\left\langle E_{\alpha\alpha}^{(P)} \right\rangle_0$, and $\left\langle E_{\alpha\alpha}^{(P)} E_{\beta\beta}^{(P')} \right\rangle_0$ for all P, P', α, and β depend only on the $c_{P\alpha}^{(1)}$'s, and the $c_{P\alpha,P'\beta}^{(2)}$'s, and not on the matrices $U_{\alpha i}^{(P)}$ that change when varying the basis. In Eq. (13) only

the matrices $U_{\alpha i}^{(P)}$ change that are explicitly shown. The thermodynamic averages $\left\langle E_{\alpha\alpha}^{(P)} \right\rangle_0$ and $\left\langle E_{\alpha\alpha}^{(P)} E_{\beta\beta}^{(P')} \right\rangle_0$ will appear frequently. We will call them one- and two-particle occupation numbers, respectively.

We minimize A_{var} in the form of Eq. (13) by partial differentiation with respect to the $c_{P\alpha}^{(1)}$'s, the $c_{P\alpha,P'\beta}^{(2)}$'s, and the $U_{\alpha i}^{(P)}$'s. We have to remember that A_0 and the occupation numbers are functions of the $c_{P\alpha}^{(1)}$'s and the $c_{P\alpha,P'\beta}^{(2)}$'s. Differentiating with respect to $c_{P\alpha}^{(1)}$ yields

$$\frac{\partial A_{var}}{\partial c_{P\alpha}^{(1)}} = \beta \left[\langle H - H_0 \rangle_0 \left\langle E_{\alpha\alpha}^{(P)} \right\rangle_0 - \left\langle (H - H_0) E_{\alpha\alpha}^{(P)} \right\rangle_0 \right], \tag{14a}$$

and with respect to $c_{P\alpha,P'\beta}^{(2)}$ yields

$$\frac{\partial A_{var}}{\partial c_{P\alpha,P'\beta}^{(2)}} = \beta \left[\langle H - H_0 \rangle_0 \left\langle E_{\alpha\alpha}^{(P)} E_{\beta\beta}^{(P')} \right\rangle_0 - \left\langle (H - H_0) E_{\alpha\alpha}^{(P)} E_{\beta\beta}^{(P')} \right\rangle_0 \right]. \tag{14b}$$

It is easy to see that for

$$c_{P\alpha}^{(1)} = \langle \alpha(P) \mid L_P \mid \alpha(P) \rangle , \tag{15a}$$

and

$$c_{P\alpha,P'\beta}^{(2)} = \langle \alpha(P)\beta(P') \mid \Phi_{PP'} \mid \alpha(P)\beta(P') \rangle \tag{15b}$$

the derivatives become zero. We can even prove that Eq. (15) will yield the absolute minimum of A_{var} (see Appendix A). We note that $\langle H \rangle_0 = \langle H_0 \rangle_0$, in contradistinction to MF where they differ by $\left\langle \frac{1}{2} \sum_{PP'} \Phi_{PP'} \right\rangle_0$.

Differentiating A_{var} with respect to $U_{\alpha i}^{(P)}$ yields

$$\begin{aligned} \frac{\partial A_{var}}{\partial U_{\alpha i}^{(P)}} &= \langle \alpha(P) \mid L_P \mid i(P) \rangle \left\langle E_{\alpha\alpha}^{(P)} \right\rangle_0 \\ &\quad + \sum_{P'} \sum_{\beta} \langle \alpha(P)\beta(P') \mid \Phi_{PP'} \mid i(P)\beta(P') \rangle \left\langle E_{\alpha\alpha}^{(P)} E_{\beta\beta}^{(P')} \right\rangle_0 , \end{aligned} \tag{16a}$$

and with respect to $U_{\alpha i}^{(P)*}$ yields

$$\begin{aligned} \frac{\partial A_{var}}{\partial U_{\alpha i}^{(P)*}} &= \langle i(P) \mid L_P \mid \alpha(P) \rangle \left\langle E_{\alpha\alpha}^{(P)} \right\rangle_0 \\ &\quad + \sum_{P'} \sum_{\beta} \langle i(P)\beta(P') \mid \Phi_{PP'} \mid \alpha(P)\beta(P') \rangle \left\langle E_{\alpha\alpha}^{(P)} E_{\beta\beta}^{(P')} \right\rangle_0 . \end{aligned} \tag{16b}$$

These derivatives need not be zero, because the matrices $U_{\alpha i}^{(P)}$ must satisfy the restriction that they remain unitary. We introduce Lagrange multipliers $\lambda_{P\alpha\beta}$, and define

$$\mathcal{A} = A_{var} - \sum_P \sum_{\alpha\beta} \lambda_{P\alpha\beta} \sum_i U_{\alpha i}^{(P)*} U_{\beta i}^{(P)}. \tag{17}$$

The derivatives of $\mathcal{A}$, rather than of A_{var}, must be equated to zero. We thus find

$$\begin{aligned}\lambda_{P\beta\alpha} = &\langle \alpha(P) \mid L_P \mid \beta(P) \rangle \left\langle E_{\alpha\alpha}^{(P)} \right\rangle_0 \\ &+ \sum_{P'} \sum_{\gamma} \langle \alpha(P)\gamma(P') \mid \Phi_{PP'} \mid \beta(P)\gamma(P') \rangle \left\langle E_{\alpha\alpha}^{(P)} E_{\gamma\gamma}^{(P')} \right\rangle_0,\end{aligned} \tag{18a}$$

and

$$\begin{aligned}\lambda_{P\alpha\beta} = &\langle \beta(P) \mid L_P \mid \alpha(P) \rangle \left\langle E_{\alpha\alpha}^{(P)} \right\rangle_0 \\ &+ \sum_{P'} \sum_{\gamma} \langle \beta(P)\gamma(P') \mid \Phi_{PP'} \mid \alpha(P)\gamma(P') \rangle \left\langle E_{\alpha\alpha}^{(P)} E_{\gamma\gamma}^{(P')} \right\rangle_0.\end{aligned} \tag{18b}$$

By taking the complex conjugate of Eq. (18a) we find

$$\lambda_{P\alpha\beta} = \lambda_{P\beta\alpha}^*. \tag{19}$$

Interchanging the indices α and β in Eq. (18b) leads to

$$\begin{aligned}&\langle \alpha(P) \mid L_P \mid \beta(P) \rangle \left\langle E_{\alpha\alpha}^{(P)} \right\rangle_0 \\ &\quad + \sum_{P'} \sum_{\gamma} \langle \alpha(P)\gamma(P') \mid \Phi_{PP'} \mid \beta(P)\gamma(P') \rangle \left\langle E_{\alpha\alpha}^{(P)} E_{\gamma\gamma}^{(P')} \right\rangle_0 \\ &= \langle \alpha(P) \mid L_P \mid \beta(P) \rangle \left\langle E_{\beta\beta}^{(P)} \right\rangle_0 \\ &\quad + \sum_{P'} \sum_{\gamma} \langle \alpha(P)\gamma(P') \mid \Phi_{PP'} \mid \beta(P)\gamma(P') \rangle \left\langle E_{\beta\beta}^{(P)} E_{\gamma\gamma}^{(P')} \right\rangle_0.\end{aligned} \tag{20}$$

This equation determines the basis $\{|\alpha(P)\rangle\}$. A method to solve it is shown in Appendix B. We only want to remark here that the method of Appendix B enables us also to determine whether the solution we obtain for Eq. (20) corresponds to a (local) minimum for A_{var}.

The "best" Hamiltonian H_0 as given by Eq. (7) can be obtained by solving Eqs. (15) and (20). These equations are not independent. We solve

both via an iterative procedure. We start by choosing a basis $\{|\alpha(P)\rangle\}$; then we calculate the $c^{(1)}_{P\alpha}$'s and the $c^{(2)}_{P\alpha,P'\beta}$'s using Eq. (15); then we calculate the occupation numbers; and finally we solve Eq. (20). This gives us a new basis $\{|\alpha(P)\rangle\}$. If this new basis differs little from the old one, then we have obtained the "best" Hamiltonian H_0. If the new basis differs to much then we repeat all calculations until convergence of the basis is reached. We have not yet addressed the problem of how to calculate the occupation numbers once numerical values for the $c^{(1)}_{P\alpha}$'s and the $c^{(2)}_{P\alpha,P'\beta}$'s are known. Neither have we said how to calculate A_0. The next subsection will deal with these matters.

B. The cluster variation method

One has only been able to calculate the thermodynamic averages $\langle X\rangle_0$ for one- and some two-dimensional cases.[22] The calculations of these thermodynamic averages pose what is called the Ising problem. Although few of these calculations have been done exactly, numerous approximation methods have been devised.[23] This subsection will deal with one of them; the cluster variation method.[24,25] We have decided against using more accurate methods, because they would probably become too involved for our purpose. Simpler approximations cannot be used as they would yield results similar to MF.[26] Furthermore, we have assumed that all molecules are equivalent. By this we mean that for any pair of molecules there is a symmetry operation of the system that relates the two molecules of the pair to each other. We then have to choose only the states of the basis $\{|\alpha(P)\rangle\}$ for one molecule. The states of all other molecules are determined by symmetry.

To simplify our notation we define

$$x_\alpha \equiv \left\langle E^{(Q)}_{\alpha\alpha}\right\rangle_0, \tag{21a}$$

and

$$y_{\alpha\beta P} \equiv \left\langle E^{(Q)}_{\alpha\alpha} E^{(P)}_{\beta\beta}\right\rangle_0. \tag{21b}$$

Here Q is a fixed molecule that is used for reference. The choice of Q is arbitrary as all molecules are considered to be equivalent. We note that in general $y_{\alpha\beta P} \neq y_{\beta\alpha P}$. The x_α's and the $y_{\alpha\beta P}$'s are not independent. The following relations hold

$$\sum_\alpha x_\alpha = 1, \tag{22}$$

$$x_\alpha = \sum_\beta y_{\alpha\beta P}, \tag{23a}$$

and

$$x_\alpha = \sum_\beta y_{\beta\alpha P}. \tag{23b}$$

Equations (23a) and (23b) are not independent, as $\sum_\beta y_{\alpha\beta P} = x_\alpha$ for every α, and $\sum_\alpha y_{\alpha\beta P} = x_\beta$ for every $\beta \neq 1$, implies $\sum_\alpha y_{\alpha 1 P} = x_1$.

The cluster variation method tries to answer the following question: "Given all one-, two- and more-particle occupation numbers, what is the free energy?" It is fairly easy to write down an expression for the energy. The problem is the entropy. For a linear chain we can use the cluster variation method for the Ising model without modifications (see Refs. 24 and 25). We derive an expression for the entropy of an ensemble of M linear chains. The total number of ways an ensemble of M linear chains with given occupation numbers x_α and $y_{\alpha\beta P}$ can be constructed if there are N molecules per chain and if we ignore end effects is

$$G = \left[\frac{\prod_\alpha (Mx_\alpha)!}{\prod_{\alpha\beta}(My_{\alpha\beta P})!}\right]^N. \tag{24}$$

The entropy for the ensemble is given by

$$S = k \ln G. \tag{25}$$

Equation (24) yields the exact entropy if there are only nearest-neighbour interactions.[24,25] No method has been found yet to determine G for an ensemble of two- or three-dimensional systems. Following Refs. 24 and 25 an approximation for G can be obtained by multiplying the right-hand-side of Eq. (24) by a correction factor

$$\Gamma = \left[\frac{\prod_\alpha (Mx_\alpha)!}{\prod_{\alpha\beta}(My_{\alpha\beta P})!}\right] \Big/ \left[\frac{M!}{\prod_\alpha (Mx_\alpha)!}\right] \tag{26}$$

for different nearest neighbours. The introduction of Γ is called the Bethe approximation.[24,25] The expression for G becomes

$$G = \left[\frac{\left(\prod_\alpha (Mx_\alpha)!\right)^{z-1}}{\left(\prod_P \prod_{\alpha\beta}(My_{\alpha\beta P})!\right)^{\frac{1}{2}} (M!)^{\frac{1}{2}z-1}}\right]^N, \tag{27}$$

with z the number of nearest neighbours. Using Stirling's approximation for the factorials we find for the entropy per molecule

$$S = k(z-1)\sum_{\alpha} x_\alpha \ln x_\alpha - \frac{1}{2}k\sum_{P}\sum_{\alpha\beta} y_{\alpha\beta P}\ln y_{\alpha\beta P}. \tag{28}$$

The expression for the energy per molecule is

$$E = \sum_{\alpha} c^{(1)}_{Q\alpha}\, x_\alpha + \frac{1}{2}\sum_{P}\sum_{\alpha\beta} c^{(2)}_{Q\alpha,P\beta}\, y_{\alpha\beta P}. \tag{29}$$

With these expressions we can determine the occupation numbers x_α and $y_{\alpha\beta P}$ by minimizing the free energy $A = E - TS$.

We perform the minimisation procedure again by differentiating. Because of the relations Eqs. (22) and (23) we introduce Lagrange multipliers λ, $\mu_{P\alpha}$ and $\nu_{P\alpha}$. We define

$$\begin{aligned}\mathcal{A} \equiv A - \lambda\sum_{\alpha} x_\alpha - \sum_{P}\sum_{\alpha}\mu_{P\alpha}\Big(x_\alpha - \sum_{\beta} y_{\alpha\beta P}\Big) \\ - \sum_{P}\sum_{\alpha\neq 1}\nu_{P\alpha}\Big(x_\alpha - \sum_{\beta} y_{\beta\alpha P}\Big).\end{aligned} \tag{30}$$

The derivatives of $\mathcal{A}$ with respect to x_α and $y_{\alpha\beta P}$ for all P, α and β must be zero. Solving the resulting equations we find

$$x_\alpha = \exp\left[-1 + \tilde{c}^{(1)}_{\alpha} + \tilde{\lambda} + \sum_{P}(\tilde{\mu}_{P\alpha} + \tilde{\nu}_{P\alpha})\right], \tag{31a}$$

and

$$y_{\alpha\beta P} = \exp\left[-1 + \tilde{c}^{(2)}_{\alpha\beta P} + 2(z-1)\tilde{\mu}_{P\alpha} + 2(z-1)\tilde{\nu}_{P\alpha}\right], \tag{31b}$$

with

$$\tilde{c}^{(1)}_{\alpha} = \frac{c^{(1)}_{Q\alpha}}{kT(z-1)}, \tag{32a}$$

$$\tilde{c}^{(2)}_{\alpha\beta P} = -\frac{1}{kT}c^{(2)}_{Q\alpha,P\beta}, \tag{32b}$$

$$\tilde{\lambda} = -\frac{\lambda}{kT(z-1)}, \tag{32c}$$

$$\tilde{\mu}_{P\alpha} = -\frac{\mu_{P\alpha}}{kT(z-1)}, \tag{32d}$$

$$\text{and}\quad \tilde{\nu}_{P\alpha} = -\frac{\nu_{P\alpha}}{kT(z-1)}. \tag{32e}$$

Here k denotes the Boltzmann constant. In writing down these equations we have put $\nu_{P1} = 0$. The Lagrange multipliers can be obtained by substituting Eq. (31) in Eqs. (22) and (23). We then get the following set of non-linear equations.

$$\tilde{\lambda} + \ln \sum_{\alpha} \exp\left[\tilde{c}_{\alpha}^{(1)} + \sum_{P} (\tilde{\mu}_{P\alpha} + \tilde{\nu}_{P\alpha})\right] = 1, \tag{33a}$$

$$\tilde{\lambda} - 2(z-1)\tilde{\mu}_{P\alpha} + \tilde{c}_{\alpha}^{(1)} + \sum_{P'} (\tilde{\mu}_{P'\alpha} + \tilde{\nu}_{P'\alpha}) - \ln \sum_{\beta} \exp\left[\tilde{c}_{\alpha\beta P}^{(2)} + 2(z-1)\tilde{\nu}_{P\beta}\right] = 0, \tag{33b}$$

$$\tilde{\lambda} - 2(z-1)\tilde{\nu}_{P\alpha} + \tilde{c}_{\alpha}^{(1)} + \sum_{P'} (\tilde{\mu}_{P'\alpha} + \tilde{\nu}_{P'\alpha}) - \ln \sum_{\beta} \exp\left[\tilde{c}_{\alpha\beta P}^{(2)} + 2(z-1)\tilde{\mu}_{P\beta}\right] = 0. \tag{33c}$$

These equations can be solved numerically via the Newton-Raphson method.[27] Equation (31) can then be used to obtain the occupation numbers. The energy and entropy are obtained via Eqs. (28) and (29). As a final remark we want to point out that if $c_{Q\alpha,P\beta}^{(2)} = c_{Q\beta,P\alpha}^{(2)}$ for all α and β, for a certain P, then $y_{\alpha\beta P} = y_{\beta\alpha P}$. For suppose $y_{\alpha\beta P} \neq y_{\beta\alpha P}$ for some α and β, then the substitution $y_{\alpha\beta P} \to \frac{1}{2}(y_{\alpha\beta P} + y_{\beta\alpha P})$ will yield the same energy, and a larger entropy, and hence a lower free energy. However, in general we have $y_{\alpha\beta P} \neq y_{\beta\alpha P}$.

3. Results

We have applied the method described in the previous section to the librational motions in β-N_2. At low pressures this phase exists between $T = 35.6\,\mathrm{K}$ and $T = 63.1\,\mathrm{K}$. At elevated pressures this phase exists even at temperatures as high as room temperature.[28] The space group is $P6_3/mmc$, and there are two molecules per unit cell (see Fig. 1).[29–31] X-ray diffraction experiments have shown no preferred orientation for the molecules. There only seems to be a slight preference for an angle of 56° between the molecular axis and the crystallographic c-axis. Different models have been contrived to account for the X-ray[29–31] and neutron[32] diffraction measurements, and also for the Nuclear Magnetic Resonance/Nuclear Quadrupole Resonance experiments.[33] One model assumes that the molecules precess freely or only slightly hindered around the c-axis.[29–32,34] Another model assumes that the molecules "choose" at random one out of a number of

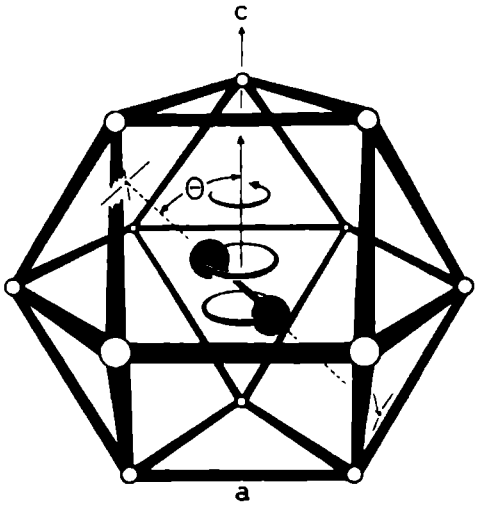

β-N_2, $P6_3/mmc$ (Z = 2)
a = 4 050 Å, c = 6 604 Å

Fig. 1 The structure of β-N_2.

fixed orientations.[29–31] And a third model assumes jumps between these orientations.[35]

In a previous paper we have reported the results of MF calculations on the librations in β-N_2.[35] We found two possible orientational probability distributions for the molecules. If the local reference frames of the two molecules in the unit cell were chosen to be identical, then a disordered phase with delocalized orientations of the molecules was found (see Fig. 2 of Ref. 35). If the local reference frames of the two molecules in the unit cell were allowed to rotate with respect to each other, then an ordered phase with localized orientations of the molecules was found (see Fig. 3 of Ref. 35) The orientations of the two molecules in the unit cell were found to be rotated by 180° about the c-axis. The ordered phase was about 0.87 kJ.mol^{-1} lower in energy at $T = 0$ K, but had also a much lower entropy. At high temperatures (above $T = 120$ K) the ordered phase showed an order-disorder transition to the disordered phase. Neither of the phases however, showed a transition to the α-phase at any reasonable temperature. For all temperatures at which the MF calculations were done the α-phase had a lower free energy. The results of the MF calculations were thus incorrect in two aspects: the molecules were found to have a preferred orientation in the β-phase, and no α-β phase transition was found. We therefore introduced the following *ad hoc* hypothesis. There are six

localized orientations that are solutions of MF. These six orientations can be transformed into each other by rotations of multiples of 60° around the c-axis. We assumed that there are free jumps between these six orientations. These free jumps yielded a delocalized picture for the orientations of the molecules. They also yielded an extra $k \ln 6$ for the entropy. This lowered the free energy of the β-phase so much that a phase transition to the α-phase at $T = 35\,\mathrm{K}$ was found. A theoretical foundation for the hypothesis could not be given, however.

As our new method is more complicated than the MF calculations we have had to limit the number of states and the number of molecules in the lattice sums. We have used six states $|\alpha(P)\rangle$ per molecule in most of our calculations, and only interactions with the twelve nearest-neighbours have been taken into account. But already in this "small" calculation a set of 133 non-linear equations has to be solved in order to obtain the occupation numbers (see Eq. (33)). Furthermore, we have assumed that all molecules are equivalent. We thus need only states for one molecule in the calculations. The states of the other molecules can be obtained via (proper) rotations. Equations (15a) and (20) have to be solved for only one molecule, and the right-hand-side of Eq. (15b) has only to be calculated for one molecule and its nearest neighbours. In Appendix B Eq. (B6) must be augmented with the restriction that $X_{ij}^{(P)} = X_{ij}^{(P')}$ for all i, j, P and P'. Even with the restriction that all molecules must be equivalent there are various possibilities for the number of sublattices and their configuration. We have found however, that the sublattices that yield the ordered phase in the MF calculations (see above) give the lowest free energy at low temperature. At high temperatures it becomes irrelevant how the sublattices are chosen (see below). The results that are presented in this paper have been obtained with the intermolecular potential of Berns and van der Avoird.[36] We have also done some calculations with the newer *ab initio* potential of van der Avoird *et al.*[37] The results of these calculations, however, do not differ qualitatively from those obtained with the Berns-van der Avoird potential. We have therefore done the calculations with the simpler potential.

We have started the calculations by choosing states for our reference basis $\{|i(P)\rangle\}$. As the calculations can only be done with a limited number of states some care must be taken in choosing these states. Although the states $|\alpha(P)\rangle$ are improved in the iterative procedure that has been described in the paragraph following Eq. (20), one has to bear in mind that one is restricted to the space that is spanned by the states $|i(P)\rangle$. The final

states will always be linear combinations of the states of the reference basis $\{|i(P)\rangle\}$. For the calculations on β-N_2 we have chosen a reference basis that might yield ordered as well as disordered phases. We have calculated the localized MF ground state at $T = 0\,\mathrm{K}$ in a basis of spherical harmonics $Y_{l,m}$ with $l_{max} = 10$ (see Ref. 35). From this state we have generated five other states by five subsequent rotations of 60° around the c-axis. The six states thus obtained we have orthogonalized. These orthogonal states form our reference basis $\{|i(P)\rangle\}$. The final states $|\alpha(P)\rangle$ can be localized or delocalized. If the calculations yield localized states of which only one is occupied then we have obtained an ordered phase. A disordered phase results when the localized states are equally occupied or when the final states are delocalized.

At low temperatures we have found an ordered phase with only one of the six initial states appreciably occupied. The other initial states are mixed to yield new but only slightly occupied states. The orientational probability distribution resembles closely that of Fig. 3 of Ref. 35. The phase is thus almost identical to the ordered phase of MF. Above $T = 30\,\mathrm{K}$ this ordered phase becomes unstable. Instead we have found a disordered phase (see Fig. 2). The states of this phase are the initial states which have become equally occupied.

This is of course radically different from MF where no stable disordered phase has been found below $T = 120\,\mathrm{K}$. Whereas the (unstable) disordered phase in MF has a high energy, the disordered phase in the new method has a very low energy. At $T = 30\,\mathrm{K}$ the energy of the disordered phase is even lower than the energy of the ordered phase at $T = 0\,\mathrm{K}$. The reason for this difference is that there is a very large correlation in the occupation of the various states for nearest-neighbours, i.e.

$$\langle E^{(Q)}_{\alpha\alpha} E^{(P)}_{\beta\beta}\rangle_0 \neq \langle E^{(Q)}_{\alpha\alpha}\rangle_0 \langle E^{(P)}_{\beta\beta}\rangle_0, \tag{34}$$

while in MF the left- and right-hand-side of Eq. (34) are intrinsically equal. We can define the orientational correlation function for a pair of molecules 1 and 2

$$\rho(\Omega_1;\Omega_2) = \frac{\sum_n \exp(-\beta E_n) \int d\Omega_3 \ldots d\Omega_N |\psi_n(\Omega_1;\ldots;\Omega_N)|^2}{\sum_n \exp(-\beta E_n)}, \tag{35}$$

with $\Omega_i = (\theta_i, \phi_i)$ and $d\Omega_i = \sin\theta_i d\theta_i d\phi_i$. The summation in this equation is over the exact eigenstates of the Hamiltonian H. In our model we approximate this function by

$$\rho(\Omega_1;\Omega_2) \approx \sum_{\alpha\beta} \left\langle E^{(1)}_{\alpha\alpha} E^{(2)}_{\beta\beta} \right\rangle_0 |\psi_\alpha(\theta_1,\phi_1)|^2 |\psi_\beta(\theta_2,\phi_2)|^2. \tag{36}$$

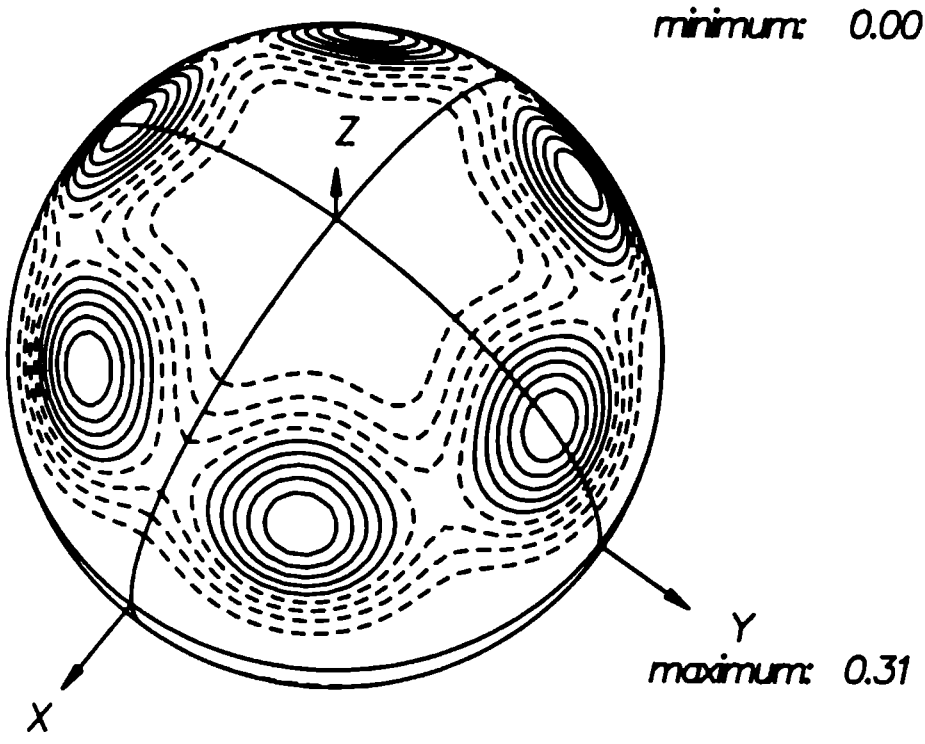

Fig. 2 Orientational probability distribution of β-N_2 according to the new method for $T > 30\,K$. The dashed contours denote a low probability; the solid contours denote a high probability. Subsequent contours differ by 10% of the maximum of the probability distribution.

The functions ψ_α correspond to the states $|\alpha(P)\rangle$. A contour plot of this function with $\theta_1 = \theta_2 = 55°$, which corresponds to the maximum of the orientational probability distribution, is shown in Fig. 3. We see that in the new method nearest-neighbours within the ab-plane prefer to be parallel to each other, but at the same time not perpendicular to the line that connects their centres of gravity. In the preferred orientations the molecules are only a few degrees from the absolute minimum of the intermolecular potential. The preferred orientations of the nearest-neighbours in adjacent layers, with respect to each other, vary. The difference of ϕ_1 and ϕ_2 ranges from 0° to 360°.

The free energy of β-N_2 as a function of temperature is shown in Fig. 4. We note that there is an unphysical discontinuity at $T = 30\,K$. This discontinuity is caused by the cluster variation method. A close inspection of the expression for the free energy that results from Eqs. (28) and (29)

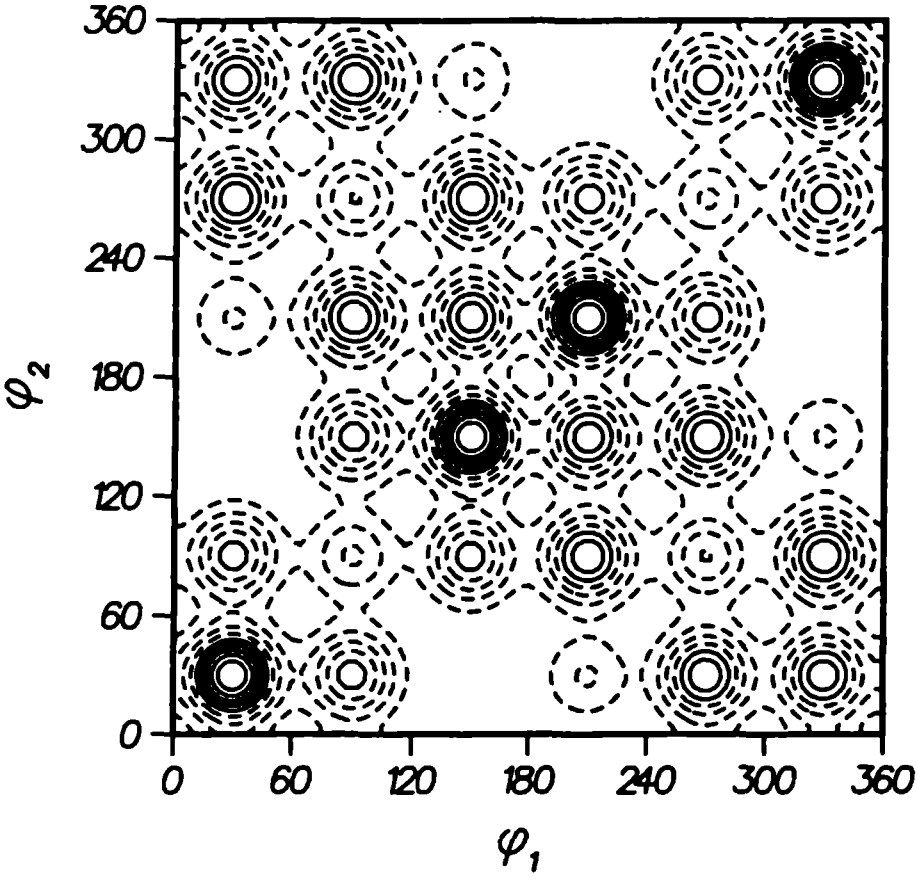

Fig. 3a Correlation function as given by Eq. (36) with $\theta_1 = \theta_2 = 55°$. The reference frame is oriented with the z-axis along the crystallographic c-axis, and the x-axis along the projection on the ab-plane of the intermolecular vector $\mathbf{R}_{12} = \mathbf{R}_2 - \mathbf{R}_1$ (continued on next page).

reveals that the free energy has two different minima at low temperature. One of them corresponds to the ordered phase. The other corresponds to the disordered phase. The free energy of the disordered phase is lower also at low temperatures. However, below $T = 26\,\mathrm{K}$ the entropy of the disordered phase, Eq. (28), becomes negative. We recall that in the derivation of Eq. (28) we introduced a correction (see Eq. (26)). It is easy to see that this correction yields a negative contribution to the entropy. If the correction becomes too large then the total entropy can become negative. It is obvious that when the entropy becomes negative the cluster variation method can no longer be used. Unfortunately, it is not clear what the free

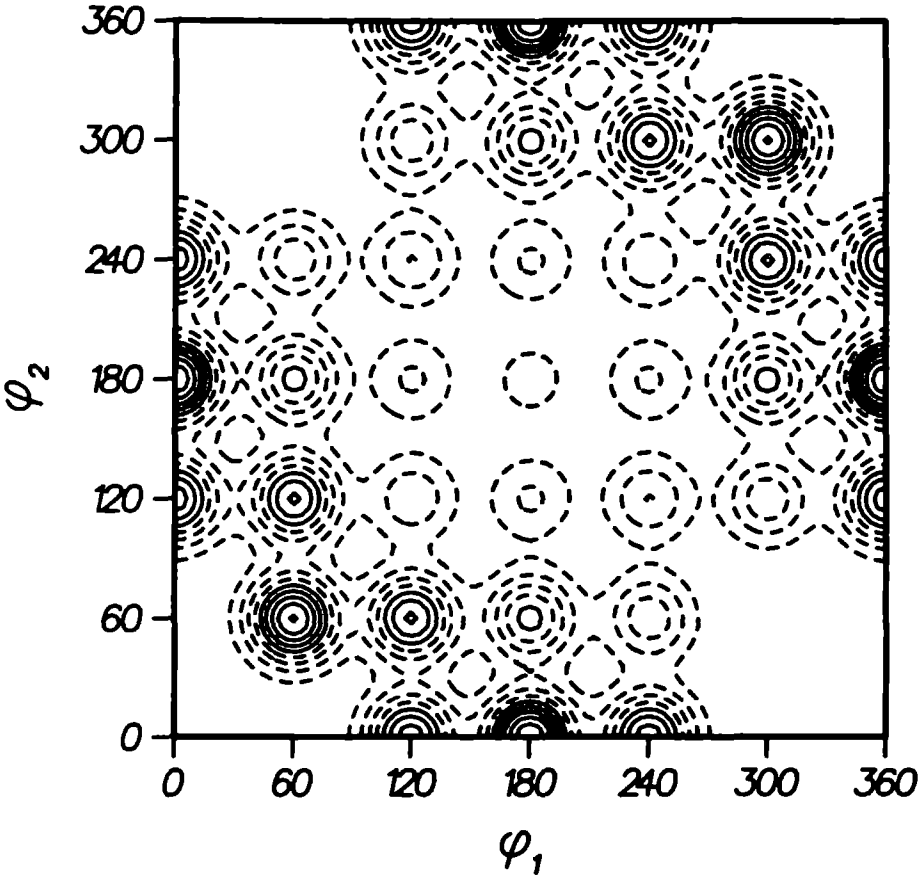

Fig. 3b Solid contours denote a high value of the correlation function, and dashed contours denote a low value. Subsequent contours differ by 10% of the maximum of the correlation function. The correlation function for in-plane nearest neighbours (a) and nearest neighbours in adjacent layers with molecule 2 higher than molecule 1 (b) are shown.

energy of the phases would be if better expressions were available. It might be that the disordered phase is the stabler one also at temperatures below 30 K but that is by no means certain.

Also shown in Fig. 4 is the free energy of α-N_2 as calculated with the new method. The calculations have been performed again using the Berns-van der Avoird potential and only nearest neighbours interactions. Four states have been used. These states have been obtained in the same way as the states in β-N_2. The only difference is that rotations of 90° around the c-axis (instead of 60°) have been used. We note that the free

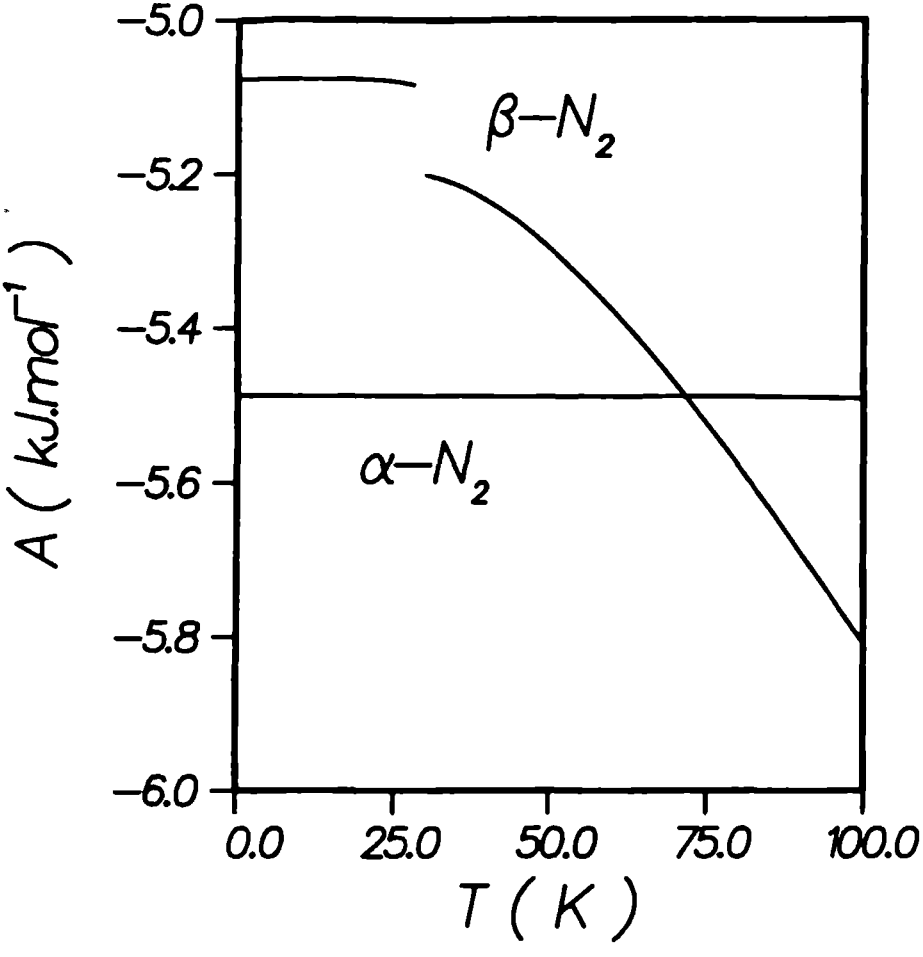

Fig. 4 Free energy of α- and β-N_2 calculated using Eqs. (28) and (29).

energy curve is an almost horizontal line. The molecules are very localized. Even at high temperatures only one of the states is occupied. The new method predicts an α-β phase transition at about $T_{\alpha\beta} = 72\,\mathrm{K}$, which is quite reasonable, given the approximations made in the calculations (e.g. only nearest-neighbours interactions). One might argue that this phase transition is rather artificial. As the molecules in the α-phase are localized a better (i.e. lower) estimate for the free energy would be obtained when some of the lower excited MF states would be included in the calculations. This is undoubtedly the case. However, inclusion of excited MF states would also lower the free energy of β-N_2. We think therefore, that as long as calculations with a large number of states is unfeasible, that it is best

Table 1. Orientational form factors $\langle S_{l,m} \rangle$ of β-N_2. The $S_{l,m}$'s are real linear combinations of spherical harmonics.[35]

	Theory			Experiment
	MF, Ref. 35		This paper	Ref. 32
	delocalized	localized		
$T =$	30 K	30 K	30 K	30 K
$\langle S_{2,0} \rangle$	-0.027	0.048	0.042	-
$\langle S_{4,0} \rangle$	-0.082	-0.233	-0.244	-
$\langle S_{6,0} \rangle$	0.029	0.042	0.057	-
$\langle S_{6,6} \rangle$	-0.016	-0.035	-0.062	-
$T =$	55 K	55 K	55 K	55 K
$\langle S_{2,0} \rangle$	-0.020	0.032	0.040	0.004±0.085
$\langle S_{4,0} \rangle$	-0.060	-0.167	-0.235	-0.311±0.326
$\langle S_{6,0} \rangle$	0.020	0.023	0.055	0.990±1.950
$\langle S_{6,6} \rangle$	-0.013	-0.013	-0.061	-0.180±2.300

to perform the calculations with similar states.

The one-particle properties in the disordered phase in β-N_2 do not change with temperature. This is a consequence of the fact that the occupation $\left\langle E_{\alpha\alpha}^{(P)} \right\rangle_0$ of the states does not change with temperature. In order to study the temperature dependence of the orientational probability distribution we have done calculations including the spherical harmonic $Y_{0,0}$ as an extra state. With this spherical harmonic the orientational probability distribution can become broader. The thermodynamic averages of some tesseral harmonics are shown in Table 1. We note that the results seem to be somewhat better than the MF results, although due to the large errors in the experimental results no definite conclusion can be drawn. The effect of temperature is very small. Probably more states need to be included for this kind of calculations.

4. Discussion and conclusions

We have presented in this paper a new method that can be used to calcu-

late the properties of orientationally disordered (and also ordered) molecular crystals. The states of the crystal are represented in this method as products of one-molecule states. A method that is improved with respect to MF because it includes the orientational pair-correlations between the molecules has been used to calculate thermodynamic averages. The states are optimized in order to yield a lowest possible free energy. We have applied the new method to the librational motions of the molecules in the β-phase of solid nitrogen. Two very important improvements with respect to prior MF calculations have been obtained. A stable disordered phase has been found at all temperatures where β-N_2 exists, and an α-β phase transition has been found at the reasonable temperature $T_{\alpha\beta} = 72\,\mathrm{K}$. In this section we will compare our new method with other methods that have been used to calculate properties of orientationally disordered molecular crystals. We will also discuss improvements that can be made and to what other systems the method can be applied.

The method that has been proved to be most useful for the calculations of properties of orientationally disordered molecular crystals is Molecular Dynamics.[2-10] The major drawback of this method is that it is a classical method. Therefore, at low temperatures and for light molecules it may give incorrect results because of quantum effects.

The most popular analytical method is a method that is unfortunately also called the Mean Field approximation.[38] It differs from what we have called Mean Field in the previous sections. Our definitions of MF refers to the time-*in*dependent Hartree method, whereas the definition of MF in Ref. 38 refers to the time-dependent Hartree method (TDH), which we call RPA.[39,40] Since in Ref. 38 the TDH or RPA method has been written in terms of susceptibilities we shall call this method in what follows the susceptibility approach. It is often used as follows. A free molecule susceptibility is calculated, corresponding to our definition of MF theory (or time-*in*dependent Hartree). The susceptibility for the crystal, corresponding to the TDH or RPA model, is calculated using the free molecule susceptibility and the intermolecular potential. The properties of the crystal can then be calculated from the crystal susceptibility. For example, the order-disorder phase transition temperature can be determined by looking for soft modes. We want to point out that this is totally incompatible with our present method. The susceptibility approach assumes that the states of the molecules are adapted to the site symmetry; i.e. delocalized states for disordered crystals.[13] We have shown however, that the states of the molecules in the disordered phase can be localized. When looking for soft

modes the susceptibility approach only tests whether these states are stable, but it does not take into account the correlations between the occupations of these states. It implicitly assumes that when the states of the molecules become localized that one of these states becomes predominantly occupied. This means that only certain order-disorder phase transitions can be described by the susceptibility approach. We have shown in a previous paper that soft modes in the Time Dependent Hartree approximation indicate an unstable MF state.[35] This means that the susceptibility approach and MF will yield identical results, because when the susceptibility approach predicts a phase transition then MF should also show that phase transition. Our method, which is an improvement of MF, shows totally different phase transitions.

A method that resembles our method is the pseudo-spin method. One can even look upon our method as a generalized pseudo-spin method.[15,16] In the pseudo-spin method the exact Hamiltonian is rewritten, making suitable approximations, in the form of the Ising Hamiltonian Eq. (8). Properties are then calculated using one of the approximations that have been devised for the Ising problem. One of the weak points theoretically of the pseudo-spin method is that there is no fixed rule for rewriting the Hamiltonian. Hence, one ends up with a Hamiltonian of the form of Eq. (7). The coefficients and the states of this Hamiltonian have however, not been optimized, but have been obtained in a more or less arbitrary way. Furthermore, the pseudo-spin method is restricted to two states per molecule. Both these deficiencies have been removed in our method.

In order to obtain also quantitatively meaningful results it is necessary to extend the calculations that have been presented in the previous section. The lattice sums have been restricted to only nearest-neighbours. It is in principle possible to include more molecules in the lattice sums of Eqs. (28) and (29). In Eq. (28) z then becomes the number of terms in the lattice sums. This would of course lead to a much larger set of equations for the Lagrange multipliers, Eq. (33). How much molecules one can include in the lattice sums depends therefore first of all on the amount of computer time one wants to spend. A much more serious problem is that the problems with negative entropies may become worse. We will show below that these problems arise because some restrictions on the two-particle occupation numbers are missing. The errors that result from neglecting these restrictions may become larger when the lattice sums are extended.

One would also like to include more states per molecule in the calculations. The problem is again that the calculations become larger, now even

in two ways. Again the number of Lagrange multipliers Eq. (33) increases, but also the number of equations for the states Eqs. (20), (B4), (B5) and (B6) increases. However, a reduction in the number of states that have to be solved is obtained when from the total number of states only a limited number is allowed to be occupied. The number of Lagrange multipliers in Eq. (33) is only determined by the number of occupied states. The number of equations for the optimisation of the states, Eqs. (20), (B4), (B5) and (B6), is still determined by the total number of states, but they simplify appreciably, which can be of help in solving them.

The most important improvement will probably be a better method for obtaining occupation numbers. The only restrictions are given by Eqs. (22) and (23). As was mentioned above, there may be more. This is most easily seen by considering three-particle occupation numbers. These are related to the two-particle occupation numbers via

$$\left\langle E_{\alpha\alpha}^{(P)} E_{\beta\beta}^{(P')} \right\rangle_0 = \sum_{\gamma} \left\langle E_{\alpha\alpha}^{(P)} E_{\beta\beta}^{(P')} E_{\gamma\gamma}^{(P'')} \right\rangle_0 , \tag{37}$$

for any P, P', P'', α, and β. It is easy to see that it is not possible to have three-particle occupation numbers that yield $\left\langle E_{11}^{(P)} E_{11}^{(P')} \right\rangle_0 = 1$, $\left\langle E_{11}^{(P)} E_{11}^{(P'')} \right\rangle_0 = 1$, and $\left\langle E_{11}^{(P')} E_{22}^{(P'')} \right\rangle_0 = 1$. This means that such combination of two-particle occupation numbers may not arise in the calculations. However, the cluster of two nearest-neighbours is simply too small to prevent these inconsistencies. These inconsistencies cause the negative entropies. The cluster variation method can thus be improved by using larger clusters; in particular closed clusters. This will involve three- and more-particle occupation numbers, however, which may complicate the calculations considerably.

An alternative for obtaining the occupation numbers may be the Monte Carlo method.[41] With this method it is possible in principle to obtain the occupation numbers with any accuracy. There are no fundamental restrictions on the number of states per molecule and the number of molecules in the lattice sums. Furthermore, the method is rather straightforward. There are however two drawbacks. One of them is that Monte Carlo is a very time consuming method. The other is that it is difficult to obtain values for the entropy and hence for the free energy. That means that the method is not suited when we want to study phase transitions like the α-β phase transition. Nevertheless, we think that the Monte Carlo method is the most appropriate method for obtaining quantitative results.

We want to comment finally on some projects that may be taken up using the new method that we have presented in this paper. First of all the method might be applied to all the other orientationally disordered molecular crystals. Thereby, the improvements mentioned above must be studied. But the method can also be applied to other systems. It would for example be very interesting to use it to study the cooperative Jahn-Teller effect. Some work has already been done in extending the method to fermion and boson systems. Hence, it may be worthwhile to apply the method to solid helium. For finite systems there is no Ising problem as the thermodynamic averages, Eq. (3a), can be obtained by direct calculation of the traces. This means that for example the correlated rotations of methyl groups in organic molecules can be studied advantageously using our method. It may even be possible to extend the method to calculate collective excitations. There is a close relation between the second-order variation of the density operator in the free energy in MF, and the collective excitations as calculated in the Time Dependent Hartree approximation. We think that there may be a similar relation between the second-order coefficients of Eq. (B5) and collective excitations.

Acknowledgments

This investigation was supported in part by the Netherlands Foundation for Chemical Research (S.O.N.) with financial aid from the Netherlands Organization for the Advancement of Pure Research (Z.W.O.).

Appendix A

In this appendix we will prove that the coefficients given by Eq. (15) yield the absolute minimum of A_{var}. We will denote here by H_0 the Hamiltonian of Eq. (7) with the specific coefficients of Eq. (15). The following definition will simplify our notation.

$$\mathcal{A}(H_1; H_2) \equiv A_{H_2} + \langle H_1 - H_2 \rangle_{H_2}, \tag{A1}$$

with

$$A_{H_2} = -\beta^{-1} \ln Z_{H_2}, \tag{A2}$$

$$\langle X \rangle_{H_2} = Z_{H_2}^{-1} \mathrm{Tr} \left[e^{-\beta H_2} X \right], \tag{A3}$$

and

$$Z_{H_2} = \mathrm{Tr}[e^{-\beta H_2}]. \tag{A4}$$

This definition implies that we can write $A_{var} = \mathcal{A}(H; H_0)$.

We now suppose that there are coefficients $c^{(1)\prime}_{P\alpha}$ and $c^{(2)\prime}_{P\alpha,P'\beta}$, different from those of Eq. (15), that yield a lower A_{var}. The corresponding Hamiltonian will be denoted by H_0'. The basis $\{|\alpha(P)\rangle\}$ of H_0' is the same as that of H_0. Using Eq. (A1) we can write

$$\mathcal{A}(H; H_0') < \mathcal{A}(H; H_0) \tag{A5}$$

It is easy to see that

$$\mathcal{A}(H_0; H_0) = \mathcal{A}(H; H_0), \tag{A6}$$

and

$$\mathcal{A}(H_0; H_0') = \mathcal{A}(H; H_0'), \tag{A7}$$

because the the non-diagonal terms of H in Eq. (5) vanish. Using Eqs. (A6) and (A7) we obtain

$$\mathcal{A}(H_0; H_0') < \mathcal{A}(H_0; H_0). \tag{A8}$$

This however is clearly impossible. We have $\mathcal{A}(H_0; H_0) = A_{H_0}$, whereas according to the Gibbs-Bogoliubov inequality Eq. (1) $\mathcal{A}(H_0; H_0') \geq A_{H_0}$ should hold. This means that Eq. (A5) cannot hold and that consequently the coefficients $c^{(1)}_{P\alpha}$ and $c^{(2)}_{P\alpha,P'\beta}$ that are related to the basis $\{|\alpha(P)\rangle\}$ by Eq. (15) yield the absolute minimum of A_{var}.

Appendix B

The derivation of Eq. (20) from Eq. (16) was meant to yield a basis $\{|\alpha(P)\rangle\}$ that minimizes A_{var}. As only $\langle H\rangle_0$ depends directly on this basis we can also say that we have tried to find the basis that minimizes $\langle H\rangle_0$. Because the basis must be orthonormal we introduced Lagrange multipliers in Eq. (17). In this appendix we will introduce new variables for which no restrictions hold. Consequently, we will be able to minimize $\langle H\rangle_0$ via direct methods. We will show that we can solve Eq. (20) and we will also prove that the solution corresponds to a minimum of $\langle H\rangle_0$ and A_{var}.

The new variables are the matrix elements of matrices $\mathbf{X}^{(P)}$ that are defined by[42,43]

$$\mathbf{U}^{(P)} = \exp(\mathbf{X}^{(P)}). \tag{B1}$$

Here $\mathbf{U}^{(P)}$ is a matrix with matrix elements $U^{(P)}_{ai}$. The matrix $\mathbf{U}^{(P)}$ in Eq. (B1) is unitary if and only if the matrix $\mathbf{X}^{(P)}$ is antihermitean. We take the lower triangle matrix elements of the $\mathbf{X}^{(P)}$'s as our new unrestricted

variables, noting that the diagonal elements are purely imaginary. $\langle H \rangle_0$ will thus be interpreted as a function of these variables.

In order to find the minimum of $\langle H \rangle_0$ we will employ the iterative Newton-Raphson method for finding minima.[27] In each iteration step $\langle H \rangle_0$ is expanded as a Taylor series in $\mathbf{X}^{(P)}$ around a trial basis. Cubic and higher order terms are discarded and the remaining quadratic expression is minimized to obtain an improved basis. To be more specific we rewrite $\langle H \rangle_0$ as in Eq. (13).

$$\begin{aligned}\langle H \rangle_0 = &\sum_P \sum_\alpha \left\langle E_{\alpha\alpha}^{(P)} \right\rangle_0 \sum_{ij} U_{\alpha i}^{(P)*} \langle i(P) \mid L_P \mid j(P) \rangle U_{\alpha j}^{(P)} \\ &+ \frac{1}{2} \sum_{PP'} \sum_{\alpha\beta} \left\langle E_{\alpha\alpha}^{(P)} E_{\beta\beta}^{(P')} \right\rangle_0 \sum_{ijkl} U_{\alpha i}^{(P)*} U_{\beta k}^{(P')*} \\ &\times \langle i(P)k(P') \mid \Phi_{PP'} \mid j(P)l(P') \rangle U_{\alpha j}^{(P)} U_{\beta l}^{(P'} \end{aligned} \tag{B2}$$

We identify the reference basis $\{|i(P)\rangle\}$ with our trial basis. The coefficients in the Taylor series, which are the derivatives of $\langle H \rangle_0$ with respect to $\mathbf{X}^{(P)}$, taken at $\mathbf{X}^{(P)} = \mathbf{0}$, are most easily calculated by first determining the derivatives of $U_{\alpha i}^{(P)}$ with respect to the $X_{ij}^{(P)}$'s. We find

$$\left(\frac{\partial U_{\alpha i}^{(P)}}{\partial X_{jk}^{(P')}} \right)_{\mathbf{X}=\mathbf{0}} = \left(\frac{\partial U_{\alpha i}^{(P)*}}{\partial X_{jk}^{(P')*}} \right)_{\mathbf{X}=\mathbf{0}} = \delta_{PP'} \delta_{\alpha j} \delta_{ik}, \tag{B3a}$$

$$\left(\frac{\partial U_{\alpha i}^{(P)}}{\partial X_{jk}^{(P')*}} \right)_{\mathbf{X}=\mathbf{0}} = \left(\frac{\partial U_{\alpha i}^{(P)*}}{\partial X_{jk}^{(P')}} \right)_{\mathbf{X}=\mathbf{0}} = -\delta_{PP'} \delta_{\alpha k} \delta_{ij}, \tag{B3b}$$

$$\begin{aligned}\left(\frac{\partial^2 U_{\alpha i}^{(P)}}{\partial X_{jk}^{(P')*} \partial X_{lm}^{(P'')}} \right)_{\mathbf{X}=\mathbf{0}} &= \left(\frac{\partial^2 U_{\alpha i}^{(P)*}}{\partial X_{jk}^{(P')*} \partial X_{lm}^{(P'')*}} \right)_{\mathbf{X}=\mathbf{0}} \\ &= \frac{1}{2} \delta_{PP'} \delta_{PP''} \left(\delta_{\alpha j} \delta_{im} \delta_{kl} + \delta_{\alpha l} \delta_{ik} \delta_{jm} \right), \end{aligned} \tag{B3c}$$

$$\begin{aligned}\left(\frac{\partial^2 U_{\alpha i}^{(P)}}{\partial X_{jk}^{(P')} \partial X_{lm}^{(P'')*}} \right)_{\mathbf{X}=\mathbf{0}} &= \left(\frac{\partial^2 U_{\alpha i}^{(P)*}}{\partial X_{jk}^{(P')*} \partial X_{lm}^{(P'')}} \right)_{\mathbf{X}=\mathbf{0}} \\ &= -\frac{1}{2} \delta_{PP'} \delta_{PP''} \left(\delta_{\alpha j} \delta_{il} \delta_{km} + \delta_{\alpha m} \delta_{ik} \delta_{jl} \right), \end{aligned} \tag{B3d}$$

$$\begin{aligned}\left(\frac{\partial^2 U_{\alpha i}^{(P)}}{\partial X_{jk}^{(P')*} \partial X_{lm}^{(P'')*}} \right)_{\mathbf{X}=\mathbf{0}} &= \left(\frac{\partial^2 U_{\alpha i}^{(P)*}}{\partial X_{jk}^{(P')} \partial X_{lm}^{(P'')}} \right)_{\mathbf{X}=\mathbf{0}} \\ &= \frac{1}{2} \delta_{PP'} \delta_{PP''} \left(\delta_{\alpha k} \delta_{il} \delta_{jm} + \delta_{\alpha m} \delta_{ij} \delta_{kl} \right), \end{aligned} \tag{B3e}$$

where for all $X_{ij}^{(P)}$ $i \geq j$ holds. The calculation of the derivatives of $\langle H \rangle_0$ is lengthy but straightforward. We find for the first derivatives

$$\begin{aligned}\left(\frac{\partial \langle H \rangle_0}{\partial X_{ij}^{(P)}}\right)_{X=0} &= \left(\frac{\partial \langle H \rangle_0}{\partial X_{ij}^{(P)*}}\right)^*_{X=0} \\ &= \langle i(P) \mid L_P \mid j(P) \rangle \left[\left\langle E_{ii}^{(P)} \right\rangle_0 - \left\langle E_{jj}^{(P)} \right\rangle_0\right] \\ &+ \sum_Q \sum_k \langle i(P)k(Q) \mid \Phi_{PQ} \mid j(P)k(Q) \rangle \\ &\times \left[\left\langle E_{ii}^{(P)} E_{kk}^{(Q)} \right\rangle_0 - \left\langle E_{jj}^{(P)} E_{kk}^{(Q)} \right\rangle_0\right]\end{aligned} \tag{B4}$$

We note the resemblance to Eq. (20). The second derivatives are given by

$$\begin{aligned}&\left(\frac{\partial^2 \langle H \rangle_0}{\partial X_{ij}^{(P)} \partial X_{kl}^{(P')}}\right)_{X=0} = \left(\frac{\partial^2 \langle H \rangle_0}{\partial X_{ij}^{(P)*} \partial X_{kl}^{(P')*}}\right)^*_{X=0} \\ &= \frac{1}{2}\delta_{PP'} \left[\delta_{jk} \langle i(P) \mid L_P \mid l(P) \rangle - \delta_{il} \langle k(P) \mid L_P \mid j(P) \rangle\right] \\ &\quad \times \left[\left\langle E_{ii}^{(P)} \right\rangle_0 - \left\langle E_{jj}^{(P)} \right\rangle_0 - \left\langle E_{kk}^{(P)} \right\rangle_0 + \left\langle E_{ll}^{(P)} \right\rangle_0\right] \\ &+ \frac{1}{2}\delta_{PP'} \sum_Q \sum_m \left[\delta_{jk} \langle i(P)m(Q) \mid \Phi_{PQ} \mid l(P)m(Q) \rangle\right. \\ &\qquad \left. - \delta_{il} \langle k(P)m(Q) \mid \Phi_{PQ} \mid j(P)m(Q) \rangle\right] \\ &\quad \times \left[\left\langle E_{ii}^{(P)} E_{mm}^{(Q)} \right\rangle_0 - \left\langle E_{jj}^{(P)} E_{mm}^{(Q)} \right\rangle_0 - \left\langle E_{kk}^{(P)} E_{mm}^{(Q)} \right\rangle_0 + \left\langle E_{ll}^{(P)} E_{mm}^{(Q)} \right\rangle_0\right] \\ &+ \langle i(P)k(P') \mid \Phi_{PP'} \mid j(P)l(P') \rangle \\ &\quad \times \left[\left\langle E_{ii}^{(P)} E_{kk}^{(P')} \right\rangle_0 + \left\langle E_{jj}^{(P)} E_{ll}^{(P')} \right\rangle_0 - \left\langle E_{ii}^{(P)} E_{ll}^{(P')} \right\rangle_0 - \left\langle E_{jj}^{(P)} E_{kk}^{(P')} \right\rangle_0\right],\end{aligned} \tag{B5a}$$

and

$$\begin{aligned}&\left(\frac{\partial^2 \langle H \rangle_0}{\partial X_{ij}^{(P)} \partial X_{kl}^{(P')*}}\right)_{X=0} = \left(\frac{\partial^2 \langle H \rangle_0}{\partial X_{ij}^{(P)*} \partial X_{kl}^{(P')}}\right)^*_{X=0} \\ &= -\frac{1}{2}\delta_{PP'} \left[\delta_{jl} \langle i(P) \mid L_P \mid k(P) \rangle - \delta_{ik} \langle l(P) \mid L_P \mid j(P) \rangle\right] \\ &\quad \times \left[\left\langle E_{ii}^{(P)} \right\rangle_0 - \left\langle E_{jj}^{(P)} \right\rangle_0 + \left\langle E_{kk}^{(P)} \right\rangle_0 - \left\langle E_{ll}^{(P)} \right\rangle_0\right] \\ &- \frac{1}{2}\delta_{PP'} \sum_Q \sum_m \left[\delta_{jl} \langle i(P)m(Q) \mid \Phi_{PQ} \mid k(P)m(Q) \rangle\right.\end{aligned} \tag{B5b}$$

$$-\delta_{ik}\langle l(P)m(Q) \mid \Phi_{PQ} \mid j(P)m(Q)\rangle]$$

$$\times \left[\left\langle E_{ii}^{(P)} E_{mm}^{(Q)}\right\rangle_0 - \left\langle E_{jj}^{(P)} E_{mm}^{(Q)}\right\rangle_0 + \left\langle E_{kk}^{(P)} E_{mm}^{(Q)}\right\rangle_0 - \left\langle E_{ll}^{(P)} E_{mm}^{(Q)}\right\rangle_0\right]$$

$$+\langle i(P)l(P') \mid \Phi_{PP'} \mid j(P)k(P')\rangle$$

$$\times \left[\left\langle E_{ii}^{(P)} E_{kk}^{(P')}\right\rangle_0 + \left\langle E_{jj}^{(P)} E_{ll}^{(P')}\right\rangle_0 - \left\langle E_{ii}^{(P)} E_{ll}^{(P')}\right\rangle_0 - \left\langle E_{jj}^{(P)} E_{kk}^{(P')}\right\rangle_0\right].$$

The following set of linear equations has to be solved in each iteration step

$$\left(\frac{\partial \langle H\rangle_0}{\partial X_{ij}^{(P)}}\right)_{\mathbf{X}=\mathbf{0}} + \sum_{P'}\sum_{\substack{kl\\ k\geq l}} \left[X_{kl}^{(P')}\left(\frac{\partial^2 \langle H\rangle_0}{\partial X_{ij}^{(P)}\partial X_{kl}^{(P')}}\right)_{\mathbf{X}=\mathbf{0}} + X_{kl}^{(P')*}\left(\frac{\partial^2 \langle H\rangle_0}{\partial X_{ij}^{(P)}\partial X_{kl}^{(P')*}}\right)_{\mathbf{X}=\mathbf{0}}\right] = 0, \tag{B6a}$$

and

$$\left(\frac{\partial \langle H\rangle_0}{\partial X_{ij}^{(P)*}}\right)_{\mathbf{X}=\mathbf{0}} + \sum_{P'}\sum_{\substack{kl\\ k\geq l}} \left[X_{kl}^{(P')}\left(\frac{\partial^2 \langle H\rangle_0}{\partial X_{ij}^{(P)*}\partial X_{kl}^{(P')}}\right)_{\mathbf{X}=\mathbf{0}} + X_{kl}^{(P')*}\left(\frac{\partial^2 \langle H\rangle_0}{\partial X_{ij}^{(P)*}\partial X_{kl}^{(P')*}}\right)_{\mathbf{X}=\mathbf{0}}\right] = 0. \tag{B6b}$$

Convergence of the Newton-Raphson method is reached in the nth iteration step when for the solution $\mathbf{X}_n^{(P)}$ of this equation in the nth step $\mathbf{X}_n^{(P)} = \mathbf{0}$ holds. This condition can only be fulfilled when the first derivatives in Eq. (B6) become zero. Hence, the Newton-Raphson method yields a solution of Eq. (20). Furthermore, the second derivatives in Eq. (B6) must form a positive definite matrix, bacause the solution must correspond to a minimum of $\langle H\rangle_0$. The second derivatives thus yield a test that we can use to determine whether we have really found a minimum for A_{var}.

We want finally to comment on how to obtain the unitary matrices $\mathbf{U}^{(P)}$ from the antihermitean matrices $\mathbf{X}_n^{(P)}$. The matrices $i\mathbf{X}_n^{(P)}$ are hermitean and can thus be diagonalized. This means that $\mathbf{X}_n^{(P)}$ can also be diagonalized. We define the unitary matrices $\mathbf{V}_n^{(P)}$ and the diagonal matrices $\mathbf{\Lambda}_n^{(P)}$ by

$$\mathbf{X}_n^{(P)}\mathbf{V}_n^{(P)} = \mathbf{V}_n^{(P)}\mathbf{\Lambda}_n^{(P)} \tag{B7}$$

The diagonal elements of $\mathbf{\Lambda}_n^{(P)}$ are purely imaginary. The matrices $\mathbf{U}_n^{(P)}$ can be defined by

$$\mathbf{U}_n^{(P)} = \mathbf{V}_n^{(P)} \exp(\mathbf{\Lambda}_n^{(P)}) \mathbf{V}_n^{(P)\dagger}. \tag{B8}$$

The matrices $\mathbf{U}^{(P)}$ are then given by

$$\mathbf{U}^{(P)} = \mathbf{U}_{n'}^{(P)} \ldots \mathbf{U}_2^{(P)} \mathbf{U}_1^{(P)}, \tag{B9}$$

where n' denotes the step in which convergence has been reached.

References

[1] J. van Kranendonk, *Solid Hydrogen* (Plenum, New York, 1983).
[2] M.L. Klein, D.Lévesque, and J.-J. Weis, J. Chem. Phys. **74**, 2566 (1981).
[3] M.L. Klein and J.-J. Weis, J. Chem. Phys. **67**, 217 (1977).
[4] M.L. Klein and I.R. McDonald, J. Chem. Phys. **79**. 2333 (1983).
[5] M. Ferrario, I.R. McDonald, and M.L. Klein, J. Chem. Phys. **84**, 3975 (1986).
[6] R.W. Impey, M. Sprik, and M.L. Klein, J. Chem. Phys. **83**, 3638 (1985).
[7] R.M. Lynden-Bell, I.R. McDonald, and M.L. Klein, Mol. Phys. **48**, 1093 (1983).
[8] R.M. Lynden-Bell, M.L. Klein, and I.R. McDonald, Z. Phys. B**54**, 325 (1984).
[9] M.T. Dove and R.M. Lynden-Bell, J. Phys. C**19**, 3343 (1986).
[10] M.T. Dove, J. Phys. C**19**, 3325 (1986).
[11] K.H. Michel and J. Naudts, J. Chem. Phys. **67**, 547 (1977).
[12] K.H. Michel, J. Chem. Phys. **84**, 3451 (1986).
[13] K.H. Michel and K. Parlinski, Phys. Rev. B**31**, 1823 (1985).
[14] K.H. Michel and J.M. Rowe, Phys. Rev. B**32**, 5818 (1985); ibid. **32**, 5827 (1985).
[15] M. Tokunaga and T. Matsubara, Prog. Theor. Phys. **35**, 581 (1966).
[16] T. Luty and R.W. Munn, J. Chem. Phys. **80**, 3321 (1984).
[17] C. Domb, Adv. Phys. **9**, 149 (1960).
[18] H.L. Friedman, *A Course in Statistical Mechanics* (Prentice Hall, London, 1985).
[19] J.G. Kirkwood, J. Chem. Phys. **8**, 205 (1940).
[20] H.M. James and T.A. Keenan, J. Chem. Phys. **31**, 12 (1959).
[21] N.R. Werthamer, in *Rare Gas Solids*, eds. M.L. Klein and J. Venables (Academic Press, London, 1976), Vol. I.

[22] R.J. Baxter, *Exactly Solved Models in Statistical Physics* (Academic Press, London, 1982).
[23] C. Domb and M.S. Green (eds.), *Phase Transitions and Critical Phenomena* (Academic Press, London, 1976).
[24] R. Kikuchi, Phys. Rev. **81**, 988 (1951).
[25] M. Kurata and R. Kikuchi, J. Chem. Phys. **21**, 434 (1953).
[26] D.M. Burley, in *Phase Transitions and Critical Phenomena*, eds. C. Domb and M.S. Green (Academic Press, London, 1976), Vol. 2.
[27] R.F. Churchhouse, *Numerical Methods*, Vol. III of *Handbook of Applicable Mathematics*, edited by W. Ledermann (Wiley, Chichester, 1981).
[28] S. Buchsbaum, R.L. Mills, and D. Schiferl, J. Phys. Chem. **88**, 2522 (1984).
[29] W.E. Streib, T.H. Jordan, and W.N. Lipscomb, J. Chem. Phys. **37**, 2962 (1962).
[30] T.H. Jordan, H.W. Smith, W.E. Streib, and W.N. Lipscomb, J. Chem. Phys. **41**, 756 (1964).
[31] A.F. Schuch and R.L. Mills, J. Chem. Phys. **52**, 6000 (1970).
[32] B.M. Powell, G. Dolling, and H.F. Nieman, J. Chem. Phys. **79**, 982 (1983).
[33] A.S. deReggi, P.C. Canepa, and T.A. Scott, J. Magn. Res. **1**, 144 (1969).
[34] J.C. Raich, N.S. Gillis, and T.R. Koehler, J. Chem. Phys. **61**, 1411 (1974).
[35] A. van der Avoird, W.J. Briels, and A.P.J. Jansen, J. Chem. Phys. **81**, 3658 (1984).
[36] R.M. Berns and A. van der Avoird, J. Chem. Phys. **72**, 6107 (1980).
[37] A. van der Avoird, P.E.S. Wormer, and A.P.J. Jansen, J. Chem. Phys. **84**, 1629 (1986).
[38] J.C. Raich, H. Yasuda, and E.R. Bernstein, J. Chem. Phys. **78**, 6209 (1983).
[39] W.J. Briels, A.P.J. Jansen, and A. van der Avoird, J. Chem. Phys. **81**, 4118 (1984).
[40] A.P.J. Jansen and A. van der Avoird, J. Chem. Phys. **86**, 3583 (1987).
[41] K. Binder, in *Monte Carlo Methods in Statistical Physics*, ed. K. Binder (Springer, Berlin, 1979).
[42] R. McQueeny, Symp. Far. Soc. **2**, 7 (1968).
[43] J. Douady, Y. Ellinger, R. Subra, and B. Levy, Comp. Phys. Comm. **17**, 23 (1979).

Ab initio description of large amplitude motions in solid N_2. III. Libron–phonon coupling

W J Briels A P J Jansen, and A van der Avoird
Institute of Theoretical Chemistry University of Nijmegen Toernooiveld, 6525 ED Nijmegen, The Netherlands

(Received 12 June 1984, accepted 28 June 1984)

A new lattice dynamics scheme is proposed for handling librons, anharmonic translational vibrations, and translational-rotational coupling in molecular crystals This scheme is an extension of earlier libron models which describe large amplitude librations or hindered rotations The formalism is based on expanding the intermolecular potential in the molecular displacement coordinates, including cubic and quartic terms, while retaining the exact orientational dependence Closed expressions are obtained via spherical tensor methods After constructing separate mean field states for the molecular rotations and translations, using bases of tesseral harmonics and 3*D* harmonic oscillator functions, respectively, the intermolecular correlations are taken into account and simultaneously the translational-rotational coupling, by solving the equations of motion for the crystal according to the time-dependent Hartree or random-phase approximation Application of the formalism to the ordered α and γ phases of solid nitrogen, using an *ab initio* potential, gave very satisfactory results

I. INTRODUCTION

As explained in any textbook, the basic tool in solid state physics is the use of wave functions, or operators in the equations of motion method, which are adapted to the translational symmetry of the lattice In the usual harmonic lattice dynamics treatments[1] the adaptation to this symmetry is easy and the original problem reduces to a set of smaller problems, one for every wave vector **q** in the first Brillouin zone If the symmetry adaptation is applied to only part of the problem, however, as in perturbational treatments of anharmonic effects,[1,2] multiple sums over the Brillouin zone will inevitably appear These multiple summations in **q** space restrict the calculation of perturbation terms to a few of the lowest orders and, therefore, make the theory inapplicable to strongly anharmonic systems

In papers I and II of this series,[3,4] we describe a lattice dynamics theory for molecular crystals which avoids multiple sums in **q** space, because the wave functions are adapted to the translational symmetry of the crystal only in the final stage Thus, we were able to treat the librations in the ordered α and γ phases of solid nitrogen and even the reorientations of the molecules in the plastic β phase, without making any approximation to the strongly anharmonic potential Just as in all previous, semiempirical, libron treatments,[5–8] the molecular centers of mass in our calculations were assumed to be fixed on the lattice sites This assumption implies the decoupling of the librons and the translational phonons In principle, one could still take the latter into account by using a translationally averaged potential for the librations, in practice, this has not been done explicitly

The coupling between librons and phonons, i e , rotational-translational coupling, is quite important, however All lattice modes are actually mixed, except those at high symmetry points in the Brillouin zone of crystals with specific space groups For calculating thermodynamic properties, which involves summation over the complete Brillouin zone, all these mixed modes must be included It has been shown in more empirical models[9–12] that rotational-translational coupling can lead to interesting phenomena such as ferroelastic phase transitions in KCN and *s*-triazine crystals

In this paper we present a new formalism for the calculation of the coupled libron–phonon modes in molecular crystals This formalism combines our previous treatment[3,4] of large amplitude librons with the explicit handling of the translational lattice modes It is applied to solid nitrogen, again, using the anharmonic anisotropic *ab initio* potential [13] Since the translational phonons are fairly well described by the harmonic model already (and even better by the quasi-harmonic self-consistent phonon model[14]), we required our formalism to be exact for harmonic lattice Hamiltonians This implies, in the general case of translations and librations, that it includes at least the translational-rotational coupling which is naturally present in the harmonic model Our formalism goes beyond the harmonic approximation, however, even for the translational phonons, by including all terms in the potential which are cubic and quartic in the molecular displacements The orientational dependence of the potential is represented exactly, as in papers I and II The above requirements are met by the following scheme First, we treat the anharmonic anisotropic lattice Hamiltonian, which depends on the translational and orientational coordinates of the molecules, in a mean field calculation for the translations and reorientations of each molecule, separately Then, we construct wave functions as products of mean field ground states and one excited mean field function, adapted to the translational symmetry The coupling between these wave functions is handled within the time-dependent Hartree (TDH) or random-phase approximation (RPA)

For the harmonic approximation to the lattice Hamiltonian the mean field states are the ground and first excited harmonic oscillator states with frequencies determined by the self forces It has been demonstrated[15,16] that the TDH/RPA equation of motion is exact in this case Moreover, it has been proved[15,16] that the TDH/RPA frequencies will be zero for uniform translations of the whole system, which implies in case of crystals that the acoustical phonon modes will correctly tend to zero frequency for wave vector zero

 0021 9606/84/214118 09$02 10

This condition is not satisfied by the simpler forms of the equation of motion based on the Tamm–Dancoff approximation,[15] which have been used in lattice dynamics also [6]

If we would separately couple the translational and/or rotational motions of the individual molecules, obtain solutions adapted to the lattice symmetry, and then introduce translational rotational coupling, we would still be hindered by the problem of multiple sums in q space mentioned at the start Instead, we have chosen to couple all mean field translational and rotational excited states simultaneously by means of the TDH/RPA scheme, applying the translational symmetry reduction directly to the full TDH problem

II. THEORY

In part A of this section we consider the intermolecular potential and bring it into a form which is suitable for the subsequent treatment In part B we deal with the translational part of the problem, including the basis functions and the matrix elements Finally, in part C we combine the results of subsection B with those of paper I, in order to describe the coupled rotational-translational motions

A. The potential

As in our first paper, we associate each molecule in the crystal with a lattice point $P = \{\mathbf{n},t\}$, with position vector $\mathbf{R}_P = \mathbf{R}_\mathbf{n} + \mathbf{r}_t$, where $\mathbf{R}_\mathbf{n}$ is the position vector of the origin of the unit cell $\mathbf{n}$ and $\mathbf{r}_t$ the position of P relative to this origin ($t = 1,2, \ldots Z$, where Z is the number of molecules per unit cell) The molecules are now supposed to oscillate and librate with their centers of mass remaining in the neighborhood of the points P; the position vectors of their mass centers relative to these points are denoted by $\mathbf{u}_P$ The orientations of the (linear) molecules with respect to a fixed lattice frame will be described by the polar angles $\Omega_P = \{\theta_P, \varphi_P\}$ of their axes The potential energy between two molecules associated with P and P', respectively, can then be written as

$$\Phi(\mathbf{U}_{PP'},\Omega_P,\Omega_{P'}) = \sum_l \varphi_l(U_{PP'}) \sum_{\mathbf{m}} \begin{pmatrix} l_1 & l_2 & l_3 \\ m_1 & m_2 & m_3 \end{pmatrix} \times C^{(l_1)}_{m_1}(\Omega_P) C^{(l_2)}_{m_2}(\Omega_{P'}) C^{(l_3)}_{m_3}(\hat{U}_{PP'}) \quad (1)$$

Here, $\mathbf{U}_{PP'} = (\mathbf{R}_{P'} + \mathbf{u}_{P'}) - (\mathbf{R}_P + \mathbf{u}_P) = \mathbf{R}_{PP'} + \mathbf{u}_{P'} - \mathbf{u}_P$ and $\hat{U}_{PP'}$ is the unit vector along $\mathbf{U}_{PP'}$ The angular functions $C^{(l)}_m$ are Racah spherical harmonics[17] and the larger brackets denote a Wigner 3-j symbol, $\mathbf{l} = \{l_1,l_2,l_3\}$ and $\mathbf{m} = \{m_1,m_2,m_3\}$ The *ab initio* N_2–N_2 potential has actually been represented in this form [13]

The potential given by Eq (1) depends on the translational degrees of freedom $\mathbf{u}_P$ and $\mathbf{u}_{P'}$ in a very intricate way In order to make this dependence explicit, which is required for the subsequent theory, we expand the factors that contain these variables in a Taylor series

$$\varphi_l(U_{PP'})C^{(l)}_m(\hat{U}_{PP'}) = \sum_{\alpha\,\alpha'} \frac{(-\mathbf{u}_P\cdot\nabla)^\alpha}{\alpha_1!} \frac{(\mathbf{u}_{P'}\cdot\nabla)^{\alpha'}}{\alpha_2!} \times \varphi_l(R_{PP'})C^{(l)}_m(\hat{R}_{PP'}) \quad (2)$$

The simplest way to evaluate this expansion is by means of the so-called gradient formula[17] in spherical tensor form

$$\mathbf{u}_P\cdot\nabla F(R_{PP'})C^{(l)}_m(\hat{R}_{PP'}) = u_P \sum_k A_{l,k}(R_{PP'})F(R_{PP'}) \times \{C^{(1)}(\hat{u}_P)\otimes C^{(k)}(\hat{R}_{PP'})\}^{(l)}_m, \quad (3)$$

where $A_{lk}(R)$ is an operator defined by

$$A_{lk}(R) = +\delta_{k,l-1}\left[\frac{l(2l-1)}{2l+1}\right]^{1/2}\left(\frac{d}{dR} + \frac{l+1}{R}\right) - \delta_{k,l+1}\left[\frac{(l+1)(2l+3)}{2l+1}\right]^{1/2}\left(\frac{d}{dR} - \frac{l}{R}\right) \quad (4)$$

while the tensor product between curly brackets is given by

$$\{C^{(l_1)}(\hat{u}_P)\otimes C^{(l_2)}(\hat{R}_{PP'})\}^{(l_3)}_{m_3} = (-1)^{l_2+l_3+m_3} \times \sum_{m_1 m_2} \begin{pmatrix} l_1 & l_2 & l_3 \\ m_1 & m_2 & -m_3 \end{pmatrix} \times C^{(l_1)}_{m_1}(\hat{u}_P)C^{(l_2)}_{m_2}(\hat{R}_{PP'}) \quad (5)$$

Using Eq (3) several times we can write Eq (2) as

$$\varphi_l(U_{PP'})C^{(l_3)}_{m_3}(\hat{U}_{PP'}) = \sum_k \sum_j {}^jW^{(l)}_k(R_{PP'},u_P,u_{P'}) \times \{\{C^{(k_1)}(\hat{u}_P)\otimes C^{(k_2)}(\hat{u}_{P'})\}^{(j)} \otimes C^{(k_3)}(\hat{R}_{PP'})\}^{(l_3)}_{m_3} \quad (6)$$

The angular independent factors are given by

$${}^jW^{(l)}_k(R_{PP'},u_P,u_{P'}) = \sum_{\alpha\,\alpha_2} \frac{(-u_P)^\alpha}{\alpha_1!} \frac{(u_{P'})^{\alpha_2}}{\alpha_2!} \times {}^jW^{(l)}_k(R_{PP'}|\alpha_1,\alpha_2) \quad (7)$$

So it is our task to calculate the coefficients ${}^jW^{(l)}_k(R_{PP'}|\alpha_1,\alpha_2)$ We do this via the following recursion relation

$$\mathbf{u}_P\cdot\nabla \sum_k \sum_j {}^jW^{(l)}_k(R_{PP'}|\alpha_1,\alpha_2)\{\{C^{(k)}(\hat{u}_P)\otimes C^{(k_2)}(\hat{u}_{P'})\}^{(j)}\otimes C^{(k_3)}(\hat{R}_{PP'})\}^{(l_3)}_{m_3} = u_P \sum_k \sum_j {}^jW^{(l)}_k(R_{PP'}|\alpha_1+1,\alpha_2)\{\{C^{(k)}(\hat{u}_P)\otimes C^{(k_2)}(\hat{u}_{P'})\}^{(j)}\otimes C^{(k_3)}(\hat{R}_{PP'})\}^{(l_3)}_{m_3} \quad (8)$$

and an analogous formula to raise the index α_2 Using the gradient formula and the expansion of a product of two spherical harmonics[17] we find that the left-hand side of Eq (8) is given by

$$u_P \sum_{k_1} \sum_{n_1} C^{(k_1)}_{n_1}(\hat{u}_P)C^{(k_1)}_{n_1}(\hat{u}_P)C^{(k_3)}_{n_1+m_3}(\hat{R}_{PP'})(2k_1+1) \sum_{k_1'k_2'} \sum_j A_{k_1',k_2'}(R_{PP'})\,{}^jW^{(l)}_{k_1',k_2'}(R_{PP'}|\alpha_1,\alpha_2) \begin{pmatrix} 1 & k_1' & k_1 \\ 0 & 0 & 0 \end{pmatrix} \times \sum_{n_1' n_2'} \sum_{\nu\mu'} \begin{pmatrix} 1 & k_1' & k_1 \\ \nu & n_1' & -n_1 \end{pmatrix} \begin{pmatrix} 1 & k_2' & j' \\ \nu & -n_1' & n_1' \end{pmatrix} \begin{pmatrix} k_1' & k_2 & j' \\ -n_1' & -n_2 & \mu' \end{pmatrix} \begin{pmatrix} j' & k_3' & l_3 \\ \mu' & n_2' & -m_3 \end{pmatrix} (-1)^{\nu+n_1'} \quad (9)$$

The last sum in this expression can be evaluated using standard angular momentum techniques,[17,18] it is equal to

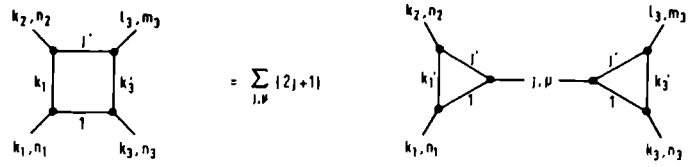

FIG 1 Recoupling scheme for expansion of the potential [Eqs (9) and (10)]

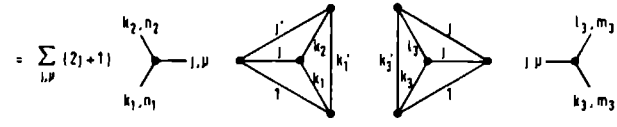

$$\sum_{\mu m} (2j+1)(-1)^{\mu+m_3} \begin{pmatrix} k_1 & k_2 & j \\ n_1 & n_2 & -\mu \end{pmatrix} \begin{pmatrix} j & k_3 & l_3 \\ \mu & n_3 & -m_3 \end{pmatrix} \begin{Bmatrix} k_1 & k_2 & j \\ j' & 1 & k_3' \end{Bmatrix} \begin{Bmatrix} j & k_3 & l_3 \\ k_3' & j' & 1 \end{Bmatrix} (-1)^{k_3'+j'+l_3} \tag{10}$$

The symbols between curly brackets are 6-j coefficients. In Fig. 1 we have given the graphical representation of this summation according to the conventions of Brink and Satchler.[18] Introducing the last two results into Eq (8) we find

$$^{j}W_{\mathbf{k}}^{(l)}(R_{PP'}\,|\alpha_1+1,\alpha_2) = (-1)^{k_1+k_3+l_3}(2j+1)(2k_1+1) \sum_{k_1' k_3'} \sum_{j'} \begin{pmatrix} 1 & k_1' & k_1 \\ 0 & 0 & 0 \end{pmatrix} \begin{Bmatrix} k_1 & k_2 & j \\ j' & 1 & k_1' \end{Bmatrix} \begin{Bmatrix} j & k_3 & l_3 \\ k_3' & j' & 1 \end{Bmatrix} A_{k_1' k_3'}(R_{PP'})$$
$$\times {}^{j}W^{(l)}_{k_1' k_2 k_3' k_3}(R_{PP'}\,|\alpha_1,\alpha_2). \tag{11}$$

In the same way a recursive relation raising the index α_2 by one unit can be derived. In the actual calculations it is most convenient to first raise one of the indices α_1 or α_2 to its final value, while keeping the other one equal to zero, and then to raise the second index This greatly simplifies the recursive relations, because, e g., when $\alpha_2 = 0$, then $k_2 = 0$ and the first 6-j coefficient in Eq (11) becomes a simple square root; moreover $j' = k_1'$ and $j = k_1$ so that the sum over j' in Eq (11) contains only one term

While the sums over $\mathbf{k}$ and j in Eqs. (6) and (7) are bounded for given α_1 and α_2, the sums over the latter indices must, in principle, be extended to infinity In testing our programs we have found that generally good results can be obtained with $\alpha_1 + \alpha_2 \leq \alpha_{max} = 4$. Indeed, taking $R_{PP'}$ equal to the nearest neighbor distance in α-N_2, and u_P and $u_{P'}$ as large as 8% of this value we found the exact value of the potential within 1%, when using $\alpha_{max} = 4$

Introducing Eqs. (6) and (7) into Eq. (1) we find with a slight change of notation:

$$\Phi_{PP'}(\mathbf{u}_P,\Omega_P,\mathbf{u}_{P'},\Omega_{P'}) = \sum_{\Lambda_1,\Lambda_2} (u_P)^{\alpha_1} C^{(k_1,l_1)}_{m_1}(\hat{u}_P) C^{(l_1,l_2)}_{m_1}(\Omega_P) X_{\Lambda_1,\Lambda_2}(P,P') C^{(l_2,l_3)}_{m'}(\Omega_{P'}) C^{(k_3,l_3)}_{n}(\hat{u}_{P'})(u_{P'})^{\alpha_2}, \tag{12}$$

which is in the required form Here Λ_1 and Λ_2 are composite indices and

$$X_{\Lambda_1,\Lambda_2}(P,P') = \frac{(-1)^{\alpha_1}}{\alpha_1!} \frac{1}{\alpha_2!} \sum_{k_2,l_2,\mu} {}^{j}W^{(l)}_{\mathbf{k}}(R_{PP'}\,|\alpha_1,\alpha_2)(-1)^{k_1+k_2+k_3+j}$$
$$\times \sum_{n_1,m_2,\mu} (-1)^{m_2+\mu} \begin{pmatrix} l_1 & l_2 & l_3 \\ m_1 & m_2 & m_3 \end{pmatrix} \begin{pmatrix} k_1 & k_2 & j \\ n_1 & n_2 & -\mu \end{pmatrix} \begin{pmatrix} j & k_3 & l_3 \\ \mu & n_3 & -m_1 \end{pmatrix} C^{(k_1,l_1)}_{m_1}(\hat{R}_{PP'}) \tag{13}$$

Construction of the crystal Hamiltonian is now straightfoward; the result is given below in Eq. (19) For convenience we do not separate the one and two particle terms in the potential, as we did in paper I Of course this does not change the physics of our model, the only result being that the mean field energies are shifted by a constant, temperature dependent, amount.

B. Translational motions

When we disregard the orientations of the molecules for the moment, we can write the crystal Hamiltonian as

$$H = \sum_P T(\mathbf{u}_P) + \frac{1}{2} \sum_{P} \sum_{P' \neq P} \Phi_{PP'}(\mathbf{u}_P,\mathbf{u}_{P'}), \tag{14a}$$

$$T(\mathbf{u}_P) = -\frac{\hbar^2}{2M} \Delta(\mathbf{u}_P), \tag{14b}$$

$$\Phi_{PP'}(\mathbf{u}_P,\mathbf{u}_{P'}) = \sum_{\lambda_1,\lambda_2} (u_P)^{\alpha_1} C^{(k_1,l_1)}_{n_1}(\hat{u}_P) X_{\lambda_1,\lambda_2}(P,P') \times C^{(k_2,l_2)}_{n_2}(\hat{u}_{P'})(u_{P'})^{\alpha_2} \tag{14c}$$

Here λ_i is the composite index $|\alpha_i,k_i,n_i|$ Treating this Hamiltonian first within the mean field approximation, in other words approximating the crystal as a generalized Einstein

crystal, we find that we must solve the coupled set of equations

$$H_P^{MF}(\mathbf{u}_P) = T(\mathbf{u}_P) + \sum_{P' \neq P} \langle \Phi_{PP'}(\mathbf{u}_P, \mathbf{u}_{P'}) \rangle_{P'} = T(\mathbf{u}_P) + \Phi_P^{MF}(\mathbf{u}_P), \tag{15}$$

where $\langle X \rangle_P$ denotes the thermodynamic average of X over the eigenstates of $H_P^{MF}(\mathbf{u}_P)$. In order to solve these equations, just as in paper I, we impose the experimentally observed symmetry on the solutions. As a result, $H_P^{MF} = H_{P'}^{MF}$ when $\mathbf{R}_{PP'}$ is equal to a primitive lattice vector, and otherwise we can use

$$\langle C_n^{(k)} \rangle_P = \sum_m \langle C_m^{(k)} \rangle_{P'} D_{mn}^{(k)}(\omega_P), \tag{16}$$

for some set of Euler angles $\{\omega_P\}$. In our case, moreover, $\langle (u_P)^\alpha \rangle_P = \langle (u_{P'})^\alpha \rangle_{P'}$ for all P and P'.

We have solved the mean field equations (15) in a basis of $3D$ harmonic oscillator functions[19]

$$\Psi_{lm}^{(n)}(\mathbf{u}_P) = A\,[2/u_P]^{1/2} A_{l+(1/2)n-l}^{l+(1/2)}(A^2 u_P^2)\, S_m^{(l)}(\hat{u}_P), \tag{17a}$$

$$A_k^\alpha(t) = \left[\Gamma(\alpha+1)\binom{k+\alpha}{k}\right]^{1/2} e^{-t/2} t^{\alpha/2} L_k^\alpha(t) \tag{17b}$$

Here $L_k^\alpha(t)$ denotes the Laguerre function and $\Gamma(k)$ the Gamma function, $l \leq n$, and l and n have the same parity. The angular functions $S_m^{(l)}$ are tesseral harmonics. The constant A is just a scaling constant, which in the case of an infinite basis has no influence. In practice, however, we restrict ourselves to a finite basis $n \leq n_{max}$ and use A to optimize this basis. If $H_P^{MF}(\mathbf{u}_P)$ would have a purely harmonic spectrum, we should use $A = [M\omega]^{1/2}$, with ω being the oscillator frequency. We have therefore chosen $A = [M(\epsilon^{(1)} - \epsilon^{(0)})]^{1/2}$, where $\epsilon^{(n)}$ is the nth mean field energy. In some cases we have tested this choice by optimizing A and it turned out that A did not appreciably change, nor did the physical results.

Matrix elements in this basis are easily obtained using

$$\frac{1}{4\pi}\int d\Omega_u\, C_m^{(l_1)}(\hat{u}) C_{m_2}^{(l_2)}(\hat{u}) C_{m_3}^{(l_3)}(\hat{u}) = \begin{pmatrix} l_1 & l_2 & l_3 \\ 0 & 0 & 0 \end{pmatrix} \begin{pmatrix} l_1 & l_2 & l_3 \\ m_1 & m_2 & m_3 \end{pmatrix} \tag{18a}$$

$$\int_0^\infty u^2\, du\, A_{(1/2)n'-l_1}^{l_1+(1/2)}(u^2) \frac{u^\alpha}{u} A_{(1/2)n-l_2}^{l_2+(1/2)}(u^2) = \frac{1}{2}(-1)^{a_1+a_2} \left[\frac{\Gamma(a_1+1)}{\Gamma(a_1+b_1+1)} \frac{\Gamma(a_2+1)}{\Gamma(a_2+b_2+1)}\right]^{1/2} \sum_{l=l_{min}}^{l_{max}} \binom{c-b_1}{a_1-l} \binom{c-b_2}{a_2-l} \binom{c+1}{l} \Gamma(c+1),$$

$$a_i = \tfrac{1}{2}(n_i - l_i), \quad b_i = l_i + \tfrac{1}{2}, \quad c = \tfrac{1}{2}(l_1 + l_2 + \alpha + 1), \quad d = \max(a_1 + b_1, a_2 + b_2) - c,$$

$$l_{min} = \begin{cases} d \text{ if } c \text{ is half-integer and } d > 0 \\ 0 \text{ otherwise} \end{cases}, \quad l_{max} = \min(a_1, a_2) \tag{18b}$$

Equation (18b) has been derived using the results of Tennyson and Sutcliffe[20], the factor u^2 in this equation originates from the volume element in u space. Matrix elements of the kinetic energy operator are calculated most easily by writing $-\Delta(\mathbf{u}) = A^2[-\Delta(A\mathbf{u}) + A^2u^2] - A^4u^2$, the matrix elements of the operator in square brackets, which is the harmonic oscillator Hamiltonian, are simply equal to $\delta_{l_1 l_2}\delta_{m_1 m_2}\delta_{n_1 n_2}(2n_1 + 3)$, while those of the remaining part can be calculated using Eq. (18b).

The final step is to construct correlated crystal states by using a restricted basis of mean field crystal states and solving the TDH equations. These equations are completely analogous to those given in Secs. II C and II D of paper I, and will not be repeated here.

C. The coupled rotational-translational problem

The Hamiltonian for the coupled problem reads

$$H = \sum_P \{T(\mathbf{u}_P) + L(\Omega_P)\} + \frac{1}{2}\sum\sum_{P \neq P'} \Phi_{PP'}(\mathbf{u}_P, \Omega_P, \mathbf{u}_{P'}, \Omega_{P'}) \tag{19}$$

Here $T(\mathbf{u}_P)$ and $L(\Omega_P)$ represent the kinetic energy operators of the translational and the rotational motions, respectively. The potential has been given in Eq. (12).

Now there are two possible ways to apply the mean field approximation to this Hamiltonian, which correspond to writing the variational Hamiltonian H_0, to be used in the Gibbs–Bogoliubov inequality, in either one of the forms

$$H_0 = \sum_P H_P^{MF}(\mathbf{u}_P, \Omega_P), \tag{20a}$$

$$H_0 = \sum_P \{H_P^T(\mathbf{u}_P) + H_P^L(\Omega_P)\} \tag{20b}$$

The first possibility has the advantage of including the correlation between the one-particle rotational and translational motions. From a practical point of view, however, it has the drawback of requiring a huge basis of product functions $C_m^{(l)}(\Omega)\Psi_{l,m_l}^{(n)}(\mathbf{u})$ in order to yield reasonably converged mean field states. We therefore choose to write H_0 as in Eq. (20b). Introducing this Hamiltonian into the Gibbs–Bogoliubov inequality, and optimizing the free energy (see papers I and II) we find the mean field equations

$$H_P^T(\mathbf{u}_P) = T(\mathbf{u}_P) + \sum_{P' \neq P} \langle \Phi_{PP'}(\mathbf{u}_P, \Omega_P, \mathbf{u}_{P'}, \Omega_{P'}) \rangle_{P'}^{L_{P'}} = T(\mathbf{u}_P) + \Phi_P^T(\mathbf{u}_P), \tag{21a}$$

$$H_P^L(\Omega_P) = L(\Omega_P) + \sum_{P' \neq P} \langle \Phi_{PP'}(\mathbf{u}_P, \Omega_P, \mathbf{u}_{P'}, \Omega_{P'}) \rangle_{P'}^{T_{P'}} = L(\Omega_P) + \Phi_P^L(\Omega_P) \tag{21b}$$

Here $\langle X \rangle_{P'}^{L_{P'}}$ denotes the thermodynamic average of X over the states of $H_{P'}^T(\mathbf{u}_{P'}) + H_{P'}^L(\Omega_{P'})$ and over those of $H_{P'}^L(\Omega_{P'})$. An analogous definition holds for $\langle X \rangle_{P'}^{T_{P'}}$. In order

to solve these coupled equations, we impose, in the usual way, the experimentally observed symmetry on the solutions and proceed iteratively A useful test on the final solutions follows from $\langle \Phi^{T}_{P}(\mathbf{u}_P)\rangle^{T_P} = \langle \Phi^{L}_{P}(\Omega_P)\rangle^{L_P}$

Our final task is to calculate the fundamental excitation energies of the crystal To this end we apply the TDH formalism as in paper I The time dependent pertubation is now $h(t) = \Sigma_P |h^{T}_{P}(\mathbf{u}_P,t) + h^{L}_{P}(\Omega_P,t)|$ and the perturbed density operator is written as $D(t) = \Pi_P d^{T}_{P}(\mathbf{u}_P,t) d^{L}_{P}(\Omega_P,t)$ Performing exactly the same steps as in paper I, we find that the excitation energies are equal to the positive eigenvalues of the matrix

$$M^{KK}_{\alpha\beta,\alpha'\beta'}(\mathbf{q}) = \delta_{\alpha\alpha'}\delta_{\beta\beta'}\delta_{ii'}\delta_{KK}(\epsilon^{(\alpha)}_{K} - \epsilon^{(\beta)}_{K}) - (P^{(\alpha)}_{K} - P^{(\beta)}_{K})\sum_{\mathbf{n}} e^{i\mathbf{q}\cdot\mathbf{R}_{\mathbf{n}}}\langle \alpha^{K}_{P}\beta^{K}_{P'} | \mathrm{Tr}'^{P,P'}_{K,K}(d^{K}_{P} d^{K}_{P'} \Phi_{PP'}) | \beta^{K}_{P}\alpha'^{K}_{P'}\rangle$$

$$- (P^{(\alpha)}_{K} - P^{(\beta)}_{K})\delta_{ii'}\delta_{KK}\sum_{Q}\langle \alpha^{K}_{P}\beta'^{K}_{P} | (\Phi_{PQ})_{Q} | \beta^{K}_{P}\alpha'^{K}_{P}\rangle, \quad \text{with } P = |\mathbf{n},i| \text{ and } P' = |\mathbf{0},i'| \tag{22}$$

Here K is equal to either T or L, and K_c is the complement of K, the same holds for K $\epsilon^{(\alpha)}_{T}$ is the mean field translational energy of the state $|\alpha^{T}_{P}(\mathbf{u}_P)\rangle$, which is an eigenstate of $H^{T}_{P}(\mathbf{u}_P)$, an analogous definition holds for $\epsilon^{(\alpha)}_{L}$ Finally, $P^{(\alpha)}_{K} = \langle \alpha^{K}_{P}|d^{K}_{P}|\alpha^{K}_{P}\rangle$ are occupation numbers corresponding with the mean field density operators d^{K}_{P} As in paper I, we omit the rows and columns for which $\epsilon^{(\alpha)}_{K} = \epsilon^{(\beta)}_{K}$ and we order the mean field states according to whether $\epsilon^{(\alpha)}_{K} > \epsilon^{(\beta)}_{K}$ or $\epsilon^{(\alpha)}_{K} < \epsilon^{(\beta)}_{K}$ If we assume that all mean field states are real, the matrix M has the simple structure

$$\mathbf{M}(\mathbf{q}) = \begin{pmatrix} \mathbf{A}^{TT} - \mathbf{B}^{TT}(\mathbf{q}) & -\mathbf{B}^{TL}(\mathbf{q}) & -\mathbf{B}^{TT}(\mathbf{q}) & -\mathbf{B}^{TL}(\mathbf{q}) \\ -\mathbf{B}^{TL}(\mathbf{q})^{\dagger} & \mathbf{A}^{LL} - \mathbf{B}^{LL}(\mathbf{q}) & -\mathbf{B}^{TL}(\mathbf{q})^{\dagger} & -\mathbf{B}^{II}(\mathbf{q}) \\ \mathbf{B}^{TT}(\mathbf{q}) & \mathbf{B}^{TL}(\mathbf{q}) & -\mathbf{A}^{TT} + \mathbf{B}^{TT}(\mathbf{q}) & \mathbf{B}^{TI}(\mathbf{q}) \\ \mathbf{B}^{TL}(\mathbf{q})^{\dagger} & \mathbf{B}^{LL}(\mathbf{q}) & \mathbf{B}^{TL}(\mathbf{q})^{\dagger} & -\mathbf{A}^{LL} + \mathbf{B}^{LL}(\mathbf{q}) \end{pmatrix} \tag{23}$$

Here $\mathbf{A}^{KK}$ is the diagonal matrix with elements $\delta_{\alpha\alpha}\delta_{\beta\beta}\delta_{ii'}\delta_{KK}(\epsilon^{(\alpha)}_{K} - \epsilon^{(\beta)}_{K})$ and the matrices $\mathbf{B}^{K\Lambda}(\mathbf{q})$ follow from Eq (22) We notice that the correlation which we lost by choosing Eq (20b) instead of Eq (20a) will partly be recovered by the last term in Eq (22) This term couples the rotations and translations on the same molecule The only B matrix in which this term appears is $\mathbf{B}^{TL}(\mathbf{q})$ In the actual calculations we have restricted the mean field basis to the ground states, the lowest three excited levels, for the translations and two excited levels for the librations These numbers correspond with the degrees of freedom As a result, in Eq (23), β is always equal to zero, i e , it represents the ground state, and α is not All calculations are performed for zero temperature, although the formalism holds for $T > 0$ as well

III. CALCULATIONS AND RESULTS

The formalism described in the preceding section has been implemented in a computer program and applied to the α, β, and γ phases of solid nitrogen The structure of these phases has been described in papers I and II, and we have used the same *ab initio* potential [15] First, we have performed the mean field calculations for the molecular librations and translational vibrations, separately, by an iterative procedure which alternately uses Eqs (21a) and (21b) For the disordered β phase we met the following problem The delocalized mean field solution for the molecular reorientations which corresponds with the observed hexagonal lattice symmetry is not stable, i e , it does not represent a minimum in the free energy (see paper II) The stable solution, which we have found also, corresponds with localized librations of the molecules around one of six equivalent axes which make an angle of 52° with the crystal c axis for the two molecules in the hexagonal unit cell equilibrium axes are rotated over 180° about the c axis Although we expect that the experimentally observed lattice symmetry can be restored by allowing rapid jumps of the molecules between these six localized librational solutions, the lower symmetry of the stable mean field solution makes it impossible to use our libron–phonon formalism as such Indeed, we find that in the mean field of the "broken symmetry" librational solution, the mean field equilibrium positions of the molecules tend to shift away from the hexagonal lattice sites Thus, the symmetry of the translational mean field solution becomes lower than the experimentally observed symmetry, as well In order to cure this problem one would have to extend our formalism with a dynamical model for the symmetry-restoring molecular jumps

For the ordered α and γ phases we have not experienced such difficulties, however, and the stable mean field solutions obtained correspond with the observed space groups of the lattices We have even determined theoretically optimized unit cell parameters in the following manner For the α phase, which exists in equilibrium with nitrogen vapor of very low pressure (practically $p = 0$), we have calculated the minimum of the Helmholtz free energy A, as a function of the cubic cell parameter a The free energy is defined as in paper I, but now we have included the translational vibrations as well This yielded the optimum cell parameter $a = 5.699$ Å (experimentally [16] $a = 5.644$ Å) and the mean field lattice cohesion energy at $T = 0$ K $\Delta E = 5.92$ kJ/mol, including zero point motions (experimentally $\Delta E = 6.92$ kJ/mol) For the γ phase which is stable above $p = 4$ kbar, we have calculated the free energy A for several values of the tetragonal cell parameters a and c, and fitted $A(a,c)$ by a quadratic function Each point (a,c) corresponds with molar volume $v = \sqrt{3}a^2c/2$ and on each curve of constant v we can determine the optimum a and c by minimizing A Using these optimum points and the corresponding free energies we have calculated the pressure $p = -\partial A/\partial v$ Thus we have found at $p = 4$ kbar that $a = 3.961$ Å, $c = 5.104$ Å in very

good agreement with the experimental values[21] $a = 3\,957$ Å, $c = 5.109$ Å

Having calculated the ground and excited mean field states of α and γ nitrogen, we have included the intermolecular correlations as well as translational-rotational coupling, by determining the eigenvalues of the TDH matrix M(q) [Eq. (23)]. In practice, we have solved the generalized Hermitean eigenvalue problem [paper I, Eq. (20)], which yields the squares of the TDH frequencies. We have tested the convergence of the frequencies with respect to the expansion length of the potential α_{max} and the sizes of the bases used for the translational modes, n_{max} and for the librons l_{max}. Characteristic results are given in Tables I and II. For $\alpha_{max} = 2$ only those terms in the potential which are harmonic in the molecular displacements are included, for $\alpha_{max} = 3$ also all cubic terms and for $\alpha_{max} = 4$ all quartic terms, as well, cf. Eq. (12). The orientational dependence of the potential as given by the spherical expansion [Eqs. (1) and (12)] is always fully taken into account. For some points in the Brillouin zone the effect of the cubic terms vanishes and the anharmonic quartic corrections to the translational frequencies are due to the quartic terms only. This is related to the inversion symmetry of the crystal; it occurs at the same points, such as the Γ point (see Table I), where the translational and librational modes are decoupled. In other points, such as the M point, the cubic corrections are nonzero but they are smaller than the quartic corrections. This may suggest that even higher terms could be important. We believe, however, that this is not the case, since the potential is represented to 1% accuracy by the terms with $\alpha_1 + \alpha_2 < 4$ for molecular displacements as large as 0.3 Å. The actual rms displacements emerging from our calculations are only about 0.1 Å (see Table III).

The size of the anharmonic corrections to the translational frequencies is comparable, for α and γ nitrogen, to the SCP corrections.[14] This is not undesirable since the SCP method appeared to work very well for the translational lattice modes in solid nitrogen.[14] There is an important difference, however, between our formalism and the SCP method.[22] The latter method neglects those terms in the potential which depend on odd powers of the molecular displacements, for any type of crystal and any point in the Brillouin zone. Our formalism includes the cubic terms, at those points where they do not vanish by symmetry. This is related to the occurrence of excited harmonic oscillator functions in the translational basis [Eq. (17)] with both even and odd n.

TABLE I α_{max} dependence of some TDH lattice frequencies for α-N_2 ($a = 5\,644$ Å, $T = 0$ K)

α_{max} =	Frequencies ω(cm^{-1}) 2 (harmonic model)	3	4
Γ(0,0,0)			
E_g	32 8	32 8	32 8
T_g	43 4	43 4	43 4
T_g	71 6	71 6	71 5
A_u	42 3	42 3	50 6
T_u	48 7	48 7	52 7
E_u	55 7	55 7	60 2
T_u	73 0	73 0	79 4
$M(\pi/a,\pi/a,0)$			
M_1	28 8	25 7	28 8
M_{12}	40 4	38 5	41 5
M_1	52 2	51 7	53 3
M_{12}	60 0	61 2	63 7
M_{12}	67 0	68 6	72 0

TABLE II l_{max} and n_{max} dependence of the free energy and the mean field excitation frequencies for α-N_2 ($\alpha_{max} = 4$, $a = 5\,699$ Å, $T = 0$ K)

l_{max} (basis size L)	n_{max} (basis size T)	A(kJ/mol)	ω_L(cm^{-1})	ω_T(cm^{-1})
6(28)	3(20)	− 5 8979	57 07	48 63
	4(35)	− 5 8980	57 07	48 63
	5(56)	− 5 8980	57 07	48 62
8(45)	3(20)	− 5 9172	51 09	48 25
	4(35)	− 5 9172	51.10	48 26
	5(56)	− 5 9172	51 10	48 24
10(66)	3(20)	− 5 9188	50 22	48.20
	4(35)	− 5 9188	50 22	48 20
	5(56)	− 5 9188	50 23	48.20

Table II illustrates that the excitation frequencies are quite well converged already for a translational basis with $n_{max} = 3$. In our further calculations we have included all basis functions up to $n_{max} = 5$, inclusive. The convergence of the librational frequencies is comparable with the pure libron calculations in paper I. In the final calculations we have used $l_{max} = 10$ for α-N_2 and $l_{max} = 12$ for γ-N_2, just as in paper I. We did not find any significant differences in the lattice frequencies between *ortho*-N_2 and *para*-N_2 solids, i.e., even l and odd l bases.

Table III lists the rms displacements of the molecules, as obtained from the mean field solutions and similar quantities for the angular oscillations. The amplitude of the motions in the γ phase are smaller than those in the α phase. The librational amplitudes are considered in both phases even at $T = 0$ K, while it should be remembered that the mean field model still has the tendency to underestimate such ampli-

TABLE III Translational and librational amplitudes from mean field calculations

α-N_2	$T = 0$ K	$p = 0$
	$\langle u_\parallel^2\rangle^{1/2} = 0.112$ Å	$u_\parallel = u_{[1\,1\,1]}$
	$\langle u_\perp^2\rangle^{1/2} = 0.107$ Å	
	$\langle u^2\rangle^{1/2} = 0.189$ Å	
	$\arccos(\langle\cos^2\theta\rangle^{1/2}) = 16.1°$	
γ-N_2	$T = 0$ K	$p = 4$ kbar
	$\langle u_z^2\rangle^{1/2} = 0.100$ Å	$u_\Gamma = u_{[1\,1\,0]}$
	$\langle u_{ab}^2\rangle^{1/2} = 0.086$ Å	$u_{1ab} = u_{[1\,\bar{1}\,0]}$
	$\langle u_\Gamma^2\rangle^{1/2} = 0.087$ Å	$u_{1c} = u_{[0,0,1]}$
	$\langle u^2\rangle^{1/2} = 0.159$ Å	
	$\arccos(\langle\cos^2\theta\rangle^{1/2}) = 12.9°$	

asymmetry parameter (rotation out of ab-plane rotation in the ab plane

$$\frac{\langle\sin^2\theta(\sin^2\varphi - \cos^2\varphi)\rangle}{\langle\sin^2\theta\rangle} = 0.05$$

TABLE IV Lattice frequencies in α N_2 (in cm^{-1}) $T = 0$ K, $p = 0$

		Experiment (Ref 24)	Semiempirical harmonic (Ref 27)	SCP (Ref 14)	TDH(libron) (Ref 3)	TDH (This work)	TDH (This work)
	a(Å)	5 644	5 644	5 796	5 644	5 644	5 699
	Γ(0,0,0)						
Librations	E_g	32 3	37 5	39 5	30 7	32 8	31 0
	T_g	36 3	47 7	48 5	41 0	43 4	41 0
	T_g	59 7	75 2	70 3	68 5	71 5	68 0
Translational vibrations	A_u	46 8	45 9	48 8		50 6	47 2
	T_u	48 4	47 7	48 4		52 7	48 8
	E_u	54 0	54 0	53 5		60 2	55 6
	T_u	69 4	69 5	72 0		79 4	73 1
	$M(\pi/a,\pi/a,0)$						
	M_{12}	27 8	29 6	32.5		28 8	27 6
	M_{12}	37 9	40 6	43 3		41 5	39 1
	M_{12}	46 8	51 8	54 0		53 3	50 2
	M_{12}	54 9	59 0	58 5		63 7	59 1
	M_{12}	62 5	66 4	64 9		72 0	66 5
	$R(\pi/a,\pi/a,\pi/a)$						
Translational vibrations	R_1	33 9	34 4	34 2		37 0	34 4
	R_{23}	34 7	35 7	35 9		38 4	35 8
	R_{23}	68 6	68 3	71 0		78 4	72 3
Librations	R_1^+	43 6	50 7	52 7	47 9	50 7	47 9
	R_{23}^+	47 2	57 8	55 7	51 0	53 6	50 8
rms deviation of librational frequencies			10.6	9 7	5 2	7 5	5 0
rms deviation of translational frequencies			0 6	1 6		6 5	2 1
rms deviation of all lattice frequencies			6 1	6 0		6 7	3 4

tudes, i.e., to overestimate the order parameters.[23]

The final frequencies from TDH calculations are given in Tables IV and V for different wave vectors q. The dispersion relations along some symmetry directions in the Brillouin zone are displayed in Fig. 2. We have not tried to apply the equivalent of Raich's libron theory[6] to the translational modes since this model which is based on the Tamm–Dancoff approximation, yields acoustical phonon branches which do not converge to zero frequency for $q \to 0$. The TDH or RPA model does show the correct limiting behavior, in this respect, but only if it is applied exactly,[15] and we had to use a translational basis, which is not too small, in order to approach this limit.

The confrontation of these final results with the experimental data[24–26] is very satisfactory, especially if we remember that the *ab initio* potential has not been adapted in order to improve the agreement, in contrast with most semiempirical calculations. Particularly, the libron frequencies are substantially improved with respect to earlier harmonic and SCP calculations[14] using the same *ab initio* potential and also with respect to semiempirical harmonic calculations.[27] This was already achieved by our previous libron calculations,[3] but the present formalism yields the frequencies of the translational and mixed modes, also in good agreement with experiment. The complete phonon dispersion curves in Fig. 2 are very close to the curves obtained from inelastic neutron scattering.[24]

IV. CONCLUSIONS

We have developed a formalism for quantitative lattice dynamics calculations on molecular crystals which is applicable to strongly anharmonic systems. It does not start from the usual harmonic model. For the orientational oscillations

TABLE V Lattice frequencies in γ N_2 (in cm^{-1}) $T = 0$ K, $p = 4$ kbar

		Experiment (Refs 25 and 26)	Semiempirical harmonic (Ref (27)(Ref 14)	SCP	TDH(libron) (Ref 3)	TDH (This work)	TDH (This work)
	a(Å)	3 957	3 940	4 100	3 957	3 957	3 961
	c(Å)	5 109	5 086	5 188	5 109	5 109	5 104
	Γ(0,0,0)						
Librations	E_g	55 0	50 5	56 5	63 8	67 5	67 6
	B_{1g}	98 1	74 8	85 2	99 6	104 2	103 3
	A_{2g}		105 1	107 1	119 9	125 1	124 4
Translational vibrations	E_u	65 0	58 3	69 3		65 0	65 2
	B_{1u}		103 1	107 4		115 8	114 9
rms deviation			14 2	7 9	6 3	8 0	7 9

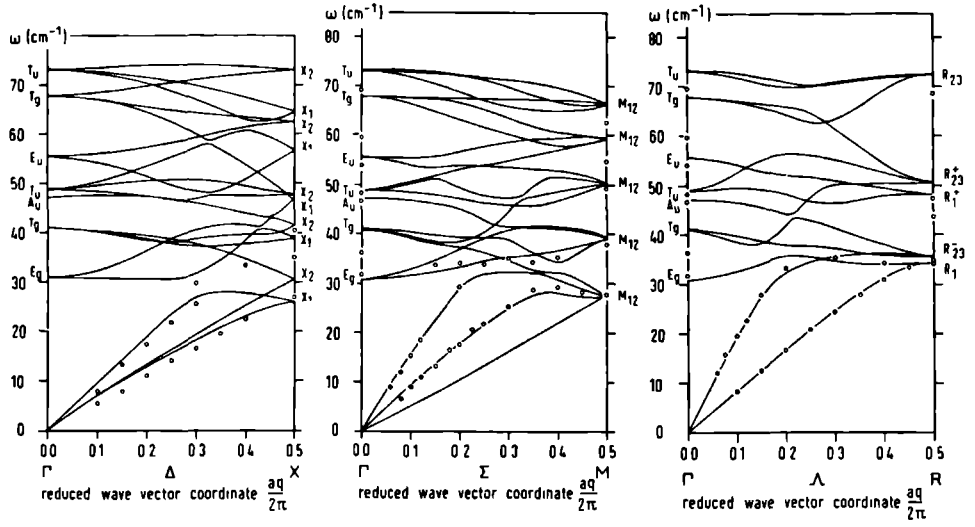

FIG 2 Calculated (TDH) dispersion curves for α-N for phonon–libron modes (a)–(c) propagating along the [001], [110], and [111] directions. The circles correspond with inelastic neutron scattering data measured at $T = 15$ K (Ref 24)

of the molecules we do not even require small amplitudes, the model is appropriate for free or hindered molecular rotations occurring in plastic phases Only when the orientational disorder in such phases is associated with jumps of the molecules between different orientations, the formalism is not applicable as such

The model has been applied to solid nitrogen, using an *ab initio* potential, with the results, lattice constants, and phonon–libron frequencies, in good agreement with experiment The observation that this agreement became systematically better with improvements of the lattice dynamics model indicates that the *ab initio* potential used should be fairly realistic

Although the formalism is certainly more complicated than the standard harmonic model, computation times for crystals of linear molecules, using extensive lattice sums, are still modest on modern computers This is promising in view of possible extension of our formalism to crystals of nonlinear molecules We can borrow several results from a recent dynamical model for van der Waals complexes comprising two nonlinear molecules [28] The spherical harmonics $C_m^{(l)}(\theta,\varphi)$ should be replaced by rotation functions $D_{km}^{(l)}(\psi,\theta,\varphi)$ both in the potential [Eq (1)] and in the basis for the molecular reorientations The matrix elements over such functions are hardly more complicated but the dimension of the summations will be extended

The formalism requires the potential to be given in the form of a spherical expansion [Eq (1)] Most semiempirical potentials are not in this form, but often they are described by an atom–atom potential model Such atom–atom or site–site potentials can be expanded in the form of Eq (1) or its generalization to nonlinear molecules,[29-32] using closed expressions for the r^{-n} terms[30-32] and for the $\exp(-\alpha r)$ terms [32]

Finally, we observe that the TDH/RPA formalism bases on mean-field states, which we have used for phonons and librons and their coupling, is similar to the spin-wave methods[33-35] applied to magnons We are trying to extend our model to the coupling between phonons, librons, and magnons in solid oxygen *Ab initio* calculations of the structure dependence of the Heisenberg exchange coupling between oxygen molecules[36,37] indicate that this coupling may have significant effects on several observed phenomena

ACKNOWLEDGMENTS

This investigation was supported in part by the Netherlands Foundation for Chemical Research (S O N) with financial aid from the Netherlands Organization for the Advancement of Pure Research (Z W O)

[1] S Califano V Schettino and N Neto *Lattice Dynamics of Molecular Crystals* Lecture Notes in Chemistry (Springer Berlin 1981), Vol 26
T H K Barrow and M L Klein in *Dynamical Properties of Solids* edited by G K Horton and A A Maradudin (North-Holland Amsterdam 1974) Vol 1
[2] A P J Jansen W J Briels and A van der Avoird J Chem Phys (to be published)
[3] A van der Avoird W J Briels, and A P J Jansen J Chem Phys (to be published)
[4] M J Mandell J Low Temp Phys 17 169 (1974) 18 273 (1975)
[5] J C Raich J Chem Phys 56 2395 (1972)
P V Dunmore J Chem Phys 57 3348 (1972) Can J Phys 55 554 (1977)

[9]T N Antsygina, V A Slyusarev, Yu A Freiman, and A I Erenburg, Sov J Low Temp Phys 8, 99, 149 (1982)
[9]J C Raich, H Yasuda, and E. R Bernstein, J Chem Phys 78, 6209 (1983)
[10]A I M Rae, J Phys C 15, 1883 (1982); 15, L287 (1982)
[11]T Luty and A van der Avoird, Chem Phys 83, 133 (1984)
[12]B de Raedt, K Binder, and K H Michel, J Chem Phys 75, 2977 (1981), K H Michel and J Naudts, *ibid* 68, 216 (1978)
[13]R M Berns and A van der Avoird, J Chem Phys 72, 6107 (1980)
[14]T Luty, A van der Avoird, and R M Berns, J Chem Phys 73, 5305 (1980)
[15]D J Rowe, *Nuclear Collective Motion* (Methuen, London, 1970)
[16]D R Fredkin and N R Werthamer, Phys Rev A 138, 1527 (1965)
[17]A R Edmonds, *Angular Momentum in Quantum Mechanics* (Princeton University, Princeton, 1957)
[18]D M Brink and G R Satchler, *Angular Momentum* (Clarendon, Oxford, 1975)
[19]J L Powell and B Craseman, *Quantum Mechanics* (Addison–Wesley, Reading, 1961)
[20]J Tennyson and B T Sutcliffe, J Chem Phys. 77, 4061 (1982)
[21]T A Scott, Phys. Rep 27, 89 (1976)
[22]N R Werthamer, in *Rare Gas Solids*, edited by M L Klein and J A Venables (Academic, London, 1976), Vol I, p 265
[23]H E Stanley, *Introduction to Phase Transitions and Critical Phenomena* (Oxford University, Oxford, 1971)
[24]J K Kjems and G Dolling, Phys Rev B 11, 1639 (1975)
[25]M M Thiery and D Fabre Mol Phys 32, 257 (1976)
[26]F Fondere, J Obriot, Ph Marteau, M Allavina, and H Chakroun, J Chem Phys 74, 2675 (1981)
[27]J C Raich and N S Gillis, J Chem Phys 66, 846 (1977)
[28]G Brocks, A van der Avoird, B T Sutcliffe, and J Tennyson, Mol Phys. 50, 1025 (1983)
[29]A van der Avoird P E S Wormer, F Mulder, and R M Berns, Topics Current Chem 93, 1 (1980)
[30]R A Sack, J Math Phys. 5, 260 (1964)
[31]J Downs, K E. Gubbins, S Murad and C G Gray Mol Phys 37, 129 (1979)
[32]W J Briels, J Chem Phys 73, 1850 (1980)
[33]C Kittel, *Quantum Theory of Solids* (Wiley, New York, 1963)
[34]D C Mattis, *The Theory of Magnetism I* (Springer Berlin, 1981)
[35]Yu B Gaididei and V M Loktev, Sov Phys. Solid State 16, 2226 (1975)
[36]M C van Hemert, P E S Wormer, and A van der Avoird, Phys. Rev Lett 51, 1167 (1983)
[37]P E S Wormer and A van der Avoird, J Chem Phys. 81, 1929 (1984)

CALCULATION OF THERMODYNAMIC PROPERTIES USING THE RANDOM PHASE APPROXIMATION: α-N_2

A.P.J. Jansen and R. Schoorl
Institute of Theoretical Chemistry
University of Nijmegen
Toernooiveld
6525 ED Nijmegen
The Netherlands

Abstract

The Random Phase Approximation (RPA) for molecular crystals is extended in order to calculate thermodynamic properties. A recursion formula for thermodynamic averages of products of Mean Field excitation and de-excitation operators is derived. With this formula the thermodynamic average of any operator can be obtained in the RPA by writing the operator in terms of Mean Field (de)excitation operators. The energy of α-N_2 is thus calculated as a function of pressure and temperature. The specific heat, free energy, cell parameter, isothermal compressibility and expansion coefficient are derived from the energy. Also the elastic constants and the Grüneisen parameters of α-N_2 are given.

1. Introduction

In previous papers we have shown how Mean Field theory (MF) and the Random Phase Approximation (RPA) can be used for lattice dynamics calculations of molecular crystals.[1,2] We have applied these formalisms to α-N_2, γ-N_2, α-O_2, and β-O_2. Accurate frequencies for the lattice vibrations were obtained. Thermodynamic properties were only calculated at the MF level, however, thus neglecting correlation effects.

In this paper we show how to include correlation effects in the calculations of the thermodynamic properties at the level of the RPA method. We will refer to the method to calculate the thermodynamic properties as an extension of RPA or (when no confusion is possible) simply RPA. The essential part of the method is a relation derived by Wallace[3] in which the thermodynamic average of a product of two operators, one of which is an excitation operator of the crystal, is related to the thermodynamic average of the commutator of these operators (see Eq. (7)).

The extension of RPA has been applied to α-N_2. The energy of α-N_2 has been calculated as a function of molar volume and temperature. Using the results of these energy calculations the specific heat, the entropy, the free energy, the cell parameter, the expansion coefficient and the isothermal compressibility have been derived. The results of these RPA calculations will be compared to the results of MF calculations and to experimental data. We will also present the results of the calculations of the elastic constants and the Grüneisen parameters. These have been obtained directly from the frequencies of the lattice vibrations.

In section 2 the theory for the calculation of the thermodynamic averages on the RPA level is given. In section 3 the results of the calculations on α-N_2 are presented and in section 4 these results are discussed and some conclusions are drawn.

2. Theory

The theory of RPA has been described amply elsewhere.[1,2,4] We will show here only how RPA can be extended to calculate thermodynamic averages. We start by writing a general operator $\hat{O}$ for the crystal as

$$\hat{O} = k^{(0)} + \sum_{\{\mathbf{R},I\}} \sum_{K} \sum_{m} \left[k^{(1,1)}_{\{\mathbf{R},I\},K,m} a^{(K)\dagger}_{\{\mathbf{R},I\},m} + k^{(1,2)}_{\{\mathbf{R},I\},K,m} a^{(K)}_{\{\mathbf{R},I\},m} \right] + \sum_{\{\mathbf{R},I\}} \sum_{\{\mathbf{R}',J\}} \sum_{K,K'} \sum_{m,m'} k^{(2,1)}_{\{\mathbf{R},I\},K,m;\{\mathbf{R}',J\},K',m'} a^{(K)\dagger}_{\{\mathbf{R},I\},m} a^{(K')}_{\{\mathbf{R}',J\},m'}$$

$$+\sum_{\{\mathbf{R},I\}}\sum_{\{\mathbf{R}',J\}}\sum_{K,K'}\sum_{m,m'}\Big[k^{(2,2)}_{\{\mathbf{R},I\},K,m;\{\mathbf{R}',J\},K',m'}a^{(K)\dagger}_{\{\mathbf{R},I\},m}a^{(K')\dagger}_{\{\mathbf{R}',J\},m'}$$
$$+\,k^{(2,3)}_{\{\mathbf{R},I\},K,m;\{\mathbf{R}',J\},K',m'}a^{(K)}_{\{\mathbf{R},I\},m}a^{(K')}_{\{\mathbf{R}',J\},m'}\Big]+\ldots. \qquad (1)$$

In a molecular crystal we distinguish different types of motions K: translational vibrations, $K=T$, and librations, $K=L$. The operator $a^{(K)\dagger}_{\{\mathbf{R},I\},m}$ denotes a MF excitation operator from the ground state to state m of type of motion K for the molecule of sublattice I in the unit cell with origin at position $\mathbf{R}$. The operator $a^{(K)}_{\{\mathbf{R},I\},m}$ denotes a MF de-excitation operator. The coefficients k in Eq. (1) can be determined by comparing matrix elements calculated with the exact form of the operator $\hat{O}$ with the matrix elements over the right-hand-side of Eq. (1). An operator that has been written already in the form of Eq. (1) in the RPA formalism is the crystal Hamiltonian. Thermodynamic averages $\langle\hat{O}\rangle$ are obtained by calculating the thermodynamic averages of the various terms in the right-hand-side of Eq. (1) and then summing. The number of terms that have to be summed is always limited in practice. For example, if $\hat{O}$ is a one-particle operator and there is only one type of motion then the right-hand-side of Eq. (1) contains only a constant term, linear terms and quadratic terms of the form $a^{(K)\dagger}_{\{\mathbf{R},I\},m}a^{(K)}_{\{\mathbf{R},I\},m'}$. Furthermore, one may neglect terms whose contributions to $\langle\hat{O}\rangle$ are small. This may even be advisable because it simplifies the calculations.

Thermodynamic averages of (products of) MF (de)excitation operators are more readily calculated when the MF (de)excitation operators are adapted to the translation symmetry of the crystal. We therefore define

$$a^{(K)\dagger}_{\mathbf{q},I,m}\equiv\frac{1}{\sqrt{N}}\sum_{\mathbf{R}}e^{i\mathbf{q}\cdot\mathbf{R}}a^{(K)\dagger}_{\{\mathbf{R},I\},m}, \qquad (2)$$

with N being the number of unit cells, and $\mathbf{q}$ a wave vector from the first Brillouin zone. Rewriting Eq. (1) in terms of these translation symmetry adapted operators, shows that we obtain (multiple) integrations over the Brillouin zone. These integrations can be reduced somewhat by using the translation symmetry of the crystal. For example, instead of the one-particle operator $\hat{O}(\{\mathbf{R},I\})$ working on molecule $\{\mathbf{R},I\}$, we take $N^{-1}\sum_{\mathbf{R}}\hat{O}(\{\mathbf{R},I\})$. Because of the translation symmetry the thermodynamic averages of both operators are the same, but there is one integration over the Brillouin zone less for the latter operator. Such a reduction can be obtained for any operator.

We can thus calculate thermodynamic averages of an operator $\hat{O}$ if we know the thermodynamic averages of (products of) translation-symmetry adapted MF (de)excitation operators. In order to obtain the latter we use the RPA ansatz in which we solve the equation of motion

$$\left[H, c_{\mathbf{q}i}\right] = \hbar\omega_{\mathbf{q}i} c_{\mathbf{q}i}, \tag{3}$$

for the excitation operators of the crystal

$$c_{\mathbf{q}i} = \sum_j \left(C_{ij} a^\dagger_{\mathbf{q}j} + \tilde{C}_{ij} a_{-\mathbf{q}j} \right), \tag{4}$$

with H the Hamiltonian of the crystal. We use the boson commutation relations obeyed by the MF (de)excitation operators (as explained below). In order to simplify our notation we have condensed in Eq. (4) the indices K, I and m of the MF (de)excitation operators into one index j. The operators $c_{\mathbf{q}i}$ are the crystal excitation operators that correspond to the collective excitations of the crystal with frequencies $\omega_{\mathbf{q}i}$. We note that the second index of $c_{\mathbf{q}i}$ adopts twice as many values as the second index of the MF (de)excitation operators. The reason for this is that $c_{\mathbf{q}i}$ can correspond to an excitation ($\hbar\omega_{\mathbf{q}i} > 0$) or a de-excitation ($\hbar\omega_{\mathbf{q}i} < 0$). The coefficients C_{ij} and $\tilde{C}_{ij}$ form the eigenvectors of the RPA matrix. Together, they form a square non-singular matrix.

Following Wallace[3] we can derive a very useful relation from Eq. (3). Repeatingly using Eq. (3) yields

$$\begin{aligned} c_{\mathbf{q}i} e^{-\beta H} &= \sum_{n=0}^{\infty} \frac{(-\beta)^n}{n!} c_{\mathbf{q}i} H^n \\ &= \sum_{n=0}^{\infty} \frac{(-\beta)^n}{n!} (H - \hbar\omega_{\mathbf{q}i})^n c_{\mathbf{q}i} \\ &= e^{\beta\hbar\omega_{\mathbf{q}i}} e^{-\beta H} c_{\mathbf{q}i}, \end{aligned} \tag{5}$$

where $\beta = (kT)^{-1}$; k being the Boltzmann constant and T the temperature. From this we can deduce the following relation for thermodynamic averages.

$$\begin{aligned} \left\langle \hat{A} c_{\mathbf{q}i} \right\rangle &= \frac{1}{Z} \mathrm{Tr}\left[e^{-\beta H} \hat{A} c_{\mathbf{q}i} \right] \\ &= e^{\beta\hbar\omega_{\mathbf{q}i}} \frac{1}{Z} \mathrm{Tr}\left[e^{-\beta H} c_{\mathbf{q}i} \hat{A} \right] \\ &= e^{\beta\hbar\omega_{\mathbf{q}i}} \left\langle c_{\mathbf{q}i} \hat{A} \right\rangle, \end{aligned} \tag{6}$$

where Z is the partition function, and $\hat{A}$ an arbitrary operator. Subtracting $\langle c_{\mathbf{q}i}\hat{A}\rangle$ from both sides of Eq. (6) we obtain Wallace's equation

$$\langle[\hat{A}, c_{\mathbf{q}i}]\rangle = \left(e^{\beta\hbar\omega_{\mathbf{q}i}} - 1\right)\langle c_{\mathbf{q}i}\hat{A}\rangle. \tag{7}$$

Now substituting Eq. (4) we obtain

$$\begin{aligned}\sum_j \left\{C_{ij}\langle[\hat{A}, a^\dagger_{\mathbf{q}i}]\rangle + \tilde{C}_{ij}\langle[\hat{A}, a_{-\mathbf{q}i}]\rangle\right\} \\ = \left(e^{\beta\hbar\omega_{\mathbf{q}i}} - 1\right)\sum_j \left\{C_{ij}\langle a^\dagger_{\mathbf{q}i}\hat{A}\rangle + \tilde{C}_{ij}\langle a_{-\mathbf{q}i}\hat{A}\rangle\right\}.\end{aligned} \tag{8}$$

which, as we shall demonstrate, enables us to calculate any thermodynamic average that we want. The coefficients C_{ij} and $\tilde{C}_{ij}$ are known from the normal RPA calculations, Eqs. (3) and (4). Thus we can look upon Eq. (8) as a set of linear equations for the thermodynamic averages on the right-hand-side. These averages can then be expressed in terms of the thermodynamic averages on the left-hand-side. If we substitute a product of n MF (de)excitation operators for $\hat{A}$ in Eq. (8) then we get, using the boson commutation relations in the left-hand-side, products of $n-1$ MF (de)excitation operators on the left and products of $n+1$ MF (de)excitation operators on the right-hand-side. So, Eq. (8) actually constitutes a recursion formula which can be applied to calculate the thermodynamic average of any product of MF (de)excitation operators.

In order to obtain $\langle a^\dagger_{\mathbf{q}i}\rangle$ and $\langle a_{\mathbf{q}i}\rangle$ we substitute the identity operator for $\hat{A}$ in Eq. (8). The left-hand-side then becomes zero, and because the coefficients C_{ij} and $\tilde{C}_{ij}$ form a non-singular matrix we find

$$\langle a^\dagger_{\mathbf{q}i}\rangle = \langle a_{\mathbf{q}i}\rangle = 0, \tag{9}$$

for all $\mathbf{q}$ and i. If we substitute a product of two MF (de)excitation operators for $\hat{A}$, then, using the boson commutation relations, the left-hand-side of Eq. (8) becomes a sum of thermodynamic averages of single MF (de)excitation operators and hence zero. Thermodynamic averages of products of three MF (de)excitation operators are thus zero too. By induction we can show that all thermodynamic averages of products of an odd number of MF (de)excitation operators are zero.

If we substitute $a_{\mathbf{q}'k}$ for $\hat{A}$ then we find

$$C_{ik}\delta_{\mathbf{q}\mathbf{q}'} = \left(e^{\beta\hbar\omega_{\mathbf{q}i}} - 1\right)\sum_j \left\{C_{ij}\langle a^\dagger_{\mathbf{q}i}a_{\mathbf{q}'k}\rangle + \tilde{C}_{ij}\langle a_{-\mathbf{q}i}a_{\mathbf{q}'k}\rangle\right\}. \tag{10}$$

We note that unless $\mathbf{q} = \mathbf{q}'$ again all thermodynamic averages on the right-hand-side become zero. Substituting $a^\dagger_{\mathbf{q}'k}$ for $\hat{A}$ we obtain

$$-\tilde{C}_{ik}\delta_{-\mathbf{q},\mathbf{q}'} = (e^{\beta\hbar\omega_{\mathbf{q}i}} - 1)\sum_j \left\{C_{ij}\langle a^\dagger_{\mathbf{q}i}a^\dagger_{\mathbf{q}'k}\rangle + \tilde{C}_{ij}\langle a_{-\mathbf{q}i}a^\dagger_{\mathbf{q}'k}\rangle\right\}. \quad (11)$$

Using Eqs. (10) and (11) we can calculate all thermodynamic averages of products of two MF (de)excitation operators. Those of the form $\langle a^\dagger_{\mathbf{q}i}a_{\mathbf{q}j}\rangle$, $\langle a_{\mathbf{q}i}a^\dagger_{\mathbf{q}j}\rangle$, $\langle a^\dagger_{\mathbf{q}i}a^\dagger_{\mathbf{q}j}\rangle$, and $\langle a_{\mathbf{q}i}a_{\mathbf{q}j}\rangle$ are the only ones that can be non-zero. Once these thermodynamic averages are known those of products of four MF (de)excitation operators can be calculated by substituting products of three MF (de)excitation operators for $\hat{A}$ in Eq. (8). As we will not need them in subsequent calculations we just note here that only the following can be non-zero; $\langle a^\dagger_{\mathbf{q}i}a^\dagger_{-\mathbf{q}j}a^\dagger_{\mathbf{q}'k}a^\dagger_{-\mathbf{q}'l}\rangle$, $\langle a^\dagger_{\mathbf{q}i}a^\dagger_{-\mathbf{q}j}a^\dagger_{\mathbf{q}'k}a_{\mathbf{q}'l}\rangle$, $\langle a^\dagger_{\mathbf{q}i}a^\dagger_{-\mathbf{q}j}a_{\mathbf{q}'k}a_{-\mathbf{q}'l}\rangle$, $\langle a^\dagger_{\mathbf{q}i}a_{\mathbf{q}j}a^\dagger_{\mathbf{q}'k}a_{\mathbf{q}'l}\rangle$, and permutations and/or hermitean conjugates of these.

3. Results

We have extended the calculations on α-N_2 using the theory of the previous section. A description of the MF and RPA calculations can be found in Refs. 1, 2, and 4. We have used a basis of 66 tesseral harmonics for the librations ($l_{max} = 10$), and 84 products of modified Laguerre functions and tesseral harmonics for the translational vibrations ($n_{max} = 5$). Two librational and three translational excited states per sublattice were included in RPA. The intermolecular potential was expanded up to fourth order terms inclusive in the displacement coordinates ($\alpha_{max} = 4$).[2] All results presented in this paper have been obtained using the Berns-van der Avoird potential.[5] Some calculations have been made with the potential of van der Avoird *et al.*,[6] but the results did not differ significantly enough to make a complete calculation with this complexer potential worthwhile.

Some properties of α-N_2 can be inferred directly from the phonon dispersion curves. These are the elastic constants and the Grüneisen parameters. The elastic constants can be calculated from the slopes of the acoustic modes at the centre of the Brillouin zone. We have calculated the phonon dispersion curves along the [1,0,0], the [1,1,0], and the [1,1,1] direction with cell parameter $a = 5.699$ Å. The nine acoustic modes in these directions have been fitted in the vicinity of the centre of the Brillouin zone with[7]

$$\omega^2 = A\sin^2(\tfrac{1}{2}qa) + B\sin^2(qa), \quad (12)$$

where q is a non-zero component of the wave vector $\mathbf{q}$. The elastic constants C_{11}, C_{12}, and C_{44} for a cubic crystal can be determined by equating the slope $\partial\omega/\partial q$ at $\mathbf{q} = \mathbf{0}$ from Eq. (12) to $\partial\omega/\partial q$ from the following relations.[8]

$$\rho\omega^2_{[1,0,0],1} = C_{11}q^2, \tag{13a}$$

$$\rho\omega^2_{[1,0,0],2} = \rho\omega^2_{[1,0,0],3} = C_{44}q^2, \tag{13b}$$

$$\rho\omega^2_{[1,1,0],1} = (C_{11} + C_{12} + C_{44})q^2, \tag{13c}$$

$$\rho\omega^2_{[1,1,0],2} = 2C_{44}q^2, \tag{13d}$$

$$\rho\omega^2_{[1,1,0],3} = (C_{11} - C_{12})q^2, \tag{13e}$$

$$\rho\omega^2_{[1,1,1],1} = (C_{11} + 2C_{12} + 4C_{44})q^2, \tag{13f}$$

$$\rho\omega^2_{[1,1,1],2} = \rho\omega^2_{[1,1,1],3} = (C_{11} - C_{12} + C_{44})q^2, \tag{13g}$$

where ρ is the density of α-N_2. The indices of ω denote the direction and the different modes. We have seven equations with three elastic constants as variables. We have used a least-square procedure to obtain the elastic constants. The results are shown in Table 1. The errors in Table 1 have been estimated using the errors in the least-square procedure. We note that the elastic constants we have calculated agree very well with those that have been determined experimentally. Also shown in Table 1 are the results that have been obtained with the libron-phonon coupling switched off, and with the harmonic approximation. In both cases we note that the agreement with experiment is bad. This indicates the importance of the anharmonic terms in the potential and the libron-phonon coupling.

Table 1. Elastic constants of α-N_2 (in kbar).

	Calculated			Experiment
	Harmonic	RPA		
	Ref. 9	This paper		Ref. 10
C_{11}	38.0	33.5± 0.4[a)]	28.5± 0.6	28.0
C_{12}	23.0	16.6± 0.4[a)]	22.0± 0.6	20.0
C_{44}	19.0	19.4± 0.4[a)]	13.3± 0.6	13.5

[a)] neglecting the libron-phonon coupling.

The Grüneisen parameters γ have been determined for the optical modes by simply repeating the calculations at different molar volumes and

calculating the derivatives

$$\gamma \equiv -\frac{\partial \ln \omega}{\partial \ln V} \tag{14}$$

numerically. Here V denotes the molar volume. The results are shown in Table 2. We note that our results are somewhat smaller than the other theoretical values. The experimental values have been obtained from pressure dependent measurements. According to Scott the failure of the experimental values to agree within extimated error is due to use of different equations of state data.[15]

Table 2. The Grüneisen parameters of α-N_2. If modes have the same symmetry then the one with the lower frequency is given first.

	Theory			Experiment	
	This paper	Ref. 11	Ref. 12	Refs. 12, 13	Ref. 14
E_g	1.94	2.92	2.24	2.45±0.25	1.95±0.06
T_g	1.91	3.00	2.14	2.30±0.25	1.63±0.06
T_g	1.73	3.16	1.89	1.95±0.25	1.68±0.06
A_u	2.41	3.08	2.82	-	-
T_u	2.69	3.11	2.98	-	-
E_u	2.73	3.12	3.01	-	-
T_u	2.88	3.31	3.12	-	-

The theory of the previous section has been used to calculate the cohesion energy of α-N_2. The operator for which the thermodynamic average must be calculated is the Hamiltonian of the crystal. As mentioned before, the Hamiltonian has already been written in the form of Eq. (1) with translation symmetry adapted operators, in order to determine the libron-phonon frequencies.[1] The constant term is the energy of the MF crystal ground state. There are no linear terms, and cubic and higher order terms have been neglected. Thus we have to perform only a single Brillouin zone integration. This integration has been carried out using a Gauss-Legendre quadrature scheme for all three dimensions.[16] Using the symmetry of α-N_2 we have only integrated over one octant of the Brillouin zone. Five integration points per dimension haver been chosen, yielding 125 integration points for the octant, and 1000 for the whole Brillouin zone. Due to the symmetry

again, we had actually to perform calculations only for the 55 points in the irreducible part of the Brillouin zone. The number of integration points is somewhat larger than the number of points that is normally chosen for this type of calculation.[17] We note furthermore that the integrand is a smooth function without singularities.

We have first calculated the energy of α-N_2 at $T = 0\,\mathrm{K}$ with $a = 5.699\,\text{Å}$. In the expression of the Hamiltonian we can distinguish six different types of terms. We have pure libron, pure phonon, and mixed libron-phonon terms, each of which can be divided further into terms that consist of an excitation and a de-excitation operator, and terms that consist of two excitation or two de-excitation operators. If we would neglect the terms that consist of two excitation or two de-excitation operators, then our Hamiltonian would become equivalent to a Hamiltonian of coupled harmonic oscillators. Such a Hamiltonian could be rewritten in terms of number operators of uncoupled harmonic oscillators. The energy would then consist of the energy of the MF crystal ground state plus the contribution from the occupation of the excited states. This latter contribution is always positive. Indeed, we have found that the terms with one excitation and one de-excitation operator always raise the total energy. The other terms bring correlation into the MF crystal ground state by mixing in doubly excited states. They lower the total energy. The net result is that at $T = 0\,\mathrm{K}$ and with $a = 5.699\,\text{Å}$ the energy of the ground state is lowered by $68.0\,\mathrm{J.mol^{-1}}$, which is about 1.1% of the MF energy of $-5.92\,\mathrm{kJ.mol^{-1}}$. The lowering of the ground state energy is mostly due (for about 80%) to the libron-phonon coupling. The rest comes from the pure phonon terms, whereas the pure libron terms raise the ground state energy slightly.

We have also investigated the temperature dependence of the energy. It is important to note that, although one is interested in the energy at finite temperatures, one must always make the MF calculations at $T = 0\,\mathrm{K}$. The reason for this is that RPA, and Eq. (1) for the Hamiltonian as given by Ref. 1 holds only at $T = 0\,\mathrm{K}$. Only in Eq. (8) a different temperature may be substituted. The results of the energy calculations at different temperatures is shown in Fig. 1. We have tried to find an analytic expression for the energy to fit the calculated values. Such an expression is necessary if one wants to calculate other properties from the energy. We have tried to make a least-square fit to the energy with a Debye function[18]

$$E = E_0 + 9kT\left(\frac{T}{\theta_D}\right)^3 \int_0^{\theta_D/T} \frac{x^3 dx}{e^x - 1}, \tag{15}$$

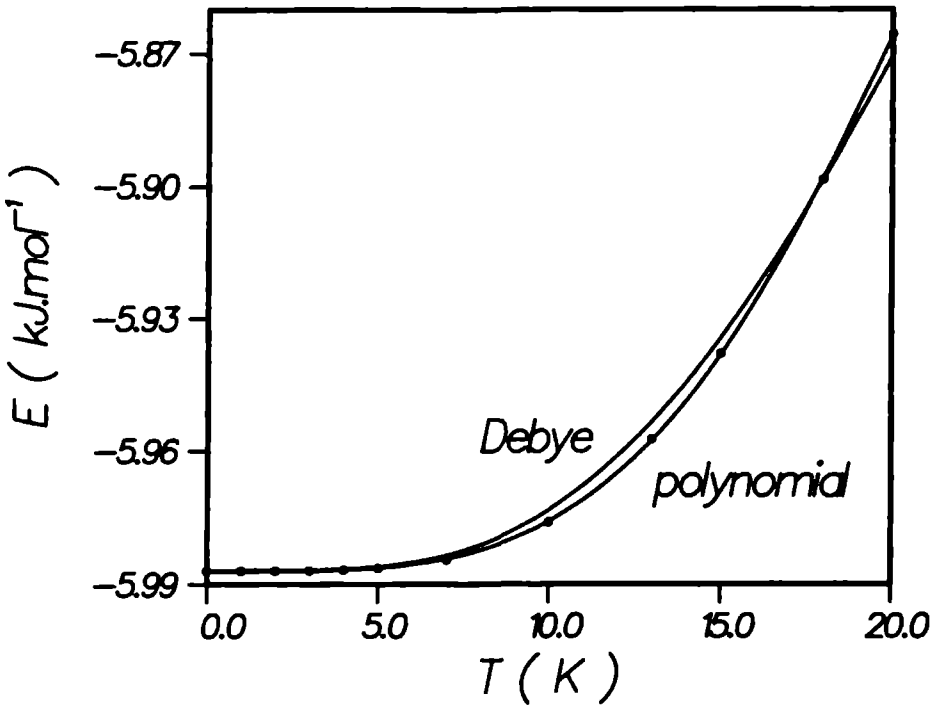

Fig. 1 The energy of α-N_2. The dots depict the calculated values. The solid lines depict the fits (see text).

where E_0 is the energy at $T = 0\,\mathrm{K}$, and θ_D the Debye temperature. Instead of the Debye function, we have also tried polynomial fits. We see in Fig. 1 that the fit with a Debye function is not very good. The curve that is shown in Fig. 1 corresponds to a Debye temperature $\theta_D = 68.7\,\mathrm{K}$. When the energies calculated at higher temperatures are left out of the procedure the Debye temperature increases. These results agree with the experimental results of Bagatskii *et al.*.[19] They found that the specific heat could only be fitted with a Debye function at temperatures below $T = 4\,\mathrm{K}$. Burford and Graham[20] have given a corresponding Debye temperature $\theta_D = 83.5\,\mathrm{K}$. They also found that the Debye temperature rapidly decreases when the temperature increases. The other curve in Fig. 1 corresponds to a fit with a polynomial of sixth order and only even powers of the temperature. The error in the fit is about $0.5\,\mathrm{J.mol^{-1}}$ over the range of temperatures shown. As the latter fit is quite good, it is this fit that has been used in subsequent calculations.

If one knows the energy as a function of the molar volume and the temperature, it is possible to calculate other thermodynamic properties.

We have therefore calculated the energy for three different molar volumes, and represented the energy dependence on the molar volume as a quadratic function. It was too expensive to use more then three molar volumes because each molar volume takes about $2\frac{1}{2}$ hours CPU-time on a NAS-9060 computer. The functional form in which we have expressed the energy is thus

$$E = \sum_{m=0}^{2} \sum_{n=0}^{3} e_{mn} V^m T^{2n}, \tag{16}$$

where e_{mn} are coefficients. Using this expression, it is quite easy to express the free energy as a polynomial in the molar volume and the temperature. We can determine the coefficients of that polynomial, using

$$E = A - T \left(\frac{\partial A}{\partial T} \right)_V, \tag{17}$$

and $(\partial A/\partial T)_V = 0$ at $T = 0\,\mathrm{K}$, which follows readily from the definition of the free energy

$$A = -\beta^{-1} \ln \mathrm{Tr} \left[e^{-\beta H} \right]. \tag{18}$$

The expression for the entropy follows from $A = E - TS$.

Before we can determine how some thermodynamic properties change with temperature, we need to know the molar volume of α-N_2 as a function of temperature. We therefore determine the minimum of the free energy for all temperatures. The result for $T = 0\,\mathrm{K}$ is $a = 5.6875\,\text{Å}$. The cell parameter decreases slightly to $5.6856\,\text{Å}$ when the temperature is raised to $T = 14\,\mathrm{K}$, and then increases more rapidly to $5.6870\,\text{Å}$ at $T = 20\,\mathrm{K}$. These calculated values of the cell parameter are slightly closer to the experimental values ($a = 5.644\,\text{Å}$ at $T = 15\,\mathrm{K}$)[10] than the MF result $a = 5.699\,\text{Å}$ at $T = 0\,\mathrm{K}$. However, the temperature dependence is clearly incorrect. As we will show in the next section this is a consequence of the fit Eq. (16). Although there is an obvious error in the calculated cell parameters we will nevertheless use it as the cell parameter at which the other properties will be calculated. We will show that this error has only a minor influence on most of these properties.

The next thermodynamic property that is easy to calculate is the specific heat c_V, defined as[21]

$$c_V \equiv \left(\frac{\partial E}{\partial T} \right)_V. \tag{19}$$

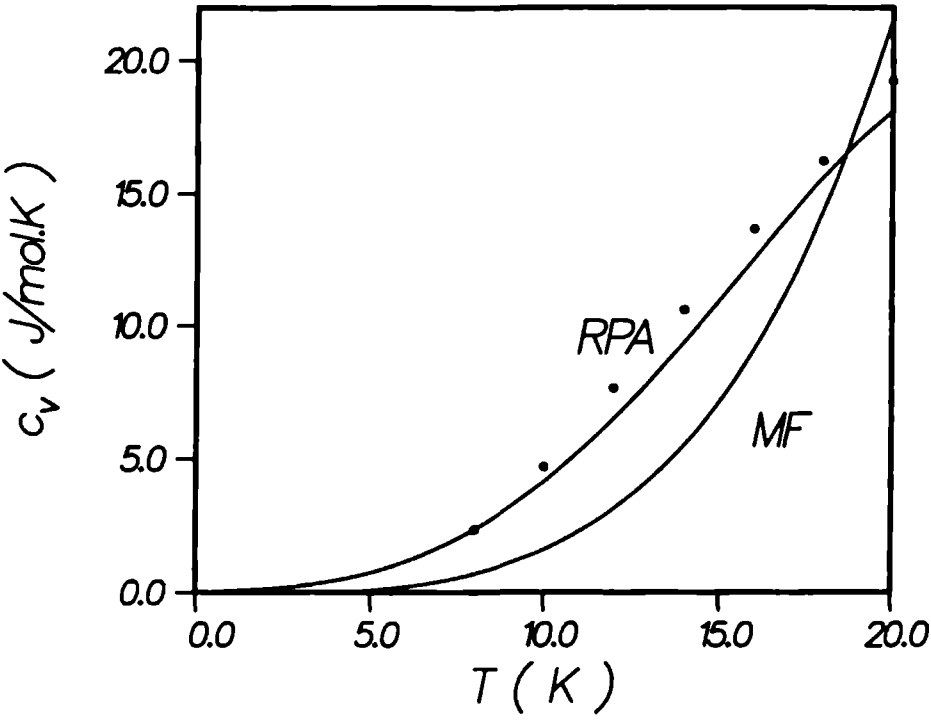

Fig. 2 The specific heat of α-N_2. The dots depict the experimental values of Ref. 15. The solid lines depict results from calculations (see text).

The results of the calculations are shown in Fig. 2. For low temperatures they are in good agreement with experiment. The RPA results are much better than the MF results, which shows that the extension to RPA described in the previous sections is a substantial improvement to MF.

It is somewhat more difficult to obtain the isothermal compressibility κ_T and the expansion coefficient α. They are defined by[21]

$$\kappa_T \equiv -\frac{1}{V}\left(\frac{\partial V}{\partial p}\right)_T, \tag{20}$$

and

$$\alpha \equiv \frac{1}{V}\left(\frac{\partial V}{\partial T}\right)_p, \tag{21}$$

where p is the pressure. In order to obtain these properties we have to transform the right-hand-sides of Eqs. (20) and (21) to derivatives of functions that have the molar volume and the temperature as variables.[18] The

resulting expressions are

$$\kappa_T = -\frac{1}{V}\left[\left(\frac{\partial p}{\partial V}\right)_T\right]^{-1}, \tag{22}$$

and

$$\alpha = -\frac{1}{V}\left[\left(\frac{\partial p}{\partial T}\right)_V \Big/ \left(\frac{\partial p}{\partial V}\right)_T\right]. \tag{23}$$

The pressure can be determined from the free energy using

$$p \equiv -\left(\frac{\partial A}{\partial V}\right)_T. \tag{24}$$

Of course, because the cell parameter decreases with increasing temperature the expansion coefficient is negative. A comparison with experimental values is thus not sensible. Calculated values for the compressibility are shown in Table 3. We note that the RPA values show an incorrect temperature dependence. The MF results seem to be better (the MF results become even better if we use the potential of van der Avoird *et al.*).[6]

Table 3. The isothermal compressibility of α-N_2 (in $10^{-10}\,m^2.N^{-1}$).

	Theory		Experiment
T (K)	MF	RPA	Ref. 22
0	5.05	3.96	-
5	5.04	3.77	-
10	5.05	3.39	4.64
20	5.14	2.77	4.82

4. Discussion and conclusions

We have calculated a number of properties of α-N_2 using RPA. A few of these properties could be calculated using the RPA formalism as it has been described in previous papers. Most of the properties, however, have been determined via an extension of RPA. We have chosen α-N_2 as the system to test this extension of RPA, as this crystal has been studied exhaustively, both experimentally and theoretically. There is much experimental data

available to benchmark a new theory. Furthermore, there is a good intermolecular potential so that there is little danger of attributing errors to the potential which are due to the theory and vice versa.

The results that have been presented in the previous section are fairly good on the whole. Where a comparison with MF theory was possible, the RPA results are mostly closer to the experimental values. However, there are still some obvious faults. In order to understand the origin of these faults, it is advisable to group the calculated properties. The libron-phonon frequencies and the energy can be obtained directly from the RPA formalism or its extension. As shown in a previous paper the libron-phonon frequencies are in good agreement with experiment.[1] The energy of the crystal at $T = 0\,\mathrm{K}$ (see Fig. 1) deviates by 13% from the experimental value of $-6.9\,\mathrm{kJ.mol^{-1}}$.[15] This, however, is probably due to the intermolecular potential (cf. results with the potential of van der Avoird *et al.* which are considerably better),[6] and the absence of three-particle terms in the Hamiltonian. The temperature dependence in RPA, on the other hand, differs from the temperature dependence in MF and seems to be quite accurate (see below).

The elastic constants and the specific heat are obtained from the libron-phonon frequencies and the energy, respectively, by a single differentiation. The results for these two properties are very good, indicating that the results for the libron-phonon frequencies and the energy, and hence the RPA formalism, are good.

The calculations of the cell parameter, the expansion coefficient, and the isothermal compressibility involve the free energy and derivatives with respect to the molar volume. The results for these properties are inaccurate. The main reason for this is the inaccuracy of the fit for the energy that was used to obtain the free energy. We have mentioned before that the error in the fit is only about $5 \cdot 10^{-4}\,\mathrm{kJ.mol^{-1}}$. This is small compared to the difference of the energy at $T = 0\,\mathrm{K}$ and $T = 20\,\mathrm{K}$, which is about $0.12\,\mathrm{kJ.mol^{-1}}$. But it is large compared to the variation in the energy at $T = 0\,\mathrm{K}$ between $a = 5.659\,\text{Å}$ and $a = 5.699\,\text{Å}$, which is only about $8 \cdot 10^{-3}\,\mathrm{kJ.mol^{-1}}$. Derivatives with respect to the molar volume will therefore be inaccurate. We can calculate the cell parameter at $T = 0\,\mathrm{K}$ also directly from the energy. We then find $a = 5.6875\,\text{Å}$, which is the same value that we have obtained from the fit. It is not very clear how accurate the isothermal compressibility is. It can again be calculated directly from the energy at $T = 0\,\mathrm{K}$. We thus obtain $\kappa_T = 4.03 \cdot 10^{-10}\,\mathrm{m^2.N^{-1}}$, which does not differ much from the value obtained from the fit. In MF theory

the situation is better, because one can calculate the free energy just as easily as the energy. One does not need to use Eqs. (16) and (17), and hence one does not introduce errors by a fit.

A question of a fundamental nature is at what temperature is it still allowed to apply the extended RPA method. We see in Fig. 2 that the error in the specific heat increases when $T = 20\,\mathrm{K}$ is approached. By using Eq. (3) it is implicitly assumed that the excited levels form ladders, as the excited states of harmonic oscillators. Indeed, the RPA method is exact at all temperatures for a system with harmonic interactions. On the other hand, we have found for a spin system (α-O_2), where the "ladders" consist of only two steps, that results become bad when the excited states become occupied. We therefore think that the extended RPA method gives reasonable results as long as the states that do not fit into a level scheme of (coupled) harmonic oscillators are not appreciably occupied. We have found that for α-N_2 the results deteriorate above $T = 20\,\mathrm{K}$. Beyond that temperature two-libron states become occupied.

In order to test the RPA formalism further it is necessary to apply it to other systems and to calculate thermodynamic averages of other operators. It would be most interesting to use the extended RPA method to calculate correlation functions; especially for orientationally disordered molecular crystals. For example, application to solid hydrogen at various pressures might lead to some new results.[23]

Acknowledgments

This investigation was supported in part by the Netherlands Foundation for Chemical Research (S.O.N.) with financial aid from the Netherlands Organization for the Advancement of Pure Research (Z.W.O.).

References

[1] W.J. Briels, A.P.J. Jansen, and A. van der Avoird, J. Chem. Phys. **81**, 4118 (1984).

[2] A.P.J. Jansen and A. van der Avoird, J. Chem. Phys. **86**, 3583 (1987).

[3] D.C. Wallace, Phys. Rev. **152**, 261 (1966).

[4] W.J. Briels, A.P.J. Jansen, and A. van der Avoird, Adv. Quant. Chem. **18** 131 (1986).

[5] R.M. Berns and A. van der Avoird, J. Chem. Phys. **72**, 6107 (1980).

[6] A. van der Avoird, P.E.S. Wormer, and A.P.J. Jansen, J. Chem. Phys. **84**, 1629 (1985).

[7] T. Luty (private communication).
[8] C. Kittel, *Introduction to Solid State Physics* (Wiley, New York, 1953).
[9] B. Kuchta, Mol. Phys. **52**, 795 (1984).
[10] J.K. Kjems and G. Dolling, Phys. Rev. B**24**, 2567 (1981).
[11] A. Zunger and E. Huler, J. Chem. Phys. **62**, 3010 (1975)
[12] V. Chandrasekharan, D. Fabre, M.M. Thiéry, E. Uzan, M.C.A. Donkersloot, and S.H. Walmsley, Chem. Phys. Lett. **26**, 284 (1974).
[13] M.M. Thiéry, D. Fabre, M. Jean-Louis, and H. Vu, J. Chem. Phys. **59**, 4559 (1973)
[14] F.D. Medina and W.B. Daniels, J. Chem. Phys. **64**, 150 (1976)
[15] T.A. Scott, Phys. Rep. **27**, 89 (1976).
[16] R.F. Churchhouse, *Numerical Methods*, Vol. III of *Handbook of Applicable Mathematics*, edited by W. Ledermann (Wiley, Chichester, 1981).
[17] T. Luty, A. van der Avoird, R.M. Berns, and T. Wasiutynski, J. Chem. Phys. **75**, 1451 (1981)
[18] L.D. Landau and E.M. Lifshitz, *Statistical Physics* (Pergamon Press, London, 1959).
[19] M.I. Bagatskii, V.A. Kucharyany, V.G. Manzhelii, and V.A. Popov, Phys. Stat. Sol. **26**, 453 (1968).
[20] J.C. Burford and G.M. Graham, Can. J. Phys. **47**, 23 (1969).
[21] K. Huang, *Statistical Mechanics* (Wiley, New York, 1963).
[22] D.C. Heberlein, E.D. Adams, and T.A. Scott, J. Low Temp. Phys. **2**, 449 (1970).
[23] M. Sprik and M.L. Klein, J. Chem. Phys. **81**, 6207 (1984).

Chapter 3
Solid Oxygen

Magnetic coupling and dynamics in solid α and β-O_2. I. An *ab initio* theoretical approach

A P J Jansen and A van der Avoird
Institute of Theoretical Chemistry University of Nijmegen, Toernooiveld, 6525 ED Nijmegen, The Netherlands

(Received 21 July 1986, accepted 24 November 1986)

This paper describes a new approach to the dynamic and magnetic properties of solid α and β oxygen which is based on two theoretical developments First, we have constructed the lattice and spin Hamiltonian for solid O_2 by including explicitly the interactions between the triplet ground state O_2 molecules as obtained mainly from recent *ab initio* calculations The spin coupling parameters in this Hamiltonian, especially the Heisenberg exchange parameter J, are strongly dependent on the positions and orientations of the molecules Secondly, we have developed an integrated scheme for lattice dynamics and spin wave calculations which uses this Hamiltonian The actual mixing between the lattice modes, phonons and librons, and the magnons appears to be small, their interaction can be largely taken into account by renormalization of the coupling terms In the lattice dynamics part of the calculation it is essential to include the Heisenberg term, since it is the extremely strong anisotropy of the coupling parameter J that explains the anomalously large libron splitting in α-O_2 The spin-wave calculation with the Hamiltonian averaged over the lattice vibrations yields reasonable values for the magnon frequencies with no empirical fit parameters

I. INTRODUCTION

Solid oxygen is one of the most interesting molecular crystals because of its behavior as a magnetic material This behavior is due to the rather unique property of the O_2 molecule of possessing a (triplet) electronic spin momentum in its ground state In the condensed phases these spin momenta can be coupled in various ways which are related to the geometrical order of the molecules, and this leads to a very rich phase diagram [1,2] Most studies have been devoted to the α and β phases Under its own vapor pressure the α phase is stable from 0 to 23 9 K and the β phase from 23 9 to 43 8 K, but the latter phase remains stable until above room temperature at higher pressures Both these phases are structurally ordered The O_2 molecules are arranged in layers parallel to the a–b plane, see Fig 1, with their axes perpendicular to this plane In the rhombohedral β phase the order within the layers is close packed hexagonal, whereas in the monoclinic α phase the hexagons are slightly distorted The α-O_2 solid is a two-sublattice antiferromagnet, with the spins preferentially aligned parallel to the $\pm$ b axis For β-O_2 short range antiferromagnetic order in three sublattices with 120° angles between the spins has been deduced from experiment It is now generally believed that the structural distortion from the geometrically most favorable close packed β phase to the α phase is driven by the magnetic (Heisenberg exchange) interaction between the molecules, the antiferromagnetic order in α-O_2 leads to a lower magnetic (and total) energy than that in β-O_2

Many more experimental data of various kinds, optical, magnetic, and thermodynamic, have been collected on α- and β oxygen [1-7] The theoretical approaches which have been made in order to interpret these data clearly fall into two categories On the one hand, one has tried to understand the elastic and optical properties via standard harmonic lattice dynamics calculations [8-10] These calculations have ignored the open shell (triplet) character of the O_2 molecules and they have used a standard empirical atom–atom potential which is common between closed shell molecules A typical feature that cannot be explained by such calculations, despite the possible variation of the parameters in the empirical potential, is the splitting of the optical ($\mathbf{q} = 0$) libron mode which occurs at the phase transition from β-O_2 to α-O_2 Given the small structural distortion of α-O_2 with respect to β-O_2, this splitting is very large indeed (more than 30 cm^{-1}) Since the lattice dynamics calculations all gave a splitting of 10 cm^{-1} at most, it was usually assumed that the higher frequency peak in the Raman spectrum of α-O_2 corresponds with a two phonon/libron or libron–magnon transition Recent experimental data[6] seem to invalidate this assumption, however, and so the anomalously large splitting has still to be explained

On the other hand, one has interpreted the magnetic data by means of spin-wave calculations based on a pure spin Hamiltonian [3,4,11,12] The following form is generally accepted for this Hamiltonian in α-O_2

$$H_{\text{spin}} = -2 \sum_{P<P'} J_{PP'} \mathbf{S}_P \mathbf{S}_{P'} + \sum_P (AS_{x_P}^2 + BS_{y_P}^2) \qquad (1)$$

The first term is the usual Heisenberg exchange term, which couples the spins $\mathbf{S}_P$ and $\mathbf{S}_{P'}$ on the lattice sites P and P' Since this term, which is isotropic in the spin, was not sufficient to explain the experimental data, one has simply added two single particle spin terms with the anisotropy parameters A and B The first of these terms, with $A > 0$, keeps the spins preferentially directed perpendicular to the molecular axes (i e , to the c^* axis which we take to be the x axis) The second single particle term with $B > 0$ determines the preferential spin axis within the a–b plane, i e , the b axis (which we take as the z axis) The parameters $J_{PP'}$, A, and B, are

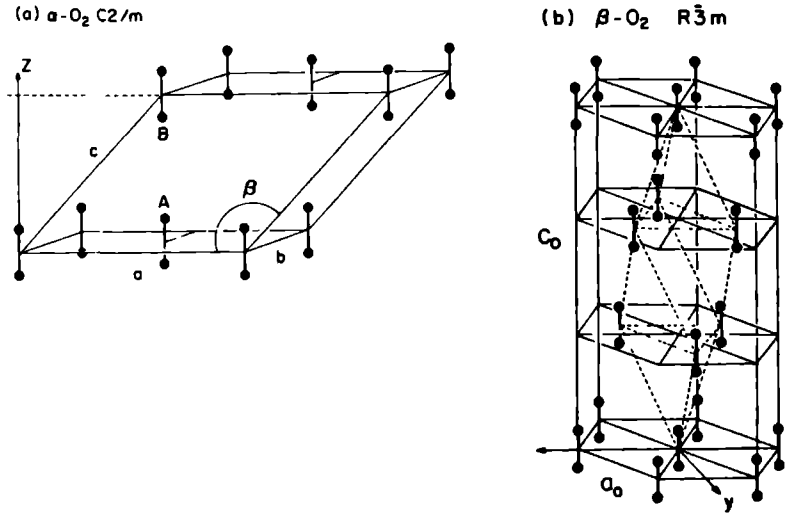

FIG 1 Crystal structures of (a) α-oxygen and (b) β-oxygen

regarded as empirical constants They must be chosen such that the properties calculated from this Hamiltonian via mean-field or spin-wave models agree with the measured data The exchange coupling constant J_{PP} is only included between nearest and next-nearest neighbors within the a–b plane and between nearest neighbors in adjacent planes, it is negative for all these pairs, i e , the coupling is antiferromagnetic In a few papers this Hamiltonian has also been applied to β-O_2 setting the in-plane anisotropy parameter B equal to zero

It will be clear from this description that the spin Hamiltonian (1) is a purely phenomenological one, it has not been derived from the properties of the interacting molecules Still, there is some justification for each of its terms The form of the Heisenberg term can be derived from first principles [11-14] The term AS_x^2 is believed to correspond to the intramolecular spin–orbit and spin–spin coupling,[15] which would indeed yield such a term for every O_2 molecule if the molecular axes are placed parallel to the x axis (the crystal c^* axis) The free molecule value of the constant A equals 5 712 K The term BS_y^2 is believed to originate from the magnetic dipole–dipole interactions between the triplet spins of the O_2 molecules The only justification for this term is that it leads to the same preferred magnetization direction (parallel to the z axis or crystal b axis) as a classical dipole–dipole interaction model, with the correct order of magnitude for the anisotropy parameter B

The treatments based on the phenomenological spin Hamiltonian (1) are unsatisfactory, however, in that they have led to very different sets of parameters J_{PP} , A, and B when the results were fitted to different experimental data This is most clearly demonstrated in DeFotis's review[3] which contains parameters from various papers that vary by an order of magnitude Although it is argued in a recent paper[4] that the results are becoming more consistent if the appropriate corrections are made, it is typical that even there the empirical values of A and B are only half the "free molecule" values In view of the small distortions of the molecular charge distributions[16] by the weak van der Waals interactions in solid O_2, this is hard to explain (at least at low pressures) Moreover, we find it very unsatisfactory that the Hamiltonian (1) represents the magnetic dipole–dipole interactions between pairs of molecules P and P' by a single particle term

From the stability considerations on the α–β phase transition it is obvious that structural changes and the magnetic coupling are strongly related in solid O_2 In some recent theoretical treatments of this phase transition[9,10,17] one has included the dependence of the Heisenberg coupling parameter J_{PP} on the distance R_{PP} between the molecules, as derived from temperature and pressure dependent measurements [18,19] From *ab initio* electronic structure calculations in our institute[20,21] the same distance dependence has been obtained, but it has been found, moreover, that J_{PP} depends very sensitively on the orientations of the molecules P and P' This being the case, the Heisenberg spin operator depends strongly on the displacements of the molecules in the lattice, both translational and orientational, and it is no longer justified *a priori* to perform separate lattice dynamics and spin-wave calculations

In a recent communication[22] it was announced that we have developed an integrated lattice dynamics and spin-wave scheme which includes the coupling between phonons, librons, and magnons This scheme starts from a Hamilto-

nian which is based on first principles The spin-independent potential V_{PP} in this Hamiltonian and the geometry dependent Heisenberg coupling parameters J_{PP} have been obtained from quantum chemical *ab initio* calculations Also the geometry dependence of the coupling parameter A in Eq (1) is explicitly included and the last term from Eq (1) is replaced by the exact two-particle operator for the magnetic dipole–dipole interactions The results of this approach are mostly in good agreement with experimental data, without any fitting of empirical parameters However, this approach does not only provide, from first principles, results which can be compared with measurements, it also offers a physical explanation of some of the observed phenomena In the present paper, this new approach is more fully presented and its results are discussed

II. THEORY

A. The spin-dependent intermolecular potential and the Hamiltonian of solid O_2

The interactions between ground state $^3\Sigma_g^-$ O_2 molecules depend on the coupling between their triplet electronic spin momenta So, for example, if we take a pair of O_2 molecules the two triplets can couple to a singlet, a triplet, or a quintet Neglecting in first instance the spin–orbit coupling and the magnetic dipole interactions, each of these three dimer spin states leads to its own potential surface It is in fact by calculating the three potential surfaces for an O_2–O_2 dimer that the leading terms in the spin-dependent O_2–O_2 potential have been obtained [20,21] The exchange interactions, in particular, cause the energy separation between the three surfaces It has been found from the *ab initio* calculations that the three O_2–O_2 potential surfaces can be accurately represented by the following expression

$$V(\mathbf{r}_{PP},\omega_P,\omega_P) - 2J(\mathbf{r}_{PP},\omega_P,\omega_P)\mathbf{S}_P\,\mathbf{S}_P \qquad (2)$$

The first, spin-independent, potential is the (multiplicity weighted) average of the $S=0$, 1, and 2 potential surfaces The second, Heisenberg, term accurately describes the splitting between the three surfaces The latter result implies that the quintet–triplet splitting is almost exactly twice the triplet–singlet splitting, for any geometry of the O_2–O_2 dimer in the van der Waals distance range The geometry of the dimer is characterized in an arbitrary system of axes by the vector $\mathbf{r}_{PP'} = \mathbf{r}_{P'} - \mathbf{r}_P$, with $\mathbf{r}_P$ and $\mathbf{r}_{P'}$ describing the center of mass positions of the molecules P and P', and by the polar angles $\omega_P = (\theta_P,\phi_P)$ and $\omega_{P'} = (\theta_{P'},\phi_{P'})$ describing the orientations of both molecules

Thus it has been found that the Heisenberg coupling parameter $J_{PP'}$ depends on the positions and orientations of the molecules P and P', just as the spin-independent potential $V_{PP'}$ Actually, the anisotropy of the parameter $J_{PP'}$ is much stronger even than the anisotropy of $V_{PP'}$ The orientational dependence of both these quantities can be explicitly expressed by the expansions

$$V(\mathbf{r}_{PP'},\omega_P,\omega_{P'}) = (4\pi)^{1/2}\sum_{L_A L_B L} v_{L_A L_B L}(r_{PP'})A_{L_A L_B L}(\hat{r}_{PP'},\omega_P,\omega_{P'}),$$

$$J(\mathbf{r}_{PP'},\omega_P,\omega_{P'}) = (4\pi)^{1/2}\sum_{L_A L_B l} J_{L_A L_B l}(r_{PP'})A_{L_A L_B l}(\hat{r}_{PP'},\omega_P,\omega_{P'}) \qquad (3)$$

in the complete orthonormal set of angular functions

$$A_{L_A L_B l}(\hat{r}_{PP'},\omega_P,\omega_{P'}) = \sum_{M_A M_B M}\begin{pmatrix} L_A & L_B & L \\ M_A & M_B & M\end{pmatrix} \times Y^{(L_A)}_{M_A}(\omega_P)\,Y^{(L_B)}_{M_B}(\omega_{P'})\,Y^{(l)}_{M}(\hat{r}_{PP'}) \qquad (4)$$

with $\hat{r}_{PP'}$ denoting the polar angles $(\Theta_{PP'},\Phi_{PP'})$ of the vector $\mathbf{r}_{PP'}$ The symbol in large brackets is a 3j coefficient and $Y^{(l)}_m(\theta,\phi)$ are normalized spherical harmonics [17] All the physical information is contained in the expansion coefficients The coefficients $v_{L_A L_B l}(r_{PP'})$ contain long range $r_{PP'}^{-n}$ contributions from electrostatic multipole interactions ($n = 5$, 7, 9, etc) and from dispersion interactions ($n = 6$, 8, 10), as well as short range (overlap) contributions from exchange and charge penetration effects which depend exponentially on $r_{PP'}$ The Heisenberg expansion coefficients $J_{L_A L_B l}(r_{PP'})$ are exponential functions of $r_{PP'}$ as they are generated purely by exchange effects Most of the contributions to the coefficients $v_{L_A L_B L}(r_{PP'})$ and the complete coefficients $J_{L_A L_B L}(r_{PP'})$ have been explicitly calculated by *ab initio* quantum chemical methods [7] Therefore, we can directly use Eqs (3) and (4) as an analytical spin-dependent O_2–O_2 potential The observation that the Heisenberg parameter $J_{PP'}$ is more strongly anisotropic than the spin-independent potential $V_{PP'}$ is reflected by the slower convergence of its spherical expansion (3) It has been found[21] in particular that the coefficient $J_{L_A L_B L}$ with $L_A = L_B = 4$ and $L = 8$ is even larger than the isotropic $L_A = L_B = L = 0$ contribution for most distances of interest This is related to the nodal character of the antibonding π_g orbitals in the O_2 molecules which contain the unpaired electrons that couple to the $^3\Sigma_g^-$ ground states

If we wish to write down the complete spin-dependent potential for a pair of interacting O_2 molecules we have to add the effects of spin–orbit and magnetic dipole (spin–spin) coupling It is well known[15] that in the free O_2 molecule the effects of spin–orbit and spin–spin coupling in the electronic ground state can be represented by the following operator

$$\sum_{m m'} A_{m\ m'}(\omega)S_m S_{m'}\begin{pmatrix} 1 & 1 & 2 \\ m & m' & -m-m'\end{pmatrix}, \qquad (5)$$

where $\omega = (\theta,\phi)$ describes the orientation of the molecular axis, $A_m(\omega)$ is a second rank tensor

$$A_m(\omega) = \tfrac{1}{3}A\sqrt{30}C^{(2)}_m(\omega), \qquad (6)$$

$C^{(2)}_m(\theta,\phi)$ is a Racah spherical harmonic [18] and S_m with $m = -1$, 0, 1 are the spherical components of the spin operator $\mathbf{S}$ Equation (5) expresses the coupling between the direction of the triplet spin momentum $\mathbf{S}$ and the direction of the molecular axis in a general coordinate frame For a free O_2 molecule the coupling constant A equals 3 96 cm^{-1} = 5 712 K, but also in van der Waals complexes of O_2 with

rare gas atoms very nearly the same value of A has been found [24,25]. So, we can include the intramolecular spin–orbit and spin–spin interactions by writing a single-particle operator of the form (5) for every O_2 molecule P. In addition we include the magnetic dipole–dipole (spin–spin) interactions between the triplet magnetic momenta $g_e \mu_B \mathbf{S}_P$ and $g_e \mu_B \mathbf{S}_{P'}$ of different molecules P and P', with $g_e = 2.0023$ and μ_B being the Bohr magneton. These interactions can be written as follows

$$\sum_{m m'} T_{-m-m'}(\mathbf{r}_{PP'}) S_{m P} S_{m' P'} \begin{pmatrix} 1 & 1 & 2 \\ m & m' & -m-m' \end{pmatrix} \quad (7)$$

with the magnetic dipole–dipole interaction tensor

$$T_m(\mathbf{r}_{PP'}) = -\sqrt{30} g_e^2 \mu_B^2 r_{PP'}^{-3} C_m^{(2)}(\hat{r}_{PP'}) \quad (8)$$

and the spin momenta $\mathbf{S}_P$ and $\mathbf{S}_{P'}$ expressed in spherical components [23].

Combining all the spin-dependent interactions we can write the complete spin Hamiltonian for solid O_2

$$\begin{aligned} H_{\text{spin}} = & -2 \sum_{P<P'} J(\mathbf{r}_{PP'}, \omega_P, \omega_{P'}) \mathbf{S}_P \mathbf{S}_{P'} \\ & + \sum_P \sum_{m m'} A_{-m m'}(\omega_P) S_{m P} S_{m' P} \\ & \times \begin{pmatrix} 1 & 1 & 2 \\ m & m' & -m-m' \end{pmatrix} \\ & + \sum_{P<P'} \sum_{m m'} T_{-m-m'}(\mathbf{r}_{PP'}) S_{m P} S_{m' P'} \\ & \times \begin{pmatrix} 1 & 1 & 2 \\ m & m' & -m-m' \end{pmatrix} \end{aligned} \quad (9)$$

This Hamiltonian has been derived from first principles and it applies to any phase of solid O_2 (and to the liquid). It has three terms just as the phenomenological spin Hamiltonian (1). All the spin coupling parameters in this new Hamiltonian (9) are dependent on the molecular positions $\mathbf{r}_P$ and orientations ω_P, however, and the last single particle anisotropic spin term in Eq. (1) has been replaced by a two-body operator.

The dependence of the spin Hamiltonian on the molecular positions and orientations, which is explicitly given by Eqs. (3)–(8), will couple the spin waves (magnons) to the lattice vibrations (phonons and librons). In order to calculate this coupling we need the complete lattice and spin Hamiltonian. This Hamiltonian reads as follows

$$H = H_{\text{ll}} + H_{\text{spin}} \quad (10)$$

with H_{spin} given by Eq. (9) and

$$H_{\text{ll}} = \sum_P T(\mathbf{r}_P) + \sum_P L(\omega_P) + \sum_{P<P'} V(\mathbf{r}_{PP'}, \omega_P, \omega_{P'}) \quad (11)$$

The latter Hamiltonian is ordinarily used in lattice dynamics calculations. It contains the kinetic energy terms for the translational and librational motions of the molecules

$$\begin{aligned} T(\mathbf{r}_P) &= -\frac{\hbar^2}{2M} \nabla^2(\mathbf{r}_P), \\ L(\omega_P) &= -\frac{\hbar^2}{2I} l^2(\omega_P) \end{aligned} \quad (12)$$

with M and I being the molecular mass and moment of inertia, respectively, and $\nabla(\mathbf{r}_P)$ and $\mathbf{l}(\omega_P)$ being the gradient and angular momentum operators. The spin-independent potential V has already been specified in Eqs. (2) and (3).

One more preparatory job has still to be performed before we can actually make lattice dynamics and spin-wave calculations with the Hamiltonian (10). All the two-body terms in Eqs. (9) and (11) contain the vector $\mathbf{r}_{PP'}$ as a variable, i.e., the difference vector of the instantaneous position vectors $\mathbf{r}_P$ and $\mathbf{r}_{P'}$. In lattice dynamics one has to know the potential explicitly as a function of the molecular displacements $\mathbf{u}_P = \mathbf{r}_P - \mathbf{R}_P$ from their equilibrium positions $\mathbf{R}_P$. This problem can be solved by expanding all functions depending on $\mathbf{r}_{PP'}$ as a double Taylor series in $\mathbf{u}_P$ and $\mathbf{u}_{P'}$, including harmonic (second order) as well as anharmonic (higher order) terms. In practice this is not simple but the procedure has been completely described in Ref. 26. Alternative procedures can be thought of, in principle, as long as they yield the potential explicitly as a function of $\mathbf{u}_P$ and $\mathbf{u}_{P'}$. So, from here on we will assume that all the terms in the potential that depend on $\mathbf{r}_{PP'}$ are now dependent on $\mathbf{u}_P$ and $\mathbf{u}_{P'}$. If we had applied the usual formalism for lattice dynamics calculations, i.e., the harmonic or quasiharmonic method, then a similar expansion for the angular displacements should have been made. By using a new method developed in our institute,[26–29] which is valid also for large amplitude librations, we avoid this problem.

We end this section by writing the different terms in the potential in a form that clearly shows on which variables they depend and, moreover, is convenient for use in the next section

$$\begin{aligned} V_{PP'} &= V(\mathbf{u}_P, \omega_P, \mathbf{u}_{P'}, \omega_{P'}) = V(\mathbf{r}_{PP'}, \omega_P, \omega_{P'}), \\ W_{PP'} &= W(\mathbf{u}_P, \omega_P, \mathbf{S}_P, \mathbf{u}_{P'}, \omega_{P'}, \mathbf{S}_{P'}) \\ &= -2J(\mathbf{r}_{PP'}, \omega_P, \omega_{P'}) \mathbf{S}_P \mathbf{S}_{P'}, \\ X_P &= X(\omega_P, \mathbf{S}_P) = \sum_{m m'} A_{-m-m'}(\omega_P) S_{m P} S_{m' P} \\ & \quad \times \begin{pmatrix} 1 & 1 & 2 \\ m & m' & -m-m' \end{pmatrix}, \\ Y_{PP'} &= Y(\mathbf{u}_P, \mathbf{S}_P, \mathbf{u}_{P'}, \mathbf{S}_{P'}) \\ &= \sum_{m m'} T_{m m'}(\mathbf{r}_{PP'}) S_{m P} S_{m' P'} \\ & \quad \times \begin{pmatrix} 1 & 1 & 2 \\ m & m & -m-m \end{pmatrix} \end{aligned} \quad (13)$$

B. Integrated lattice dynamics and spin-wave formalism

Both the common spin-wave formalism[11,30] and the lattice dynamics methods developed in our institute[26–29] for large amplitude librons and for libron–phonon coupling use the time-dependent Hartree (TDH) method or random phase approximation (RPA). Therefore, it seemed convenient to use the same method for an integrated formalism that includes magnon–phonon and magnon–libron coupling as well. We start with the mean field (MF) approximation and, in analogy with the phonon–libron method,[26] we write sepa-

rate MF single particle Hamiltonians for the translational vibrations,

$$H_P^T(\mathbf{u}_P) = T(\mathbf{u}_P) + \sum_{P' \neq P} \langle V(\mathbf{u}_P,\omega_P,\mathbf{u}_{P'},\omega_{P'}) \rangle_{T_P L_{P'}}^{L_{P'}} + \sum_{P' \neq P} \langle W(\mathbf{u}_P,\omega_P,\mathbf{S}_P,\mathbf{u}_{P'},\omega_{P'},\mathbf{S}_{P'}) \rangle_{T_P L_P S_{P'}}^{L_{P'} S_{P'}} + \sum_{P' \neq P} \langle Y(\mathbf{u}_P,\mathbf{S}_P,\mathbf{u}_{P'},\mathbf{S}_{P'}) \rangle_{T_P S_{P'}}^{S_{P'}} \quad (14)$$

for the librations

$$H_P^L(\omega_P) = L(\omega_P) + \sum_{P' \neq P} \langle V(\mathbf{u}_P,\omega_P,\mathbf{u}_{P'},\omega_{P'}) \rangle_{T_{P'} L_P}^{T_{P'}} + \sum_{P' \neq P} \langle W(\mathbf{u}_P,\omega_P,\mathbf{S}_P,\mathbf{u}_{P'},\omega_{P'},\mathbf{S}_{P'}) \rangle_{T_{P'} L_P S_{P'}}^{T_{P'} S_{P'}} + \langle X(\omega_P,\mathbf{S}_P) \rangle^{S_P} \quad (15)$$

and for the spins

$$H_P^S(\mathbf{S}_P) = \sum_{P' \neq P} \langle W(\mathbf{u}_P,\omega_P,\mathbf{S}_P,\mathbf{u}_{P'},\omega_{P'},\mathbf{S}_{P'}) \rangle_{T_{P'} L_P S_P}^{T_{P'} L_P} + \langle X(\omega_P,\mathbf{S}_P) \rangle_{L_P} + \sum_{P' \neq P} \langle Y(\mathbf{u}_P,\mathbf{S}_P,\mathbf{u}_{P'},\mathbf{S}_{P'}) \rangle_{T_P S_{P'}}^{T_{P'}} \quad (16)$$

The different potential terms are defined in Eq (13) The subscripts and superscripts on the angle brackets denote MF Hamiltonians over which the thermodynamic averages should be taken, and so the MF problems for the translations, librations, and spins have to be solved self-consistently The only difference with the usual MF procedure is that the three problems are coupled, but this can be taken care of in the iterative process that is required to reach self-consistency

The manner to diagonalize the MF Hamiltonians in practice is to introduce a basis for each type of "motion" of the molecules For the translational motions we use a basis of three-dimensional spherical harmonic oscillator functions $|\chi_k^{(n)}{}_\mu(\mathbf{u}_P)\rangle$ and for the librational motions a basis of tesseral harmonics $|S_m^{(l)}(\omega_P)\rangle$, just as in Ref 26 For the single-molecule spin states the basis is given by the three triplet spin functions $|S,M_S\rangle$ with $S = 1$ and $M_S = -1$, 0 and 1 Diagonalizing Eqs (14), (15), and (16) in these bases produces the MF states

From the single-molecule MF states the crystal states can be constructed

$$|\psi_{(i_T,i_L,i_S)}\rangle = \prod_P \otimes |\psi_{i_T}^{T_P}(\mathbf{u}_P)\rangle \otimes |\psi_{i_L}^{L_P}(\omega_P)\rangle \otimes |\psi_{i_S}^{S_P}(\mathbf{S}_P)\rangle \quad (17)$$

The ground state is obtained by setting $i_T = i_L = i_S = 0$ for all molecules P Singly excited states have one of these indices i_K not equal to zero We can define excitation operators $a_{P i_K}^{(K)\dagger}$ for each type of motion $K = T, L$, or S, that replace $\psi_0^{K_P}$ on particle P by $\psi_{i_K}^{K_P}$ In the MF method the motions of the individual molecules are still uncorrelated In our particular MF scheme we have further neglected the coupling between the translational and the librational motion of a given molecule and the orientation of its spin momentum (apart from averaging or renormalization effects) Correlation can be introduced by the RPA or TDH method which produces collective excitations, i e , phonons, librons, and magnons in our case Moreover, the RPA/TDH method takes into account the magnon–phonon, magnon–libron, and phonon–libron coupling For the last this has already been demonstrated in Ref 26 in pure lattice dynamics calculations We also refer to this paper for details of the formalism, here we only present the outlines of the theory for $T = 0$ K The method consists of approximating the exact Hamiltonian (9)–(11) by a Hamiltonian which is quadratic in the excitation operators $a_{P i_K}^{(K)\dagger}$ and their Hermitian conjugates $a_{P i_K}^{(K)}$

$$H = \sum_{P P'} \sum_{K K'} \sum_{i_K j_{K'}} A_{P P'}^{K K'}(i_K, j_{K'}) a_{P i_K}^{(K)\dagger} a_{P' j_{K'}}^{(K')} + \sum_{P \neq P'} \sum_{K \leq K'} \sum_{i_K j_{K'}} [B_{P P'}^{K K'}(i_K, j_{K'}) a_{P i_K}^{(K)\dagger} a_{P' j_{K'}}^{(K')\dagger} + \text{Hermitian conjugate}] \quad (18)$$

These operators $a_{P i_K}^{(K)\dagger}$ and $a_{P j_K}^{(K)}$ are assumed to obey boson commutation relations The terms with $K' = K$ lead to pure phonons ($K = T$), librons ($K = L$), and magnons ($K = S$), the coupling terms with $K \neq K'$ yield also mixed excitations Even the single-particle coupling terms ($K \neq K', P = P'$) which have been neglected at the MF level are thus reincluded into the formalism The expressions for the coupling coefficients $A_{P P'}^{K K'}(i_K, j_{K'})$ and $B_{P P'}^{K K'}(i_K, j_{K'})$ can be obtained by equating the matrix elements of the Hamiltonian (18) to those of the exact Hamiltonian (10) in the basis (17)

In order to be able to diagonalize the Hamiltonian (18) for the infinite crystal, we first apply the translational symmetry by writing excitation operators

$$a_{I i_K}^{(K)}(\mathbf{q})^\dagger = \frac{1}{\sqrt{N}} \sum_{\mathbf{R}} e^{-i\mathbf{q}\cdot\mathbf{R}} a_{(\mathbf{R}I) i_K}^{(K)\dagger}, \quad (19)$$

where $\mathbf{q}$ is a vector in the first Brillouin zone, $\mathbf{R}$ a primitive translation vector of the crystal, I labels the different sublattices, and N is the number of unit cells A specific molecule P in the crystal is thus labeled by the position vector $\mathbf{R}$ of the origin of its unit cell and by its sublattice index I Substituting the operators (19) and their Hermitian conjugates into the Hamiltonian (18), the latter becomes a direct sum of independent Hamiltonians for every wave vector $\mathbf{q}$ The exact excitation operators of the crystal $C_\lambda(\mathbf{q})^\dagger$ must satisfy the following equation of motion

$$[H, C_\lambda(\mathbf{q})^\dagger] = \hbar\omega_\lambda(\mathbf{q}) C_\lambda(\mathbf{q})^\dagger \quad (20)$$

by expressing these operators as

$$C_\lambda(\mathbf{q})^\dagger = \sum_{K I i_K} [x_{K I i_K}^{(\lambda)*} a_{I i_K}^{(K)}(\mathbf{q})^\dagger + x_{K I i_K}^{(\lambda)} a_{I i_K}^{(K)}(-\mathbf{q})] \quad (21)$$

Equation (20) with the Hamiltonian (18) will be exactly solved, if the expansion coefficients $(\mathbf{x}^{(\lambda)*}, \mathbf{x}^{(\lambda)})$ are the eigenvectors of the following matrix

$$\begin{pmatrix} E^{(L)}+\Phi^{(LL)} & \Phi^{(LT)} & \Phi_1^{(LS)} & -\Phi^{(LT)} & -\Phi^{(LT)} & -\Phi_2^{(LS)} \\ \Phi^{(LT)} & E^{(T)}+\Phi^{(TT)} & \Phi_1^{(TS)} & -\Phi^{(LT)*} & -\Phi^{(LT)} & -\Phi_2^{(TS)} \\ \Phi_1^{(LS)*} & \Phi_1^{(TS)*} & E^{(S)}+\Phi_1^{(SS)} & -\Phi_1^{(LS)*} & -\Phi_1^{(TS)*} & -\Phi_3^{(SS)} \\ \Phi^{(LL)} & \Phi^{(LT)} & \Phi_1^{(LS)} & -E^{(L)}-\Phi^{(LL)} & -\Phi^{(LT)} & -\Phi_2^{(LS)} \\ \Phi^{(LT)} & \Phi^{(TT)} & \Phi_1^{(TS)} & -\Phi^{(LT)*} & -E^{(T)}-\Phi^{(TT)} & -\Phi_2^{(TS)} \\ \Phi_2^{(LS)*} & \Phi_2^{(TS)*} & \Phi_4^{(SS)} & -\Phi_2^{(LS)*} & -\Phi_2^{(TS)*} & -E^{(S)}-\Phi_2^{(SS)} \end{pmatrix} \tag{22}$$

The sub-blocks of this matrix which are labeled by $K=T$, $K=L$, and $K=S$ for phonons, librons and magnons, respectively, are defined as follows, with the operators written as in Eq (13)

$$(E^{(K)})_{l_K,j_K} = \delta_{IJ}\delta_{i_K j_K}\Delta\epsilon_{i_K}^{(K)}$$

$$(\Phi^{(LL)})_{l_L,j_L} = \sum_{\mathbf{R}} e^{i\mathbf{q}\cdot\mathbf{R}}\langle\psi_{i_L}^{L(\mathbf{0},I)}\psi_{j_L}^{L(\mathbf{R},J)} \times|V_{(\mathbf{0},I)(\mathbf{R},J)}+W_{(\mathbf{0},I)(\mathbf{R},J)}|\rangle,$$

$$(\Phi^{(TT)})_{l_T,j_T} = \sum_{\mathbf{R}} e^{i\mathbf{q}\cdot\mathbf{R}}\langle\psi_{i_T}^{T(\mathbf{0},I)}\psi_{j_T}^{T(\mathbf{R},J)} \times|V_{(\mathbf{0},I)(\mathbf{R},J)}+W_{(\mathbf{0},I)(\mathbf{R},J)}+Y_{(\mathbf{0},I)(\mathbf{R},J)}|\rangle,$$

$$(\Phi_1^{(SS)})_{l_S,j_S} = \sum_{\mathbf{R}} e^{i\mathbf{q}\cdot\mathbf{R}}\langle\psi_{i_S}^{S(\mathbf{0},I)} \times|W_{(\mathbf{0},I)(\mathbf{R},J)}+Y_{(\mathbf{0},I)(\mathbf{R},J)}|\psi_{j_S}^{S(\mathbf{R},J)}\rangle,$$

$$(\Phi_2^{(SS)})_{l_S,j_S} = \sum_{\mathbf{R}} e^{i\mathbf{q}\cdot\mathbf{R}}\langle\psi_{j_S}^{S(\mathbf{R},J)} \times|W_{(\mathbf{0},I)(\mathbf{R},J)}+Y_{(\mathbf{0},I)(\mathbf{R},J)}|\psi_{i_S}^{S(\mathbf{0},I)}\rangle,$$

$$(\Phi_3^{(SS)})_{l_S,j_S} = \sum_{\mathbf{R}} e^{i\mathbf{q}\cdot\mathbf{R}}\langle\psi_{i_S}^{S(\mathbf{0},I)}\psi_{j_S}^{S(\mathbf{R},J)} \times|W_{(\mathbf{0},I)(\mathbf{R},J)}+Y_{(\mathbf{0},I)(\mathbf{R},J)}|\rangle,$$

$$(\Phi_4^{(SS)})_{l_S,j_S} = \sum_{\mathbf{R}} e^{i\mathbf{q}\cdot\mathbf{R}}\langle|W_{(\mathbf{0},I)(\mathbf{R},J)} + Y_{(\mathbf{0},I)(\mathbf{R},J)}|\psi_{i_S}^{S(\mathbf{0},I)}\psi_{j_S}^{S(\mathbf{R},J)}\rangle,$$

$$(\Phi^{(LT)})_{l_L,j_T} = \sum_{\mathbf{R}} e^{i\mathbf{q}\cdot\mathbf{R}}\langle\psi_{i_L}^{L(\mathbf{0},I)}\psi_{j_T}^{T(\mathbf{R},J)} \times|V_{(\mathbf{0},I)(\mathbf{R},J)}+W_{(\mathbf{0},I)(\mathbf{R},J)}|\rangle + \delta_{IJ}\sum_{P}\langle\psi_{i_L}^{L(\mathbf{0},I)}\psi_{j_T}^{T(\mathbf{0},P)}|V_{(\mathbf{0},I)P}+W_{(\mathbf{0},I)P}|\rangle,$$

$$(\Phi_1^{(LS)})_{l_L,j_S} = \sum_{\mathbf{R}} e^{i\mathbf{q}\cdot\mathbf{R}}\langle\psi_{i_L}^{L(\mathbf{0},I)}|W_{(\mathbf{0},I)(\mathbf{R},J)}|\psi_{j_S}^{S(\mathbf{R},J)}\rangle + \delta_{IJ}\sum_{P}\langle\psi_{i_L}^{L(\mathbf{0},I)}|W_{(\mathbf{0},I)P}|\psi_{j_S}^{S(\mathbf{0},J)}\rangle + \delta_{IJ}\langle\psi_{i_L}^{L(\mathbf{0},I)}|X_{(\mathbf{0},I)}|\psi_{j_S}^{S(\mathbf{0},J)}\rangle,$$

$$(\Phi^{(LS)})_{l_L,j_S} = -\sum_{\mathbf{R}} e^{i\mathbf{q}\cdot\mathbf{R}}\langle\psi_{i_L}^{L(\mathbf{0},I)}\psi_{j_S}^{S(\mathbf{R},J)}|W_{(\mathbf{0},I)(\mathbf{R},J)}|\rangle + \delta_{IJ}\sum_{P}\langle\psi_{i_L}^{L(\mathbf{0},I)}\psi_{j_S}^{S(\mathbf{0},P)}|W_{(\mathbf{0},I)P}|\rangle$$

$$(\Phi_1^{(TS)})_{l_T,j_S} = \sum_{\mathbf{R}} e^{i\mathbf{q}\cdot\mathbf{R}}\langle\psi_{i_T}^{T(\mathbf{0},I)} |W_{(\mathbf{0},I)(\mathbf{R},J)}+Y_{(\mathbf{0},I)(\mathbf{R},J)}|\psi_{j_S}^{S(\mathbf{R},J)}\rangle + \delta_{IJ}\sum_{P}\langle\psi_{i_T}^{T(\mathbf{0},I)}|W_{(\mathbf{0},I)P}+Y_{(\mathbf{0},I)P}|\psi_{j_S}^{S(\mathbf{0},I)}\rangle,$$

$$(\Phi_2^{(TS)})_{l_T,j_S} = \sum_{\mathbf{R}} e^{i\mathbf{q}\cdot\mathbf{R}}\langle\psi_{i_T}^{T(\mathbf{0},I)}\psi_{j_S}^{S(\mathbf{R},J)} \times|W_{(\mathbf{0},I)(\mathbf{R},J)}+Y_{(\mathbf{0},I)(\mathbf{R},J)}|\rangle + \delta_{IJ}\sum_{P}\langle\psi_{i_T}^{T(\mathbf{0},I)}\psi_{j_S}^{S(\mathbf{0},P)}|W_{(\mathbf{0},I)P}+Y_{(\mathbf{0},I)P}|\rangle \tag{23}$$

Here $\Delta\epsilon_{i_K}^{K}$ is a MF excitation energy to the state i_K of the MF Hamiltonian H_P^K Single-molecule ground states have been omitted from the notation of the matrix elements for brevity The eigenvalues of the matrix (22) are the excitation energies of the crystal $\hbar\omega_\lambda(\mathbf{q})$, and the corresponding deexcitation energies, which in principle correspond to mixed phonon–libron–magnon ($K=L,T,S$) excitations

C. Separate lattice dynamics and spin-wave treatments

As shown by the results (Sec III) of applying Sec II B, the actual mixing between phonons and librons, on the one hand, and magnons, on the other, is small in the case of α and β oxygen, except for some isolated points in the Brillouin zone This is caused by the smallness of the TS and LS coupling blocks in the matrix (22) So it is possible to describe most of the properties of these systems in good approximation by separate lattice dynamics and spin-wave treatments These treatments are still essentially different from the earlier separate treatments, however In principle, we base each formalism on the complete lattice and spin Hamiltonian (9)–(11) The mean-field calculations for the translational vibrations, for the librations and for the spins are made as in Sec II B, Eqs (14)–(16), and the separation only implies that we solve the RPA problems separately for the phonons and librons and for the spin waves Although from the point of view of the calculations this is not a great simplification, conceptually the separation is advantageous We treat the lattice vibrations in the averaged field of the spins and the spin waves in the average field of the vibrating molecules Or, in the actual calculations, those terms in the complete Hamiltonian (9)–(11) that depend both on the lattice vibrations and the spins are averaged over the spins when calculating

the lattice modes and averaged over the molecular vibrations when calculating the spin waves This thermodynamic averaging, sometimes called renormalization, is performed in the sense of MF theory Moreover, the separation allows practical simplifications because some of the renormalized terms are insignificant

Let us now be specific about the essential differences between our separated treatment and the earlier calculations In the older lattice dynamics calculations[8-10] only the Hamiltonian H_0, given by Eq (11), has been taken into account In our lattice dynamics calculations we have included, moreover, the first two terms from the spin Hamiltonian (9), averaged over the spin states from a MF calculation Especially the Heisenberg term with the spin factor $\langle \mathbf{S}_P\ \mathbf{S}_{P'} \rangle_{S_P}^{S_{P'}}$ turns out to be crucial, see Sec III, because of the extremely strong dependence of the coupling parameter J on the molecular orientations ω_P The third term in Eq (9) appears to be insignificant for the lattice dynamics calculations, and also the effects of the second term are of minor importance

In our spin-wave calculations we have used the spin Hamiltonian (9) with coupling parameters $\langle J(\mathbf{r}_{PP'}, \omega_P, \omega_{P'}) \rangle$, $\langle A_m(\omega_P) \rangle$, and $\langle T_m(\mathbf{r}_{PP'}) \rangle$ averaged over the vibrational wave functions of the molecules When we identify these averaged parameters with the spin-coupling constants in Eq (1), our spin Hamiltonian (9) becomes conceptually similar to the phenomenological one in Eq. (1) Two essential differences persist, however Our coupling parameters have been obtained from *ab initio* calculations, not by fitting the experimental data Secondly, the third term in Eq (9) is a two-body term obtained from a first principles expression for the intermolecular spin–spin interactions, in Eq (1) it is a single-molecule term

As an illustration we now briefly present a simplified spin-wave theory for α-O$_2$ based on the first principles spin Hamiltonian (9) Just as in the older spin-wave theory[11] based on Eq (1), the RPA problem can be solved analytically in this case First we define the averaged coupling parameters

$$\begin{aligned} J_{PP'} &= \langle J(\mathbf{r}_{PP'}, \omega_P, \omega_{P'}) \rangle_{T_P T_{P'}}^{L_P L_{P'}}, \\ A_m &= \langle A_m(\omega_P) \rangle^{L_P}, \\ T_{mPP'} &= \langle T_m(\mathbf{r}_{PP'}) \rangle_{T_P}^{T_{P'}}, \end{aligned} \tag{24}$$

and the $\mathbf{q}$-dependent lattice sums

$$\begin{aligned} J(\mathbf{q})^{\text{intra}} &= \sum_{\mathbf{R} \neq \mathbf{0}} J_{PP'}\, e^{i\mathbf{q}\cdot\mathbf{R}} \quad \text{for } I' = I, \\ J(\mathbf{q})^{\text{inter}} &= \sum_{\mathbf{R}} J_{PP'}\, e^{i\mathbf{q}\cdot\mathbf{R}} \quad \text{for } I' \neq I, \\ T_m(\mathbf{q})^{\text{intra}} &= \sum_{\mathbf{R} \neq \mathbf{0}} T_{mPP'}\, e^{i\mathbf{q}\cdot\mathbf{R}} \quad \text{for } I' = I, \\ T_m(\mathbf{q})^{\text{inter}} &= \sum_{\mathbf{R}} T_{mPP'}\, e^{i\mathbf{q}\cdot\mathbf{R}} \quad \text{for } I' \neq I \end{aligned} \tag{25}$$

for molecules $P = \{\mathbf{0}, I\}$ and $P' = \{\mathbf{R}, I'\}$ Then, the mean-field spin Hamiltonian for a molecule P on a given sublattice reads as follows

$$\begin{aligned} H_P^{\text{S}}(\mathbf{S}_P) = &-2 \sum_{P' \neq P} J_{PP'}\, \mathbf{S}_P\, \langle \mathbf{S}_{P'} \rangle_{S_{P'}} \\ &+ \sum_{m m'} A_{m\ -m} S_{m'} S_{m'} \begin{pmatrix} 1 & 1 & 2 \\ m & m' & -m-m' \end{pmatrix} \\ &+ \sum_{P' \neq P} \sum_{m m'} T_{(-m)\ -m'\ PP'} S_{m_P} \\ &\times \langle S_{m'_{P'}} \rangle_{S_{P'}} \begin{pmatrix} 1 & 1 & 2 \\ m & m' & -m-m' \end{pmatrix} \end{aligned} \tag{26}$$

and we have to diagonalize this Hamiltonian between the triplet spin states $|1\rangle$, $|0\rangle$, and $|-1\rangle$ of molecule P The average spin directions $\langle \mathbf{S}_{P'} \rangle$ on the molecules P' are assumed to be parallel when they are on the same sublattice in α-O$_2$ and antiparallel when they are on a different sublattice If the monoclinic b axis is taken as the spin quantization axis (the z axis) the 3×3 Hamiltonian matrix is blocked and the MF ground state for the molecule P can be written as

$$|g\rangle = |1\rangle \cos(\alpha/2) - |-1\rangle \sin(\alpha/2) e^{i\beta} \tag{27a}$$

in terms of two variational parameters α and β The ground state sublattice magnetizations lie along the crystal b axis, i e , $\langle S_x \rangle = \langle S_z \rangle = 0$ The first excited state is simply given by

$$|e_1\rangle = |0\rangle \tag{27b}$$

In this simple model it is assumed, as in the older spin wave treatments, that the second excited state $|e_2\rangle$, which corresponds to two-magnon excitations, is irrelevant and that the temperature equals zero Then the average magnetization is a simple function of the parameter α

$$\langle S_z \rangle = \cos \alpha \tag{28}$$

and the MF equations (26) can be written analytically as

$$\begin{aligned} \beta &= \arctan[\text{Im}(A_2)/\text{Re}(A_2)] \\ \alpha &= 2 \arctan\left[\frac{|A_2|}{(X^2 \cos^2 \alpha + |A_2|^2)^{1/2} - X \cos \alpha} \right] \end{aligned} \tag{29}$$

with the constant

$$\begin{aligned} X = &-2\sqrt{5}[J(\mathbf{0})^{\text{intra}} - J(\mathbf{0})^{\text{inter}}] \\ &+ \sqrt{\tfrac{5}{3}}[T_0(\mathbf{0})^{\text{intra}} - T_0(\mathbf{0})^{\text{inter}}] \end{aligned} \tag{30}$$

and the parameters A_2, $J(\mathbf{0})$, and $T_0(\mathbf{0})$ given by Eqs (24) and (25) From Eq (29) α can easily be found self consistently, starting from $\alpha = 0$, whereas β is directly given The MF excitation energy is found to be

$$\Delta\epsilon = [\tfrac{1}{2}(X^2 \cos^2 \alpha + A_2|^2)]^{1/2} - \sqrt{\tfrac{7}{10}} A_0 \tag{31}$$

The second step in the spin-wave method involves the solution of the RPA equation, cf Sec II B This problem is more complicated than the usual spin-wave problem[11] with the Hamiltonian (1), due to the explicit consideration of the dipole–dipole interaction as a two-body operator and due to the tensorial character of the coupling parameters A and $T_{PP'}$ Still it can be solved analytically and the magnon frequencies are given by

$$\begin{aligned} \omega_{1,2}(\mathbf{q})^2 = &|\Delta\epsilon + Y^{\text{intra}}|^2 - |Y^{\text{inter}}|^2 + Z^{\text{inter}}|^2 - Z^{\text{intra}}|^2 \\ &\pm 2[\ (\Delta\epsilon + Y^{\text{intra}}) Z^{\text{inter}} - Y^{\text{inter}} Z^{\text{intra}\ 2} \\ &- \{\text{Im}(Z^{\text{intra}} Z^{\text{inter}*})\}^2]^{1/2} \end{aligned} \tag{32}$$

The constants Y and Z (both for intra/inter) are fairly complicated combinations

$$Y = -2J(\mathbf{q}) - \frac{1}{\sqrt{30}}T_0(\mathbf{q}) - \frac{1}{\sqrt{5}}\sin\alpha\,\mathrm{Re}(e^{-i\beta}T_2(\mathbf{q})),$$

$$Z = e^{i\beta}\Big[2J(\mathbf{q})\sin\alpha + \frac{1}{\sqrt{30}}T_0(\mathbf{q})\sin\alpha + \frac{1}{\sqrt{5}}\mathrm{Re}(e^{-i\beta}T_2(\mathbf{q})) + i\cos\alpha\,\mathrm{Im}(e^{-i\beta}T_2(\mathbf{q}))\Big] \tag{33}$$

of the $\mathbf{q}$ dependent lattice sums $J(\mathbf{q})$ and $T_m(\mathbf{q})$ defined by Eq (25)

The lattice sum $J(\mathbf{q})$ is easily calculated Because of the exponential decay of $J_{pp'}$ with the intermolecular distance $r_{pp'}$ only the nearest and next-nearest neighbors within the layers parallel to the a–b plane and the nearest and next-nearest neighbors in the adjacent layers contribute The lattice sums $T_m(\mathbf{q})$ over the (magnetic) dipole–dipole interaction converge very slowly when taken in direct space In order to evaluate these sums we have invoked the $\mathbf{q}$ dependent Ewald formula[31] which writes part of the sum in reciprocal space and which leads to rapid convergence The macroscopic term which occurs[31] for $\mathbf{q} = 0$ vanishes for antiferromagnetic lattices The magnon frequencies obtained by this simple analytical expression (32) can be compared with some of the numerically calculated eigenvalues of the full RPA matrix, Eq (22), or with the eigenvalues of the pure spin blocks (SS) of this matrix Thus, the results, which are discussed in Sec III, inform us about the separability of the lattice dynamics and spin-wave problems and about the validity of the simplified model for the spin waves

III. RESULTS AND DISCUSSION

A. General remarks

The *ab initio* calculations on the O_2–O_2 dimer[21] have provided the spin-independent O_2–O_2 potential $V_{pp'}$ and the geometry dependent Heisenberg coupling parameter $J_{pp'}$ directly in the form of a spherical expansion as in Eq (3) For the expansion coefficients we have chosen the following forms

$$v_{L_A L_B L}(r_{pp'}) = C^{\exp}_{L_A L_B L}\exp(-\alpha_{L_A L_B L}r_{pp'} - \beta_{L_A L_B L}r_{pp'}^2) + C^{\mathrm{mult}}_{L_A L_B L}r_{pp'}^{-(L_A+L_B+1)} + C^{(6)}_{L_A L_B L}r_{pp'}^{-6} + C^{(8)}_{L_A L_B L}r_{pp'}^{-8} + C^{(10)}_{L_A L_B L}r_{pp'}^{-10} \tag{34}$$

and

$$J_{L_A L_B L}(r_{pp'}) = C'^{\exp}_{L_A L_B L}\exp(-\alpha'_{L_A L_B L}r_{pp'} - \beta'_{L_A L_B L}r_{pp'}^2) \tag{35}$$

The exponential contribution to Eq (34) is due to overlap (exchange and charge penetration) effects, the second term is due to the electrostatic multipole interactions and the last three terms arise from dispersion interactions The expansion coefficients of the Heisenberg coupling parameter, Eq (35), just contain an exponential term because this coupling is caused merely by exchange effects All the coefficients occurring in these equations have been explicitly calculated in Ref 21, except for the $C^{(n)}_{L_A L_B L}$ Apart from the leading isotropic coefficient $C^{(6)}_{0,0,0}$, good values for these coefficients are not available in the literature either So we have estimated these parameters $C^{(n)}_{L_A L_B L}$ via simple model considerations In order to check whether this uncertainty influences the conclusions, three different sets of parameters $C^{(n)}_{L_A L_B L}$ have been tested The first set (A) has been obtained by assuming that the O_2–O_2 dispersion interactions can be represented by a $C^{(6)}r^{-6}$ atom–atom potential, which is approximately equal to the potentials used by Kobashi *et al.*,[8] and by expanding this atom–atom r^{-6} potential in the form of Eq (3) Explicit formulas for such expansions have been derived[32] The second set (B) has been obtained by using the same model, but now we have scaled $C^{(6)}$ in the atom–atom potential to the value that reproduces the experimental cell parameters in α-O_2 when the free energy is minimized by isotropic expansion of the lattice In constructing the third set (C) we have started from the accurate semiempirical value[33] of $C^{(6)}_{000}$ and taken the anisotropy factors $C^{(6)}_{L_A L_B L}/C^{(6)}_{000}$ from *ab initio* calculations[34] The higher coefficients $C^{(n)}_{L_A L_B L}$ for $n = 8,10$ were then related to the coefficients with $n = 6$ by using the same ratios calculated for the N_2–N_2 potential.[35] Some adjustments of these ratios had to be made, however, in order to obtain a reasonable lattice energy for α-O_2 and optical libron frequency in β-O_2 All the three sets of parameters $C^{(n)}_{L_A L_B L}$ are listed in Table I Together with the parameters given in Ref 21 and with the O_2 bond length and the values of the intra- and intermolecular spin coupling parameters, also given in Table I, these parameters completely specify the spin-dependent O_2–O_2 potential

The cell parameters used in our calculations on α-O_2 and β-O_2 are listed in Table II It would have been possible to optimize these cell parameters by minimizing the free energy, as we have done for nitrogen[26] We found this too expensive, however, and not very meaningful because of the uncertainty in the dispersion coefficients

Next we specify the basis sets used in our (mean-field) calculations The translational vibrations of the molecules have been expanded in a basis $|\chi^{(n)}_{\lambda\mu}(\mathbf{u}_p)\rangle$ of three-dimensional harmonic oscillator functions For the displacement vectors $\mathbf{u}_p$ we have used polar coordinates, so that the angular parts of the (isotropic) oscillator functions are given by spherical (or in practice, tesseral) harmonics and the radial parts by modified Laguerre functions, see Ref 26 Convergence of the MF states was reached for $n_{\max} = 3$, but in order to ensure the correct behavior of the acoustic phonon branches in the RPA calculation, we had to include all oscillator functions with $n \leq n_{\max} = 5$ As explained in Ref 26, this is related to the translational invariance property of the lattice dynamics formalism, which is satisfied for the RPA method, but only in the limit of a complete basis set The librational states of the molecules have been expanded in tesseral harmonics, i e , real combinations of spherical harmonics $|Y^{(l)}_m(\omega_p)\rangle$ For homonuclear[16] O_2 molecules, we only need functions with odd l because of the zero nuclear spin momentum and the $^1\Sigma_g$ symmetry character of the electronic ground state Since the librational states of the O_2

TABLE I Expansion coefficients $C^{(n)}_{L_A L_B L}$, Eq (34), (kJ mol^{-1} nm^n) and some other parameters in the potential, Eqs (6) and (8)

	L_A	L_B	L	$C^{(6)}_{L_A L_B L}$	$C^{(8)}_{L_A L_B L}$	$C^{(10)}_{L_A L_B L}$
Potential *A*	0	0	0	-0.3990×10^{2}	-0.1456×10^{1}	-0.3966×10^{0}
	2	0	2		-0.1042×10^{1}	-0.4525×10^{0}
	2	2	0			-0.8868×10^{0}
	2	2	2			0.1514×10^{0}
	2	2	4			-0.4876×10^{0}
	4	0	4			-0.9713×10^{0}
Potential *B*	0	0	0	-0.5819×10^{2}	0.2123×10^{1}	-0.5783×10^{0}
	2	0	2		-0.1519×10^{1}	-0.6598×10^{0}
	2	2	0			-0.1293×10^{0}
	2	2	2			0.2208×10^{-1}
	2	2	4			-0.7110×10^{0}
	4	0	4			-0.1416×10^{1}
Potential *C*	0	0	0	-0.3574×10^{2}	-0.2489×10^{1}	-0.1892×10^{0}
	2	0	2	-0.2850×10^{1}	-0.4972×10^{0} [a]	-0.5629×10^{0} [a]
	2	2	0	-0.1108×10^{-4}	-0.1795×10^{-5}	-0.6641×10^{0}
	2	2	2	-0.1324×10^{-4}	0.3014×10^{-5}	0.1085×10^{0}
	2	2	4	-0.1064×10^{-1}	-0.1443×10^{-3}	-0.3567×10^{0}

$d_{O\text{-}O} = 0.1208$ nm
$A = 5.712$ K
$g_r^2 \mu_B^2 = 2.497\times10^{-1}$ K nm^3

[a] In pure libron calculations the values $C^{(8)}_{202} = -0.4144\times10^{4}$ kJ mol^{-1} nm^8 and $C^{(10)}_{202} = 0.4691\times10^{5}$ kJ mol^{-1} nm^{10} have been taken

molecules in the α and β solids are fairly localized, we needed rather many of these free rotor functions for convergence. For $l \leqslant l_{max} = 13$ the MF ground state was converged to within 1 cm^{-1}, the first two excitation energies to within 2 cm^{-1}. The spin basis is simply given by the triplet functions $|S,M_S\rangle$ with $S = 1$ and $M_S = -1$, 0, and 1

It has been explained in Sec II B that the pair terms in the potential, which depend on the intermolecular distances $r_{PP'}$, have to be written as explicit functions of the displacement coordinates $\mathbf{u}_P$ and $\mathbf{u}_{P'}$. We have achieved this by means of a double Taylor expansion, including all terms in $u_P^{\alpha_1} u_{P'}^{\alpha_2}$ up to powers $\alpha_1 + \alpha_2 < 4$. The calculations on solid nitrogen,[26] where the same method has been used, show that these terms are largely sufficient to take into account all the anharmonicity in the translational vibrations. Let us emphasize at this point that our method is also valid for strongly anharmonic librations with very large amplitudes, because it retains the full orientational dependence of the potential. In some of the calculations, where we focus on the librons and magnons, we have kept the molecular centers of mass fixed on the lattice sites.

TABLE II Cell parameters of solid oxygen

α-O_2	$a = 5.403$ Å
	$b = 3.429$ Å
	$c = 5.086$ Å
	$\beta = 132.53°$
β-O_2	$a = 3.272$ Å
	$c = 11.277$ Å

In calculating the lattice sums for the pair terms in the potential we have generally taken a distance of 9 Å between the molecular centers of mass as the truncation distance. This implies that we have included 96 molecules in α-O_2 and 84 molecules in β-O_2. Only for the magnetic dipole-dipole interactions we had to extend the summations beyond this radius and to use Ewald's method for accelerating convergence, see Sec II C.

B. Mean-field results

The results of the MF calculations for the translational vibrations, the librations and the spins of the O_2 molecules may be summarized as follows. Translationally the molecules in α-O_2 vibrate as three-dimensional, nearly harmonic, oscillators. Two of the fundamental frequencies that correspond with the vibrations in the *ab* plane are nearly equal, the third fundamental frequency for the vibration in the c^* direction is about 50% larger. Apparently the potential is stiffer in the c^* direction. This is confirmed by the smaller amplitude of vibration in this direction, see Table III. In β-O_2 the small anisotropy in the *ab* plane has disappeared, of course, and all the amplitudes have slightly increased.

The librational states of the molecules are rather localized in α-O_2, and even in β-O_2. They look like weakly anharmonic two-dimensional oscillator states, anisotropic in the case of α-O_2 and isotropic for β-O_2. The lower frequency in α-O_2 corresponds with libration about the *a* axis, the higher one with libration about the *b* axis. The root-mean-square angular displacements are only about 11°, as compared with 16° (at $T = 0$ K) for α-nitrogen.[26,27] This agrees well with experimental data[36] and with some of the earlier lattice dynamics calculations,[37,38] whereas in other calculations[10] the

TABLE III Translational and librational amplitudes from MF calculations (potential C) [a]

α O_2	$T = 0$ K
$\langle u_x^2 \rangle^{1/2}$	= 0 1092 A
$\langle u_y^2 \rangle^{1/2}$	= 0 1115 A
$\langle u_z^2 \rangle^{1/2}$	= 0 0889 A
$\arccos(\langle \cos\theta \rangle^{1/2})$	= 10 84°
Asymmetry parameter [a] $\dfrac{\langle \sin^2\theta(\sin\phi - \cos\phi) \rangle}{\langle \sin\theta \rangle}$	= 0 126
β-O_2	$T = 30$ K
$\langle u_x \rangle^{1/2}$ = $\langle u_y^2 \rangle^{1/2}$	= 0 1200 A
$\langle u_z^2 \rangle^{1/2}$	= 0 0940 A
$\arccos(\langle \cos\theta \rangle^{1/2})$	= 11 16°

[a] The libration angles θ and ϕ are here defined as polar angles in a crystal frame with $x = a$, $y = b$, and $z = c^*$.

amplitudes are substantially higher, both for the translations and the librations It has been suggested[8 19] that the molecular axes in α and β oxygen are tilted with respect to the c^* axis, but we have found no such tilt in β-O_2 and only a very small tilt angle in α-O_2 (-0 3° about the b axis)

The effective Heisenberg coupling parameters which can be used in separate spin-wave calculations, see Sec II C, are listed in Table IV Only four of such couplings are significant All coupling parameters are raised in absolute value by the averaging over the translational vibrations, but lowered by librational averaging The latter effect dominates The resulting values for the nearest neighbor intersublattice couplings in α-O_2 and β-O_2 fall well within the range of experimental data quoted in DeFotis's review,[1] but they are less negative than the more recent experimental values [4 11 18] These more negative values are mainly based on magnetic susceptibility data, however, which have only been interpreted via MF theory The ratios $J_{NNN}/J_{NN} = 0$ 39 for α-O_2 and $J_{NN}(\beta\text{-}O_2)/J_{NN}(\alpha\text{-}O_2) = 0$ 76 are in agreement with experiment [4 11] The interlayer couplings are small and they become even smaller by librational averaging This agrees with the experimental data that suggest α- and β-O_2 to be quasi-two-dimensional magnetic systems,[4 11 19] but the sign of our interlayer coupling parameters does not agree with experiment [5] We expect that the positive sign of the *ab initio* values for J' may be incorrect, because the geometry of the interlayer neighbor pairs is close to geometries for which the calculated J' values change sign [21] Although our calculated positive J' would lead to a magnetic ground state of α-O_2 with reversed spins an alternating layer, we have still based our MF and RPA calculations on the experimentally observed magnetic ground state The drawback of this discrepancy is that the spin waves in our RPA calculations will become soft for some $\mathbf{q}$ vectors along the c^* direction Since the effect of the weak interlayer coupling on most properties is small indeed, we have, at this stage, not tried to correct this error

In β-O_2 the interlayer coupling causes still another problem It has been pointed out by one of us[40] and by others,[41 42] that the three-sublattice structure which is favored by the antiferromagnetic intralayer exchange coupling will be distorted by the interlayer coupling So, in the ground state the magnetic structure of β-O_2 will be incommensurate[40 42] and via the geometry dependence of the Heisenberg coupling terms, the symmetry of the lattice will be distorted too This would complicate our calculations to a large extent Since the effects of the interlayer exchange coupling are very small, we have omitted this coupling from our calculations on β-O_2 and based ourselves on the experimentally observed geometry with the antiferromagnetic three-sublattice structure Also the magnetic dipole dipole coupling has been left out of our spin-wave calculations on β-O_2, and both anisotropic spin terms have been left out of the lattice dynamics calculations since they would lead to similar problems

By calculating the Helmholtz free energy both for α- and β-oxygen as a function of the temperature, we have investigated whether the spin-dependent potential correctly predicts the α–β transition It is indeed found, as shown in Fig 2, that the α phase is more stable at low temperature and

TABLE IV Effective exchange coupling parameters (in K) calculated with potential C [a]

			Averaged over		
		At equilibrium structure	librations	translations	librations and translations
α O_2 ($T = 0$ K)	$J_{\perp\perp}$	− 12 677	− 10 133	− 14 311	− 11 550
	$J_{\perp\perp\perp}$	− 5 164	− 3 858	− 5 915	− 4 479
	$J_{\parallel\perp}$	0 538	0 352	0 547	0 346
	$J_{\parallel\perp\perp}$	0 368	0 274	0 374	0 272
β O_2 ($T = 30$ K)	$J_{\perp\perp}$	− 9 561	− 7 391	− 11 120	− 8 714
	$J_{\perp\perp\perp}$	− 0 002	− 0 001	− 0 002	− 0 001
	$J_{\parallel\perp}$	0 487	0 322	0 499	0 318

The Heisenberg exchange parameters J and J' refer to the intra- and interlayer couplings, respectively the subscripts refer to (next) nearest neighbors

[a] These results and also those in Table VII are slightly different from those in Ref 22 because the latter have been calculated with potential B

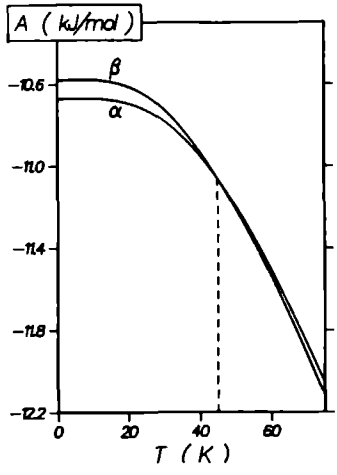

FIG 2 Free energy (at zero pressure) for α and β oxygen from MF calculations with potential C

the β phase at higher temperature The calculated transition temperature, 45 K, (experimentally 23 9 K) is too high, however But, as one can observe in Fig 2, the intersection of the two free energy curves is fairly hard to determine Since we have not varied the lattice parameters and in view of the uncertainty in the dispersion terms of our potential, the error in $T_{\alpha\beta}$ is not surprising These dispersion terms are spin-independent and not very anisotropic, so they will play little role in most of the properties discussed in the next section They are important for the lattice stability, however, and thus for the α–β transition temperature Also the free energy calculated for α-O_2 at $T = 0$ K, 10 67 kJ/mol, is in reasonable but not perfect agreement with the experimental[43] cohesion energy of 8 66 kJ/mol

C. RPA results

Some results from the integrated lattice dynamics and spin-wave calculations are shown in Table V The magnetic

TABLE V Phonon, libron, and magnon frequencies at $\mathbf{q} = \mathbf{0}$ in α-O_2 (potential C)

ω (cm^{-1})	Character
6 7	magnon <0 1% libron
22 1	99 7% magnon 0 3% libron
39 3	99 2% libron 0 8% magnon (B_g)
49 8*	pure phonon
55 3*	pure phonon
70 0*	libron <0 1% magnon
74 1	libron <0 1% magnon (A_g)
86 8*	pure phonon
101 3	magnon <0 1% libron
101 5	magnon <0 1% libron
124 4*	libron <0 1% magnon

* These modes correspond to modes at $\mathbf{q} = (0\ 2\pi/b\ 0)$ in the Brillouin zone of the structural lattice

unit cell in α-O_2 is twice as large as the structural unit cell We have used the larger unit cell that contains two molecules in our RPA calculations and so we find six phonon modes, four libron modes, and four magnon modes for every wave vector $\mathbf{q}$ in the (smaller) Brillouin zone The dispersion of these modes for $\mathbf{q}$ perpendicular to the ac plane is shown in Fig 3 and we have especially looked at the mixing between the lattice modes, phonons and librons, and the magnons In general we find this mixing to be very small It should originate mainly from the Heisenberg exchange term, but if we write the spin operator $\mathbf{S}_p \cdot \mathbf{S}_{p'}$ in second quantization[44] we observe that the magnon creation and annihilation operators for the lower excited spin states do not occur linearly So the Heisenberg term only couples the lattice modes with the higher excited spin states, the so-called two-magnon states Additional, but also small, coupling is caused by the second term in the spin Hamiltonian (9), so that, altogether, the TS and LS coupling blocks in the RPA matrix (22) remain very small The only substantial amount of mixing occurs in those regions of the Brillouin zone where the dispersion curves for the lattice modes and those for the magnons would cross Even the weak coupling then leads to an avoided crossing and to an interchange of character of the modes involved This is demonstrated in Fig 4, where an example of phonon-libron mixing is shown as well Some of the corresponding results for β-O_2 are listed in Table VI

The lower magnon frequencies in Table V may be compared with the results from the simple analytical spin wave treatment presented in Sec II C The latter results are shown in Table VII, first column The agreement is very good in-

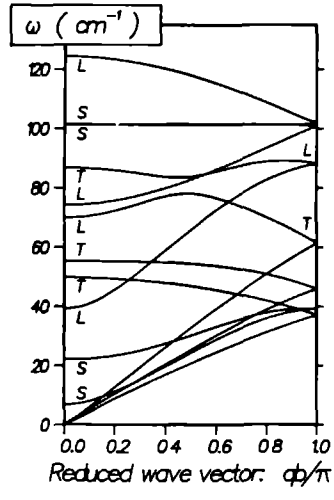

FIG 3 Calculated (RPA) dispersion curves for α O for phonon (T) libron (L) and magnon (S) modes propagating along the b axis Note the avoided crossing and the interchange of T/L character between two phonon–libron branches at $qb/\pi \approx 0.45$

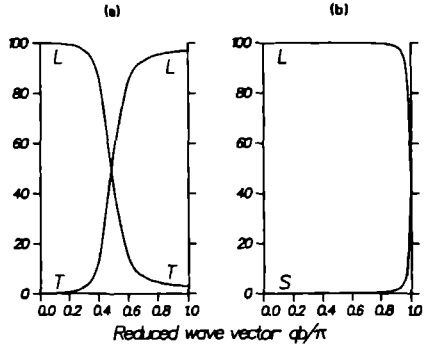

FIG 4 (a) Percentage of libron character of the two libron–phonon branches that show an avoided crossing in Fig 3 (b) Percentage of libron character of the two upper libron–magnon branches in Fig 3 that become degenerate at $qb/\pi = 1$

deed, given the negligible amount of mixing between the magnons and the lattice modes at $\mathbf{q} = \mathbf{0}$ this could be expected The agreement with the measured magnon frequencies[3] is also very satisfactory, especially if one considers that none of the parameters in our spin-dependent Hamiltonian have been fitted The different dispersion coefficients chosen in the spin-independent potential, see Table I, practically do not affect the magnon frequencies

In order to compare our first principles spin Hamiltonian (9) with the phenomenological one, Eq (1), we have also made spin-wave calculations on α-O_2 with the latter We have set the Heisenberg parameters J_{pp} equal to the calculated values, see Table IV For the first anisotropy parameter we have taken the free molecule value, $A = 5\ 712$ K, and for the second parameter we have adopted the value $B = 0\ 26$ K that yields the same spin-anisotropy field as a classical dipole model The results are listed in the second column of Table VII The higher magnon frequency, which is mostly determined by the values of J and A is almost the same as for the spin Hamiltonian (9) In the latter Hamiltonian the coupling parameter A has been multiplied by a sec

TABLE VI Phonon libron and magnon frequencies at $\mathbf{q} = \mathbf{0}$ in β-O_2 (potential C)

ω (cm^{-1})	Degeneracy	Character
0 0	1	pure magnon
15 0	2	pure magnon
39 5*	2	phonon <0 1% libron
53 4*	2	99 8% phonon 0 2% libron
54 3	2	pure libron (E_g)
70 8*	2	93 4% phonon 6 6% libron
71 7	1	pure magnon
71 8	2	pure magnon
96 4*	2	99 8% libron 0 2% phonon
96 4*	2	92 7% libron 7 3% phonon

*The modes correspond to modes at $\mathbf{q} = 2\pi/9a$ (1 $\sqrt{3}$ 0) and $\mathbf{q} = 2\pi/9a$ (1 $-\sqrt{3}$ 0) in the Brillouin zone of the structural lattice

ond rank tensor, see Eq (6), whose components have to be averaged over the librational states of the molecules, see Eq (24) The anisotropy component along the x axis (the crystal c^* axis) is still 95% of the free molecule value, however, and the components in the ab plane are smaller than 1% This explains the observed similarity The lower magnon frequency, which is mainly determined by J and B, is rather different for the spin Hamiltonians (1) and (9) We conclude that it is not justified to replace the exact magnetic dipole–dipole interaction operator in Eq (9) by an effective single-molecule term in Eq (1)

Let us now discuss the lattice modes in α- and β-oxygen, especially the two libron modes that correspond with $\mathbf{q} = \mathbf{0}$ in the structural unit cell These modes have been observed by Raman spectroscopy [6 36] In the hexagonal β phase they are degenerate with E_g symmetry, at a frequency of 48 cm^{-1} In the monoclinic α phase the a and b axes are no longer equivalent and, in principle, one finds two branches, one with B_g symmetry for the librations about the crystal a axis and one with A_g symmetry for librations about the b axis The splitting between the two Raman peaks observed (at 42 and 74 cm^{-1}) for α-O_2 is very large, however, in view of the small structural distortion Lattice dynamics calculations[8 10] have never yielded a splitting more than 10 cm^{-1} Therefore, it has mostly been assumed that the A_g and B_g modes remain accidentally degenerate at about 42 cm^{-1} and that the higher frequency mode should be interpreted as a two phonon/libron or libron–magnon transition [8] In support of this explanation, it has been suggested by Kuchta[45] on the basis of model calculations that the Heisenberg exchange term would help in restoring the A_g–B_g degeneracy Etters *et al* [37] have proposed that the higher frequency belongs to a libron mode which lies at the edge of the Brillouin zone for the structural lattice, but which has $\mathbf{q} = \mathbf{0}$ in the magnetic Brillouin zone This mode could become visible in Raman spectroscopy when there is a strong coupling between the librons and the spins The weakest point of all these interpretations is, however, that under various temperatures and pressures no indication of the doublet character of the lowest peak in α-O_2 has been observed Recent temperature dependent Raman measurements[6] suggest that the lower frequency peak corresponds with the B_g mode and the higher one with the A_g mode, so that the splitting would be about 32 cm^{-1} indeed

Our calculations offer a clear explanation of this problem It can be observed in Table VIII that, for any of the three potentials that we have taken the splitting between the B_g and A_g libron modes lies between 30 and 40 cm^{-1} Most of the splitting disappears if the Heisenberg term is omitted from the calculations Therefore, the older lattice dynamics calculations which have not included this term[8 10] or included it via a simple empirical model,[45] have failed to find this splitting It is only by the extremely strong anisotropy of the Heisenberg coupling parameter J, which has been found from the *ab initio* calculations,[21] that the large splitting is correctly reproduced This is confirmed by the plot of the lattice potential in Fig 5 along the normal coordinates for the B_g and A_g librons, with and without the contribution of the Heisenberg term We observe that this term lowers the

TABLE VII Optical ($q = 0$) magnon frequencies in α-O (potential C)

	Calculated		
	First principles from Eq (9)	Semiempirical from Eq (1) with B = 0 26 K	Experiment Ref 3
ω(cm $^{-1}$)	6 7	4 7	6 4
	22 2	22 7	27 5

lattice energy of α-O_2 at the equilibrium geometry At the same time it drastically increases the stiffness of the potential in the A_g direction, but much less in the B_g direction Actually this was clearly visible already in Fig 2 of Ref 21

The calculations with the different potentials A, B, and C also yield the correct relative magnitudes of the B_g and A_g libron frequencies in α-O_2 with respect to the E_g frequency in β-O_2 In any case, the inclusion of the Heisenberg term appeared to be essential The values of the frequencies are best reproduced by potential C, which has been partly adjusted to the E_g frequency in β-O_2

IV. CONCLUSIONS

We have proposed a lattice and spin Hamiltonian for solid O_2 with a form that is completely derived from first principles, and we have developed an integrated lattice dynamics and spin-wave formalism that can be used with this Hamiltonian Apart from the kinetic energy and the spin-independent intermolecular potential, which are present in any molecular crystal, the Hamiltonian describes the coupling between the O_2 triplet spin momenta The first of the spin-coupling terms is the usual Heisenberg exchange term, which is isotropic in spin space, the second one is due to the intramolecular spin–orbit and spin–spin coupling and the third term describes the magnetic dipole (spin–spin) interactions between different molecules Using well-known properties of the O_2 $^3\Sigma_g^-$ ground state and the results of *ab initio* calculations[21] on the O_2–O_2 dimer, all the spin-coupling parameters have been given (analytically) as functions of the (instantaneous) positions of the molecules in the lattice and their orientations The integrated lattice dynamics and spin-wave formalism, which is based on the random phase approximation, is an extension of a recent lattice dynamics approach [26–29] This approach has been developed for the description of large amplitude motions in molecular crystals and it has been applied already to solid N_2 We have applied the extended formalism to solid O_2 in the α and β phases

Since especially the Heisenberg exchange coupling parameter is strongly anisotropic and dependent on the intermolecular distance, a substantial coupling between the lattice vibrations in solid O_2 and its magnetic properties could be expected The actual mixing between the lattice modes, phonons and librons, and the magnons appears to be small, however Except for those (isolated) points in the Brillouin zone where the relevant dispersion curves show avoided crossings, this mixing can be neglected Thus, it is possible to treat the lattice dynamics and the spin waves separately

The lattice dynamics and spin-wave calculations which we have then made separately, are still substantially different from the earlier treatments In the lattice dynamics Hamiltonian we have retained the spin-coupling terms, with averaged spin operators Especially the inclusion of the Heisenberg term with its strong anisotropy appears to be crucial The spin factor $\langle \mathbf{S}_p \cdot \mathbf{S}_{p'} \rangle$ changes from ≈ -1 for the nearest neighbors in α-O_2 to ≈ -0.5 for those in β-O_2, which yields a discontinuity in the anisotropic potential at the α–β phase transition The coupling parameters in our spin hamiltonian have been obtained by averaging (renormalizing) the *ab initio* parameter functions over the lattice vibrations So, in contrast with the earlier spin-wave treatments, we were not obliged to fit any empirical parameters Another essential improvement upon these treatments is the explicit consideration of the magnetic dipole–dipole interaction as a two-body spin operator The only non *ab initio* data in our approach are the long range dispersion coefficients in the spin independent potential By choosing different values for these coefficients we have demonstrated, however, that our conclusions do not depend on this choice

The optical ($q = 0$) magnon frequencies from the spin wave calculations on α-O_2 are in fair agreement with the values from infrared and Raman spectrometry Especially if one considers that no parameter fitting was involved in these

TABLE VIII Optical ($q = 0$) libron frequencies in α and β O from pure libron calculations (cm $^{-1}$)

		Putting $J = 0$			Including $J(r_{pp'}, \omega_p, \omega_{p'})$			Experiment Ref 6	
Potential		A	B	C	A	B	C		
α-O_2	B_g	23 9	19 7	38 9	25 3	21 5	39 9	42 6/42 0	(T = 13/20 K)
	A_g	37 8	34 7	50 7	63 1	60 7	72 2	74 2/72 0	
β-O_2	E_g	28 4	24 6	42 9	42 4	39 6	53 6	48 0/42 0	(T = 25/40 K)

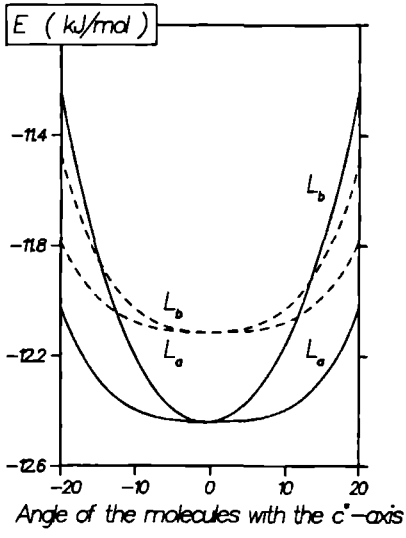

FIG 5 Variation of the potential energy of the α O crystal along the normal coordinates L_b and L_a of the B_g and A_g optical librations respectively The dashed curves denote the potential without the Heisenberg exchange contribution in the solid curves this contribution (see Fig 2 of Ref 21) has been added

calculations this is very satisfactory and it supports the validity of our first principles Hamiltonian A more detailed study of the magnetic properties of solid O_2 will be described in a subsequent paper [46]

The lattice dynamics results are even more rewarding They have led to a unique assignment of the Raman ($\mathbf{q} = \mathbf{0}$) libron peaks in α- and β O_2 The large splitting between the peaks in α-O_2 which could not be explained by any of the previous lattice dynamics calculations appears to be caused by the extremely strong anisotropy of the Heisenberg exchange coupling parameter For this reason, it was crucial to include the Heisenberg term in the lattice dynamics calculations and to know its dependence on the molecular orientations from *ab initio* calculations

ACKNOWLEDGMENTS

We thank Dr Paul Wormer and Dr Wim Briels for valuable discussions This investigation was supported in part by the Netherlands Foundation for Chemical Research (S O N) with financial aid from the Netherlands Organization for the Advancement of Pure Research (Z W O)

B Olinger R L Mills and R B Roof J Chem Phys **81** 5068 (1984)
H J Jodl F Bolduan and H D Hochheimer Phys Rev B **31** 7376 (1985)
G DeFotis Phys Rev B **23** 4714 (1981) and references therein
[P W Stephens and C F Majkrzak Phys Rev B **33** 1 (1986)
R J Meier and R B Helmholdt Phys Rev B **29** 1387 (1984)
[K D Bier and H J Jodl J Chem Phys **81** 1192 (1984)
H J Jodl W Loewen and D Griffith (to be published)
[K Kobashi M L Klein and V Chandrasekharan J Chem Phys **7** 843 (1979)
R D Etters A A Helmy and K Kobashi Phys Rev B **28** 2166 (1983)
A A Helmy K Kobashi and R D Etters J Chem Phys **80** 2782 (1984)
[V A Sivusarev Yu A Freiman and R P Yankelevich Sov J Low Temp Phys **6** 105 (1980) **7** 265 (1981)
R J Meier J H P Colpa and H Sigg J Phys C **17** 4501 (1984)
F A Matsen D J Klein and D C Foyt J Phys Chem **75** 1866 (1971)
[N Fuchikami and R Block Physica B **112** 369 (1982)
[M Mizushima *The Theory of Rotating Diatomic Molecules* (Wiley New York 1975)
[P W Stephens Phys Rev B **31** 4491 (1985)
[Yu B Gaididei and V M Loktev Sov J Low Temp Phys **6** 614 (1984)
[R J Meier C J Schinkel and A de Visser J Phys C **15** 1015 (1982)
[C Uyeda K Sugiyama and M Date J Phys Soc Jpn **54** 1107 (1985)
M C van Hemert P E S Wormer and A van der Avoird Phys Rev Lett **51** 1167 (1983)
[P F S Wormer and A van der Avoird J Chem Phys **81** 1929 (1984)
A P J Jansen and A van der Avoird Phys Rev B **31** 7500 (1985)
D M Brink and G R Satchler *Angular Momentum* (Clarendon Oxford 1968)
[A van der Avoird J Chem Phys **79** 1170 (1983)
J Metten B Heymen P Verhoeve J Reuss W C Laine and G Brocks Chem Phys **92** 9 (1985)
[W J Briels A P J Jansen and A van der Avoird J Chem Phys **81** 4118 (1984)
[A P J Jansen W J Briels, and A van der Avoird J Chem Phys **81** 3648 (1984)
[A van der Avoird W J Briels and A P J Jansen J Chem Phys **81** 3658 (1984)
[W J Briels A P J Jansen and A van der Avoird Adv Quantum Chem **18** 131 (1986)
[G T Trammel J Appl Phys Suppl **31** 362 (1960)
M Born and K Huang *Dynamical Theory of Crystal Lattices* (Clarendon Oxford 1954)
W J Briels J Chem Phys **73** 1850 (1980)
D J Margoliash and W J Meath J Chem Phys **68** 1426 (1978)
[F Visser P E S Wormer and W P J H Jacobs J Chem Phys **82** 3753 (1985)
[R M Berns and A van der Avoird J Chem Phys **72** 6107 (1980)
[J E Cahill and G E Leroi J Chem Phys **51** 97 (1969)
R D Etters K Kobashi and J Belak Phys Rev B **32** 4097 (1985)
[G E Jelinek L J Slutsky and A M Karo J Chem Phys Solids **33** 1279 (1972)
[J C Laufer and G E Leroi J Chem Phys **55** 993 (1971)
[A P J Jansen Phys Rev B **33** 6352 (1986)
[R J Meier Phys Lett A **107** 275 (1985)
[B Kuchta and T Luty Chem Phys Lett **126** 506 (1986)
[M P Orlova Sov J Phys Chem **12** 1603 (1966)
[C Kittel *Quantum Theory of Solids* (Wiley New York 1963)
[B Kuchta Chem Phys **95** 391 (1985)
[A P J Jansen and A van der Avoird (to be published)

SYMMETRY ANALYSIS OF THE LATTICE VIBRATIONS/SPIN WAVES OF α-O_2

A.P.J. Jansen
Institute of Theoretical Chemistry
University of Nijmegen
Toernooiveld
6525 ED Nijmegen
The Netherlands

Abstract

After determining the magnetic space group of α-O_2, we have made a symmetry analysis of the phonons, librons, and magnons in the context of the RPA formalism, and determined at which points in the Brillouin zone there is a mixing of the magnons and the librons/phonons. It is shown that the time reversal operator yields doubly degenerate modes at some points on the boundary of the Brillouin zone. We have derived the selection rules for IR and Raman spectroscopy. The magnons appear to be both IR and Raman active via their coupling with the magnetic dipole field of the radiation. This may be verified by experiments with polarized IR radiation.

1. Introduction

Solid oxygen is a unique system. It combines the properties of a molecular crystal with those of a magnetic material. The coupling of the structural and magnetic interactions leads to very interesting but also very complex phenomena. This is also apparent from the phase-diagram;[1] already at low pressures there are three phases instead of the ordinary one or two.

Experimental research on solid oxygen dates back to the beginning of this century.[2] However, the interpretation of these early and also of later measurements is still controversial.[3] It is very difficult to obtain single crystals of the α and β phase. Only recently the first experiments on single crystals of α-O_2 have been reported.[4] These experiments have proved to be very valuable, but most measurements today are still done on powder samples.

Until recently theorists have been treating the structural and magnetic properties separately.[5-11] In our institute we have developed a formalism to describe the coupling between the spin waves and the lattice vibrations. It is an extension of a formalism we developed to describe phonons, librons and their coupling in solid nitrogen.[12,13] Because of the close resemblance of our phonon-libron formalism to the usual spin wave theory we were able to integrate both schemes. Using this lattice vibrations/spin wave formalism we could explain the large libron-splitting in α-O_2 and the relative magnitudes of the libron frequencies in α- and β-O_2, basing ourselves on a spin-dependent Hamiltonian for the lattice dynamics calculations.[14,15]. Furthermore, our calculations yielded reasonable values for the optical magnon frequencies and detailed information on the coupling between magnons and librons/phonons.

In this paper we will investigate the symmetry aspects of this coupling in α-O_2. We will determine the symmetries of the lattice vibrations/spin waves. In the literature, only the symmetry assignment of the optical phonons and librons can be found.[16] This assignment is based on the harmonic approximation. The group theoretical analysis with this approximation has been described by Maradudin and Vosko.[17] We will use the Random Phase Approximation (RPA) as it applies both to librons/phonons and magnons. In cases where the harmonic approximation or the classical spin wave theory holds, the RPA formalism yields identical results. For a detailed description of the RPA formalism we refer to Ref. 13 and 15. A symmetry analysis for classical spin waves has been given by Sahni and Venkataraman.[18] We will also determine the selection rules for IR and Ra-

man spectroscopy, and suggest an experiment with polarized IR radiation.

2. The magnetic space group of α-O_2

The non-magnetic space group of α-O_2 as determined by X-ray diffraction measurements is C_{2h}^3 $(C2/m)$.[19] This group is not appropriate, however for a group theoretical analysis that includes the magnetic properties. For this purpose, we have to determine the magnetic space group of α-O_2, which is determined by the magnetic structure as obtained from neutron diffraction measurements.[20]

The magnetic space group contains a non-magnetic space group as a subgroup.[21] It is obvious that this subgroup must also be a subgroup of C_{2h}^3. From C_{2h}^3 we have to omit those primitive translations that connect the molecules in the two different magnetic sublattices. Thus we obtain the space group $C_{2h}^1(P2/m)$. The crystal, including the magnetic structure, is invariant under this space group. As it is a subgroup of C_{2h}^3 with index two, it must be the non-magnetic space group that we are looking for. In order to obtain the magnetic space group we add symmetry operations that relate the molecules on different sublattices to each other. An operation $\{\theta \,|\, \mathbf{r}(\theta)\}$ that reverses all spins and then translates all molecules by an intermolecular vector between nearest neighbours, interchanges the magnetic sublattices. Combining this operation with the elements of C_{2h}^1 we obtain the magnetic space group of α-O_2. Its Hermann-Mauguin symbol is C_P2/m in the notation of Opechowski and Guccione.[21] We write its elements as $\{\alpha \,|\, \mathbf{R}\}$ and $\{\alpha\theta \,|\, \mathbf{R}+\mathbf{r}(\theta)\}$, where $\alpha \in C_{2h}$, and $\mathbf{R}$ is a primitive translation of C_{2h}^1.

3. The equation of motion

The RPA formalism is based on the following equation of motion[13,15]

$$[H, c] = \hbar\omega c \tag{1}$$

where H is the Hamiltonian of the system, c an excitation operator, and $\hbar\omega$ an excitation energy. We will associate with every element $\{\alpha \,|\, \mathbf{R}\}$ or $\{\alpha\theta \,|\, \mathbf{R}+\mathbf{r}(\theta)\}$ of the magnetic space group of α-O_2 an operator $\hat{O}(\{\alpha \,|\, \mathbf{R}\})$ or $\hat{O}(\{\alpha\theta \,|\, \mathbf{R}+\mathbf{r}(\theta)\})$ that operates on the same Hilbert space as the Hamiltonian. These operators commute with the Hamiltonian. Suppose we have a complete set of excitation operators $\{c_i\}$. Then every operator $\hat{O}(\{\alpha \,|\, \mathbf{R}\})$ $c_i\hat{O}(\{\alpha \,|\, \mathbf{R}\})^{-1}$ and $\hat{O}(\{\alpha\theta \,|\, \mathbf{R}+\mathbf{r}(\theta)\})c_i\hat{O}(\{\alpha\theta \,|\, \mathbf{R}+\mathbf{r}(\theta)\})^{-1}$ is also an excitation operator with the same excitation energy as c_i. If we express these

operators as linear combinations of operators of the set $\{c_i\}$, we obtain (co)representations of the magnetic space group.[22] Assuming that there is no accidental degeneracy, the (co)representations are irreducible. The irreducible (co)representations of C_P2/m thus give us the degeneracies and and symmetries of the lattice vibrations/spin waves of α-O_2. In what follows we will determine these irreducible co-representations, and how they relate to RPA.

4. The symmetries of the single molecule MF states

In the RPA formalism the Hamiltonian and the excitation operators are expressed in terms of MF excitation operators (cf. Eq. (6)). These are in turn defined in terms of single molecule MF states. We thus start by looking at the symmetries of the single molecule MF states.

The transformation properties of these states under the point group $\{\alpha, \alpha\theta \mid \alpha \in C_{2h}\}$ are determined by a group of operators isomorphic to this point group. The operators corresponding with the elements of C_{2h} are defined as follows[23]

$$\hat{O}(\alpha)\psi(x) = \psi(\alpha^{-1}x) \tag{2}$$

for librational ($x = (\theta, \phi)$) or translational states ($x = \mathbf{r}$). If we write the spin states in the standard representation[24] then they transform as spherical harmonics under rotations. They are invariant under inversion.

The operator that yields the reversal of the spin momenta is the time reversal operator that is given by[24]

$$\hat{O}(\theta) = K_0 e^{-i\pi S_y}, \tag{3}$$

where K_0 is the complex conjugation operator. Again the spin states must be in standard representation. We note that the operators of Eq. (2) are unitary, whereas $\hat{O}(\theta)$ is antiunitary.

The symmetries of the single molecule MF states can be determined by inspection of the results of the MF calculations. However, we can also use some physical arguments. The $S = 1$ spin states transform according to the irreducible representation $D^{(1)+}$ of the direct product of the rotation group and the group C_i.[24] This representation decomposes under C_{2h} into $2B_g + A_g$. The MF ground spin state must have B_g symmetry because the state of A_g symmetry (i.e. $|m_s = 0\rangle$) has no spin momentum along the monoclinic axis. The two excited MF spin states must then be of A_g and B_g symmetry.

The total single molecule state must be symmetric under permutation of the nuclei (nuclear spin momentum $I = 0$ for $^{16}O_2$). The electronic ground state ($^3\Sigma_g^-$) is odd under this permutation, and the vibrational and translational factors are even, so that the librational states are ungerade. Librational states with A_u symmetry have a nodal plane perpendicular to the monoclinic axis. The equilibrium orientation is also perpendicular to the monoclinic axis, and therefore the librational MF ground state will have B_u symmetry. The librational MF excited states have A_u and B_u symmetry. The translational MF ground state will have no nodal plane and thus have A_g symmetry. The first three translational excited states will have one nodal plane and thus have A_u symmetry (a nodal plane perpendicular to the monoclinic axis) and B_u symmetry (the nodal plane contains the monoclinic axis; there are two of these states). The operator $\hat{O}(\theta)$ has no effect on the librational and translational MF states as they are real. It interchanges the corresponding MF spin states of the two magnetic sublattices.

5. Transformation properties of the MF (de)excitation operators

The MF crystal states are defined in terms of the single molecule MF states

$$\Psi_{\{m\}\{n\}\{k\}} \equiv \prod_P \psi^{(L)}_{m_P}(\Omega_{\mathbf{R}_P})\psi^{(T)}_{n_P}(\mathbf{r}_{\mathbf{R}_P})\psi^{(S)}_{k_P,I_P}(\sigma_{\mathbf{R}_P}). \tag{4}$$

The superscripts denote the types of motions; L stands for librations, T for translations and S for spin. Furthermore, I_P and $\mathbf{R}_P$ denote the sublattice to which molecule P belongs and the position of the molecule, respectively. We can define a group of operators, called the symmetry group of the Hamiltonian, that determines the transformation properties of these states under $C_P 2/m$, as follows

$$\begin{aligned}
&\hat{O}\left(\{\alpha \,|\, \mathbf{R}\}\right)\Psi_{\{m\}\{n\}\{k\}} \\
&\quad \equiv \hat{O}(\alpha)\prod_P \psi^{(L)}_{m_P}(\Omega_{\{\alpha\,|\,\mathbf{R}\}\mathbf{R}_P}) \\
&\qquad \times \psi^{(T)}_{n_P}(\mathbf{r}_{\{\alpha\,|\,\mathbf{R}\}\mathbf{R}_P})\psi^{(S)}_{k_P,I_P}(\sigma_{\{\alpha\,|\,\mathbf{R}\}\mathbf{R}_P}), \qquad (5a) \\
&\hat{O}\left(\{\alpha\theta \,|\, \mathbf{R}+\mathbf{r}(\theta)\}\right)\Psi_{\{m\}\{n\}\{k\}} \\
&\quad \equiv \hat{O}(\alpha)\prod_P \psi^{(L)}_{m_P}(\Omega_{\{\alpha\,|\,\mathbf{R}+\mathbf{r}(\theta)\}\mathbf{R}_P}) \\
&\qquad \times \psi^{(T)}_{n_P}(\mathbf{r}_{\{\alpha\,|\,\mathbf{R}+\mathbf{r}(\theta)\}\mathbf{R}_P})\psi^{(S)}_{k_P,I_{P,c}}(\sigma_{\{\alpha\,|\,\mathbf{R}+\mathbf{r}(\theta)\}\mathbf{R}_P}), \qquad (5b)
\end{aligned}$$

where $\hat{O}(\alpha)$ is defined by Eq. (2) but now it operates on all single molecule MF states, and $I_{P,c}$ denotes the sublattice that is not given by I_P. The operators in Eq. (5a) are unitary, whereas those in Eq. (5b) are antiunitary. We obtain the MF crystal ground state Ψ_0 if we put all m's, n's and k's in Eq. (4) equal to zero. We note that this state, combined with all electronic states of the molecules, is invariant under $C_P 2/m$. We get singly excited MF crystal states by taking one of the m's, n's and k's not equal to zero. Using the singly excited MF crystal states we can define the following operators

$$a^{\dagger}_{L,P,m} \equiv \left[\prod_{P' \neq P} \otimes \mathbf{1}_{P'}\right] \tag{6}$$
$$\otimes \left| \psi^{(L)}_m(\Omega_{\mathbf{R}_P}) \psi^{(T)}_0(\mathbf{r}_{\mathbf{R}_P}) \psi^{(S)}_{0,I_P}(\sigma_{\mathbf{R}_P}) \right\rangle \left\langle \psi^{(L)}_0(\Omega_{\mathbf{R}_P}) \psi^{(T)}_0(\mathbf{r}_{\mathbf{R}_P}) \psi^{(S)}_{0,I_P}(\sigma_{\mathbf{R}_P}) \right|$$

(and analogous operators for the translation and the spin). These operators yield singly excited MF crystal states when working on the MF crystal ground state Ψ_0. They transform as

$$a^{\dagger}_{K,P,m} \xrightarrow[\{\alpha\theta \,|\, \mathbf{R}+\mathbf{r}(\theta)\}]{\{\alpha \,|\, \mathbf{R}\}} \hat{O}\begin{pmatrix} \{\alpha \,|\, \mathbf{R}\} \\ \{\alpha\theta \,|\, \mathbf{R}+\mathbf{r}(\theta)\} \end{pmatrix} a^{\dagger}_{K,P,m} \hat{O}^{\dagger}\begin{pmatrix} \{\alpha \,|\, \mathbf{R}\} \\ \{\alpha\theta \,|\, \mathbf{R}+\mathbf{r}(\theta)\} \end{pmatrix}. \tag{7}$$

We adapt these operators to the translational symmetry of the crystal

$$a^{\dagger}_{\mathbf{q},K,I,m} \equiv \frac{1}{\sqrt{N}} \sum_{P \in \text{sublattice } I} e^{i\mathbf{q}\cdot\mathbf{R}_P} a^{\dagger}_{K,P,m}, \tag{8}$$

where N denotes the number of unit cells. The transformation properties of the translationally adapted operators under $C_P 2/m$ are given by

$$\hat{O}(\{\alpha \,|\, \mathbf{R}\})\, a^{\dagger}_{\mathbf{q},K,I,m}\, \hat{O}^{\dagger}(\{\alpha \,|\, \mathbf{R}\}) = S_{\alpha K m}\, e^{-i\alpha\mathbf{q}\cdot\mathbf{R}}\, a^{\dagger}_{\alpha\mathbf{q},K,I,m}, \tag{9a}$$

$$\hat{O}(\{\alpha\theta \,|\, \mathbf{R}+\mathbf{r}(\theta)\})\, a^{\dagger}_{\mathbf{q},K,I,m}\, \hat{O}^{\dagger}(\{\alpha\theta \,|\, \mathbf{R}+\mathbf{r}(\theta)\}) = S_{\alpha K m}\, e^{i\alpha\mathbf{q}\cdot(\mathbf{R}+\mathbf{r}(\theta))}\, a^{\dagger}_{-\alpha\mathbf{q},K,I_c,m}, \tag{9b}$$

where $S_{\alpha K m} = \pm 1$ (see Table 1), and I_c denotes the sublattice that is not given by I.

In deriving Eq. (9b) we have used that $\hat{O}(\{\alpha\theta \,|\, \mathbf{R}+\mathbf{r}(\theta)\})$ is antiunitary and that also for an antiunitary operator A

$$A\big(|\,\psi\rangle\langle\phi\,|\big)A^{\dagger} = \big(A\,|\,\psi\rangle\big)\,\big(\langle\phi\,|\,A^{\dagger}\big) \tag{10}$$

Table 1. The factor $S_{\alpha Km}$ in Eq. (9).

		$\alpha \in C_{2h}$			
K	symmetry of $\psi_m^{(K)}$	E	C_2	I	σ
L	A_u	1	−1	1	−1
	B_u	1	1	1	1
T	A_u	1	1	−1	−1
	B_u	1	−1	−1	1
S	A_g	1	−1	1	−1
	B_g	1	1	1	1

holds. We observe that the values for $S_{\alpha Km}$ are not the characters of the irreducible representations of C_{2h} which are spanned by the states ψ_m. The reason for this is that the single molecule MF ground states do not all have A_g symmetry.

The excitation operators of Eq. (6) play the same role in the RPA formalism as the displacement coordinates in the harmonic approximation. In particular their transformation properties are the same.

6. The transformation properties of the RPA matrix and its eigenvectors

We can now determine the transformation properties of the RPA matrix. Let us first write the Hamiltonian in second quantized form

$$H = \langle \Psi_0 \mid H \mid \Psi_0 \rangle + \sum_{\mathbf{q}} \Bigg[\sum_{KK'} \sum_{IJ} \sum_{mn} {}^{\mathbf{q}}V_{IJ}^{KK'}(m,n) a^{\dagger}_{\mathbf{q}KIm} a_{\mathbf{q}K'Jn} + \sum_{\substack{KK' \\ K \le K'}} \sum_{IJ} \sum_{mn} {}^{\mathbf{q}}W_{IJ}^{KK'}(m,n) a^{\dagger}_{\mathbf{q}KIm} a^{\dagger}_{-\mathbf{q}K'Jn} + \text{h.c.} \Bigg]. \tag{11}$$

This Hamiltonian must be invariant under $C_P 2/m$. Using Eq. (9a) we find for the coefficients

$$ {}^{\alpha\mathbf{q}}V_{IJ}^{KK'}(m,n) = {}^{\mathbf{q}}V_{IJ}^{KK'}(m,n) S_{\alpha Km} S_{\alpha K'n}, \tag{12a}$$

$$ {}^{\alpha\mathbf{q}}W_{IJ}^{KK'}(m,n) = {}^{\mathbf{q}}W_{IJ}^{KK'}(m,n) S_{\alpha Km} S_{\alpha K'n}, \tag{12b}$$

and using Eq. (9b) we find

$$^{-\alpha\mathbf{q}}V^{KK'}_{I_cJ_c}(m,n)^* = {}^{\mathbf{q}}V^{KK'}_{IJ}(m,n)S_{\alpha Km}S_{\alpha K'n}, \tag{13a}$$

$$^{-\alpha\mathbf{q}}W^{KK'}_{I_cJ_c}(m,n)^* = {}^{\mathbf{q}}W^{KK'}_{IJ}(m,n)S_{\alpha Km}S_{\alpha K'n}. \tag{13b}$$

The RPA equation is obtained by substituting

$$c^{\chi}_{\mathbf{q}} = \sum_{KIm}\left[c^{(\chi+)}_{\mathbf{q}KIm}a^{\dagger}_{\mathbf{q}KIm} + c^{(\chi-)}_{\mathbf{q}KIm}a_{-\mathbf{q}KIm}\right] \tag{14}$$

into Eq. (1). It is an eigenvalue equation of the matrix

$$R(\mathbf{q}) = \begin{pmatrix} {}^{\mathbf{q}}A & -({}^{-\mathbf{q}}B) \\ {}^{\mathbf{q}}B^* & -({}^{-\mathbf{q}}A)^T \end{pmatrix}, \tag{15}$$

with

$$^{\mathbf{q}}A_{KIm,K'Jn} = {}^{\mathbf{q}}V^{KK'}_{IJ}(m,n), \tag{16}$$

and

$$^{\mathbf{q}}B_{KIm,K'Jn} = \begin{cases} {}^{\mathbf{q}}W^{KK}_{JI}(n,m) + {}^{\mathbf{q}}W^{KK}_{IJ}(m,n), & \text{if } K = K' \\ {}^{\mathbf{q}}W^{KK'}_{JI}(n,m), & \text{if } K > K' \\ {}^{-\mathbf{q}}W^{K'K}_{IJ}(m,n), & \text{if } K < K'. \end{cases} \tag{17}$$

Now, defining

$$\tilde{\Gamma}\left(\mathbf{q};\, {}^{\{\alpha\,|\,\mathbf{R}\}}_{\{\alpha\theta\,|\,\mathbf{R}+\mathbf{r}(\theta)\}}\right) \equiv \begin{pmatrix} \Gamma\left(\mathbf{q};\, {}^{\{\alpha\,|\,\mathbf{R}\}}_{\{\alpha\theta\,|\,\mathbf{R}+[\mathbf{r}(\theta)\}}\right) & 0 \\ 0 & \Gamma\left(\mathbf{q};\, {}^{\{\alpha\,|\,\mathbf{R}\}}_{\{\alpha\theta\,|\,\mathbf{R}+\mathbf{r}(\theta)\}}\right) \end{pmatrix} \tag{18}$$

with

$$\Gamma(\mathbf{q};\{\alpha\,|\,\mathbf{R}\})_{KIm,K'Jn} = e^{-i\mathbf{q}\cdot\mathbf{R}}S_{\alpha Km}\delta_{KK'}\delta_{IJ}\delta_{mn}, \tag{19a}$$

$$\Gamma(\mathbf{q};\{\alpha\,|\,\mathbf{R}+\mathbf{r}(\theta)\})_{KIm,K'Jn} = e^{-i\mathbf{q}\cdot(\mathbf{R}+\mathbf{r}(\theta))}S_{\alpha Km}\delta_{KK'}\delta_{IJ_c}\delta_{mn}, \tag{19b}$$

we obtain using Eqs. (12), (13), (15)–(17)

$$\tilde{\Gamma}(\mathbf{q};\{\alpha\,|\,\mathbf{R}\})\,R(\mathbf{q})\,\tilde{\Gamma}(\mathbf{q};\{\alpha\,|\,\mathbf{R}\})^{\dagger} = R(\alpha\mathbf{q}), \tag{20a}$$

$$\left[\tilde{\Gamma}(\mathbf{q};\{\alpha\theta\,|\,\mathbf{R}+\mathbf{r}(\theta)\})K_0\right]R(\mathbf{q})\left[\tilde{\Gamma}(\mathbf{q};\{\alpha\theta\,|\,\mathbf{R}+\mathbf{r}(\theta)\})K_0\right]^{\dagger} = R(-\alpha\mathbf{q}). \tag{20b}$$

The matrices (18) form a co-representation of $C_P 2/m$ if the wave vector $\mathbf{q}$ lies in the interior of the Brillouin zone. Equation (20) shows that the solutions of the RPA equation with wave vector $\mathbf{q}$ form bases for the irreducible co-representations of the subgroup of $C_P 2/m$ with elements $\{\alpha \,|\, \mathbf{R}\}$ and $\{\alpha\theta \,|\, \mathbf{R} + \mathbf{r}(\theta)\}$ with $\alpha\mathbf{q} = \mathbf{q}$ and $\alpha\mathbf{q} = -\mathbf{q}$, respectively. Bases for the irreducible co-representations of $C_P 2/m$ are obtained by collecting those solutions of the RPA equations that correspond with the different wave vectors of a star.

If we place the coefficients $c^{(x\pm)}_{\mathbf{q}KIm}$ in Eq. (14) in a column vector $\mathbf{c_q}$ we find using Eq. (9)

$$\mathbf{c_q} \xrightarrow{\{\alpha \,|\, \mathbf{R}\}} \tilde{\Gamma}(\mathbf{q}; \{\alpha \,|\, \mathbf{R}\})\mathbf{c_q}, \tag{21a}$$

$$\mathbf{c_q} \xrightarrow{\{\alpha\theta \,|\, \mathbf{R}+\mathbf{r}(\theta)\}} \tilde{\Gamma}(\mathbf{q}; \{\alpha\theta \,|\, \mathbf{R} + \mathbf{r}(\theta)\})K_0\mathbf{c_q}, \tag{21b}$$

if $\alpha\mathbf{q} = \mathbf{q}$ and $\alpha\mathbf{q} = -\mathbf{q}$, respectively. Actually these transformations led us to Eqs. (18)–(20).

If $\mathbf{q}$ lies on the zone boundary we have to take a subgroup of $C_P 2/m$ with $\alpha\mathbf{q} = \mathbf{q}+\mathbf{Q}$ and $\alpha\mathbf{q} = -\mathbf{q}+\mathbf{Q}$, where $\mathbf{Q}$ is a primitive translation of the reciprocal lattice. For some wave vectors we must make some sign changes in Eq. (19b), according to Eq. (21b). However, this is really immaterial. In what follows we will only need to know the irreducible representations of non-magnetic space groups.

7. The symmetries of the lattice vibrations/spin waves

We can now determine the symmetries of the lattice vibrations/spin waves for every wave vector $\mathbf{q}$. There are essentially three steps. First, we have to determine the subgroup $\{\{\alpha \,|\, \mathbf{R}\}, \{\alpha\theta \,|\, \mathbf{R} + \mathbf{r}(\theta)\}\}$ of $C_P 2/m$ with $\alpha\mathbf{q} = \mathbf{q} + \mathbf{Q}$ for the non-magnetic elements and $\alpha\mathbf{q} = -\mathbf{q} + \mathbf{Q}$ for the magnetic elements. Secondly, we have to determine the irreducible representations with wave vector $\mathbf{q}$ of the subgroup of this subgroup that consists of all non-magnetic elements. Thirdly, we have to check whether the magnetic elements yield extra degeneracies.

All three steps are easy. The first step is trivial. The subgroup of the second step is a symmorphic space group. The irreducible representations are found by looking up the irreducible representations of the point group of the elements for which $\alpha\mathbf{q} = \mathbf{q} + \mathbf{Q}$ holds and then multiply with $\exp(-i\mathbf{q}\cdot\mathbf{R})$. The irreducible co-representations that give the symmetries of the lattice vibrations/spin waves are determined in the third step.

Table 2. The symmetry of the lattice vibrations/spin waves.

		symmetry of the single molecule MF state that is excited					
		librations		translations		spin	
point in the Brillouin zone[25]	$\{\alpha\|\alpha\mathbf{q} = \mathbf{q}+\mathbf{Q}\}$	A_u	B_u	A_u	B_u	A_g	B_g
general	C_1	-	-	-	-	-	-
plane $ABΓY$	C_s	A''	A'	A''	A'	A''	A'
plane $EDZC$	C_s	$A'+A''$	$A'+A''$	$A'+A''$	$A'+A''$	$A'+A''$	$A'+A''$
line ZC	C_2	B	A	A	B	B	A
lines AE and BD	C_2	$A+B$	$A+B$	$A+B$	$A+B$	$A+B$	$A+B$
Γ and Y	C_{2h}	B_g	A_g	A_u	B_u	B_g	A_g
Λ	C_2	B	A	A	B	B	A
Z and C	C_{2h}	B_g+B_u	A_g+A_u	A_g+A_u	B_g+B_u	B_g+B_u	A_g+A_u
A and B	C_{2h}	A_u+B_g	A_g+B_u	A_u+B_g	A_g+B_u	A_u+B_g	A_g+B_u
E and D	C_{2h}	A_g+B_g	A_g+B_g	A_u+B_u	A_u+B_u	A_g+B_g	A_g+B_g
		librons		phonons		magnons	

We know from group theory that the irreducible co-representations of a magnetic group are characterized by the irreducible representations of the subgroup of all non-magnetic elements that they subduce.[22] There are three possibilities. If the irreducible co-representation is of the first kind it subduces one irreducible representation; if it is of the second kind it subduces two equivalent irreducible representations and if it is of the third kind it subduces two non-equivalent irreducible representations. There is a doubling of the degeneracy if the irreducible co-representation is of the second or third kind. Fortunately, the following simple character test enables us to classify the irreducible co-representation.

$$\sum_{\substack{\alpha,\mathbf{R} \\ \alpha\mathbf{q}=-\mathbf{q}+\mathbf{Q}}} \chi(\{\alpha\theta\,|\,\mathbf{R}+\mathbf{r}(\theta)\}^2) = M, -M, \text{ or } 0, \tag{22}$$

where M is the number of terms in the summation and χ is the character of an irreducible representation. The different results of the summation hold for an irreducible co-representation of the first, second and third kind, respectively. We note that we only need to know the irreducible representations of a non-magnetic space group.

As the third step we thus take all irreducible representations that we have found in the second step and apply the character test above. The result indicates from what kind of irreducible co-representation the irreducible representation is subduced. The final results are shown in Table 2. The modes are labelled using the wave vector and the label of the irreducible representation of the point group. A plus sign denotes an irreducible co-representation that subduces two irreducible representations. The labels denote these two irreducible representations. The two irreducible representations that are subduced by the same irreducible co-representation of the third kind can be determined by operating with $\{\theta\,|\,\mathbf{r}(\theta)\}$ on the basis of the irreducible representations. We note that all irreducible co-representations are of the first or of the third kind. Those of the first kind are one-dimensional and those of the third kind are two-dimensional. The symmetry assignments of the phonons and librons are the same as we would have obtained when working with the harmonic approximation and two molecules per unit cell.[17] We can visualize the irreducible co-representations of the third kind as follows. Imagine that only the molecules of one sublattice participate in an excitation. The excitation has a certain point group symmetry. The operation $\{\theta\,|\,\mathbf{r}(\theta)\}$ translates the excitation to the other sublattice, thereby changing its symmetry (see Fig. 1 for two examples).

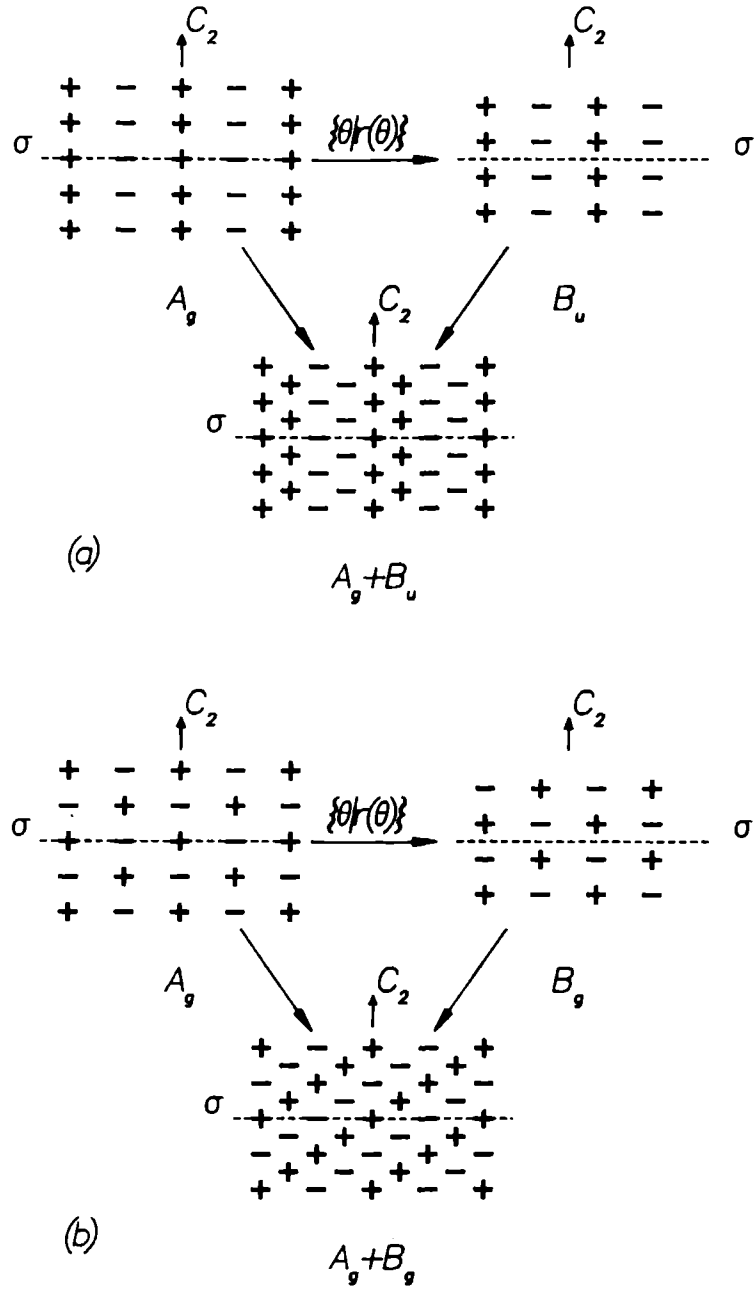

Fig. 1. Signs of the coefficients in the basis vectors of the irreducible co-representations $A_g + B_u$ of the A-point (a) and $A_g + B_g$ of the E-point (b). The basis vectors are expressed in terms of the excitation operators of Eq. (6). (Only operators with A_g symmetry are considered.)

8. Selection rules for IR and Raman spectroscopy

A practical application of the group theoretical analysis is the determination of the selection rules for IR and Raman spectroscopy. According to the symmetry analysis for α-oxygen based on the harmonic approximation, two libron modes, one with A_g and one with B_g symmetry, should be Raman active. No modes should be IR active.[16] This analysis, however, does not apply to magnons.

If we restrict ourselves to one-phonon, -libron, and -magnon modes then only optical ($\mathbf{q} = \mathbf{0}$) modes can be IR or Raman active.[26] The dominant interaction with radiation fields for IR adsorption is normally the electric dipole interaction. Other interactions that are linear in the field strength are the magnetic dipole and the electric quadrupole interactions. We can neglect the last interaction because of the long wavelength of the IR radiation.[27] The electric dipole operator has one component with A_u and two components with B_u symmetry. The optical phonons thus may be IR active by coupling to the electric dipole field. The magnetic dipole operator has one component with A_g and two components with B_g symmetry. The optical librons and magnons thus may be IR active by coupling to the magnetic dipole field. The intensity in Raman scattering is quadratic in the electric and magnetic dipole operators.[28] The relevant entities are the electric polarisability, the magnetic susceptibility and a mixed susceptibility term which is a combination of an electric and a magnetic transition dipole. The former two can be decomposed into parts having A_g and B_g symmetry, and the mixed term into parts having A_u and B_u symmetry. All modes thus may be Raman active.

From this analysis it seems that more modes are IR or Raman active than are actually observed experimentally. Optical phonons are observed neither in IR nor in Raman spectra. The reason for this is as follows. In Table 2 we can observe that the optical phonons do not couple to the magnons. This means that they can be labelled according to the non-magnetic space group C_{2h}^3 of α-O_2. Their wave vector then will lie on the boundary of the Brillouin zone corresponding to the structural unit cell. In other words, the excitations on nearest neighbours for the optical phonons are out-of-phase, and consequently the optical phonons will be neither IR nor Raman active.

As the coupling between the librons and the magnons is small,[15] this holds also for half of the librons. The other two libron modes, which are Raman active, are not observed in IR spectra because the magnetic transition

dipole moments are probably too small. The $\mathbf{q} = \mathbf{0}$ magnons are observed in IR as well as in Raman spectra. As has been pointed out above, they are IR active because they couple to the magnetic dipole field. The magnetic transition dipole moments for the magnons are large. Therefore, it is probably the magnetic susceptibility that leads to the observation of magnon excitations in Raman experiments.

9. Conclusions

We have derived the symmetries of the lattice vibrations/spin waves of α-oxygen by looking at the solutions of the RPA equations. Because of the non-zero electronic spin momentum of the O_2 molecules, a magnetic space group is required to describe the symmetry of α-O_2. The symmetry group of the Hamiltonian consequently contains antiunitary operators. This in turn leads to the use of co-representations.

The results differ in several aspects from those which are obtained when neglecting the magnetic structure of α-O_2. Except for the Γ-, E- and D-point in the Brillouin zone, the magnons couple to the librons and the phonons. For the Γ-, E- and D-point the magnons only couple to the librons. At the boundary of the Brillouin zone the lattice vibrations/spin waves may become degenerate due to the time-reversal symmetry. The results as shown in Table 2 confirm the results of the numerical calculations we have made.[15] There are some slight errors in the dispersion curves in Fig. 3 of Ref. 15. Some forbidden crossings were not detected due to the smallness of the coupling between the magnons and the phonons/librons.

The selection rules derived from the group theoretical analysis for IR and Raman spectroscopy agree with experiment. The magnon peaks in IR spectra can be explained by the coupling of the magnons to the IR radiation via the magnetic dipole interaction. Inspection of the results of the numerical calculation[15] shows that the magnons at 6.4 and 27.3 cm^{-1} have B_g symmetry. This means that no adsorption should be observed in an experiment with a single crystal and polarized IR radiation with the magnetic dipole field parallel to the monoclinic axis. On the other hand, the libron at 42 cm^{-1} [29] may be observed in this experiment, depending on the strength of the libron-magnon coupling. The libron at 72 cm^{-1} [29] may be observed if the IR radiation is polarized with the magnetic dipole field perpendicular to the monoclinic axis. It would be interesting to perform these experiments.

Acknowledgments

This investigation was supported in part by the Netherlands Foundation for Chemical Research (S.O.N.) with financial aid from the Netherlands Organization for the Advancement of Pure Research (Z.W.O.).

References

[1] B. Olinger, R.L. Mills, and R.B. Roof Jr., J. Chem. Phys. **81**, 5068 (1984).
[2] A. Perrier, and H. Kamerlingh Onnes, Leiden Comm. **139c**, 25 (1914).
[3] G.C. DeFotis, Phys. Rev. B**23**, 4714 (1981) and references therein.
[4] A.F. Prikhot'ko, Yu.G. Pikus, L.J. Shanskiĭ, and D.G. Danilov, JETP Lett. **42**, 251 (1985).
[5] K. Kobashi, M.L. Klein, and V. Chandrasekharan, J. Chem. Phys. **71**, 843 (1979).
[6] R.D. Etters, A.A. Helmy, and K. Kobashi, Phys. Rev. B**28**, 2166 (1983).
[7] A.A. Helmy, K. Kobashi, and R.D. Etters, J. Chem. Phys. **80**, 2782 (1984).
[8] R.D. Etters, K. Kobashi, and J. Belak, Phys. Rev. B**32**, 4097 (1985).
[9] V.A. Slyusarev, Yu.A. Freiman, and R.P. Yankelevich, Sov. J. Low Temp. Phys. **6**, 105 (1980); **7**, 265 (1981).
[10] Yu.B. Gaididei, and V.M. Loktev, Sov. Phys. Solid State **16**, 2226 (1975).
[11] R.J. Meier, J.H.P. Colpa, and H. Sigg, J. Phys. C**17**, 4501 (1984).
[12] W.J. Briels, A.P.J. Jansen, and A. van der Avoird, J. Chem. Phys. **81**, 4118 (1984).
[13] W.J. Briels, A.P.J. Jansen, and A. van der Avoird, Adv. Quant. Chem. **18**, 131 (1986).
[14] A.P.J. Jansen, and A. van der Avoird, Phys. Rev. B**31**, 7500 (1985).
[15] A.P.J. Jansen, and A. van der Avoird, J. Chem. Phys. **86**, 3583 (1987).
[16] J.E. Cahill, and G.E. Leroi, J. Chem. Phys. **51**, 97 (1969).
[17] A.A. Maradudin, and S.H. Vosko, Rev. Mod. Phys. **40**, 1 (1968).
[18] V.C. Sahni, and G. Venkataraman, Adv. Phys. **23**, 547 (1974).
[19] C.S. Barrett, L. Meyer, and J. Wasserman, J. Chem. Phys. **47**, 592 (1967).
[20] R.J. Meier, and R.B. Helmholdt, Phys. Rev. B**29**, 1387 (1984).
[21] W. Opechowski, and R. Guccione, in *Magnetism*, edited by G.T. Rado and H. Suhl (Academic Press, New York, 1965), Vol. II A.
[22] L. Jansen, and M. Boon, *Theory of Finite Groups. Application in Physics* (North-Holland, Amsterdam, 1967).
[23] E.P. Wigner, *Group Theory* (Academic Press, New York, 1965).
[24] A. Messiah, *Quantum Mechanics* (North-Holland, Amsterdam, 1969).

[25] G.F. Koster, in *Solid State Physics*, edited by F. Seitz and D. Turnbull (Academic Press, New York, 1957), Vol. 5, p. 173.
[26] A.P. Cracknell, Adv. Phys. **23**, 673 (1974).
[27] R. Loudon, *The Quantum Theory of Light* (Clarendon Press, Oxford, 1973).
[28] M. Born, and K. Huang, *Dynamical Theory of Crystal Lattices* (Clarendon Press, Oxford, 1954).
[29] K.D. Bier, and H.J. Jodl, J. Chem. Phys. **81**, 1192 (1984).

Section 3.3

Magnetic structure of β-oxygen

A P J Jansen
Institute of Theoretical Chemistry, University of Nijmegen, Toernooiveld, 6525 ED Nijmegen, The Netherlands
(Received 8 October 1985)

Treating the spins classically, we show that for β-O_2 the two-dimensional three-sublattice structure is unstable with respect to interlayer exchange couplings The energetically most favorable structure is found to be incommensurate Quantum-mechanical spin-wave calculations agree with the conclusions from the classical magnetic-structure calculations

I INTRODUCTION

The combination of magnetic and molecular properties makes solid oxygen a unique system Although it has been studied for a long time, much remains unexplained One of the unsolved problems is the magnetic structure of the β phase This phase consists of stacked triangular layers forming a structure with space group $R\bar{3}m$ (see Fig 1) [1]

Magnetic susceptibility measurements[2,3] indicate that β-O_2 is a triangular antiferromagnet The main feature of *triangular antiferromagnets is an intrinsic frustration effect* If only intralayer nearest-neighbor exchange interactions are taken into account, we already have a complex system If the spins are treated classically, it can be proved that they adopt a three-sublattice structure, i e, the nearest-neighbor spins make angles of 120° [4,5] However, a quantum-mechanical treatment of $S=\frac{1}{2}$ spins on such lattice has shown that there are other structures, which are energetically more favorable [6] This may be true for β-O_2 ($S=1$) also Actually, the situation is more complex because of the interlayer exchange interactions In most papers it is assumed that the layers adopt the three-sublattice structure, and that there is no interaction between the layers [7,8] The latter assumption follows from the former in this sense, that if the spins are treated classically, then the field for a given spin due to the spins in other layers vanishes exactly The first assumption of a perfect three-sublattice structure is, however, in contradiction with neutron diffraction, which shows only short-range but no long-range order [9]

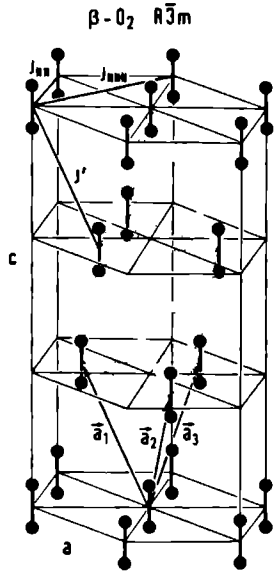

FIG 1 Structure of β-O_2

In a recent paper[10] a magnetic structure calculation was done for a system with a comparable lattice (i e, C_6Eu) It was shown, using a model worked out by Nagamiya,[11] that the three-sublattice structure lost its long-range order due to the interlayer exchange coupling In this paper we determine the magnetic structure of β-O_2, using the same model We check whether β-O_2 shows the same distortion of the three-sublattice structure as C_6Eu, thus explaining the neutron-diffraction experiment Moreover, we compare the results of this classical model with those from quantum-mechanical spin-wave calculations

II THEORY

As we have shown in a previous paper,[12] the spin-dependent part of the Hamiltonian of solid oxygen can be written as a sum of three terms

$$H=H_{ex}+H_{s.o.}+H_{dip} \tag{2.1}$$

The first term is the well-known Heisenberg exchange term, the second term is due to the intramolecular spin-spin and spin-orbit coupling, which couples the spin to the molecular axis, and the third term describes the magnetic dipole-dipole coupling between the spin momenta Wormer and van der Avoird[13] have shown that the exchange-coupling constant J in

$$H_{ex}=-2\sum_{(a,m)}J_{a-m}\mathbf{S}_a\,\mathbf{S}_m \tag{2.2}$$

strongly depends on the positions and the orientations of the molecules In this equation the sum runs over all spin pairs The composite index $\mathbf{n}=\{n_1,n_2,n_3\}$ denotes the spin at $\mathbf{R}_n=n_1\mathbf{a}_1+n_2\mathbf{a}_2+n_3\mathbf{a}_3$, $\mathbf{a}_1$, $\mathbf{a}_2$, and $\mathbf{a}_3$ being primitive translations (see Fig 1) Also, the other two terms contain position- and orientation-dependent factors [12] However, in a mean-field (MF) sense we can take statistical averages over the lattice vibrations and make the Hamiltonian of Eq (2 1) only spin dependent The Heisenberg term then remains formally the same, with the coupling parameter J replaced by its average value The second term $H_{s.o.}$ for the β phase simplifies further if we assume that the librations of the molecules are small so that effectively the molecular axes are fixed along the crystallographic c axis, which we take as the z axis (see Fig 1) This leads to the form in which this term is normally used [14]

$$H_{s.o.}=A\sum_{\mathbf{n}}S_{\mathbf{n}z}^2 \quad (A>0) \tag{2 3}$$

As the dipole-dipole term is much smaller than the other two, we neglect it altogether (usually, instead of the dipole-dipole term, one takes an in-plane anisotropy term, which is zero in β-O_2) [15]

In order to determine the magnetic structure, we follow a standard method that treats the spins classically [11] We start by taking only the Heisenberg term into account Defining

$$J(\mathbf{q})=\sum_{\mathbf{n}}J_{\mathbf{n}}e^{i\mathbf{q}\cdot\mathbf{R}_{\mathbf{n}}} \tag{2 4a}$$

and

$$\mathbf{S}(\mathbf{q})=N^{-1/2}\sum_{\mathbf{n}}\mathbf{S}_{\mathbf{n}}e^{i\mathbf{q}\cdot\mathbf{R}_{\mathbf{n}}}, \tag{2 4b}$$

the energy pertaining to the Heisenberg term can be written as

$$E_{ex}=-\sum_{\mathbf{q}}J(\mathbf{q})\mathbf{S}(\mathbf{q})\cdot\mathbf{S}(-\mathbf{q}) \tag{2 5}$$

The magnetic structure is obtained by minimizing this energy with the restriction that $\mathbf{S}_{\mathbf{n}}^2=S^2=1$ for all $\mathbf{n}$ The minimum energy is given by

$$-NS^2J(\mathbf{Q}) \tag{2 6}$$

Here $\mathbf{Q}$ is a vector that maximizes $J(\mathbf{q})$ The spin orientations are given by

$$\mathbf{S}_{\mathbf{n}}=N^{-1/2}[e^{-i\mathbf{Q}\cdot\mathbf{R}_{\mathbf{n}}}\mathbf{S}(\mathbf{Q})+e^{i\mathbf{Q}\cdot\mathbf{R}_{\mathbf{n}}}\mathbf{S}(-\mathbf{Q})], \tag{2 7}$$

where $\mathbf{S}(\mathbf{Q})$ $[=\mathbf{S}(-\mathbf{Q})^*]$ is arbitrary with the restriction on $\mathbf{S}_{\mathbf{n}}^2$ mentioned above We note that in the minimum-energy configuration all spins lie in a plane As the Heisenberg Hamiltonian is isotropic in spin space, it is clear that we can choose the plane we want the spins to lie in If we interpret the operator $S_{\mathbf{n}x}$ classically as the z component of the spin $\mathbf{S}_{\mathbf{n}}$, we see that, as $A\sum_{\mathbf{n}}S_{\mathbf{n}x}^2\geq 0$, we can minimize this term if we put all spins parallel to the crystallographic a-b plane. The orientations of the spins then become

$$\begin{aligned} S_{\mathbf{n}x}&=S\sin(\mathbf{Q}\cdot\mathbf{R}_{\mathbf{n}}),\\ S_{\mathbf{n}y}&=S\cos(\mathbf{Q}\cdot\mathbf{R}_{\mathbf{n}}),\\ S_{\mathbf{n}z}&=0 \end{aligned} \tag{2 8}$$

The foregoing discussion shows that this structure minimizes the energy of the total Hamiltonian, and thus that Eqs (2 8) denote the orientations that the spins will adopt in the ground state of the crystal

In order to get further support for the results of these classical calculations, via a quantum-mechanical treatment of the spins, we have computed magnon frequencies using the MF formalism followed by the random-phase approximation (RPA), starting from the three-sublattice structure If only the Heisenberg term is taken into account, MF yields the same magnetic ground state as the classical model [11] However, we can impose the translational symmetry of the three-sublattice structure on the MF solution MF then yields this structure and RPA yields the corresponding magnon frequencies This method is well known, therefore, we just refer to Refs 12, 16, and 17 for details As we are interested in the stability of the three-sublattice structure, we have to scan reciprocal space to see if there are magnon modes with imaginary frequency [18] In that case it can be proved that the three-sublattice structure is not stable [19–22] From the q vectors of such modes and the solutions of the corresponding RPA equations one can deduce in what way the three-sublattice structure will distort

III RESULTS

As the exchange-coupling constants decrease very fast with increasing distance between the molecules, the summation in the definition of $J(\mathbf{q})$, Eq (2 4a), can be truncated after a few terms The dominant terms pertain to the nearest-neighbor pairs, with $J_{NN}<0$ Although β-O_2 is often considered a two-dimensional system,[7 8 15] we will show that this is not correct For this purpose we have to take into account the coupling J' between neighboring molecules in different layers Furthermore, also the intralayer next-nearest-neighbor constant J_{NNN} turns out to be important The three interactions are indicated in Fig 1 We can express $J(\mathbf{q})$ in terms of J_{NN}, J_{NNN}, and J'

$$\begin{aligned} J(\mathbf{q})=2J_{NN}&\left[\cos(aq_x)+2\cos\left(\frac{aq_x}{2}\right)\cos\left(\frac{aq_y\sqrt{3}}{2}\right)\right]+2J_{NNN}\left[\cos(aq_y\sqrt{3})+2\cos\left(\frac{3aq_x}{2}\right)\cos\left(\frac{aq_y\sqrt{3}}{2}\right)\right]\\ &+2J'\left[\cos\left(-\frac{aq_y\sqrt{3}}{3}+\frac{cq_z}{3}\right)+2\cos\left(\frac{aq_x}{2}\right)\cos\left(\frac{aq_y\sqrt{3}}{6}+\frac{cq_z}{3}\right)\right] \end{aligned} \tag{3 1}$$

Here $a = 0.3272$ nm and $c = 1.1277$ nm are the cell parameters. In order to find the vector Q that maximizes $J(\mathbf{q})$, we have used the method of steepest descent [23]. This is the simplest method to determine the maximum or minimum of a function of more than one variable, but certainly not the most efficient. However, it took generally less than 1 sec of central-processing-unit time on a NAS-9040 computer to find Q, so that little would be gained by using more sophisticated methods. The error in the angle between neighboring spins thus found is less than 0.01°. When more became known about the most stable structure, the numerical computations could be supplemented and refined analytically.

Setting $J_{NNN} = J' = 0$ we have found that $J(\mathbf{q})$ was maximal for $\mathbf{Q} = \frac{1}{3}(\mathbf{b}_1 - \mathbf{b}_2)$ (and symmetry-related points). Here $\mathbf{b}_1$, $\mathbf{b}_2$, and $\mathbf{b}_3$ denote the primitive translations of the reciprocal lattice. So the neglect of J_{NNN} and J' leads to the three-sublattice structure that is assumed in the two-dimensional models of β-O_2 [7,8,15]. However, as J_{NNN} and J' are not likely to be zero, a number of different phases becomes possible. In Fig. 2 we show the phase diagram for $J' < 0$. In crossing a phase boundary, Q can change continuously, in which case the boundary is drawn as a dashed line, or discontinuously, and then the boundary is indicated by a thick solid line. We observe that the sign of J_{NNN} is very important for the magnetic structure, as the line $J_{NNN} = 0$ is a discontinuous transition line for $J'/J_{NN} < 3$. In Fig. 3 we show the magnetic structures of the different phases. Phases I and II have commensurate structures, phase II is the magnetic structure we find in α-O_2. All other phases are incommensurate. The angle α between the spins in phase III goes to 120° if $J_{NNN} \to \infty$. For finite values of J_{NNN} this angle is greater, depending on J'. The angle α in phase IV goes to 120° if J' goes to zero. If $J'/J_{NN} < 1.5$, then $\alpha \to 120°$ if $J_{NNN} \to \infty$. In phase V the angle α increases from 120° to

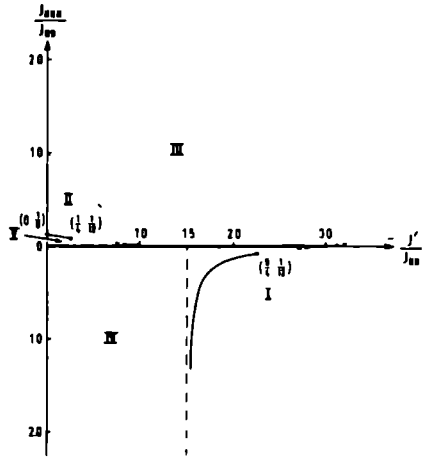

FIG. 2. Phase diagram for $J' < 0$.

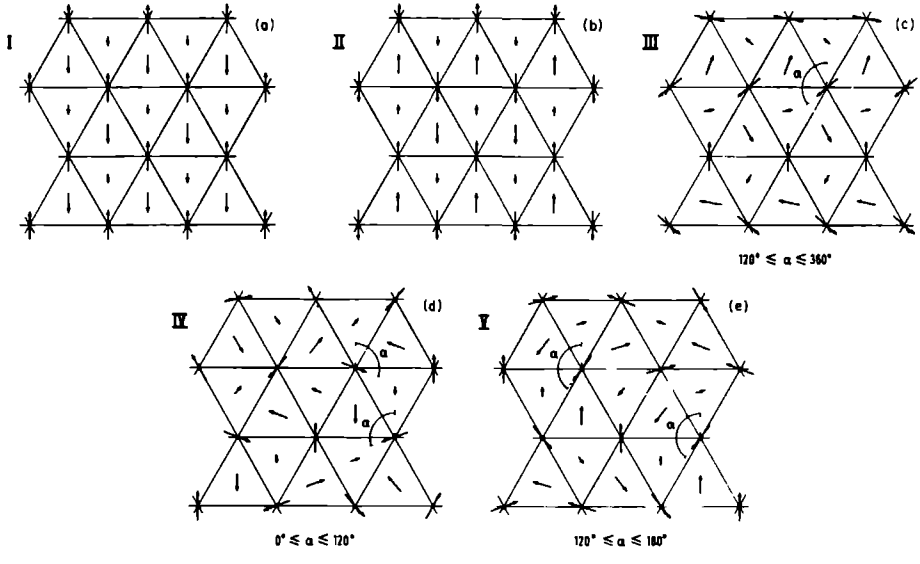

FIG. 3. Magnetic structures for the phases of Fig. 2. Three adjacent layers are shown. The middle layer is depicted by the large connected arrows. The short arrows and the arrows of intermediate length depict the lower and upper layer, respectively.

180° on approaching the boundary with phase II

The phase diagram for $J'>0$ is identical to Fig 2 if we put $-J'/J_{NN}$ on the horizontal axis We can get the magnetic structures of the phases by reversing the small arrows and those of intermediate length in Fig 3

The magnon frequencies for the three-sublattice structure have been calculated with two (de)excitation operators per molecule, one for each excited state Because of the second term, $H_{s.o.}$ of Eq (2 1), the two excited states interact This implies that there are six magnon modes for every q vector (there are three spins per unit cell of the three-sublattice structure)

We have found that there is always a mode with imaginary frequency with wave vector Q, the vector that maximizes $J(\mathbf{q})$ This agrees with the magnetic-structure calculations, which predict a structure with wave vector Q that is more stable than the three-sublattice structure However, the reverse statement, i e , that the q vector of a mode with imaginary frequency maximizes $J(\mathbf{q})$, is not true As there are no discontinuities in the dispersion curves, there is always a range in reciprocal space of modes with imaginary frequencies So the vector Q may only be determined approximately from the spin-wave calculations But there are also modes with imaginary frequencies with q vectors that yield small values for $J(\mathbf{q})$ This becomes clear if we realize that the Brillouin zone of the three-sublattice structure is smaller than the Brillouin zone corresponding to the unit cell of Fig 1 Suppose that Q lies outside the Brillouin zone of the three-sublattice structure Then there is a magnon with imaginary frequency with vector $\mathbf{Q}-\mathbf{K}$ in this Brillouin zone, where K is a primitive translation of the reciprocal lattice of the three-sublattice structure However, $J(\mathbf{Q}-\mathbf{K})$ is, in general, much smaller than $J(\mathbf{Q})$

IV DISCUSSION AND CONCLUSION

The results of the magnetic-structure calculations show that the three-sublattice structure is not the structure with the lowest energy if $J'\neq 0$ and $J_{NNN}\neq 0$ The instability is primarily caused by the interlayer exchange coupling (if $J'=0$ and $J_{NNN}/J_{NN}<\frac{1}{8}$, then the three-sublattice structure is still stable) The intralayer next-nearest-neighbor exchange coupling also has an important influence, however, as Fig 2 clearly shows

It is well known that the nearest-neighbor exchange coupling dominates the system This means that β-O_2 adopts the structure of phase IV, V, or, if $J'>0$, the corresponding phases with reversed spins in alternating layers, which we denote by IV' and V' Thus, according to the classical model and MF, we can conclude that β-O_2 has an incommensurate magnetic structure No other magnetic-structure calculation[4,5,24] has yet led to this conclusion In a recent paper Meier[24] pointed out that a nonzero interlayer exchange coupling might lead to a distortion of the three-sublattice structure However, his model was too crude to draw any definite conclusions concerning the magnetic structure Moreover, he did not realize the importance of the intralayer next-nearest-neighbor exchange coupling Loktev[4] and Kuchta[5] included only nearest-neighbor interactions in their calculations and thus concluded that the three-sublattice structure was most stable Kuchta's generalized MF theory excluded incommensurate structures So his results would probably not change if the interlayer exchange would be included

Neutron-diffraction experiments show only diffuse magnetic scattering[9] No long-range order is observed However, the observed and calculated magnetic peaks are weak Therefore, we think that an incommensurate magnetic structure is compatible with the neutron-diffraction experiments It would be interesting to take a closer look at the magnetic scattering to see if there are indications of an incommensurate structure

To determine the actual magnetic structure we have to know the values of the exchange-coupling constants Using the Wormer–van der Avoird potential[13] and putting the molecules parallel to the crystallographic c axis, we have found $J_{NN}=-9\,6$ K, $J_{NNN}=-2\,3\times10^{-3}$ K, and $J'=0\,49$ K This means that the magnetic structure of β-O_2 is given by phase V' with $\alpha=121\,7°$ Neutron diffraction has shown, however, that J' is negative and small[9] So β-O_2 most probably adopts phase V The angle α can be calculated from the relation

$$12\frac{J_{NNN}}{J_{NN}}\cos^2\alpha+2\cos\alpha+1-3\frac{J_{NNN}}{J_{NN}}+\frac{J'}{J_{NN}}=0 \qquad (4\,1)$$

ACKNOWLEDGMENTS

I would like to thank Professor A van der Avoird for his comments and suggestions, and Dr T Janssen for helpful discussions This investigation was supported by the Netherlands Foundation for Chemical Research [Stichting Scheikundig Onderzoek in Nederland (SON)], with financial aid from the Netherlands Organization for the Advancement of Pure Research [Nederlandse Organisatie voor Zuiver-Wetenschappelijk Onderzoek (ZWO)]

[1] I N Krupskii, A I Prokhvatilov, Yu A Freiman, and A I Erenburg, Fiz Nizk Temp 5, 271 (1979) [Sov J Low Temp Phys 5, 130 (1979)]
[2] G C DeFotis, Phys Rev B 23, 4714 (1981), and references therein
[3] R J Meier, C J Schinkel, and A de Visser, J Phys C 15, 1015 (1982)
[4] V M Loktev, Fiz Nizk Temp 5, 295 (1979) [Sov J Low Temp Phys 5, 142 (1979)]
[5] B Kuchta, Phys Lett 103A, 202 (1984)
[6] P Fazekas and P W Anderson, Philos Mag 30, 423 (1974)
[7] V A Slyusarev, Yu A Freiman, and R P Yankelevich, Fiz Nizk Temp 6, 219 (1980) [Sov J Low Temp Phys 6, 105 (1980)]
[8] R D Etters, A A Helmy, and K Kobashi, Phys Rev B 28, 2166 (1983)
[9] R J Meier and R B Helmholdt, Phys Rev B 29, 1387 (1984)
[10] T Sakakibara, J Phys Soc Jpn 53, 3607 (1984)
[11] T Nagamiya, in *Solid State Physics*, edited by F Seitz and D Turnbull (Academic, New York, 1967), Vol 20, p 305

[12]A. P. J. Jansen and A. van der Avoird, Phys. Rev. B 31, 7500 (1985).
[13]P. E. S. Wormer and A. van der Avoird, J. Chem. Phys. 81, 1929 (1984).
[14]E. J. Wachtel and R. G. Wheeler, Phys. Rev. Lett. 24, 233 (1970).
[15]V. A. Slyusarev, Yu. A. Freiman, and R. P. Yankelevich, Fiz. Nizk. Temp. 7, 536 (1981) [Sov. J. Low Temp. Phys. 7, 265 (1981)].
[16]J. C. Raich and R. D. Etters, Phys. Rev. 168, 425 (1968).
[17]A. P. J. Jansen, W. J. Briels, and A. van der Avoird, J. Chem. Phys. 81, 3648 (1984).
[18]A. Lagendijk (private communication).
[19]D. R. Fredkin and N. R. Werthamer, Phys Rev 138, A1527 (1965).
[20]D. J. Thouless, Nucl. Phys 21, 225 (1960).
[21]J. Čížek and J Paldus, Phys. Rev A 3, 525 (1971).
[22]A van der Avoird, W. J Briels, and A. P. J. Jansen, J Chem Phys. 81, 3658 (1984).
[23]R. F. Churchhouse, *Numerical Methods*, Vol III of *Handbook of Applicable Mathematics*, edited by W Ledermann (Wiley, Chichester, 1981)
[24]R. J. Meier, Phys. Lett. 107A, 275 (1985).

Magnetic coupling and dynamics in solid α and β-O_2. II. Prediction of magnetic field effects

A P J Jansen and A van der Avoird
Institute of Theoretical Chemistry University of Nijmegen, Toernooiveld, 6525 ED Nijmegen The Netherlands

(Received 21 July 1986, accepted 24 November 1986)

Via simple thermodynamic arguments and via quantitative lattice dynamics and spin-wave calculations, we predict that the phase transition temperature $T_{\alpha\beta}$ in solid oxygen and the optical libron frequencies in the α and β phases will both be lowered by an external magnetic field The lowering of $T_{\alpha\beta}$ varies from about 0 1 K at 7 5 T to about 1 2 K at 30 T The lowering of the B_g and A_g libron peaks in the Raman spectrum of α-O_2 and of the E_g peak in the β-O_2 spectrum varies between 1 5 and 2 9 cm $^{-1}$ at 30 T These shifts can be explained by the magnetic field induced changes in the sublattice magnetizations, which affect the Heisenberg exchange contribution to the intermolecular potential From *ab initio* calculations it is known that the Heisenberg coupling parameter J is extremely anisotropic

I. INTRODUCTION

In the preceding paper I[1] we have discussed some properties of solid O_2, both as a molecular crystal and as a magnetic material A lattice and spin-Hamiltonian has been derived from first principles and it has been shown that the dynamical and the magnetic properties of solid O_2 are directly related by coupling terms in the Hamiltonian which contain spin operators as well as structure dependent factors Especially in the Heisenberg exchange term the dependence of the coupling parameter J on the positions and orientations of the molecules is very strong [2,3] Lattice dynamics and spin-wave calculations that take into account these coupling terms yield good agreement with the measured magnon and libron frequencies in α and β-O_2 In particular, they explain the anomalously large libron splitting in α-O_2, which could not be understood from previous lattice dynamics calculations, but which appears to be caused by the extreme anisotropy of the Heisenberg coupling parameter J [1,4]

The most direct demonstration of the importance of the coupling terms in our first principles Hamiltonian would be the measurement of an effect of external magnetic fields on some properties that are normally determined by a spin-independent intermolecular potential Typical properties of this type are the phonon and libron frequencies and the transition temperature between different solid phases In solid O_2 it should be possible to change the transition temperature between the α and β phases, as well as the libron frequencies in each of these phases, by applying an external magnetic field. The important question is, however, whether the changes are detectable for those field strengths that can be obtained in practice (up to about 30 T in static fields) [5] In the present paper we estimate the size of the magnetic field effects via theoretical calculations, in order to predict whether they will indeed be measurable

II THEORY

The theoretical framework for the calculations has been completely described in paper I The Hamiltonian is defined by Eqs (9)–(11) The spin-dependent terms, Eq (9), are the Heisenberg exchange term, the intramolecular spin-orbit and spin–spin coupling term and the intermolecular spin–spin (magnetic dipole) coupling term The dependence of the Heisenberg coupling parameter J on the positions and orientations of the molecules, Eqs (3) and (35), has been obtained via *ab initio* calculations [3] The geometry dependence of the other spin coupling parameters is well known, see Eqs (6) and (8) Lattice dynamics and spin-wave calculations with this Hamiltonian start by the construction of separate mean field (MF) states for the molecular vibrations, translations, and librations, and for the spins, see Eqs (14)–(16) Next, the correlation between the motions of the individual molecules as well as the coupling between the phonons, librons, and magnons is introduced via the random phase approximation (RPA), Eqs (18)–(23)

The extension of this formalism for the calculations in the present paper is very simple To the spin part of the Hamiltonian, Eq (9), we have to add the Zeeman interaction

$$H_Z = g_e \mu_B \sum_p \mathbf{B}\cdot\mathbf{S}_p \qquad (1)$$

with the external magnetic field $\mathbf{B}$ Since this terms depends only on the single-molecule spins $\mathbf{S}_p$, we just need to add it to the MF Hamiltonian for the spins, Eq (16) The MF states for the spins will thus be changed, and via the thermodynamic averages over the spin states in Eqs (14)–(16), those for the translational vibrations and for the librations will change too The RPA Hamiltonian (18), that yields the final phonon–libron–magnon states via Eqs (19)–(23), will be affected via the excitation and deexcitation operators

$a^{(\lambda)+}_{p'i_\lambda}$ and $a^{(\kappa)}_{p'i_\kappa}$

which are defined on the basis of the MF states Just as in paper I, it is possible to make separate calculations for the lattice modes, the phonons and librons, and for the magnons, since there is very little mixing between these The separation only occurs at the RPA level, however and the coupling terms in the Hamiltonian have to be included in both calculations In the spin-wave calculations they should be averaged over the (MF) molecular vibrations and in the lattice

 0021 9606/87/063597 05$02 10

TABLE I Magnetic susceptibilities (in 10^{-6} cm^3 g^{-1})

	α-O_2 Calculated				Experiment (Ref 6)
	χ_1*				
T(K)	$\chi_1 = \chi_b$	χ_a	χ_c	χ	χ
5	0 9	262 0	253 6	172 2	48 1
10	3 3	262 0	253 6	173 0	48 6
15	21 2	262 0	253 7	179 0	50 6
20	56 0	262 0	253 8	190 6	55 5
22 5	76 7	262 0	253 9	197 5	60 1
		β − O_2 Calculated			Experiment (Ref 6)
T(K)		χ_c	$\chi_a = \chi_b$	χ	χ
25		290 1	299 6	296 4	104 3
42		275 6	282 8	280 4	130 4

*Equation (2) yields $\chi_1 = 262\ 2 \times 10^{-6}$ cm^3 g^{-1}

dynamics calculations they must be averaged over the (MF) spin states At specific points in the Brillouin zone of the structural Bravais lattice, for example at $q = 0$, the phonons and librons in α- and β-O_2 do not mix either

III. MAGNETIC PROPERTIES

Before looking at the α–β phase transition temperature and the libron frequencies in α and β-O_2, we first consider the response of the spin systems to external magnetic fields The α phase is a two-sublattice collinear antiferromagnet with the sublattice magnetizations directed along the b axis of the monoclinic lattice This preferential magnetization direction is usually imposed by a phenomenological spin Hamiltonian with two anisotropic single-particle spin terms, as in Eq (1) of paper I In paper I it is demonstrated, however, that it also follows from a spin Hamiltonian from first principles as in Eq (9) Applying a small external field **B** in the b direction or perpendicular to it, we have calculated both the resultant overall magnetization and the free energy lowering and from both quantities we have extracted the magnetic susceptibilities $\chi_\parallel$ and $\chi_\perp$ This calculation has been performed at the MF level at various temperatures T, the results are given in Table I Although we have included the anisotropic spin terms in the Hamiltonian of Eq (9), paper I, the result for $\chi_\perp$ nearly satisfies the simple MF relation

$$\chi_\perp = Ng_c^2\mu_B^2|4J(0)^{\text{inter}}|^{-1} \tag{2}$$

which has been derived from the Heisenberg term only The lattice sum $J(0)$ has been defined in Eq (25) of paper I The experimental data are given in Table I too and we observe that our calculated values of $\chi_\parallel$ and $\chi_\perp$ are considerably too high

Also for β-O_2 the calculated susceptibility values are too high, by about the same factor, see Table I In this phase the magnetic anisotropy within the ab plane is absent and all components of the susceptibility are nearly equal

From the calculated sublattice magnetizations, as a function of temperature, we have derived the Neel temperature T_N of α-O_2 The relation $\chi_\parallel(T_N) = \chi_\perp(T_N)$ is approximately satisfied by the susceptibilities given in Table I, but not exactly because of the anisotropic spin terms in the Hamiltonian The value $T_N = 49\ 5$ K thus obtained cannot be directly compared with experiment since the α phase is not stable above 23 9 K (at low pressure), but it is not far from estimated values [6,7]

When α-O_2 is placed in a stronger magnetic field along the sublattice magnetization axis (the b axis) the spin momenta will change directions by about 90° Experimentally, the so-called spin-flop field was found to be $7\ 5 \pm 0\ 5$ T [8] In our calculations we can simulate this situation by increasing the field strength and we find the spin-flop field to lie at 7 1 T (at 0 K)

According to the simple relation (2) derived from MF theory the too high susceptibility values would indicate that the calculated Heisenberg coupling parameter J is considerably too small in absolute value This has indeed been concluded in a recent paper [9] We have evidence for the contrary, however Our values of J, together with the well known free molecule values for the parameters in the anisotropic spin Hamiltonian from first principles, Eq (9) of paper I, yield fairly good values for the optical magnon frequencies in α-O_2, which have been directly measured by infrared and Raman spectroscopy Also the calculated Neel temperature and spin-flop field are quite realistic Moreover, if the absolute value of J would be substantially in error, then the absolute values of its main anisotropic components would probably be incorrect too The latter values enter directly into the calculated difference of the optical libron frequencies in α-O_2, which was found to be in very good agreement with the Raman spectra [10,11] Actually, in paper I this libron splitting has, for the first time, been quantitatively explained So we believe that the values of J extracted from the *ab initio* calculations[3] are not seriously in error, but that the error in the calculated susceptibilities will be mainly caused by the use of the mean field model [12,13]

IV THE α–β PHASE TRANSITION TEMPERATURE

The α phase of solid O_2 is stabilized with respect to the β phase by the magnetic interactions, in particular by the Heisenberg exchange coupling So one expects that changes in the magnetic structure which may be caused by an external magnetic field will affect the phase transition temperature From a simple thermodynamic argument we can derive a relation between the change in the phase transition temperature and the applied field strength We start from the expression for the Helmholtz free energy differential

$$dA = -S\,dT - p\,dV - M\,dB \tag{3}$$

with S being the entropy, T the temperature, p the pressure, V the volume, M the magnetization, and B the magnetic field strength as usual We have to use[14] the form $-M\,dB$ for the magnetic contribution since the interaction of the magnetic dipole moments with the external field is explicitly included in the Hamiltonian, and thus in the free energy Assuming that the magnetic susceptibility is field independent, we can write the free energy at field B as

$$A(B) = A(0) + \int_0^B \left[\frac{\partial A}{\partial B'}\right]_{TV} dB'$$
$$= A(0) - \int_0^B \chi B'\, dB'$$
$$= A(0) - \tfrac{1}{2}\chi B^2 \qquad (4)$$

which holds for any temperature T For temperatures close to the phase transition temperature $T_{\alpha\beta}$ we expand the free energy of the α phase as

$$A_\alpha(B,T) = A_\alpha(B,T_{\alpha\beta}) + (T - T_{\alpha\beta})\left[\frac{\partial A_\alpha}{\partial T}\right]_{B\,T_{\alpha\beta}} \qquad (5)$$

while neglecting the higher order terms Equation (4) can be directly substituted into the first term of Eq (5) and it can also be put into the first derivatives

$$\left[\frac{\partial A_\alpha}{\partial T}\right]_{B\,T_{\alpha\beta}} = \left[\frac{\partial A_\alpha}{\partial T}\right]_{0\,T_{\alpha\beta}} - \frac{1}{2}\left[\frac{\partial \chi_\alpha}{\partial T}\right]_{T_{\alpha\beta}} B^2$$
$$= -S_\alpha(T_{\alpha\beta}) - \frac{1}{2}\left[\frac{\partial \chi_\alpha}{\partial T}\right]_{T_{\alpha\beta}} B^2 \qquad (6)$$

The same equations can be written for the β phase Since, by definition

$$A_\alpha(0,T_{\alpha\beta}) = A_\beta(0,T_{\alpha\beta}) \qquad (7)$$

and

$$A_\alpha(B,T) = A_\beta(B,T)\,, \qquad (8)$$

if T is the transition temperature in the external field B, we easily arrive at the following relation

$$\Delta T = -\frac{\Delta\chi B^2}{2\Delta S + B^2\Delta(\partial\chi/\partial T)} \qquad (9)$$

with

$$\Delta\chi = \chi_\beta(T_{\alpha\beta}) - \chi_\alpha(T_{\alpha\beta})\,,$$
$$\Delta S = S_\beta(T_{\alpha\beta}) - S_\alpha(T_{\alpha\beta})\,,$$
$$\Delta\left(\frac{\partial\chi}{\partial T}\right) = \left[\frac{\partial\chi_\beta}{\partial T}\right]_{T_{\alpha\beta}} - \left[\frac{\partial\chi_\alpha}{\partial T}\right]_{T_{\alpha\beta}}\,,$$
$$\Delta T = T - T_{\alpha\beta} = T_{\alpha\beta}(B) - T_{\alpha\beta}(0) \qquad (10)$$

By estimating the quantity $\Delta(\partial\chi/\partial T)$ from the measurements,[6,7,15] we have found that, for fields up to 30 T, the second term in the denominator of Eq (9) may be safely neglected Thus, the relation between the shift in the transition temperature and the applied field strength becomes simply

$$\Delta T = -\frac{\Delta\chi}{2\Delta S} B^2 \qquad (11)$$

Both from experiment and from our calculations, see Table I, we know that $\Delta\chi > 0$, mainly because the parallel component of the susceptibility $\chi = \frac{1}{3}\chi_\parallel + \frac{2}{3}\chi_\perp$ is considerably smaller in the α phase Since the calculated values for χ are not very reliable, we use the average experimental values of DeFotis[6] $\chi_\alpha = 60.1\times10^{-6}$ cm^3 g^{-1} (at $T - 22.5$ K) and $\chi_\beta = 104.3\times10^{-6}$ cm^3 g^{-1} (at $T = 25$ K) Also the entropy change ΔS is positive, since the β phase is stable at higher temperatures, from the heat of transition, 92 J mol^{-1},[16] we calculate that $\Delta S = 3.85$ J mol^{-1} K^{-1} Substituting these data into Eq (11) we find that the α–β transition temperature is lowered by the magnetic field by an amount of 1.83 mK/T^2 At a field strength of 30 T the lowering of the phase transition temperature would thus be 1.65 K

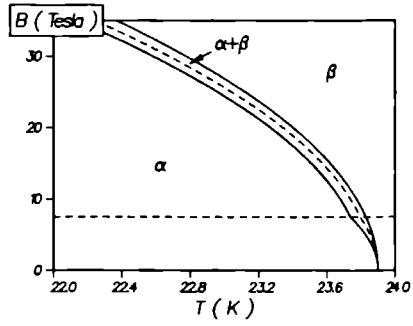

FIG 1 Magnetic field strength dependence of the α–β phase transition temperature The dashed curve depicts the average transition temperature The solid curves indicate the range of transition temperatures in a powder sample Note the effect of the spin flop in α O$_2$ at 7.5 T

The actual shift at higher magnetic field strengths will be smaller, however At 7.5 T the α phase exhibits a spin flop which increases the parallel susceptibility component to about the same value as the perpendicular component, and thus decreases $\Delta\chi$ The effect of this spin flop on the change in $T_{\alpha\beta}$ is clearly visible in Fig 1 The resulting ΔT is about 0.1 K at 7.5 T and about 1.2 K at 30 T, a small but possibly still measurable shift

Another interesting phenomenon is observed by looking in detail at the anisotropy In the β phase the susceptibility is nearly, but not exactly isotropic, see Table I In α-oxygen $\chi_\parallel$, i e, the component along the b axis, is about half of $\chi_\perp$ at the phase transition temperature [6] Taking the susceptibility ratios from Table I, we estimate that the shifts in the transition temperature will be -2.88 mK/T^2 for a magnetic field along the b axis, -1.37 mK/T^2 for a field along the a axis and -1.25 mK/T^2 for a field along the c^* or c axis (the molecular axis) Such differences can only be measured in single crystals, of course In powder samples the α–β phase transition in a magnetic field will take place over a range of temperatures, see Fig 1

V. MAGNETIC FIELD EFFECTS ON THE LIBRON FREQUENCIES

It has been suggested by several authors[10,17,18] that it would be useful to measure the Raman spectrum of solid O$_2$ in an external magnetic field The reason for this suggestion was that the two peaks observed in α-O$_2$ could not be assigned in a satisfactory manner It was believed that the peak at lower frequency contains two accidentally degenerate B_g and A_g libron modes The peak at higher frequency should then correspond with a two-libron or libron–magnon transition[17,18] or with a libron or mixed libron–magnon mode which lies at the boundary of the Brillouin zone of the structural lattice but in the center of the magnetic Brillouin

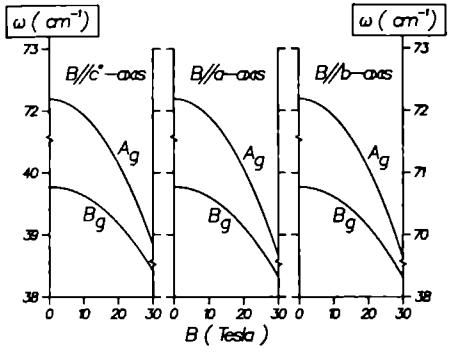

FIG 2 Magnetic field induced lowering of the optical libron frequencies in α O_2

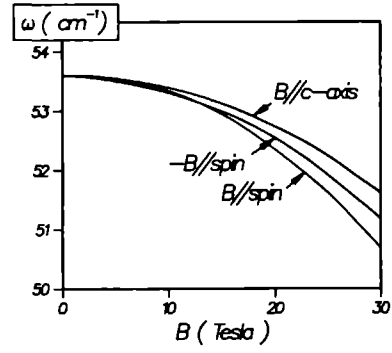

FIG 3 Magnetic field induced lowering of the optical libron frequency in β-O_2 The lower two curves have been calculated with the field parallel or antiparallel to one of the sublattice magnetizations within the *ab* plane

zone [19] In a magnetic field the possible magnon character of these modes could be detected by a change of their frequencies, whereas pure libron modes would not shift

In paper I and in Ref 4 we have made a different assignment of the Raman spectrum on the basis of *ab initio* calculations [3] The two peaks in α-O_2 have been identified as the B_g and A_g libron modes, respectively, and the large splitting was shown to be caused by the Heisenberg exchange term in the (spin-dependent) potential So we think that both modes are pure libron modes, but that they will still be shifted by an external magnetic field which changes the magnetization and, thus, affects the spin factor $\langle \mathbf{S}_P \cdot \mathbf{S}_P \rangle$ in the Heisenberg term Here we report the explicit calculation of such shifts, as a function of the magnetic field strength, in α and β-O_2

The calculations have been made as explained in Sec II Since we are mainly interested in the optical ($\mathbf{q} = \mathbf{0}$) libron modes which do not mix with the phonons, because of the symmetry in α and β-O_2, we have kept the centers of mass of the molecules fixed at the lattice sites As it is primarily the Heisenberg exchange term from which we expect the libron shifts, we have retained the full geometry dependence of the Heisenberg coupling parameter J, as in Eqs (3) and (35) of paper I, but we have replaced the anisotropic spin terms in the Hamiltonian of Eq (9) in paper I by their semiempirical forms from Eq (1), in order to simplify the calculations

The magnetic structure of α-O_2 is fairly rigid There is some frustration due to the antiferromagnetic coupling between the intralayer next-nearest neighbors which belong to the same sublattice In a magnetic field the spins in the same sublattice will remain parallel, however, and thus this frustration cannot be removed The magnetic order is further stabilized by the anisotropic spin terms, especially by the out of-plane anisotropy So one needs high fields to distort the magnetic structure to an appreciable extent and the resulting shifts in the libron frequencies will not be large Figure 2 shows these shifts for the optical B_g and A_g librons They amount up to 2 5 cm^{-1} for fields up to 30 T They vary only slightly (by about 0 1 cm^{-1}) for different field directions, so that in a powder sample they should be measurable too When the magnetic field lies along the *b* axis there is a discontinuity at 7 5 T, due to the spin flop At this field strength the shifts are still too small for the discontinuity to be visible, however

In β-O_2 we have assumed that the spins adopt the three-sublattice structure The spin momenta lie in the *ab* plane, which situation is stabilized by the out-of-plane anisotropic spin terms A magnetic field along the *c* axis gives the same *c* component to every spin This distortion is not very favorable and the effect on the E_g libron frequency will be relatively small, see Fig 3 If the field direction is parallel to the *ab* plane, the spin momenta can have all possible angles relative to this field We have treated the extreme cases, i e , we have placed the field parallel to one of the sublattice magnetizations or antiparallel to it The three-sublattice order is a frustrated structure and it has been shown by several authors[20–22] that it can easily be distorted We have found that this is indeed so, for fields parallel to the *ab* plane The effects on the E_g libron mode frequency are displayed in Fig 3

Another interesting effect occurs in β-O_2 when we place the magnetic field parallel to the *ab* plane The angles between nearest neighbor spins are no longer the same for all neighbor pairs Via the average spin factors $\langle \mathbf{S}_P \cdot \mathbf{S}_P \rangle$ in the Heisenberg exchange term the intermolecular potential differs for various neighbor pairs and the trigonal symmetry of the structural lattice is distorted The unit cell of the distorted lattice contains three molecules The Brillouin zone must be folded accordingly, and there will be phonons and librons at the zone boundary of the undistorted Brillouin zone that lie in the center of the distorted Brillouin zone So, in a magnetic field parallel to the *ab* plane extra phonon or libron peaks may become visible in the infrared or Raman spectra Their intensity will probably be small, however, as they differ only slightly from the phonons and librons that lie at the zone boundary in the absence of the field Also the threefold symmetry axis has disappeared and the E_g mode will therefore be split According to our calculations this splitting is small (less than 0 03 cm^{-1} for fields up to 30 T),

and so we expect the other symmetry breaking effects to be small too

In Fig 3 one can observe that for β-O_2 the shift of the E_g libron frequency depends rather strongly on the magnetic field direction So, in powder samples we expect, in contrast with α-O_2, that the Raman peak will not only be shifted but also broadened by the magnetic field

VI. CONCLUSION

We have quantitatively predicted the effects of external magnetic fields on the α–β phase transition temperature in solid oxygen, as well as on the libron frequencies in each of these phases For the phase transition temperature $T_{\alpha\beta}$ we have used simple thermodynamic arguments to show that $T_{\alpha\beta}$ is lowered by the magnetic field, to such an extent that it might be measurable in the highest static magnetic fields that can be reached in practice (up to about 30 T) For the libron frequencies we have made quantitative calculations similar to those in paper I The magnetic field induced shifts of these frequencies are caused by the Heisenberg exchange term in the spin-dependent lattice potential, via the extremely strong dependence of the coupling parameter J on the molecular orientations

We have found the largest shift for the E_g libron frequency in β-O_2, when the magnetic field is parallel to the ab plane It is questionable whether this shift (2 9 cm^{-1} at 30 T) can be measured, however, since the width of the observed Raman line[10] is 13 to 20 cm^{-1} and, in powder samples, this width will be further increased by the magnetic field The shifts in the B_g and A_g libron frequencies are somewhat smaller (1 5 and 2 5 cm^{-1}, respectively, at 30 T) and the A_g peak is fairly broad too Especially the shift in the lower frequency B_g peak, which has a linewidth of less than 1 cm^{-1}, should be visible in the Raman spectrum, however, even at somewhat weaker fields According to the earlier interpretations[17–19] of the Raman spectra, the peak at the lower frequency should not shift at all. We end this paper by an appeal to the experimentalists It would be very useful as a verification of the theoretical models that have been proposed for solid oxygen, if the magnetic field induced changes of the α–β phase transition temperature and the libron frequencies in α and β-O_2 could indeed be measured

ACKNOWLEDGMENTS

This investigation was supported in part by the Netherlands Foundation for Chemical Research (S O N) with financial aid from the Netherlands Organization for the Advancement of Pure Research (Z W O)

[1]A P J Jansen and A van der Avoird J Chem Phys **86** 3583 (1987)
[2]M C van Hemert, P E S Wormer, and A van der Avoird Phys Rev Lett **51**, 1167 (1983)
[3]P E S Wormer and A van der Avoird J Chem Phys **81** 1929 (1984)
[4]A P J Jansen and A van der Avoird Phys Rev B **31** 7500 (1985)
[5]K van Hulst, C J M Aarts A R de Vroomen and P Wyder J Magn Magn Mat **11**, 317 (1979), M J Leupold and Y Isawa J Phys (Paris) C **1**, 41 (1984)
[6]G DeFotis, Phys Rev B **23** 4714 (1981) and references therein
[7]C Uyeda, K Sugiyama, and M Date J Phys Soc Jpn **54** 1107 (1985)
[8]R J Meier, J H P Colpa, and H Sigg J Phys C **17** 4501 (1984)
[9]P W Stephens and C F Majkrzak Phys Rev B **33** 1 (1986)
[10]K D Bier and H J Jodl, J Chem Phys **81** 1192 (1984)
[11]J E Cahill and G E Leroi J Chem Phys **51** 97 (1969)
[12]M E Lines, Phys Rev **133** A841 (1964)
[13]M E Lines Phys Rev **156** 534 (1967)
[14]C J Adkins *Equilibrium Thermodynamics* (McGraw Hill London 1968)
[15]R J Meier, C J Schinkel, and A de Visser, J Phys C **15** 1015 (1982)
[16]M P Orlova, Sov J Phys Chem **12**, 1603 (1966)
[17]K Kobashi, M L Klein, and V Chandrasekharan, J Chem Phys **7**, 843 (1979)
[18]B Kuchta, Chem Phys **95**, 391 (1985)
[19]R D Etters, K Kobashi, and J Belak, Phys Rev B **32**, 4097 (1985)
[20]A P J Jansen Phys Rev B **33**, 6352 (1986)
[21]R J Meier, Phys Lett A **107**, 275 (1985)
[22]B Kuchta and T Luty, Chem Phys Lett **126**, 506 (1986)

SUMMARY

Theoretical approach to the optical, thermodynamic and magnetic properties of solid nitrogen and solid oxygen

In this thesis the development of new lattice dynamics methods for molecular crystals and the application of these methods to various phases of solid nitrogen and solid oxygen have been presented. Thermodynamic, optical and (for oxygen) magnetic properties have been calculated and have been compared with experimental results.

The new methods that have been developed for lattice dynamics calculations on molecular crystals are based on the Mean Field theory (MF) and on the Random Phase Approximation (RPA). They are quantum mechanical methods that resemble methods used for electronic structure calculations in quantum chemistry; viz. Self-Consistent Field and Configuration Interaction methods. The methods complement each other. Calculations are begun with MF, which is an independent-particle method. Correlation between the motions of molecules is then taken care of in RPA, using the states that have been obtained with MF. The results of the RPA calculations are the collective excitations of the crystals. The motivation for developing and applying these methods has been the inadequacy of the (quasi)-harmonic methods to handle large amplitude motions (see chapter 1). In molecular crystals motions in which the molecules change their orientations (librations or rotations) are such large amplitude motions. Therefore, MF and RPA have been applied initially to librations (section 2.1 and 2.2). After this application yielded good results the methods have been extended to include translational vibrations, and the coupling of librations and translational vibrations (section 2.4). Later on, the methods have been extended further to include the spin waves in solid oxygen (section 3.1).

Besides MF and RPA, some other methods have been used when particular problems were encountered. For one system (β-O_2) the precise nature of the magnetic structure was not known. A classical model in which the magnetic energy is minimized has been invoked to solve this problem (see below and section 3.3). For another system (α-O_2) a symmetry analysis has been made in order to gain a deeper understanding of some results of the numerical calculations (see below and section 3.2). In section 2.3 a new method has been developed to handle orientationally disordered crystals. In such crystals the correlation between the orientations may lead to incorrect results when using MF. The new method is based on a generalized

Ising Hamiltonian. This method can lead to orientational disorder although the various states for the individual molecules correspond to well-defined orientations.

Calculations have been made for α-, β-, and γ-N_2, and for α- and β-O_2. The α- and γ-phases of solid nitrogen are both ordered phases. Using MF we have calculated the orientations of the molecules in these phases, and the amplitudes of the librations and translational vibrations (section 2.1 and 2.4). With RPA we have obtained the frequencies of the librons (collective librations), the phonons (collective translational vibrations), and the mixed libron-phonon modes (section 2.4). We have compared these calculated results with experimental data, finding good agreement. The RPA calculation for α-N_2 has been extended (section 2.5). Most thermodynamic properties have been calculated in this thesis on the MF-level. For α-N_2, however, they have also been calculated with the extended RPA method. The results that have been obtained with RPA agree better, in general, with experimental results than the results obtained with MF.

The β-phase of solid nitrogen is an orientationally disordered phase. Initially, a disordered structure was found in MF. The RPA calculation, however, yielded librons with imaginary frequencies, which could be shown to indicate that the MF solution was not stable. Indeed, another structure has been found with a considerably lower energy and with real libron frequencies. Unfortunately, this structure was ordered. We made an *ad hoc* hypothesis in which jumps between six well-defined orientations for each molecule were assumed (section 2.2). Later we developed a new theory to account for these jumps explicitly. Using this theory it has been shown that each molecule in β-N_2 has an equal probability to be in one of the six orientations. There is a strong correlation between the orientations of nearest neighbours (section 2.3).

The α- and β-phases of solid oxygen are also ordered phases. Due to the triplet ground state of the oxygen molecules these phases have a magnetic structure. Besides the librons and phonons, there are also magnons in α- and β-O_2. Quantum chemical calculations have shown that magnetic interactions between oxygen molecules depend strongly on the distance between and the orientations of the molecules. Using MF and RPA the libron, phonon and magnon frequencies have been calculated (section 3.1). A correct splitting of the librons in α-O_2 has been obtained. We have shown that this splitting is due to the anisotropy in the magnetic interactions, which are normally neglected in lattice dynamics calculations of solid oxygen. Predictions have been made for the effects of a magnetic field on the libron

frequencies and on the α-β phase transition temperature (section 3.4). The coupling between the magnons and the libron/phonons has been investigated via a symmetry analysis, using co-representations of the magnetic space group. An experiment has been suggested for testing the selection rules that have been derived from the analysis (section 3.2). The magnetic structure of β-O_2 has been calculated by minimizing the magnetic energy. This structure was found to be incommensurate (section 3.3).

SAMENVATTING

Theoretische aanpak van de optische, thermodynamische en magnetische eigenschappen van vast stikstof en vast zuurstof

In dit proefschrift zijn de ontwikkeling van nieuwe roosterdynamica methoden voor moleculaire kristallen en de toepassing van deze methoden op verschillende fasen van vast stikstof en vast zuurstof gepresenteerd. Thermodynamische, optische en (voor zuurstof) magnetische eigenschappen zijn berekend en vergeleken met experimentele resultaten.

De nieuwe methoden die ontwikkeld zijn voor de roosterdynamica berekeningen aan moleculaire kristallen zijn gebaseerd op de Mean Field theorie (MF) en de Random Phase Approximation (RPA). Dit zijn quantummechanische methoden die lijken op methoden die gebruikt worden voor elektronenstruktuurberekeningen in de quantumchemie, nl. Self-Consistent Field en Configuratie Interactie methoden. De methoden vullen elkaar aan. Berekeningen worden begonnen met MF, wat een independent-particle methode is. Correlaties in de bewegingen van moleculen worden daarna meegenomen in RPA, gebruik makend van de toestanden die verkregen zijn m.b.v. MF. De uitkomsten van RPA zijn de collectieve excitaties van de kristallen. De reden waarom deze methoden ontwikkeld en toegepast zijn is dat de (quasi)-harmonische methoden niet in staat zijn grote amplitude bewegingen te behandelen (zie hoofdstuk 1). De bewegingen in moleculaire kristallen waarbij de moleculen hun oriëntatie veranderen (librations of rotations) zijn zulke grote amplitude bewegingen. Daarom zijn MF en RPA eerst toegepast op librations (sectie 2.1 en sectie 2.2). Nadat deze toepassing goede resultaten opleverde zijn de methoden uitgebreid voor translatie-vibraties, en de koppeling van librations met translatie-vibraties (sectie 2.4). Later zijn de methoden verder uitgebreid voor spingolven in vast zuurstof (sectie 3.1).

Naast MF en RPA zijn er enkele andere methoden ontwikkeld en toegepast wanneer specifieke problemen optraden. Van één systeem (β-O_2) was de preciese aard van de magnetische struktuur niet bekend. Een klassiek model, waarbij de magnetische energie wordt geminimaliseerd, is gebruikt om dit probleem op te lossen (sectie 3.3). Voor een ander systeem (α-O_2) is een symmetrie analyse gemaakt om een beter begrip te krijgen van de resultaten van de numerieke berekeningen (sectie 3.2). In sectie 2.3 is een nieuwe methode ontwikkeld om oriëntationeel wanordelijke kristallen te behandelen. In dergelijke kristallen kan MF door de corre-

latie in de oriëntaties tot onjuiste resultaten leiden. De nieuwe methode is gebaseerd op een gegeneraliseerde Ising Hamiltoniaan. Deze methode kan oriëntationele wanorde beschrijven hoewel de verschillende toestanden van de individuele moleculen corresponderen met goed gedefinieerde oriëntaties.

Er zijn berekeningen uitgevoerd voor α-, β- en γ-N_2, en voor α- en β-O_2. De α- en γ-fase van vast stikstof zijn beide geordende fasen. We hebben m.b.v. MF de oriëntaties van de moleculen en de amplitudes van de libraties en de translatie-vibraties in deze fasen berekend (sectie 2.1 en 2.4). M.b.v. RPA hebben we de frequenties van de libronen (collectieve libraties), de fononen (collectieve translatie-vibraties) en de gemengde libron-fonon modes verkregen (sectie 2.4). We hebben deze berekeningen vergeleken met experimentele resultaten en een goede overeenstemming gevonden. In RPA berekeningen aan α-N_2 is de methode verder uitgebreid (sectie 2.5). De meeste thermodynamische grootheden zijn in dit proefschrift berekend op MF-niveau. Voor α-N_2 zijn ze echter ook berekend m.b.v. de uitgebreide RPA methode. In het algemeen kloppen de resultaten van RPA beter met de experimentele resultaten dan die van MF.

De β-fase van vast stikstof is een oriëntationeel wanordelijke fase. Aanvankelijk werd m.b.v. MF een wanordelijke struktuur gevonden. De RPA berekeningen leverden echter libronen met imaginaire frequenties op, waarvan aangetoond kon worden dat dit wijst op een instabiele MF oplossing. Er is dan ook een andere struktuur gevonden met een aanzienlijke lagere energie en met reële libronfrequenties. Helaas was deze struktuur geordend. We hebben een *ad hoc* hypothese opgesteld waarbij werd aangenomen dat er sprongen tussen zes goed gedefinieerde oriëntaties plaats vonden. Later hebben we een nieuwe theorie ontwikkeld om deze sprongen expliciet te verklaren. M.b.v. deze theorie is aangetoond dat elk molecuul in β-N_2 een gelijke waarschijnlijkheid heeft om één van de zes oriëntaties aan te nemen. Er is een sterke correlatie tussen de oriëntaties van naaste buren (sectie 2.3).

De α- en β-fase van vast zuurstof zijn ook geordende fasen. Ten gevolge van de triplet grondtoestand van de zuurstofmoleculen hebben deze fasen een magnetische struktuur. Naast de libronen en de fononen zijn er ook magnonen in α- en β-O_2. Quantumchemische berekeningen hebben laten zien dat de magnetische interacties tussen zuurstofmoleculen sterk afhangen van de afstand tussen en de oriëntaties van de moleculen. M.b.v. MF en RPA zijn de libron-, fonon- en magnonfrequenties berekend (sectie 3.1). Een correcte opsplitsing van de libronen in α-O_2 werd verkregen. We hebben laten zien dat deze opsplitsing het gevolg is van de anisotropie in

de magnetische interacties, die normaal verwaarloosd worden in de roosterdynamica berekeningen aan vast zuurstof. Voorspellingen zijn gedaan voor de effecten van een magnetisch veld op de libronfrequenties en op de α-β faseovergangstemperatuur (sectie 3.4). De koppeling tussen de magnonen en de libronen/fononen is onderzocht via een symmetrie analyse, m.b.v. co-representaties van de magnetische ruimtegroep. Een experiment is voorgesteld om de selectieregels die afgeleid zijn van de analyse te testen (sectie 3.2). De magnetische struktuur van β-O_2 is berekend door de magnetische energie te minimaliseren. Hierbij werd een incommensurabele struktuur gevonden (sectie 3.3).

CURRICULUM VITAE

van

Antonius Petrus Johannes Jansen,
geboren 2 december 1959 te Maastricht

juni 1978

Eindexamen VWO aan het Stedelijk Lyceum en HAVO te Maastricht.

september 1978

Aanvang studie Scheikunde aan de Katholieke Universiteit Nijmegen.

maart 1981

Kandidaatsexamen S4 (cum laude): hoofdvakken Schei- en Wiskunde en bijvak Natuurkunde.

juni 1983

Doctoraalexamen Scheikunde (cum laude): hoofrichting Theoretische Chemie en bijvakken Molecuulspectroscopie en Capita uit de Natuurkunde.

juli 1983

Aanstelling als SON/ZWO-medewerker bij het Instituut voor Theoretische Chemie van de Katholieke Universiteit Nijmegen op het promotieonderwerp: dynamica van moleculaire kristallen.

STELLINGEN

1. De één-deeltjes Hamiltoniaan die Soulard *et al.* gebruiken voor de verklaring van de Raman en inelastische neutronverstrooiingsexperimenten aan vast 4-methyl pyridine (C_6H_7N en C_6D_7N) is onzinnig.

   L. Soulard, F. Fillaux, G. Braaten, N. Le Calvé en B. Pasquier, *Chem. Phys. Lett.* **125**, 41 (1986).

2. Bij het bepalen of hexasilabenzeen (Si_6H_6) een vlakke dan wel een stoelconformatie aanneemt vergeten Nagase *et al.* de moleculaire vibraties.

   S. Nagase, H. Taramae en T. Kudo, *J. Chem. Phys.* **86**, 4513 (1987).

3. Bij de vergelijking van moleculaire dynamica en roosterdynamica gaat Righini uit van een te beperkte groep van roosterdynamicamethoden.

   R. Righini, *Physica* **131B**, 234 (1985).

4. Het gebruik van kromlijnige coördinaten in de harmonische benadering heeft geen enkel voordeel, maar wel enige nadelen.

   S. Dasgupta en S. Sengupta, *J. Phys.* **C20**, 1611 (1987).
   W.J. Briels, A.P.J. Jansen en A. van der Avoird, *Adv. Quant. Chem.* **18**, 131 (1986).

5. De magnetische structuur van de δ-fase van zuurstof geadsorbeerd aan grafiet die Hardouin Duparc en Etters geven is niet stabiel.

   O.B.M. Hardouin Duparc en R.D. Etters *J. Chem. Phys.* **86**, 1020 (1987).

6. Gibson's voorspelling dat zijn Padé approximant methode ook geschikt is voor de berekening van thermodynamische grootheden van een double well oscillator is niet te rechtvaardigen met zijn resultaten voor een deeltje in een doos, een rigid rotor en een (an)harmonische oscillator.

   W.G. Gibson, *J. Phys.* **A17**, 1877 (1984); *ibid.* **A17**, 1891 (1984).

7. Berekeningen aan de translatie-rotatie-koppeling in oriëntationeel wanordelijke kristallen zijn niet goed gefundeerd aangezien er te weinig bekend is van de rotatie-dynamica in dit soort kristallen.

   K.H. Michel en J. Naudts, *J. Chem. Phys.* **67**, 547 (1977).
   S. Galam, *Phys. Lett.* **122**, 271 (1987).

8. Zetwerk vervaardigd m.b.v. een tekstverwerker met afbreekalgoritme dient men goed te controleren op afbreekfouten. Immers, een lid van de regering zal het niet op prijs stellen indien hij/zij gedegradeerd wordt tot een minister. Maar zelfs als het afbreken in principe goed is kunnen rare effecten ontstaan. Zo kan beter vermeden worden dat een bisschop in een massagebed terecht komt.

   D.E. Knuth, *The TEXbook* (Addison Wesley, Reading, 1986).
   Battus, *Opperlandse taal- & letterkunde* (Querido, Amsterdam, 1985).

A.P.J. Jansen
10 september 1987